

THE PRODUCTION OF METAL MATRIX COMPOSITES USING THE STIR CASTING TECHNIQUE

By

Jasmi Hashim B Sc (Mech), M Sc (Mater)

This thesis is submitted to
Dublin City University
in part fulfilment of the requirement for the award of the degree of
Doctor of Philosophy

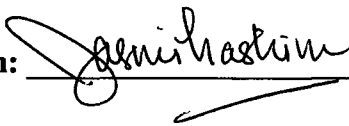
School of Mechanical and Manufacturing Engineering
Dublin City University
Ireland

Supervisors Professor M S J Hashmi, Dr L Looney

August, 1999

DECLARATION

I hereby certify that this material, which I now submit for assessment on the programme of study leading to the award of Doctor of Philosophy is entirely my own work and has not taken from the work of others save and to the extent that such work has been cited and acknowledged within the text of my work.

Sign:  _____

ID No: 95971785

Date: _____

ACKNOWLEDGEMENT

I would like to express my sincerest gratitude to my supervisors, Professor M S J Hashmi and Dr L Looney for their guidance, support and encouragement throughout this research

Sincere thanks are due to Mr Brain Corcoran, and to school technicians especially to Mr Liam Domican, Mr Martin Johnson, Mr Jim Barry and Mr Keith Hickey, for their generous assistance

Financial support received from Dublin City University and from University Teknologi Malaysia is gratefully acknowledged

Finally I would like to express my special thanks to my wife, Norhayati Ahmad, my son Muhammad Afif, Assoc Prof Dr Esah Hamzah (UTM) and Assoc Prof Dr Hishamudin Jamaluddin (UTM) for their encouragement to complete this project

THE PRODUCTION OF METAL MATRIX COMPOSITES USING THE STIR CASTING TECHNIQUE

Jasmi Hashim B Sc (Mech), M Sc (Mater)

ABSTRACT

The fabrication of Metal Matrix Composites (MMCs) using the stir casting technique is the focus of this study. A significant part of the work consists of the design of a specialised rig for this high temperature processing method. Following preliminary tests, graphite was chosen as the main vessel material, and a crucible was designed with a bottom pouring mechanism. In order to optimise stirring conditions, a computer program was used to stimulate the fluid flow in the process crucible.

The main research challenge was to solve the problem of poor wettability between particulate SiC and molten aluminium (A359 alloy), materials which are potentially suitable to the proposed fabrication approach as reinforcement and matrix materials respectively. The percentages of SiC particles used were in the range of 5 to 25 volume percent, samples were cast into ingot or tensile specimen, and some samples were heat treated by precipitation hardening with T6 artificial ageing. It was found that both increasing the silicon carbide content, and T6 artificial treatment increase the mechanical properties such as hardness and tensile strength of the matrix alloy. Characterization of

the MMCs produced included observation of microstructure, porosity content measurement, tensile strength, microhardness, and compression strength measurements

The fabrication approach was successful in producing cast MMCs samples which have reasonable mechanical properties. The use of clean SiC particles, magnesium as a wetting agent, and continuous stirring while the MMC slurry is solidifying were found to promote the wettability of SiC and A359 matrix alloy. Decreasing the solidifying time was found to improve the wettability significantly.

CONTENTS

DECLARATION	I
ACKNOWLEDGEMENT	II
ABSTRACT	III
CONTENTS	V
LIST OF SYMBOLS	XI
1. LITERATURE REVIEW	1
1 1 BACKGROUND	1
1 2 LITERATURE REVIEW	7
1 3 MATERIAL SELECTION	9
1 3 1 Compatibility	10
1 3 2 Thermal Properties	11
1 3 3 Fabrication Method	12
1 3 4 Application	13
1 3 5 Cost	14
1 3 6 Properties	15
1 3 7 Recycling	16
1 4 SELECTION OF MATRIX MATERIALS	16
1 5 THE SELECTION OF REINFORCING MATERIALS	20
1 5 1 Fibre	21
1 5 2 Short Fibre	22
1 5 3 Whiskers	23

1 5 4	Particles	24
1 6	MMC FABRICATION METHODS	28
1 6 1	Liquid Phase Fabrication Methods	28
1 6 2	Solid State Fabrication Process	31
1 6 3	Spray Casting	33
1 6 4	Secondary Processing	34
1 7	STIR CASTING FABRICATION METHOD	35
1 7 1	Fabrication Process	35
1 7 2	Solidification of Metal Matrix Composite	44
1 7 2 1	Particles Pushing or Engulfed	45
1 7 2 2	Particle Floating or Settling	47
1 7 2 3	Solidification Rate of the Melt	48
1 7 2 4	Viscosity and Casting Fluidity of the Slurry	52
1 7 3	Post Solidification Processing	54
1 8	PROBLEMS IN STIR CASTING	55
1 8 1	PARTICLE DISTRIBUTION	56
1 8 1 1	Particle Incorporation	57
1 8 1 2	Particle Characteristics	58
1 8 1 3	Mixing	61
1 8 1 4	Solidification	62
1 8 2	WETTABILITY	67
1 8 2 1	Definition	72
1 8 2 2	Factors Which Retard Wettability	71

1 8 2 3	Methods Used to Promote Wettability	73
1 8 3	POROSITY	80
1 8 4	CHEMICAL REACTION	87
1 9	HEAT TREATMENT OF METAL MATIRX COMPOSITE	91
1 9 1	Heat Treatment Procedure	92
1 9 2	Effect of Reinforcement Particles	94
1 10	MECHANICAL PROPERTIES OF CAST, PARTICLE REINFORCED METAL MATRIX COMPOSITE	100
2.	FEA COMPUTER SIMULATION OF PARTICLE DISTRIBUTION IN CAST METAL MATRIX COMPOSITE	
2 1	INTRODUCTION	103
2 2	STIRRING	105
2 3	SIMULATION	107
2 4	RESULTS AND DISCUSSION	110
2 4 1	Effect of Stirring Speed	111
2 4 2	Effect of Position	113
2 4 3	Effect of Fluid Viscosity	114
2 4 4	Interaction of Effect	114
2 4 5	Comparison with Visualisation Experiment	118
2 4 6	Limitation of the CFD model	118
2 5	CONCLUSION	118

3.	EXPERIMENTAL EQUIPMENT AND PROCEDURE	
3 1	INTRODUCTION	120
3 2	DESIGNING OF EXPERIMENTAL RIG	121
3 2 1	Preliminary Design	121
3 3	WETTABILITY EXPERIMENTS	134
3 3 1	Wettability Testing	136
3 3 2	Point Counting Method	143
3 4	MMC FABRICATION	144
3 4 1	Materials	147
3 4 2	Fabrication Method	149
3 5	SAMPLE PREPARATION	152
3 5 1	Metallography Preparation	153
3 5 2	Preparation for Porosity Measurement	155
3 5 3	Micro Hardness and Compression Testing	156
3 5 4	Tensile Testing	157
3 6	HEAT TREATMENT	161
4.	RESULTS AND DISCUSSION	
4 1	INTRODUCTION	164
4 2	WETTABILITY	165
4 3	MMC FABRICATION METHOD	181
4 4	METALOGRAPHY AND MICROSTRUCTURAL ANALYSIS	183
4 5	POROSITY	192

4 6	COMPRESSION STRENGTH	197
4 7	MICROHARDNESS	198
4 7 1	Effect of Heat Treatment on Micro Hardness	203
4 8	TENSILE PROPERTIES	206
5.	CONCLUSION AND RECOMMENDATIONS	
5 1	CONCLUSION	212
5 2	RECOMMENDATIONS FOR FUTURE WORK	215
	REFERENCES	217
	APPENDIX	
	Appendix A (Schematic Drawings of Casting Equipment Found In the Literature)	A1
	Appendix B (Detailed Drawings of Present Rig)	B1
	Appendix C (Temperature Measurements)	C1
	Appendix D (Graphical Method of Wettability Measurement)	D1
	Appendix E (Density Measurements)	E1
	Appendix F (Micro Hardness, As-cast Condition)	F1
	Appendix G (Micro Hardness - After T6 Treatment)	G1
	Appendix H (Compression Testing)	H1
	Appendix I (Tensile Testing)	I1
	Appendix J (Graphs)	J1
	Appendix K (Publications)	K1

LIST OF SYMBOLS

ε	= Thermal mismatch strain
$\Delta\alpha$	= Difference between coefficient of thermal expansion
ΔT	= Difference in temperature change
V_c	= Theoretical critical velocity
L	= Latent heat of diffusion per unit volume
A_o	= Atomic spacing of the liquid
V_o	= Atomic volume of the liquid
D	= Diffusion coefficient of liquid
KT	= Boltzman factor
R	= Particle radius
V_p	= Settling velocity of the particles
R_p	= particle radius
ρ_p	= particle density
ρ_m	= matrix density
μ	= Viscosity of the molten metal
η	= Coefficient of viscosity
τ	= Shear stress
γ	= Shear rate
η_a	= Apparent viscosity

γ_{sv}	= Specific energy of the solid-vapor interface
γ_{sl}	= Specific energy of the liquid-solid interface
γ_{lv}	= Specific energy of the liquid-vapor interface
W_a	= Work of adhesion
θ	= Contact angle
Ω	= Angular velocity
α	= Rupture strength
P	= Applied load

CHAPTER ONE

LITERATURE REVIEW

1.1 BACKGROUND

The application of Metal Matrix Composites (MMCs) as structural engineering materials has received increasing attention in recent years. Their high strength and toughness at elevated temperatures coupled with low-density makes them suitable for use in applications where conventional engineering materials, such as steel are used. MMCs exhibit significantly higher stiffness and mechanical strength compared to matrix alloys, but often suffer from lower ductility and inferior fracture toughness. MMCs gain the ability to withstand higher tensile and compressive stresses by the transfer and distribution of an applied load from the ductile matrix to the reinforcement material. This load transfer is only possible due to the existence of an interfacial bond between the reinforcement elements and the matrix material. Therefore, appropriate selection of reinforcement material and its properties coupled with a good fabrication method both of which effect this bond will significantly influence the resulting MMC.

There are different routes by which MMCs may be manufactured, and among all the liquid-state processes, stir casting technology is considered to have the most potential for engineering applications in terms of production capacity and cost efficiency. Casting techniques are economical, easier to apply and more convenient for mass production with regard to other manufacturing techniques. There are also various types of the reinforcement material: continuous and discontinuous fibre, or particle. Although the

mechanical properties of the MMC with discontinuous fibre or particles (DRMMC), are not as good as those of continuous fibre reinforced composites, the isotropic properties and low cost of DRMMCs make them potentially useful materials. Silicon carbide and aluminium alloys have been widely used as reinforcement and matrix material respectively, because of the compatibility between these materials, and their potential properties when combined.

The main factors controlling the properties of MMCs fabricated using casting techniques include: reinforcement distribution, wetting of reinforcement by matrix alloy, reactivity at the reinforcement/matrix interface and porosity content in the solidified casting. The effective introduction of a reinforcement element into the liquid matrix is difficult owing to insufficient wetting of the ceramic particles by the liquid alloy. Increasing the liquid temperature [1], coating or oxidizing the ceramic particles, adding some surface-active elements such as magnesium or lithium into the matrix [2] and stirring the molten matrix alloy for an adequate time during incorporation are some ways of improving the wettability and making the mixing and retention of the ceramic particles easier. The selection of high silicon content aluminium alloy was found to delay the chemical reaction [68, 205] whereas the use of inert atmosphere, and the controlled stirring parameters was found to minimise the porosity content.

The present study was aimed at investigating a different approach of fabricating cast MMC, with the main focus towards solving the wettability between silicon carbide particles (SiCp) and aluminium matrix. Emphasis was also place on minimising other problems such as chemical reaction between these two substances, achieving as uniform

as possible a distribution of the SiCp in the matrix, and to keep the porosity level to a minimum as possible. The main part of this study involved the design of a purpose built rig to produce cast MMC, and investigates the influence of the process parameters

In this research, A359 aluminium alloy was used as the matrix material and SiCp as the reinforcement material. A series of wettability tests have been carried out using SiC particles and A359 alloy material. The application of magnesium as a wetting agent, and stirring the slurry in a semi-solid condition was used to improve the wettability. Preheating of the SiC particles was also tried to investigate any possible beneficial effects.

The synthesis of MMCs using the stir casting method was carried out according to the following procedure. All the substances A359 alloy, SiC and magnesium as a wetting agent, were placed in a graphite crucible, and then all of them were heated up in an inert atmosphere. Stirring was started after the matrix alloy melted, and was continued until the matrix alloy became partly solidified. The slurry was then re-melted and re-stirred before being poured into a mould from the bottom of the crucible. The slurry was cast into ingot and tensile specimen shapes. The cast MMC produced by this method was studied. The microstructures of the samples were observed, the porosity contents were measured, tensile strength, microhardness, and compression strength of MMC produced were measured, before and after precipitation hardening with high temperature artificial aging (T6 treatment). The percentage of SiC particle used was in the range of 5 to 25 volume percent. In order to achieve a better mixing effect of the SiCp and molten

matrix, a computer simulation was carried out and this model was validated by comparison with visualization experiments

The experimental data shows that the approach used to produce cast MMC is successful. The proposed method can be used to solve the wettability problems associated with this technique. Microstructural observation shows that the distribution of SiC particles in the matrix alloy is relatively good. The values of the tensile strength, and microhardness are also comparable with the data for MMC produced by other methods, reported by other researches. It was found that the properties of the particulate composites are controlled by the properties of the matrix and the reinforcement, the grain size of the matrix, the porosity content of the composites, the volume fraction and distribution of the reinforcing particles. The precipitation hardening also contributed significantly to improving the properties of the cast MMC.

This research work as shown in the Figure 1.1, can be sub divided into six sections such as

- i) Literature review
- ii) FEA simulation
- iii) Designing of rig
- iv) MMC fabrication
- v) MMC evaluation
- vi) Mechanical testing

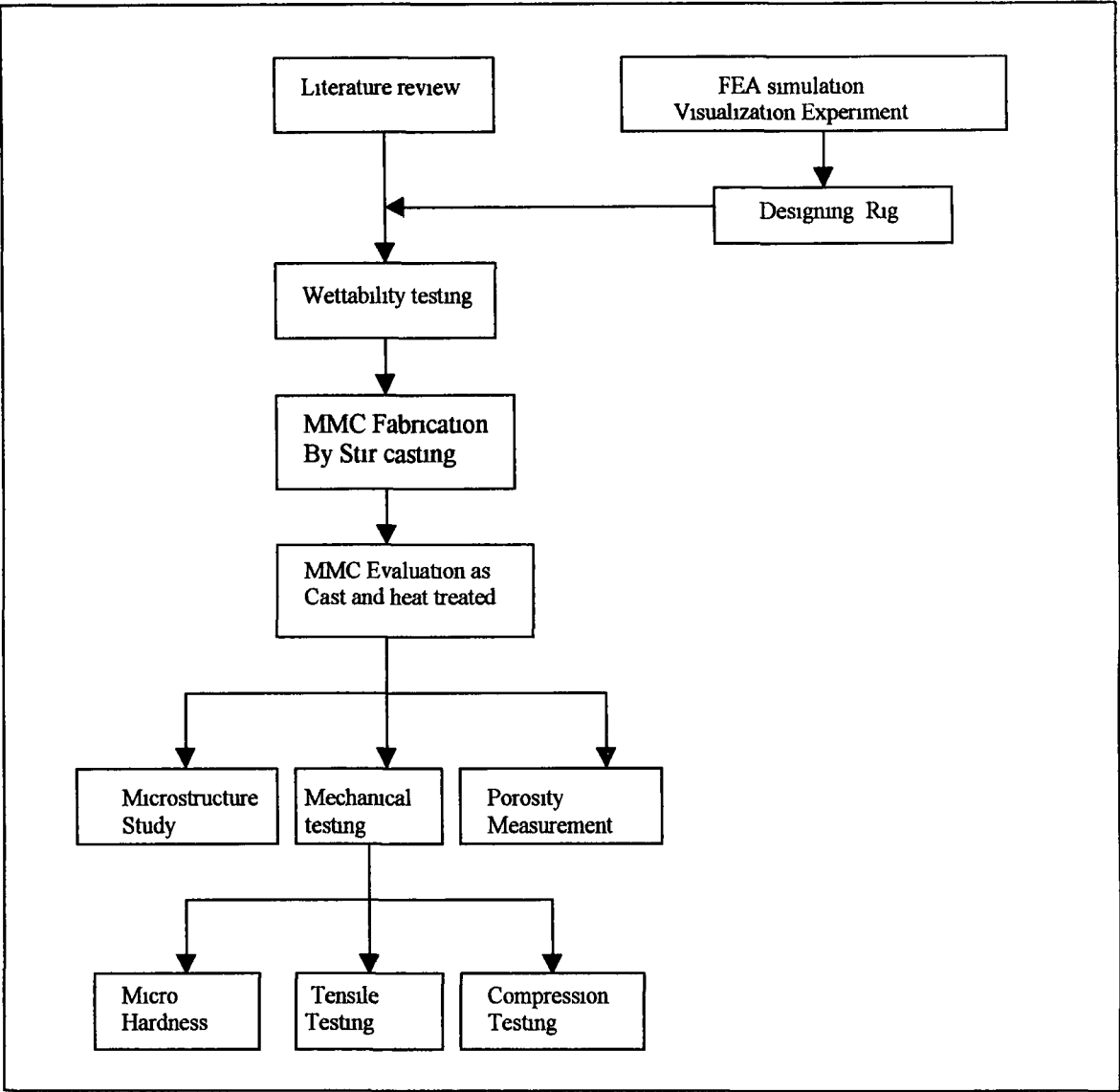


Figure 1 1 Flow chart of the research work

This thesis contains five chapters. The first chapter deals with the introduction to the present research work, and literature review carried out for this research includes the topics of material selection, MMC fabrication methods, problems in stir casting and mechanical properties of cast, particles reinforced MMC. FEA computer simulation of particle distribution in cast MMC is presented in Chapter 2. Chapter 3 describes the

experimental equipment and procedure carried out, including designing of rig, wettability experiments, samples preparation, and mechanical testing. Result and discussion based on the experimental works are presented in Chapter 4. All graphs were produced using SPSS Processor. Finally chapter 5 contains the conclusions from this present research, and provides suggestions for future work, which is related to this field of study.

1.2 LITERATURE REVIEW

Extensive research and development in composite material began in the 1960s. However, interest in MMCs diminished in the early 1970s and polymer matrix composites became the dominant materials. Nowadays composite material is widely recognized according to its matrix materials. Accordingly, composites are classified into three main groups as Metal Matrix Composite (MMC), where metal is used as the matrix material, Polymer Matrix Composite (PMC), where polymer is used as the matrix material and, Ceramic Matrix Composites (CMC) where ceramic is used as the matrix material. Among them PMC are still the most mature of composite technologies. CMC are the least mature and the latest development, and MMC systems lie somewhere between the two.

Composites are a combination of at least two different materials with an interface separating the constituents. The suitability of these composite materials for a given application, however, lies in the judicious selection of synthesizing or processing technique, matrix and reinforcement materials. Matrices can be selected from a number of metal or alloy candidates such as aluminium alloys, and the reinforcement material can have different size and morphology as well as material. This reinforcement can be combined with different matrix materials, which will result in a large number of possible composite material systems. By combining the matrix and reinforcing elements appropriately, new materials with dramatic improvements in strength, elastic modulus, fracture toughness, density and coefficient of thermal expansion (CTE) can be

manufactured. Controlling these properties depends on both a successful selection of the reinforcing phase and an efficient bonding between the matrix and the reinforcing element.

In the context of metal based composites, their development has resulted from an attempt to achieve an improvement in structural efficiency, reliability and overall performance through either reductions in weight or increases in strength to weight ratio. A reduction in material density can be directly translated to reduction in structural weight. This leads the aerospace industry to develop new materials with combinations of low density, improved stiffness and high strength as alternatives to existing high strength aluminium alloys.

In a broader sense, cast composites where the volume and shape of reinforcing phase is governed by a phase diagram, for example, cast iron and aluminium-silicon alloys, have been produced by foundries for a long time. The modern composites are different in the sense that any selected volume, shape and size of reinforcement can be artificially introduced into the matrix. The modern composites are non-equilibrium combinations of metal and ceramics, where there is less thermodynamic restriction on the relative volume percentages, shape and size of ceramic elements. Structurally, MMCs consist of continuous or discontinuous fibres, whiskers, or particles in an alloy matrix reinforcing the matrix or providing it with requisite properties, which are not achievable in monolithic alloys.

1.3 MATERIAL SELECTION

The aim of designing metal matrix composite materials is to combine the desirable attributes of metal and ceramics. The addition of high strength, high modulus refractory particles to a ductile metal matrix will produce a material whose mechanical properties are intermediate between the matrix alloy and the ceramic reinforcement. Metals have a useful combination of properties such as high strength, ductility, and high temperature resistance, but sometimes some of them have a low stiffness value, whereas ceramics are normally stiff and strong, but brittle. For example, aluminium and silicon carbide have very different mechanical properties with Young's moduli of 70 GPa and 400 GPa, coefficients of thermal expansion of $24 \times 10^{-6}/^{\circ}\text{C}$ and $4 \times 10^{-6}/^{\circ}\text{C}$, and yield strength of 350 MPa and 600 MPa respectively. By combining these materials e.g. AA6061 (at T6 condition) with 17 volume fraction of SiC particle, a MMC with Young's modulus of 96.6 GPa, and yield strength of 510 MPa can be produced [3]. By carefully controlling the relative amount and distribution of the ingredients of the composites, as well as the processing conditions these properties can be further improved.

There are a number of criteria that need to be considered before a right selection of the material can be made. Some of these criteria are inter-related. Several criteria for the selection of matrix and reinforcement materials are as follows [4,5]

- i Compatibility
- ii Thermal properties
- iii Fabrication method

iv	Application
v	Cost
vi	Properties
vii	Recycling

1.3.1 Compatibility

The chemical stability, wettability, and compatibility of the reinforcement with the matrix material are important, not only for materials fabrication, but also for application. Not all reinforcement is compatible with every matrix alloy. The wetting and bonding or, on the other hand, excessive chemical reactions between the matrix and ceramic are generally regarded as the major issue in producing most MMC materials [6]. The wettability can be defined as the ability of a liquid to spread on a solid surface, and this phenomenon will be discussed in greater detail in section 1.7.2. If a chemical reaction occurs, it can change the composition of the matrix alloy. Alternatively, some of the chemical reactions at the interface may lead to a strong bond between the matrix and the reinforcement, but a brittle reaction product can be highly detrimental to the performance of the composite. Table 1.1 shows examples of interaction in selected reinforcement-matrix systems [7]. The detail about chemical reactions between reinforcement and matrix materials will be discussed separately in section 1.7.4. Among the many ceramic reinforcements considered for making aluminum matrix composites, Al_2O_3 and SiC have been found to have an excellent compatibility with the aluminum matrix [8] since SiC offers an adequate thermal stability with aluminum alloy during the synthesis and application.

1.3.2 Thermal Properties

These properties can be important for an application where the component is often subjected to thermal cycling, or when the material cannot be allowed to expand, (where close tolerances are needed)

Table 1 1 Examples of interaction in selected reinforcement- matrix systems [7]

System	Interaction	Approx. temp. of significant interaction (°C)
C-Al	Formation of Al_4C_3	550
B-Al	Formation of borides	500
B-Ti	Formation of TiB_2	750
SiC-Al	No significant reaction below melting point	Melting point, 660
SiC-Ti	$TiSi_2$, Ti_5Si_3 and TiC form	700
SiC-Ni	Formation of Nickel silicides	800
$Al_2O_3 - Al$	No significant reaction below melting point	Melting point, 660

It is also important to have small differences in the coefficients of thermal expansion (CTE) when different materials are combined, to avoid internal stress and thermal mismatch strain being generated in the composites [9] In general, the CTE of the reinforcement material is low compared to the matrix alloy For example, in the case of an Al-SiC composite, the CTE of aluminium is $24 \times 10^{-6}/K$ whilst it is $3.8 \times 10^{-6}/K$ for SiC The CTE of the composite depends on the volume fraction of the

reinforcement, which normally decreases the CTE with increasing particle content [10] The thermal mismatch strain, ϵ , between reinforcement and matrix is an essential consideration for composites that will be exposed to thermal cycling This strain is a function of the difference between the CTE of the reinforcement and matrix $\Delta\alpha$, according to the following expression [11],

$$\epsilon = \Delta\alpha\Delta T \quad (1)$$

Where ΔT is the temperature change It is important that the temperature change be minimum in order to minimize strain accumulation However, unavoidably on cooling from high temperatures during materials processing, a thermal mismatch strain is generated across the interface between the two components of the composite For example the value of coefficient of thermal expansion of aluminium alloy and silicon carbide particle is $24 \times 10^{-6}/^{\circ}\text{C}$ and $4 \times 10^{-6}/^{\circ}\text{C}$, and this will give $\Delta\alpha$ of about $20 \times 10^{-6}/^{\circ}\text{C}$ During solidification from melting temperature of about 700°C to room temperature of about 20°C will give ΔT of about 680°C Therefore the amount of a thermal mismatch strain that will generated during solidification process of aluminium-silicon carbide composite is about 0.0136

1.3.3 Fabrication Method

There are several fabrication techniques available to manufacture MMC materials A powder metallurgy (PM) route is the most common method for the preparation of

discontinuous reinforced MMC [10, 13-16]. Since no melting and casting is involved, this leads to less interaction between the matrix and the reinforcement, consequently minimizing interfacial reaction and leading to improved mechanical properties. In some cases this technique will permit the preparation of composites that cannot be prepared through liquid metallurgy. For example, SiC whiskers will dissolve in a molten Ti-alloy matrix, therefore using PM route [17] can minimize dissolution. It has been shown that SiC fibre are highly compatible with solid aluminum but only fairly compatible with liquid aluminum [18]. In liquid metal processing, the ceramic particles spend considerable time in contact with the molten alloy matrix, and this can result in reaction between the two. In the stir casting method, the use of reinforcement material such as fibre, or filament seems not to be suitable. This is because the stirring action, which is essential to disperse reinforcement material in the molten matrix, would break them [88].

1.3.4 Application

If the composite is to be used in a structural application, the moduli, strength and density will be important, which requires high moduli, low-density reinforcement. In this case particle shape may also be a factor, since angular particles can act as local stress raisers, thus potentially reducing ductility. If the composite is to be used in a thermal structural management application, the CTE and thermal conductivity are important. The CTE is generally important because it influences the long-term strength of the composite. Repeated application in many thermal cycles from ambient to approximately 200° C will cause internal stress to be regenerated at each cycle, and it is possible that excessive plastic strain could be developed which is greater than the allowable creep strain [19].

1.3.5 Cost

Recent developments in MMC fabrication are aimed at cheaper and simple techniques. Liquid state processing incorporating various casting methods, powder metallurgy methods and, in-situ processing are being used in current production of particulate reinforced aluminium matrix composites. However, the powder metallurgy route is difficult to automate, and for this reason may not be the right answer for economical production of aluminium matrix composites. The most economical techniques are found among the liquid state and in-situ processes, and among them the most simple, inexpensive and widely used methods are casting methods [20]. In some fabrication techniques, the size and shape of component are limited and standard metal working and machining methods normally cannot be applied. Machining of MMC components will always give a very bad surface finished, and a special tool has to be used. Consequently, the production costs of these materials remain high [21]. Figure 1.1(a) shows the relative costs of various processing techniques and reinforcement materials.

Processing method	Cost	Reinforcement type
Diffusion Bonding	High	Mono filaments
Powder Metallurgy	↑	Whiskers
Spray Methods	↓	Fibre
Liquid State Processes	Low	Particle

Figure 1.1(a) Relative cost effect of various processing method and reinforcement [21]

Alternative reinforcement phase morphologies has to be investigated in order to reduce the cost of MMCs while retaining the attractive properties. These approaches typically involve the use of less expensive, discontinuous reinforcement phase and powder metallurgy and casting techniques. A major reason for using particles is to reduce the cost of the composites. So the reinforcement has to be readily available in the quantities, size and, shape required at low cost.

1.3.6 Properties

Low density MMCs can readily be developed by selecting low density alloys, such as those based on aluminium and magnesium, as the matrix material. When structural requirements demand optimal strength-density ratio in combination with thermal stability, nickel and titanium based alloys can also be selected. Whereas most metallic matrices exhibit reasonably high thermal conductivity, their CTEs are substantially higher than most of the available reinforcement material. It was found that the presence of a discontinuous reinforcement phase in a metal matrix increases the fatigue life [310]. This is influenced by the mutually interactive effects of individual properties of the composite constituents, size of the reinforcement phase, spatial distribution of the reinforcement in the matrix and intrinsic nature of the reinforcement-matrix interface [9]

Aluminium alloy has lower hardness values compared to, for example, steel or cast iron. This alloy cannot therefore be used in applications where the material is subjected to extensive abrasion. If a hard reinforcement is added to the matrix, the new

material could be used in applications where abrasion resistance is of consent. The wear resistance normally increases with the amount of reinforcement. However, the combination of a number of properties is very important. It is not always justified to choose aluminium matrix composite because of its high specific properties only, e.g. the low weight and the resulting weight saving. The ductility decreases with increasing amount of reinforcement material added. Coarser particles should be avoided to minimize particle fracture [22].

1.3.7 Recycling

The production cost of aluminium is expensive compared to other commercial materials such as steel, but if aluminium is recycled, great savings in energy consumption can be gained. The energy consumed when aluminium is recycled is only about 5% of that used in primary production [23]. It is important to choose matrix and reinforcement with the consideration that detrimental inter-metallic may be formed that will make recycling difficult. The formation of certain intermediate phases will decrease the possibilities of recycling. This problem is possible to avoid by carefully selecting reinforcements having compatibility with the matrix.

1.4 SELECTION OF MATRIX MATERIAL

In MMC, metals or alloys are used as the matrix material. The matrix acts as the bonding element and its main function is to transfer and distribute the load to the

reinforcement materials. This transfer of load depends on the bonding between the matrix and the reinforcement. However, the bonding depends on the type of the matrix and the reinforcement as well as to the fabrication technique. For the matrix material, factors such as density, and strength retention at elevated temperature and ductility are considered to be important [24]. To achieve higher composite strength, metal alloys are used as the matrix instead of pure metal. The matrix material is used in various forms for different fabrication methods, for example, powder is used in powder metallurgy techniques and liquid matrix material is used in liquid metal infiltration, squeeze casting and compocasting.

Matrix selection depends not only on desirable properties but also on which material is best suited for a particular composite manufacturing technique. The matrix alloy should be chosen after giving careful consideration to the chemical compatibility with the reinforcement or its coating, to its ability to wet, its own characteristic properties and processing behaviour [25]. Generally, Al, Ti, Mg, Ni, Cu, Pb, Fe, and Zn are used as the matrix material [25], but Al, Ti and Mg are widely used. Nowadays, the main focus is given to aluminium alloy as the matrix material [26] because of its unique combination of good corrosion resistance, low density and excellent mechanical properties. This is also because aluminium is light, which is the first requirement in the most potential applications of MMC. Additionally, it is inexpensive in comparison to other light metals such as titanium and magnesium. Among all excellent aluminium alloys, the precipitation hardenable alloys, such as Al-Mg-Si and Al-Si are normally selected. Other aluminium alloy systems that have been used as a matrix material are 2XXX (Copper-Aluminium

good effect of L₁ is that when it is alloyed to aluminum, it simultaneously decreases the densities and increases the elastic moduli of the alloys [27] The typical properties of some metals used as matrices in composites are shown in Table 1.2 [28]

Table 1.2 Typical properties of metal matrix constituent [28]

Metal	Density [gcm⁻³]	Melting Point [°C]	CTE [x10⁻⁶°C⁻¹]	Tensile Strength [MPa]	Modulus [GPa]
Aluminum	2.8	590	23.4	310	70
Beryllium	1.9	1280	11.5	620	290
Copper	8.9	1083	17.6	340	120
Lead	11.3	320	28.8	20	10
Nickel	8.9	1140	13.3	760	210
Niobium	8.6	2470	6.8	280	100
Steel	7.8	1460	13.3	2070	210
Tantalum	16.6	2990	6.5	410	190
Tin	7.2	230	23.4	10	40
Titanium	4.4	1650	9.5	1170	110
Zinc	6.6	390	27.4	280	70

Another important structural aerospace metal is titanium. Titanium has been used in aero-engines mainly for compressor blades and discs, due to its elevated temperature resistant properties. Although it has higher density than Al, it still shows excellent strength to weight and stiffness to weight ratios. The melting point of titanium is relatively high and it retains strength at much higher temperatures than aluminum. As the corrosion and oxidation resistance of Ti is good, it is an ideal material, for example, for jet engines in aerospace industry [29-31]. However, titanium is a very expensive material. It is rather soft and its corrosion resistance is based on a surface oxidation layer. It is not

its corrosion resistance is based on a surface oxidation layer. It is not very wear resistant, and it cannot resist combined wear and corrosion. Hard ceramic particles in titanium matrix may improve the wear resistance significantly.

Magnesium is the lightest of structural metal, approximately 35% lighter than aluminium. Magnesium is readily available and it is relatively easy to cast. Magnesium is a potential material to fabricate composites for making reciprocating components in motors and for making pistons, dudgeon pin, and spring caps. It is also used in aerospace applications due to its low CTE and high stiffness properties with low-density [32]. The mechanical properties of magnesium matrix composites are comparable to those of aluminum based material. However, its corrosion properties are poor, and this is usually minimized by painting and coating techniques.

Inter-metallic compounds have also been developed as matrix materials. Their high temperature capability and oxidation resistance is higher than those of titanium matrix composites. Among them are Ni_3Al , Ti_3Al , and MoSi_2 [36]. These intermetallic materials have high strength, high elastic moduli and good creep resistance. The major disadvantage of these materials is their low ductility at room temperature, and this makes the processing method of structural components more difficult. However this problem can be reduced by the addition of certain alloying elements.

Stainless steel and superalloy have been used as matrix materials [30,31]. In this case a modern highly alloyed PM super-duplex stainless steel. Its yield strength is more than two times higher than for standard austenitic grades. Despite the high strength the impact toughness of these materials remains high, and they have a very good resistance against

pitting corrosion The wear resistance of this steel is improved when ceramic particles are added

1.5 SELECTION OF REINFORCING MATERIALS.

In general the prime role of the reinforcement material in the matrix metal is to carry load The reinforcement may be divided into two major groups continuous and discontinuous The MMCs produced by these are therefore named continuously reinforced composite and discontinuously reinforced composite In general the reinforcement increases strength, stiffness, and temperature resistance capacity but lowers the density fracture toughness and ductility of the MMC's The correct selection of reinforcement type, geometry or shape is important in order to obtain the best combination of properties at substantially low cost When selecting the reinforcement materials the following aspect must be considered [34,35]

- i Shape – continuous fibre, chopped fibre, whiskers, spherical or irregular particles, or flakes
- ii Size – diameter and aspect ratio
- iii Surface morphology – smooth or corrugated and rough
- iv Structural defects – voids etc
- v Inherent properties – such as strength, moduli and density
- vi Chemical compatibility with the matrix

In terms of shape, the reinforcement material may be sub-divided into four major category [24]

- i Continuous fibres
- ii Short fibres (chopped fibres are not necessarily all the same length)
- iii Whiskers
- iv Particles or platelet, and

1.5.1 Fibre

Continuous fibres exhibit highest strength when they are oriented unidirectionally, but the composite then has low strength in the direction perpendicular to the fibre orientation. Whereas, whiskers and particles giving a better strength when distributed uniformly in the matrix. Carbon, boron, SiC and Al₂O₃ are the most researched continuous reinforcements. The density of carbon fibre is the lowest, accordingly, it can offer significant weight savings. Boron fibres show the greatest strength in comparison with other fibres. However the cost of these fibres is very high [36].

The continuous fibre reinforced composite offers the best combination of strength and stiffness, compared to other types of reinforcement. Among the greatest benefits are the increased strength with increased temperature. Aluminium based fibre MMCs have useful strength up to 400°C [37]. However the cost of these systems is very high, mainly because of high costs of the continuous fibres and the composite production cost [38]. These expensive materials have military applications, where weight saving is of great importance compared to the production cost. However, continuous fibres suffer from fibre damage especially during secondary processing [39], such as rolling and extrusion.

These materials are not recyclable Properties some of continuous fibre are shown in Table 1 3 [36].

Table 1 3 Characteristic some of continuous fibres [36]

Fibre-composition	Filaments per Yarn	Mean Diameter [μm]	Specific Gravity	Young's Modulus[GPa]	Failure Strength[GPa]
B (cvd on W)	1	140	2 6	410	4 1
Al ₂ O ₃	900	10-13	3 9	350	2 1
Al ₂ O ₃ -20SiO ₂	960	10	3 1	160	1 6
Al ₂ O ₃ -15SiO ₂	1000	17	3 25	210	1 8
C	1000 - 12000	7	1 76	230	3 5
C	1000 - 6000	6 5	1 81	390	2 7
SiC (+O)	500	15	2 55	200	2 8
SiC (+O + Ti)	200 -1600	8-9	2 3-2 5	200	2 8
S-glass	1000	9	2 49	80	4 14
E-glass	1000	9	2 49	70	2 7

1.5.2 Short Fibre

Short fibres are used mainly for refractory insulation purposes due to their low strength, and fibres such as saffil and kaowool are used as the reinforcement materials in automobile engine components In term of price, short fibres are normally cheaper than both fibre and whiskers [40] Characteristic some of these short fibres are shown in Table

Table 1 4 Characteristics of ceramic short fibres [40]

Short fibre	Length [mm]	Diameter size [μm]	Density [g cm^{-3}]	UTS [Gpa]	E [Gpa]
Carbon	2.5	7.8	1.75	3.45	2.30
SiC Nicalon	1-6	10-15	2.55	3	195
Al_2O_3	3-6	15-25	3.96	1.7	380

1.5.3 Whiskers

Numerous materials, including metal, oxides, carbides, halide and organic compounds have been prepared under controlled conditions into the form of whiskers. The whiskers based composites are more costly than the particles based ones. But in general they offer higher strength than particle based composites. Compared to discontinuous reinforcement, such as polycrystalline flake, particle or chopped fibres, single crystal whiskers usually have a much greater tensile strength. Whisker reinforced composite offers the potential for enhanced properties, but suffers from whisker breakage and damage during secondary fabrication [41]. Discontinuous fibres and whiskers are not as expensive as continuous fibres, however the whiskers having a higher cost than discontinuous fibres. The whiskers reinforced material retains strength up to 250°C [42]. Mechanical properties whiskers fibres are shown in Table 1 5 [41].

Table 1 5 Mechanical Properties of some whisker reinforcement [41]

Material	Tensile Strength [MPa]	Density [gcm ⁻³]	Young Modulus [MPa]	Specific Strength	Specific Modulus [MPpa]
Alumina	21	3 96	430	5 3	110
Silicon carbide	21	3 21	490	6 5	150
Graphite	20	1 66	710	12 0	430
Boron carbide	14	2 52	490	5 6	190
Silicon nitride	14	3 14	380	4 4	120

1.5.3 Particles

Particles are the most common and cheapest reinforcement. This type of reinforcement material produces discontinuous reinforced composites with isotropic properties. Another advantage is that conventional fabrication methods may be used to produce a wide range of product forms, making them relatively inexpensive compared to composites that are reinforced with continuous fibre or filaments. The useful temperature range of particle reinforced aluminium based composite is 20–150°C. Because of their relatively low cost, these materials are likely to find extensive applications [42].

Particle shape and size play an important role since angular particles can act as stress raisers, whereas rounded or globular particles are favoured for the impact properties. Spherical particles should give better ductility than angular shapes [42]. Several different particles or powder shapes are as shown in Figure 1 2. It has been found

that fine particles are more effective in strengthening the composites than coarse particles of the same volume fraction [43]

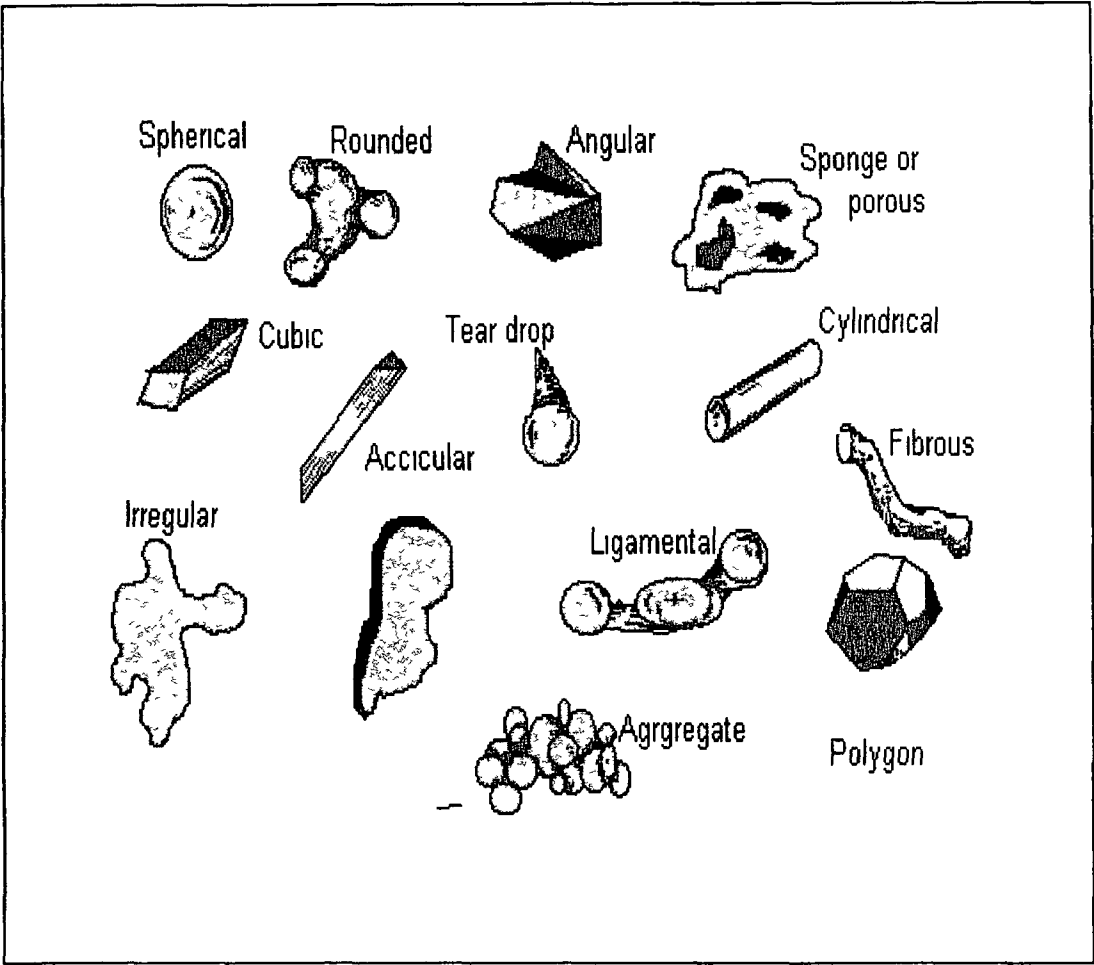


Figure 1 2 Different shape of particles [42]

Finer particles result in a closer inter-particle spacing. Coarser particles are in general easily incorporated in liquid melts but are more susceptible to gravity settling and can result in a heavily segregated casting [46]. Coarse particles are more susceptible to cracking under stress, resulting in poor mechanical properties of the composite [44]. Larger particles show a greater propensity to crack than smaller particles having a higher

probability of containing defect. However, fine particles in a melt matrix pose difficulty due to the clustering of the particles and other problems associated with the larger surface area of the particles, such as increased viscosity of the melt, making processing more difficult. Most molten metal processing use ceramic particle in the size range of 10-20 μm [46]. It has been observed that the increase in load capacity given by cubic particles results in a decrease in ductility [45].

The preferred and most used of the particles materials, for aluminum alloy matrix composites is silicon carbide (SiC), due to its favorable combination of mechanical properties, density and cost [47]. Another widely used particle reinforcement in aluminium matrix composites is Al_2O_3 . In comparison to SiC , it is more inert in aluminum and it is also oxidation resistant. Accordingly, it is more suitable for high temperature fabrication and use. Some other particle reinforcement also has been investigated. For example, graphite can give the composite specific tribological properties, and B_4C reinforced materials may have nuclear application because of neutron capturing properties of boron [48].

It is well established that uniformly distributed reinforcements of finer size and clean interface are essential for improvement of mechanical properties [109]. Moreover, improved elevated temperature properties can be obtained in these composites, if the reinforcements, especially the interfaces are stable at such temperatures over a prolonged period of time. Table 1.6 shows the characteristics of ceramic particles, which are often used in MMC, fabrication [40]. Optimizing alloy development ought to include

considerations of all the fundamental aspect of particles including their shape, size, volume fraction and mechanical properties.

Table 1.6 : Characteristics of ceramic particles [40].

Particle	Size [μm]	Density [g cm ³]	UTS [GPa]	E [GPa]
Graphite	40-250	1.6 – 2.2	20	910
SiC	15 – 340	3.2	3	480
SiO ₂	53	2.3	4.7	70
TiC	46	4.9	-	320
BN	46	2.25	0.8	100 – 500
ZrO ₂	75 – 180	5.65 6.15	0.14	210
B ₄ C	40 – 340	2.5	6.5	480
Al ₂ O ₃	40 – 340	3.97	8	460
Glass	30 – 120	2.55	3.5	110

Initial interest in whiskers and particle reinforcements has declined because of realisation of the health hazard posed in their handling [24]. Skin, eye and respiratory protection must be used during the handling of these powders to prevent over exposure in the event of accidental spillage during mixing [12, 309]. Very fine whiskers in particular may cause respiratory disorders, and can be carcinogenic. In addition, care must also be taken during mixing because of the explosive nature of a collection of very fine (size <5 μm) particles. Electro-static charges can build up during mixing which can initiate ignition and explosion. This is particularly relevant to metal powders.

1.6 MMC FABRICATION METHODS

Discontinuous Reinforced Metal Matrix Composites (DMMC) have achieved a dominant position in the metal matrix composite field because of low production cost as compared to continuously reinforced materials. In an effort to optimize the structure and properties of particle reinforced metal matrix composite, various processing techniques have been evolved over the last twenty years. Processing of DMMC materials generally involves at least two operations – production of the composites materials itself, and fabrication of this composite into useful product forms. Both operations can effect the properties and interfacial characteristics of the final product. The methods, which are commonly employed to manufacture DMMC, can be grouped depending on the temperature of the metallic matrix during processing

- i Liquid phase processes, and
- ii Solid state processes

1.6.1 Liquid Phase Fabrication Methods

Generally there are three liquid phase fabrication methods or casting routes, which are currently in practice – stir casting, liquid metal infiltration and squeeze casting. The application of this high temperature processing method is limited by poor wettability and a high tendency for chemical reaction of the reinforcement with liquid metal. However, there are a number of techniques used to control this phenomenon. Normally

this type of fabrication method is carried out under vacuum or using an inert gas atmosphere to minimize the oxidation of the liquid metal

In the stir casting method, the ceramic particles are incorporated into a molten matrix using various techniques, followed by mixing or pressing, and casting the resulting MMC. In this process, a strong bond between the matrix and reinforcement is achieved by using high processing temperatures, and often, alloying the matrix with an element which can interact with the reinforcement to produce a new phase which improves wetting between the matrix and the reinforcement material. There is variation in stir casting methods, in the way the liquid metal is stirred in fully liquid state, such as by vortex method, or in a partially solidified state such as in the compocasting method [49]. In the vortex method, the reinforcement is introduced into a vortex created in the liquid metal by stirring. Reinforcement is efficiently distributed throughout the melt, and the resulting composites can be cast. Whereas in the compocasting, or rheocasting technique, the melt is vigorously stirred as it cools below the liquidus temperature. This produces a slurry in which the metal solid has a non-dendritic or rounded form. The mixture is cast, often using pressure to ensure flow of the viscous material. It is possible to incorporate an addition during the stirring stage to produce a composite, hence the descriptive term of compocasting. Incorporation of the reinforcement particles within the semi-solid alloy is claimed to be advantageous because the solid mechanically entraps the reinforcement and agglomeration, and settling or floatation is avoided [51].

Figure 1.3 shows schematic diagram of vortex method [52]. The detail of this process, so called stir casting will be discussed in the section 1.6. More recently, semi-solid processing has attracted considerable attention as a direct result of its intrinsic

ability to yield fine-grained microstructures and provide improved mechanical property [306] Semi-solid processing involves the agitation of a metal alloy, as solidification begins Mehrabian et al [50] found that, even in cases where the ceramic particles are not wetted by the matrix, the ceramic particles were prevented from settling, floating or agglomerating by the partially solidified matrix They also found that increasing the mixing times promotes metal-ceramic bonding

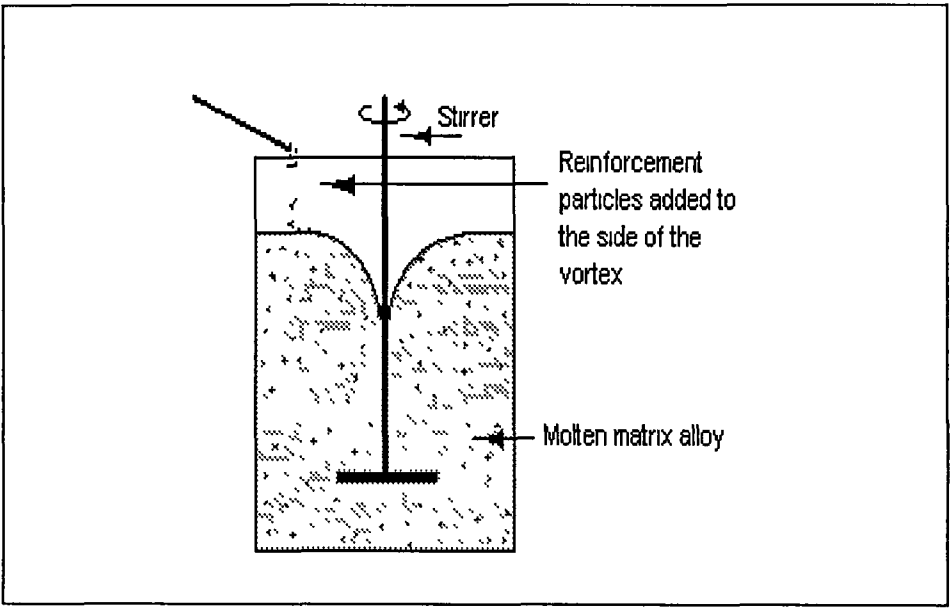


Figure 1 3 Schematic diagram of producing MMC slurry
using a vortex method [52]

Squeeze infiltration is the most successful form for MMC production In this technique the molten metal is forced-infiltrated into fibre bundles or preformed, expelling all absorbed and trapped gasses This method involves placing a preheated preform of reinforcement into a preheated die, filling the die with molten matrix metal, squeezing the molten metal into the preform using a hydraulic press with a preheated ram, holding the

pressure during solidification, releasing the pressure and ejecting the resulting composite. The preheated reinforcement, usually in the form of a pre-compacted and inorganically bonded preform, is placed in a preheated metal die. Superheated liquid metal is introduced into the die and pressure is applied to drive the metal into the interstices between the reinforcing materials. The pressure required to combine matrix and the reinforcement is a function of the friction effects due to viscosity of the molten matrix as it fills the ceramic preform. Squeeze casting produces components, which are free from gas or shrinkage porosity. Figure 1.4 shows squeeze casting schematically [53].

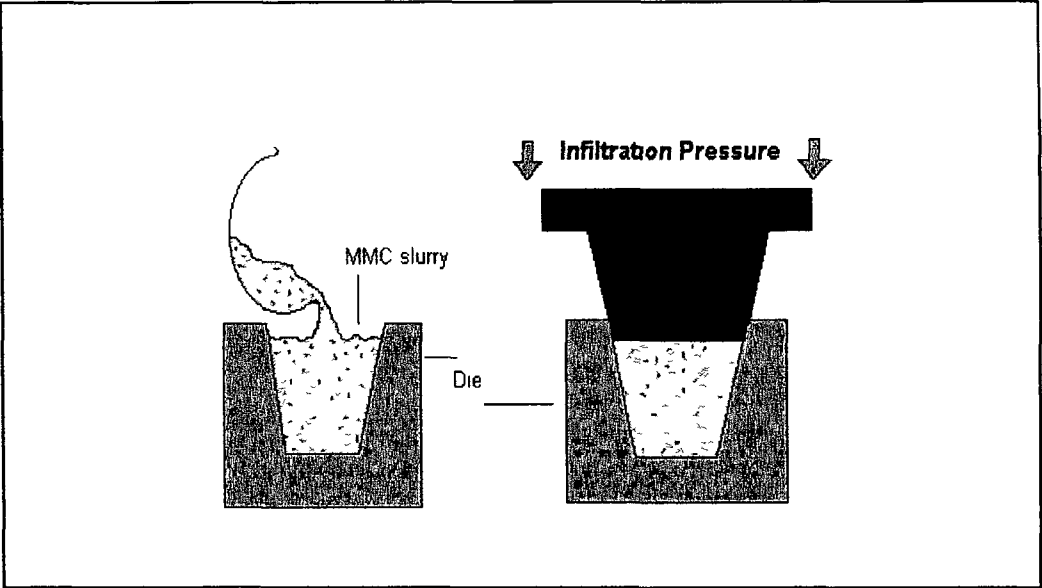


Figure 1.4 Squeeze casting process [53]

1.6.2 Solid State Fabrication Process

Solid state processes are generally used to obtain the highest mechanical properties in MMCs, particularly in discontinuous MMCs. This is because segregation effects and brittle reaction product formation are at a minimum for these processes,

especially when compared with liquid state processes. Powder Metallurgy (PM) is the common method for fabricating DRMMC [54].

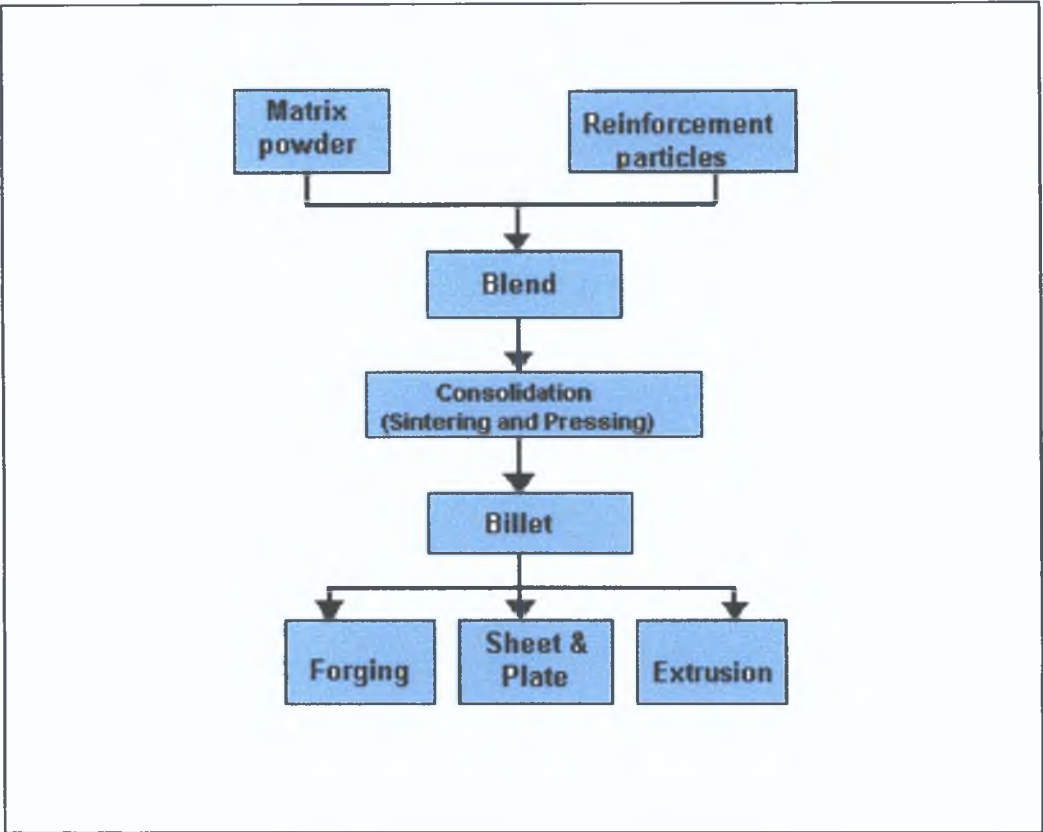


Figure 1.5: The flow chart of the powder metallurgy process to fabricate MMC [54].

The technique used to produce MMC by powder metallurgy is similar to those used for powder metallurgy processing of un-reinforced materials. In this process, after blending the matrix alloy powder with reinforcement material and binder, the resulting mixture is feed into a mould of the desire shape. Cold isostatic pressing is utilized to obtain a green compact. The main difficulties encounter in this process is the removal of the binder used to hold the powder particles together. The organic binders often leave

residual contamination that causes deterioration of the mechanical properties of the composites. In order to facilitate the bonding of powder particles, the compact is then heated to a temperature below the melting point but high enough to develop significant solid state diffusion (sintering). Sometimes it becomes necessary to maintain the consolidation temperature slightly above the solidus to minimize deformation stress and to avoid the damage of particles or whiskers. The consolidated composites are subsequently extruded or forged into desired shape [55]. Figure 1.5 shows a schematic diagram of the PM technique [54]. Table 1.7 shows a comparative evaluation of different processes, which are commonly used for discontinuously reinforced metal matrix composite production [57].

1.6.3 Spray Casting

Other methods of manufacturing MMCs are the spray casting or also called spray deposition method. This method also can be used on unreinforced materials. In this process, a controlled stream of molten metal is produced. The stream is converted to a spray of molten droplets in an inert atmosphere, for example in Nitrogen gas. The size of the droplets are approximately 20-50 μm in diameter. The droplets are impacted onto a collecting surface, and allowed to coalesce. It is possible to add solid particles such as SiC and Al_2O_3 to the atomised metal stream. The advantage with this process is the short contact time between the liquid matrix and reinforcement that will reduce chemical reactions. However the production cost of this process is very high [307-309].

1.6.4 Secondary Processing

Secondary processing of DRMMC such as extrusion and rolling, leads to break up of particle (or whisker) agglomerates, reduction or elimination of porosity, and improved particles-to-particle bonding, all of which tend to improve the mechanical properties of these materials. When composite sheet or product are required, rolling follows extrusion. Because compressive stresses are lower in the rolling operation than in the extrusion, edge cracking is a serious problem with these materials. It was found that rolling of DRMMC is most successful in the range of 0.5Tm using relatively low rolling speeds. As in the case of extrusion, further break-up of particulate agglomerates takes place during rolling [56].

Table 1.7 A comparative evaluation of different techniques used for discontinuously reinforced metal matrix composite fabrication [57]

Method	Range of shape and size	Metal yield	Range of volume. fraction	Damage to reinforcement	Cost
Liquid metallurgy (Stir casting)	Wide range of shapes, larger size to 500 kg	Very high, >90%	Up to 0.3	No damage	Least expensive
Squeeze casting	Limited by preform shape Up to 2 cm height	Low	Up to 0.45	Severe damage	Moderate expensive
Powder metallurgy	Wide range, restricted size	High	0.3-0.7	Fibre or particle fracture	Expensive
Spray casting	Limited shape, large size	Medium			Expensive

1.7 STIR CASTING FABRICATION METHOD

Among the variety of manufacturing processes available for discontinuous metal-matrix composites, stir casting is generally accepted, and currently practiced commercially. Its advantages lie in its simplicity, flexibility and applicability to large-scale production and, because in principle it allows a conventional metal processing route to be used, and its low cost. This liquid metallurgy technique is the most economical of all the available routes for metal matrix composite production [58], allows very large sized components to be fabricated, and is able to sustain high productivity rates. According to Skibo et al [59], the cost of preparing composites materials using a casting method is about one-third to one-half that of a competitive methods, and for high volume production, it is projected that costs will fall to one-tenth.

1.7.1 Fabrication Process

In general stir casting of MMCs involves producing a melt of the selected matrix material, followed by the introduction of a reinforcing material into the melt, obtaining a suitable dispersion through stirring. The next step is the solidification of the melt containing suspended particles to obtain the desired distribution of the dispersed phase in the cast matrix. The schematic diagram of this process is as shown in Figure 1.6. In composites produced by this method, particle distribution will change significantly depending on process parameters during both the melt and solidification stages of the process. The addition of particles to the melt drastically changes the viscosity of the melt,

and this has implications for casting processes. It is important that solidification occur before appreciable settling has been allowed to take place.

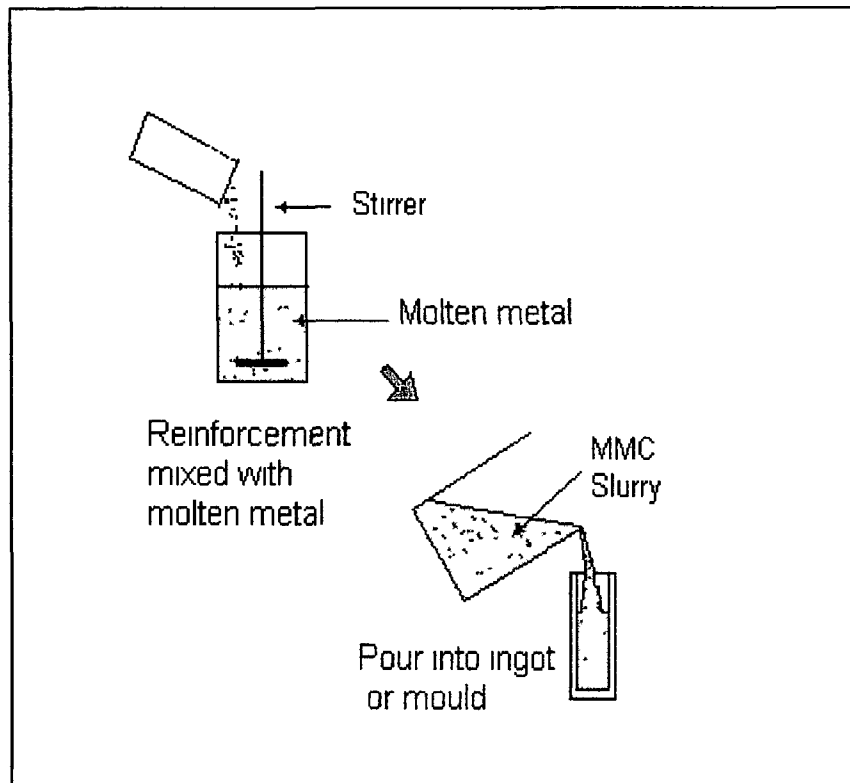


Figure 1.6 Schematic Diagram of Stir Casting

The earlier approaches to producing metal matrix composite used solid particles produced within the melt through a chemical reaction. This results in dispersed phases as in precipitation hardening of Al-4wt% Cu alloy. Other approaches to produce metal matrix composites involve the introduction of second phase particles in the metal melt. The foundry technique involves the mixing of reinforcement particles by stirring the molten alloy matrix.

The process is generally carried out at two different ranges of temperature of the melt, beyond the liquidus temperature [60-63] or at the melt temperature maintained within the partially solid range of the alloy [64-66]. The technique involving the latter range of temperature is called the compocasting process and it is very effective in making cast composites with higher particle content [50]. The reinforcement particles are added gradually while stirring continues at a constant rate. According to Miwa [67], in order to get good incorporation, the addition rate needs to be reduced with a decrease in size of the particles. Lee et al [68] introduced particles at 4-5g/hour, and Salvo [69] takes about 5-10 minutes to incorporate silicon carbide particles into the melt. In some cases the particles were introduced through a nitrogen gas stream [73,74].

The reinforcement particles used normally are one of two types: either in as-received condition, or heat-treated (artificially oxidized). Oxidation has taken place at 1000°C for 1.5 hours in air [70], at 1100°C for 12 hours [71] or one and half hours [72], and at 850°C for 8 hours. Additionally, gas absorbed on the surface of SiC, which was prepared in air, can be removed by preheating at a certain temperature for a certain period of time. For example, particles have been heated to 554°C for one hour [70,75], 850°C for 8 hours [76], or at the temperature of 900°C [77], 799°C [74,78] and 1100°C [69].

Most previous researches have used the matrix metal alloy in the ingot form [68,69,74,80] or extruded bar [69]. As a starting point the ingot is generally melted to above the liquidus temperature, for example to 50°C above the liquidus temperature [68]. A different approach has been proposed by Young and Clyne [81] and in their work

slurry was prepared from powdered material. Composite melt may be prepared in a graphite crucible [70,73,74,82], silicon carbide crucible [69,72], alumina crucible [76,83,84], or concrete crucible [79]. In order to keep the melt as clean as possible the ingot is melted under a cover of an inert gas such as nitrogen, or in a vacuum chamber [74] or in a pressure chamber [69]. There also helps to minimize the oxidation of the molten metal [77], or reduces porosity (under pressure). McCoy et al [79] prepared composite with the whole apparatus being sealed within a glove box which was filled with nitrogen gas. According to Yamada et al [80] the molten aluminium should be subjected to a high vacuum atmosphere to degas hydrogen, before the reinforcement materials are completely added. Gupta and Surappa [77] treated the metal ingot in different ways. In their work the metal ingot, before melting, was treated with a warm alkaline solution and washed with a mixture of acids, in order to reduce the thickness of the oxide film and to eliminate other surface impurities.

The most significant requirement when using a stir casting technique is continuous stirring of the melt with a motor driven agitator to prevent settling of particles. If the particles are more dense than the host alloy, they will naturally sink to the bottom of the melt [88]. This means that some method of stirring the melt must be introduced before casting to ensure that the particles are properly distributed throughout the casting. Some of the stirrer which are normally be used is shown in Figure 1.7

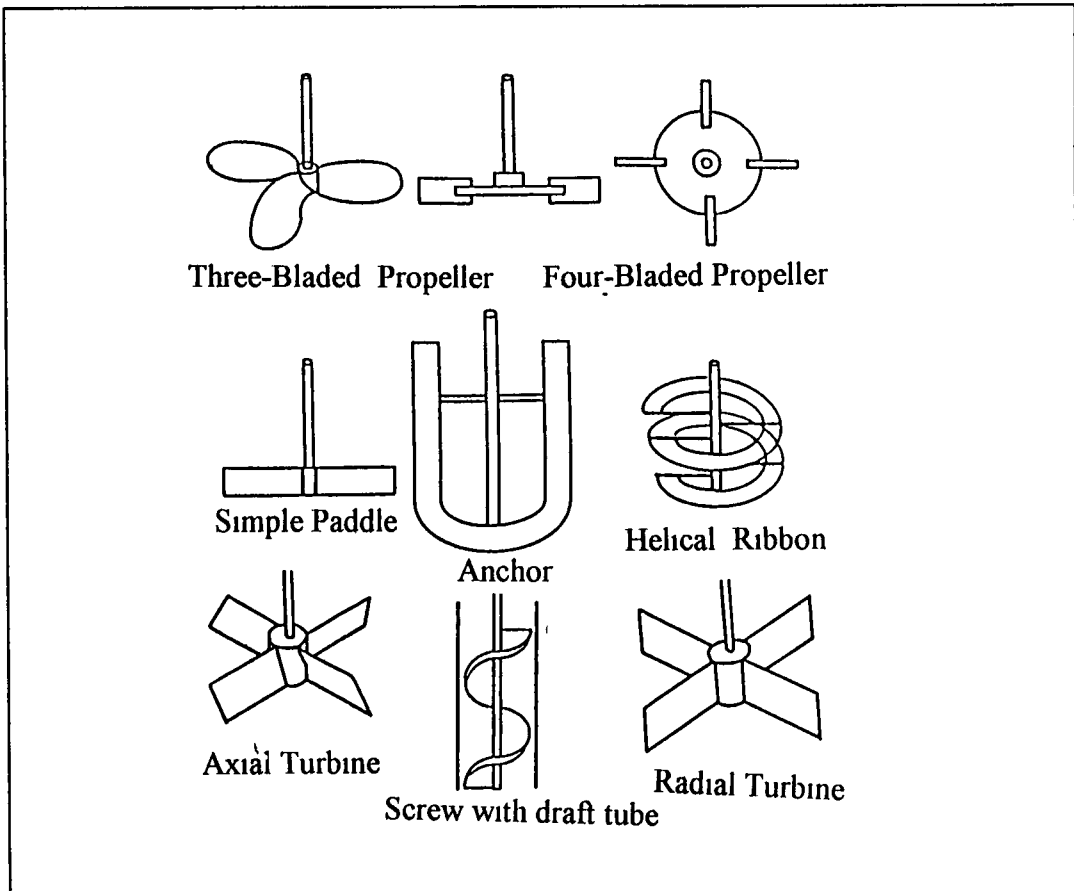


Figure 1 7 Several type of stirrer [88]

Dispersion by stirring with the help of a mechanical stirrer has become widely used after this method was introduced by Ray [86]. This external force is used to mix a non-wettable ceramic phase into a melt, and also to create a homogeneous suspension in the melt. The uniformity of particle dispersion in a melt before solidification is controlled by the dynamics of the particle movement in agitated vessels. The composite slurry may be agitated using a various types of mechanical stirrer [85] such as graphite stirrer [70], steel stirrer coated with ceramic [79], four bladed alumina spray-coated stirrer [84] or alumina stirrer. The vortex method is the most frequently used [70,73,77-80, 85] since

any stirring of a melt naturally results in a formation of a vortex. Ceramic particles are introduced through the side of a vortex which is created in the melt with a mechanical impeller at different agitation speeds such as at 100 rpm [70,68], 580 rpm [70], 600 rpm [76,80, 84], 1000 rpm [73], or 400-1500 rpm [74]. Particles have, for example, been continuously stirred after being incorporated into the melt, for 45 minutes [79], or for 15 minutes [75]. Some foundries use a slowly rotating propeller for continuous stirring.

Introducing reinforcement particles to the stirred molten matrix sometimes will entrap not only the particles but also other impurities such as metal oxide and slag, which is formed on the surface of the melt. During pouring, air envelopes may form between particles, which can alter the interface properties between particles and the melt, retarding the wettability between them. In the case where the temperature of the particles added are not at the same as the temperature of the molten slurry, the viscosity of the slurry increases very rapidly. The development of a vortex during stirring has been found to be helpful for transferring the particles into the matrix melt. In this method, the reinforcement particles are added to the top of the stirred liquid, and are drawn toward the center of the vortex. In other words, the vortices formed tend to concentrate particles added to the surface at the center of the mould. A pressure difference between the inner and outer surface of the melt sucks the particles into the liquid [74]. However, air bubbles are also sucked by the same mechanism into the liquid metal, resulting in high porosity in the cast product. However, vigorously stirred melts will also entrap gas, which is extremely difficult to remove as the viscosity of the slurry increases. Gibson et al [87] dispersed graphite powder in agitated slurry of Al-Si alloys by using a special rotor

design to prevent surface agitation of the melt and consequent air entrapment. Slag that forms on the surface of the aluminium melt will also entrap the reinforcement particle and result in slag or particle clusters that lead to poor dispersion. It is important therefore that the matrix materials be as clean as possible. An inert cover gas such as dry argon can help to prevent atmospheric contamination of the melt. It has been possible to reduce the extent of porosity by the use of vacuum [80,84]

The melt particle slurry prepared by stirring will have to be transported to a die or casting bay either by using a slurry pump or by being held in a ladle. During the holding the slurry must be stirred continuously if the holding time is long enough to allow considerable settling, leading to a non-uniform distribution of the particles in the cast components. The settling rate is a function of volume fraction of particles in the slurry [89]. The utilization of fine particles with large volume fraction will reduce the settling. If a mixture of fine and coarse particles is used in slurry, the coarse ones will settle faster than the fine particles. In a large mass of liquid, such as in the furnace or crucible, there may be thermal current flowing around the melt, which helps to keep the particles in suspension. However, if the melt is not continuously stirred, it is important to remember to stir it immediately before pouring, whether or not it was stirred while melting and holding [90]. The particle distribution or homogeneity will be maintained if their settling has been controlled.

Table 1 8 Summary of several stir casting techniques

MMC system	Processing route	Melting and Mixing	Mould	Ref
A6061 Al ₂ O ₃ p	A6061 in ingot form Preheated Al ₂ O ₃ at 799°C	Graphite Crucible Vortex, stir at 400-1500rpm for 240 sec before pouring	Steel sprayed with water	Gosh & Ray [74]
A356 SiCw	A356 in ingot form In vacuum chamber, and Whiskers incorporated via nitrogen gas	Graphite crucible Vortex, 500 – 1000 rpm	-	Giro et al [14]
A6061 Al ₂ O ₃	Preheated Al ₂ O ₃ at 799°C	Graphite crucible Vortex, 7-25 rps	Steel	Ghosh & Ray[66]
A6061 SiCp	Process in glove box filled with Argon Preheated SiC in glove box at 100 – 500°C	Concrete crucible, ceramic coated stirrer Vortex, stir at 580 rpm for 45 min	Copper	McCoy et al [79]
A356 SiCp	-	Using two graphite impellers, 600 rpm	Steel	Yamada et al [80]
A356 SiCp	A356 in ingot form SiC oxidized in air at 1100°C	Slurry reheated to 700°C before pouring	Preheated mould.	Ribes & Suery [91]]
A356 SiCp	Using Nitrogen gas to protect melt from oxidation	Graphite crucible Stirring speed 1000 rpm	Under pressure	Milhere & Suery [73]
A6061 Al ₂ O ₃ w	A6061 in ingot form Al ₂ O ₃ preheated.	Stirring at 200-400 rpm	Preheated mould and under pressure	Lee H C [68]
A356 SiCp	Preheated at 850°C for 8 hours	Alumina crucible Alumina stirrer, at 600 rpm	Graphite preheated at 838K	Wang & Ahesh [76]
A356 SiCp	-	Graphite crucible Melt at 740°C	Aluminium coated with graphite	Yarrandi et al [82]
A2024 SiCw	SiCw preheated at 554° for 1 hour	Stirr at 250 rpm	Crucible dropped in the water bath	Miwa et al [67]
A6061 SiCp	A6061 in ingot form SiC oxidized in air at 1100°C	SiC crucible, Vigorously agitated, melt reheated at 700°C before pouring	Preheated steel Casting under pressure	Miwa et al [75]
A356 SiCp	SiC oxidized in air at 1000°C, for 1 5 hours	Graphite stirrer 400 rpm, reheated to 700°C for 1 minute before pouring	Graphite preheated at 300°C	Yilmaz & Altintas [72]
A356 SiCp	SiC oxidized in air at 850°C for 8 hours	Alumina crucible Alumina stirrer, 600 rpm.	Graphite -preheated at 838K	Wang & Ajesh [84]
A5083 SiCp	SiC oxidized in air at 1100°C for 12 hours	SiC crucible, 600-640 rpm, reheated to 720°C for 5 minutes before pouring	Under pressure	Zhong et al [72]
A6061 SiCp	A6061 in ingot form Preheated SiC at 900°C	Melting under Nitrogen gas Vortex	Cast iron	Gupta & surappa [77]

p = particle, w = whiskers

Table 1 9 Recommendation from manufacturer for stir casting processes [92]

Precaution in respect of	Manufacture's recommendations	
	Duralcan, USA	COMALCO, Australia
Pre-melting	Ingot, Clean, preheated for drying Implements Clean, coated and dried.	Clean dry tools and mould All steel tools coated with chromium/alumina/zircon/boron nitride
Melting	Purge furnace with inert gas – dry argon Continue the gas flow throughout melting Do not degas or flux the melt Temperature control is mandatory if there is possible of chemical reaction	Inert gas may be used. Skim surface oxides during air melting Avoid fluxing and degassing Temperature control necessary to avoid undesirable chemical reaction
Stirring	Necessary to counter particle settling Avoid turbulence	Gentle stirring but quite at surface Induction stirring is not enough If interrupted, stir again for ten minutes at worst case
Pouring	Avoid turbulence May used ceramic foam filters or screens	Prefer bottom pouring with continued stirring May use woven fibre or preheated ceramic foam filters
Casting sprues	Reduce feeding distance by 65% of that for base alloy May required additional riser	Enlarge section sizes of gates and by 25% over that of the base alloy

After the incorporation of the particle into the melt is completed (in the case in which the stirring action was performed in semi-solid condition) the slurry need to be re-melted to a temperature above the liquidus before being poured into the mould. The re-melted temperature used varies from 700°C for one minute [69, 72,80] and 720°C for 5 minutes [72]. The composites slurry is then poured into a steel mould [69,78], copper mould [79], graphite mould [72,84] or in cast iron mould [77]. Normally the mould is preheated and has been to 300°C [72,69], 370°C [82] and 565oC [76,84]. In some cases the casting is solidified under pressure to prevent porosity [68,69,72,80]. The viscosity of the melt-particles slurry is higher than that of the base alloy, and this may offer greater

resistance to flow in the mould cavity Table 1 8 summaries stir casting processing of MMC reported in literature The table has been restricted to include aluminium-based composite only Table 1 9 shows ingot manufacturers recommendations for casting practice in metal matrix composite fabrication

1.7.2 Solidification of Metal Matrix Composites

During solidification it is important to have an understanding of particle movements and distribution, as the properties of composite are known to critically depend on the distribution of the reinforcement The solidification synthesis of cast metal-ceramic particle composites involves producing a melt of matrix material, followed by the introduction of the particles into the melt, and the final step is solidification of the melt into a certain shape, such as an ingot or a billet form The solid particles are present virtually in unchanged form, both in the liquid and the solid metal The incorporation of the reinforcement particle will immediately increase the viscosity of the matrix melt For example, if 15 volume percent of reinforcement particles is added into the fully melted matrix mixture, this means that the melt will be occupied by 15 percent of solid particle, or in the other word, the slurry is partially solidified [93]

It is established that the formation of the microstructure in cast particle reinforced composites is mainly influenced by the following phenomena particle pushing or engulfed by the solidification front, particle settling or floatation in the melt, the solidification rate of the melt, and chemical reaction between particles and the matrix

1.7.2.1 Particles Pushing or Engulfed

During solidification the reinforcement particle acts as a barrier to solute diffusion ahead of the liquid solid interface, and the growing solid phase will avoid the reinforcement in the same way that two growing dendrites avoid one another. The individual particles may be pushed by the moving solid-liquid interface into the last freezing inter-dendritic regions, or the growing cell may capture them [94]. The ceramic particles, which generally have lower thermal conductivity than that of the melt, are often surrounded by the last freezing fraction of the molten alloy during solidification of slurry. Therefore the last portion of the metal to solidify will be located close to, or at the reinforcement-matrix interface. This phenomenon has been interpreted by several researchers such as Uhlmann et al [95], in terms of particle pushing by the solidification front, or interaction of particles with a planar solidification front. They observed that for every size of particle, there is a critical velocity of solidification front, below which the particles are pushed by the front, and above which the particles are to be engulfed by the solidifying phase [95,96]. There are several prediction models of particle pushing including the Uhlman, Chalmers and Jackson's model [96] and Bolling and Cisse's model [97]. The first model is a kinetic approach to particle pushing, which assumes that a particle is pushed in front of the solid-liquid interface. Repulsion between the particles and the solid occurs when the sum of the particle-liquid and liquid-solid interfacial free energies is less than the particle-solid interfacial free energy. This model introduced critical velocities, above, which the particles should be entrapped, and below which the particles are rejected by the moving solid-liquid interface. The critical velocity is given by

$$V_c = \frac{1}{2}(n + 1)LA_oV_oD/KTR^2 \quad (2)$$

Where,

V_c = theoretical critical velocity

L = Latent heat of diffusion per unit volume

A_o = Atomic spacing liquid

V_o = Atomic volume of liquid

D = Diffusion coefficient of liquid

KT = Boltzmann factor

R = particle radius

n = is a constant approximately equal to 5.0 [95]

If the growing solid metal captures the reinforcement particles, little redistribution of the particles will occur during solidification, and hence the particle distribution in the solidified material will be as uniform as in the liquid state. On the other hand, if the particles are pushed by the solidification front, they will be redistributed, to be finally segregated in the last pool of liquid matrix to solidify. This is represented in Figure 1.8 [98]. According to Rohatgi et al [99], when the reinforcement is relatively movable within the solidifying matrix, the particles pushing effect can be important. This will effect the distribution of the particles, which are generally found between individual dendrite arms.

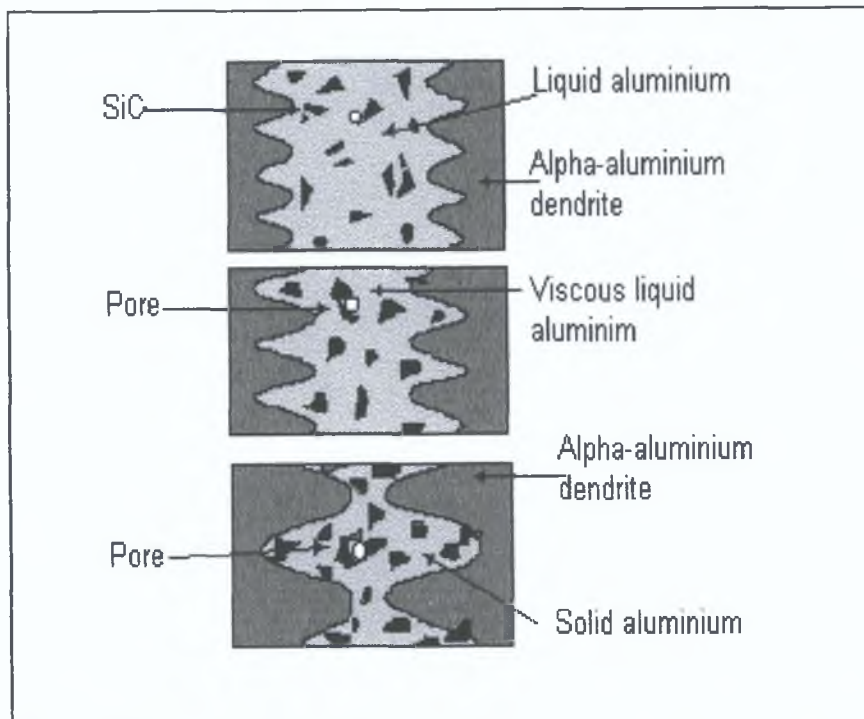


Figure 1.8: The different stages of particles pushing and pore formation in SiC reinforced composites during solidification [98].

1.7.2.2 Particle Floating or Settling

One of the main problems associated with the production of particle-reinforced composites using a conventional melt technology is that of particles settling in the melt. Particle enriched zones may be formed either because of gravity segregation of particles of different densities in the melt, during holding or during slow solidification. It becomes important to identify and control the process parameter related to this problem in order to maintain the uniform distribution of these particles in the matrix alloy. Mechanical stirring is usually used during melt preparation, and the stirring condition, melt temperature and the type, amount and nature of the particulate reinforcement are some of

the main factors to consider when investigating this phenomenon. In general, particle settling or floating may occur because of density differences. If the original distribution of particles in the melt is uniform, the theoretical prediction of settling can be made by using Stoke's Law [as stated in reference no 100], which assumes that the particles are spherical, and that no interaction occurs between particles. Stokes predicted the settling rate of particles using

$$V_p = \frac{2R_p^2(\rho_p - \rho_m)g}{9\mu} \quad (3)$$

where,

V_p = settling velocity of the particles

R_p = particle radius

ρ_p = particle density

ρ_m = matrix density

μ = viscosity of molten metal

The result of the settling experiments of Sekkar et al [101] indicate that the silicon carbide particles show a tendency to segregate in aluminium alloy as a result of settling. It was concluded that as holding time in the molten state increase, the particles settling will also be increased.

1.7.2.3 Solidification Rate of the Melt

In recent years attempts have been made to rapidly solidify composite melts to combine the advantages of a dispersed ceramic phase, and rapidly solidified structure of

the matrix. The microstructure of rapidly solidified composite has finer dendrite size, and this permits fewer reinforcement particles to be segregated in the intercellular and interdendritic boundaries, giving a more homogeneous particle distribution. Samuel et al [98] studied the effect of the solidification rate on the silicon carbide particle distribution in an A359 alloy. They found that the inter-particle distance distribution for the silicon carbide particle composites proved that finer dendrites arm spacing produces a more uniform distribution, while higher spacing leads to particle clustering. The presence of fibers influences the secondary dendrite arm coarsening process, leading to the elimination of all dendrite arms at sufficiently low cooling rate [102]. The resulting microstructure consists of a solute-poor primary phase away from the fibres, and a solute-rich primary phase with secondary phases concentrated at the fibre/matrix interface. Kang et al [103] have investigated one dimensional heat transfer during solidification of aluminium-alumina slurry and concluded that the particles are surrounded by solute rich liquid cooling at a relatively slow rate.

The grain size in a casting is determined by the nucleation rate which results in grain multiplication [104] as well as the presence of fluid flow during solidification. The nucleation rate is influenced by the cooling rate and by the presence of heterogeneous nucleation catalyst. The particulate reinforcement can influence each of these processes, and hence modify the resulting grain size in the matrix. If the reinforcement surface serves as a propitious site for heterogeneous nucleation of the matrix, a much finer grain size will result. Titanium carbide is a material that is known to act as a grain refiner in aluminium [105].

The dendrite arm spacing is fine in the case of a fast cooling rate. Due to this fine dendrite arm spacing, the number of reinforcement particles, which are accommodated at each dendrite boundary, is less as compared to the case where the dendrites are larger at slower cooling rates. The greater the dendrite arm spacing, the greater will be the segregation due to particle pushing. A rapidly solidified structure therefore has a better distribution of the reinforcement particles. According to Girod et al [14], there is an increased tendency for dendrites to form at the top of the ingot due to the settling of the solid phase. This depends on the viscosity of the slurry, and the extent of the dendrite growth increases with the lowering of the holding temperature, stirring speed and the size of the impeller.

The cooling curve of the A356 alloy is shown in Figure 1.9 [106]. The liquidus and solidus temperature are 615°C and 543°C respectively. Backerud et al [107] determined the solidification curve of A357 alloy, which is similar to the A356 in the study of Jeng et al [106]. The liquidus temperature determined by Backerud et al was 615°C and was in agreement with the result of Jeng et al. The principle characteristics of the solidification curves determined for the A356 and A357 alloy were similar. The solidification rate was relatively constant in the beginning, and a sharp increase of the solidification rate occurred at 570°C, and the rate decreased again toward the end of solidification. The cooling curves and the solidification curves of the A356 alloy and its composites are similar, as shown in Figure 1.9. However an approximately ~10°C deviation of the liquidus temperature has been found.

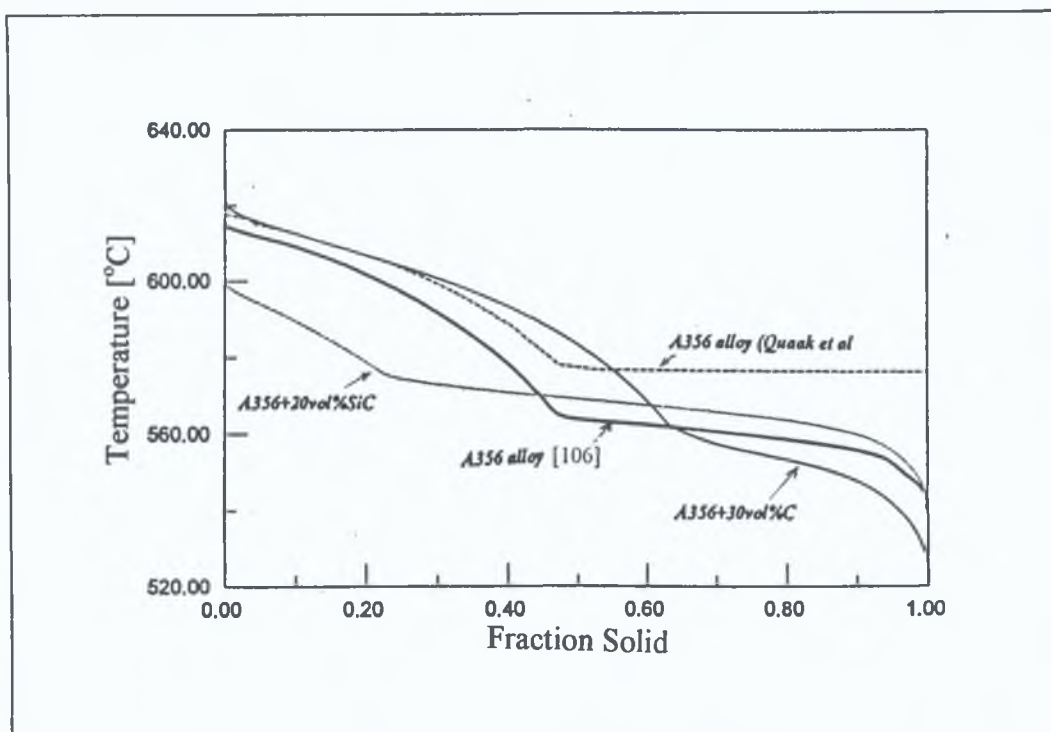


Figure 1.9: Solidification curve of A356 alloy and its composite [106].

Table 1.10: The liquidus and solidus temperatures for some Al-Si alloys and composites [106].

Alloy/composites	Liquidus Temperature [°C]	Solidus Temperature [°C]
Al-10wt Si	584	-
A356	615	534
A356+30vol.%SiC	622	525
A356+20vol.% SiC	605	548

Kaufmann et al [108] made a comparison between the cooling curve of the A356 alloy and its composite which was reinforced by 15 vol. % SiC. The liquidus temperature of the composite was 5.5°C higher than that of un-reinforced A356. The addition of ceramic

particles in the molten metal introduces more nucleation sites, and reduces the effect of under-cooling. Thus the determined of liquidus temperature in the composites could be higher. This is as shown in Table 1.10 [106].

1.7.2.4 Viscosity and Casting Fluidity of the Slurry

Slurry of molten metal-alloy containing particles has more resistance to flow than the melt alone. Molten metals or alloys generally behave as Newtonian fluids: the shear stress, τ , required to initiate and maintain laminar flow is linearly proportional to the velocity gradient or shear rate, γ . The coefficient of viscosity, η , characterizing the resistance to flow is constant [109]. This relationship can be shown as:

$$\eta = \tau/\gamma = \text{Constant} \tag{4}$$

Melt-particle slurries generally behave differently and the shear stress is not linearly proportional to the strain rate. The ratio of shear stress to strain rate is termed apparent viscosity, η_a ,

$$\eta_a = \tau/\gamma = k(\gamma)^m \tag{5}$$

where ,

k and m are constant.

The viscosity reduces as the shear rate caused by stirring increases as shown in Figure 1.10. At higher shear rates, the clusters of particle are broken reducing the resistance to

flow. Also the apparent viscosity increases with the volume fraction of particles in slurry. Higher viscosity helps to enhance the stability of the slurry by reducing the settling velocity, but also create resistance to flow in mould channels during casting [110]

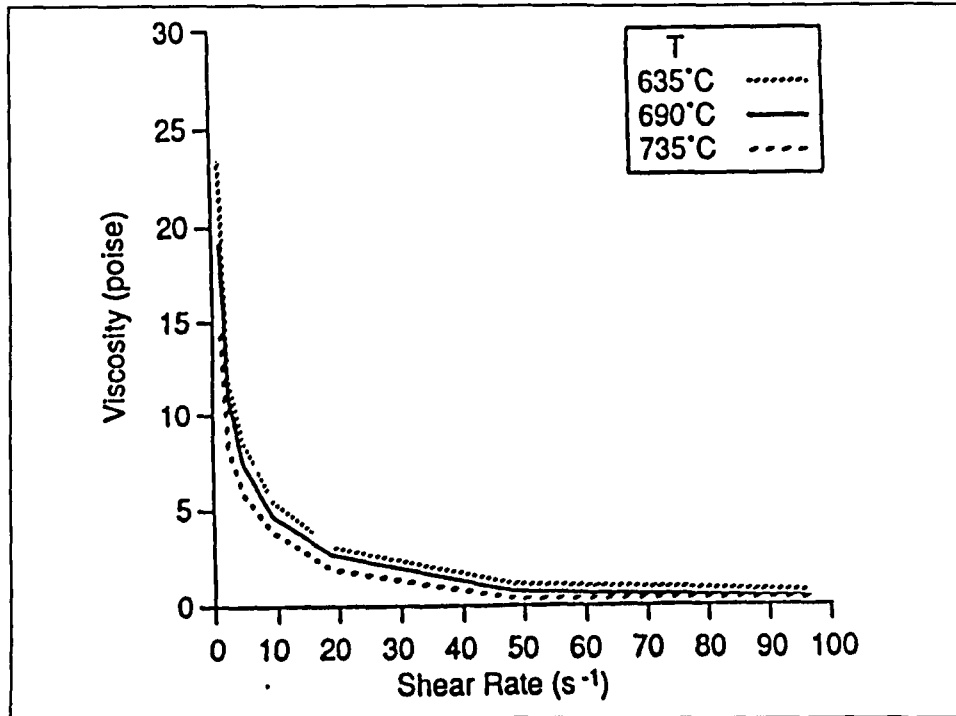


Figure 1 10 Influence of shear rate on the viscosity of A356-SiC composite [135]

The strong shear thinning behaviour of the semisolid slurries in steady state conditions is attributed to compete agglomeration processes of the primary phase globules. Strong agglomeration at low shear rates produces a large amount of entrapped liquid and, as a consequence, an increase in the effective fraction of solid, resulting in a high viscosity. At higher shear rates the bond between primary phase globules are broken by shearing forces and a lower viscosity is found. The viscosity increases with the volume fraction of the reinforcement, and with a decrease in the particle size. The apparent viscosity's of the

composite slurry will furthermore decrease with increasing shear rate over a wide range of shear rate, corresponding to non-Newtonian pseudoplastic behaviour

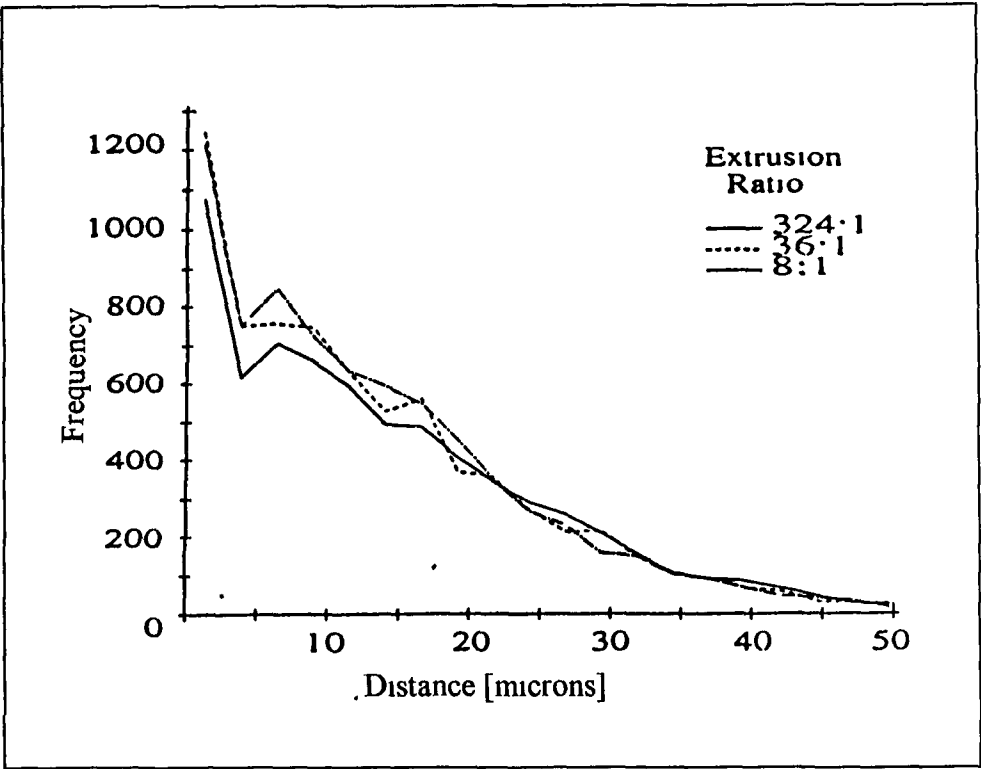


Figure 1.11 The effect of extrusion ratio on the particle distribution [8]

1.7.3 Post Solidification Processing

The composite can be used in the as-cast condition, for shape casting applications, or the ingot can be secondary processed by techniques including hot extrusion or rolling. This secondary processing will modify the particle distribution. According to Lloyd et al, [152] secondary fabrication processes, such as extrusion, can modify the particle distribution but complete declustering cannot be achieved even at the highest extrusion ratio. Figure 1.11 shows the effect of extrusion ratio on the particle distribution [8]. It

shows that extrusion rapidly homogenize the distribution at quite low extrusion ratios, and the particle distribution does not change significantly with greater degree of extrusion. However secondary processing may change the particle distribution by cracking the particle [153]. Use of an appropriate reinforcement particle size range, and correct fabrication practice minimises particle fracture.

1.8 PROBLEMS IN STIR CASTING

In preparing metal matrix composites by stir casting, there are several factors that need consideration including

- i The difficulty of achieving a uniform distribution of reinforcement material
- ii The poor wettability between the two main substances
- iii The propensity for porosity in the cast metal matrix composite
- iv Chemical reaction between reinforcement material and matrix alloy

In order to achieve the optimum properties of the metal matrix composite, the distribution of the reinforcement materials in the matrix alloy must be uniform, and the wettability of bonding between these two substances should be optimized. The chemical reaction between reinforcement materials and the matrix alloy and porosity must be avoided or minimised. The high Al-SiC interface bonding strength is the main reason for the composite relatively high specific mechanical properties. A sufficient bond is achieved only when good wetting of the reinforcement by the matrix is obtained, and this is dependent on the surface properties of the two phases [111]. It is believed that a strong

interface permits transfer and distribution of load from the matrix to the reinforcement, resulting in an increase in elastic modulus and strength [75] Fracture in discontinuously reinforced composites can result mainly from de-bonding of particles from the matrix [112]

1.8.1 PARTICLE DISTRIBUTION

The distribution of the particle reinforcement in the matrix alloy is significantly influence by three main stages the melt stage, solidification and post-solidification process Melt and solidification stages are inter-related and need to be continuously controlled Post-solidification process could help to homogenize the distribution of the particles in the final product

Particle distribution in the matrix material during the melt stage of the casting process mainly depends on the viscosity of the slurry, the extend to which particles are successfully incorporated in the melt, and the characteristics of the reinforcement particles The characteristics of the reinforcement particles influence settling rate, and the effectiveness of mixing in breaking up agglomerates, minimising gas entrapment and attaining distribution of the particles

Casting of particle reinforced metal matrix composites generally occurs in the semi solid state as it is advantageous compared with conventional casting where the alloy is completely melted This is because when the composite slurry is in the temperature

range where the matrix itself is partly solid as in compocasting, little or no gravity-induced segregation of the ceramic reinforcement occurs, even if the slurry is at rest [113] This occurs as the solid matrix phase has about the same density as the liquid metal, so it neither settles nor floats in the slurry, and holds the reinforcement in place

1.8.1.1 Particle Incorporation

In general there are two types of barrier to particle incorporation into a liquid melt. These are mechanical barriers such as a surface oxide film, and thermodynamic barriers, which are usually referred to in terms of wettability. Mechanical barriers can be reduced by good foundry practice, but overcoming thermodynamic barriers is more difficult. Generally ceramic reinforcements used in MMCs are non-wettable by the metallic melt, requiring an external driving force to overcome the surface energy barriers. This force is provided by stirring the melt with a mechanical stirrer or using electromagnetic stirring. It has been shown that alloy chemistry, temperature of particle addition and stirring rate are some of the parameters controlling wetting of the reinforcement by the melt [120]. Once the particles are transferred into the liquid and the energy barrier is overcome, the surface energy or surface forces will not change with position inside the melt. The dynamics of particles in the melt will be governed by other forces including gravity, buoyancy or by stirring action. However, two problems complicate the incorporation process: (i) particle agglomerates must be broken up before complete dispersion and wetting can occur, and (ii) it is energetically conducive for the particles to become attached to gas bubbles.

During particle addition, there is some local solidification of the melt induced by the particles, and the entire matrix melt temperature can fall below the solidus, depending on the temperature of the particles. It was also found that the perturbation in the solute field due to the presence of particles can change the dendrite tip radius, and the dendrite tip temperature [121]. These effects give rise to a dendrite-to cell transition as the density of particles is increased. Also the length of the dendrite is reduced in the presence of the particles.

The method of particle introduction to the matrix melt is a very important aspect of the casting process. There are a number of techniques [99,122] for introducing and mixing the particles. However, some of these methods have several disadvantages. Gas injection of particles for example will introduce a quantity of gas into the melt, some methods are not very effective in dispersing the particles and some, such as the ultrasonic technique are very expensive, and are difficult to scale to production level. Whereas, by using centrifugal action, the distribution of the particles varies from the inner to outer part of a billet because of the differences in centrifugal force [123].

1.8.1.2 Particle Characteristics

One major processing problem is that particles either sink or float, depending on the particle-to-liquid density ratio. In foundry operations, segregation of the particles may occur between the time stirring has stopped, and the melt has solidified. Clustering of the particles is a contributory problem, making the particles settle more quickly. Therefore,

the particles may be unevenly distributed macroscopically (denuded region due to settling) and microscopically (clusters of particles) [56,119] Particle enriched zones may form either as a consequence of gravity segregation of particles in melts during holding, or during slow solidification or as a consequence of selective segregation under the action of centrifugal acceleration in centrifugal casting [124] In foundry operations, where composite ingots are re-melted for product casting, there may be problems of clustering if the melt is not intensively stirred

At sufficiently long holding times, top parts of the casting are completely denuded of particles, which settle to the lower parts of the casting, as a function of time [46,59,125] Therefore the melt must be re-stirred prior to casting if long holding times in the molten state are used According to Geiger et al [126] the settling rate will also be a function of the particle density and size, with particle shape and size possibly playing a role [46] At high volume fractions, particles interact with each other and settling is hindered [127] Hindered settling for spherical particles has been modelled by Richardson and Zaki [128] with the particle velocity, V_c is given by $V_c = V_o(1-f)^n$ where, V_o is the Stokes's velocity, f is the volume fraction of particles, and n is a factor dependent on the Reynolds number, the particle diameter and the container diameter, and which increases with increasing particle diameter The studies on the settling indicate that the finer the dispersions and the higher their volume fraction, the slower the rate of settling Hanumanth et al [129] using an average particles size of 90 μ m found a slurry of 0.2 volume fraction of SiC particles settled completely in about 300 seconds resulting in loosely packed particles at the bottom of an aluminium alloy matrix At lower volume

fraction of particles the settling time is less. So, it is apparent that slurry with large size particles will have to be stirred all the time until casting. In practice the situation is complicated by the fact that there is a range of particle shapes and sizes. As large, irregular particles sink, the liquid they displace can influence the settling rate of other particles [130]. Settling is not a concern during initial mixing because of the turbulence in the mixer, but it is important in any subsequent molten metal transfer. Thomas [131] studied the state of dispersion of particles in slurry under dynamic conditions of flow, and in this context it was found that the particle shape and size are the most important parameters. The flow behaviour of the slurries has been summarised as follows:

- i Particles below 10 μm size are almost always carried fully suspended in the liquid, and gravitational effects are negligible.
- ii Gravitational effect is not negligible for particles in the size range of 10 μm to 100 μm , and a particle concentration gradient will develop.
- iii Particles ranging from 100 to 1000 μm in size, are fully suspended at high velocities and often deposit at the bottom of the channel at lower flow velocities.

According to Ray [132], when the flow velocity is above a critical value for a given size of particle, the suspension will remain homogeneous during flow. If the flow velocity is reduced below the critical value, the suspension becomes inhomogeneous. If the flow velocity is further reduced, the particles will sediment at the bottom of the channel and move by tumbling over each other.

1.8.1.3 Mixing

It is essential to produce as uniform a distribution as possible without any gas entrapment, since any gas bubbles will attach to reinforcement particles leading to poor bonding with the matrix. Excessive gases content can result from over agitated melts, which lead to unacceptable porosity content in the ingot. Even in inert gas or vacuum operated processes, top melt surface agitation is known to cause problems.

Stirring is a complex phenomenon, and it can be a problem to control the process such that a uniform distribution of particles is achieved. Mechanical stirring being usually used during melt preparation or holding, the stirring condition, melt temperature, and the type, amount and nature of the particles are some of the main factors to consider when investigating this phenomenon [133, 134]. Settling and segregation are both to be avoided. In creating a homogeneous distribution of particles in a molten alloy, the high shear rate caused by stirring the slurry should result in a fairly uniform particle distribution in the radial direction, and also prevent particles from settling. Secondary flow in the axial direction results in transfer of momentum from high to low momentum regions and causes lifting of particles. To correlate particle lifting with flow parameters, one defines a Particle Dispersion Number (PDN) as the ratio of the axial velocity of secondary flow to the terminal settling velocity. If PDN is greater than one, the settling velocity is smaller than the axial velocity of the secondary flow, and the particles will be carried to the top of the melt. On the other hand if PDN is smaller than one, the particles will remain at the bottom. For homogeneous dispersion PDN should be greater than four.

[135] To correlate particle lifting with flow parameters, one defines a Particle Dispersion Number (PDN) as the ratio of the axial velocity of secondary flow to the terminal settling velocity. If PDN is greater than one, the settling velocity is smaller than the axial velocity of the secondary flow, and the particles will be carried to the top of the melt. On the other hand, if PDN is smaller than one, the particles will remain at the bottom. For homogeneous dispersion, PDN should be greater than four [135]. PDN is given by

$$PDN = \frac{H_o (\mu \Omega)^{1/2}}{r_i^{1/4} d^{3/4} V_t} \quad (6)$$

where H_o is the height of the melt, Ω the angular velocity of the stirrer, r_i the radius of the inner cylinder, d the gap between the inner and outer cylinder, V_t the particles settling velocity and μ the viscosity of the slurry.

It is generally accepted that the liquid movement around the particles creates a shear rate, which helps to 'wash' the particle surfaces of detrimental oxides or other contaminants. This washing action constantly refreshes the liquid presented to the particle.

1.8.1.4 Solidification

There are essentially three mechanisms, which will affect particle redistribution during solidification processing. These are agglomeration, sedimentation and particle engulfment or rejection (pushing) ahead of the solidification front. The prevalence of one or more of these mechanisms is dependent upon elements of the processing technique as

well as the physical and chemical properties of the particle and the matrix [136] The distribution of particles in the resulting solid may or may not follow the distribution in the liquid The actual distribution of particles that one obtains in the solidified material will largely depend upon the morphology of the interface that is present under given experimental conditions When the particles are trapped by a plane front or cells, the distribution remains similar to that present in the liquid prior to solidification On the other hand, when a dendritic structure is present during solidification, then the solidification of particles in the solid can be significantly different from that in the liquid The trapping of particles between dendrites usually occurs just behind the tip, within the first ten secondary branches These secondary branches close to the dendrite tip have smaller branches The particles which are trapped between these branches, as close to the tip will remain between these branches as the dendrites grows The particles that have been trapped a few branches behind the tip may appear to be trapped at the base of the dendrite in metallic systems [121]

The result of extensive particle redistribution during processing can be to create large particles-free regions in a casting, large particles agglomerates and cluster, interdendritic distribution of the reinforcement In order to generate uniform stress distributions during service, a homogeneous distribution of the reinforcement phase is desirable and it is suggested that this is achieved by minimising holding and casting times, thus avoiding extensive settling, and by stimulating particle engulfment into the primary matrix grain or dendrites during freezing

During solidification of a liquid containing dispersed second phase particles, the particles in the liquid melt can migrate towards, or away from the freezing front. It has been found that those small particles are entrapped between the secondary arms, while comparatively large particles are entrapped between primary dendritic arms [138,139]. When the composite slurry is poured into a cold mould, the temperature of the melt drops rapidly at the mould boundary. Thus dendrites appear on the mould boundaries first and push the particles in a direction opposite to heat transfer as the temperature in the mould decreases. According to Xiao et al [137], in MMC castings there is a boundary layer over which (due to friction at the boundaries and the growing mechanism of dendrites), only few particles are entrapped. This results in a lower volume fraction of particles near the boundaries.

It is now well established that depending on the interfacial energies, a growing crystal can either engulf or reject particles [99,134,140]. Engulfment of the reinforcement means that not only the particles unlikely to be associated with brittle inter-metallic phases and other particles in the inter-dendritic and inter-granular regions, but the fact that engulfment occurs suggests that reinforcement wetting has taken place, and that the interfacial bonding between the particles and the matrix must be good. Two mechanisms have been suggested for particle pushing from fluid flow [141,142]. In the first mechanism, the particle is in contact with the solid and it is moved over the surface by the fluid flow as the solid grows. Whereas in the second mechanism, the particle which is located near the solidification front becomes trapped because of the roughness of the solidification front. When the particle is rejected by the growing crystals and pushed

ahead of the advancing interface, a viscous force is generated and this tends to prevent the pushing of the particle. Hence, it is the balance of these counteracting forces which decides the rejection or engulfment of the particle. It is parameters such as relative density difference, relative difference in thermal conductivity and heat diffusivity between the particle and the metallic melt, and alloy composition will affect the shape of the solidification front and determine the magnitude of these forces [99,140]. Particle pushing suggests that the solid metal has no affinity for the reinforcement and that the interfacial bonding is weak. Strong interfacial bonding is essential for effective load transfer from the matrix to the particle and for delaying the onset of particle-matrix decohesion, both of which have a profound effect on the strength and stiffness of the composite.

Solidification rate will influence the size of dendrite arm spacing. At high cooling rates where the dendrite arm spacing is smaller than the particle size, particles become virtually immobile and no solidification induced segregation results. Therefore finer DASs either close to, or even greater than, the average particle size will produce a more uniform distribution of the particles in the matrix. Increasing the dendrite arm spacing leads to particle clustering, and clustering increases with increases in particle content. However according to Jin and Lloyd [144], the reinforcement does not normally nucleate Al dendrites, and does not affect the as-cast grain size.

Engulfment and nucleation both require that a low particle-solid interfacial energy be present, just as particle incorporation requires a low particles-liquid interfacial energy.

This is usually achieved through the solid and particles sharing the same crystal structure and lattice parameter. Ceramic material known to act as grain refiner such as TiB_2 and TiC , are likely to be engulfed within the metal grain rather than be pushed to the boundaries. It is also established that a finer grain size will give better mechanical properties. In this context Kennedy et al [145] incorporated particles of TiB_2 , TiC and B_4C into aluminium alloy melt. This was done without the use of external mechanical agitation. A wetting agent which produce K-AL-F based slag in the melt surface was also added.

A variety of casting techniques have been used to cast molten alloys containing suspended ceramic particles. The choice of casting technique and configuration of mould are important. A sand mould was used [146] to cast aluminium-containing particles Al_2O_3 , SiC and glass, and some settling of coarse particles was observed. This is because of the slow cooling rate allowed by the sand mould. It was suggested that a metal chips could be introduced in the sand mould to enhanced the solidification and reduce the floating or settling tendency of the particles [147]. Aluminium based composites have also been cast by Deonath et al [148], demonstrating good distribution of particles as a result of reasonably rapid freezing. While in centrifugally cast aluminium-graphite [149], lighter graphite particles segregated to the inner periphery of the casting, and similar results have been reported for porous alumina [150], and mica [151], dispersed in aluminium alloys. However, during centrifugal casting of aluminium alloy containing zircon particles, the heavier zircon particles segregate near the outer periphery of the hollow casting.

1.8.2 WETTABILITY

Casting of metal matrix composites is an attractive processing method since it is relatively inexpensive and offers a wide selection of materials and processing conditions. Good wetting of the reinforcement particle is an essential condition for the generation of a satisfactory bond between a solid ceramic phase and a liquid metal matrix during casting of composite [154]. In spite of the importance of wettability in the manufacture of composites, relatively few quantitative studies have been conducted, and many fundamental questions remain unanswered. Many of the problems encountered in the fabrication of aluminum-ceramic composites are consequences of the characteristic of the interface wettability between ceramic reinforcement and matrix material.

The mechanical properties of metal matrix composites are controlled to a large extent by the structure and properties of the reinforcement-metal interface [155-158]. It is believed that a strong interface permits transfer and distribution of load from the matrix to the reinforcement, resulting in an increased elastic modulus and strength. From metallurgical consideration the desired interfacial region in a composite relies on several factors [227]

- 1 An intimate contact between the reinforcement and the matrix to
 established satisfactory wetting of the reinforcement by the matrix

- 11 A very low rate of chemical reaction at the interface and no or little inter-
 diffusion between the component phases so that the reinforcement is not
 degraded

1.8.2.1 Definition

Wettability can be defined as the ability of a liquid to spread on a solid surface. Wettability also describes the extent of interface contact between the liquid and the solid. Consider a drop of liquid resting on a solid substrate as shown in Figure 1.13. The contact angle at equilibrium is determined by equation (7), often referred to as Young-Dupre equation [205]

$$\gamma_{sv} = \gamma_{sl} + \gamma_{lv} \cos \theta \quad (7)$$

where, γ_{sv} = the specific energy of the solid-vapor interface, γ_{sl} = the specific energy of the liquid-solid interface, γ_{lv} = the specific energy of liquid-vapour interface. The three forces are the specific energies of surface tension, i.e. energy per unit area. When a liquid drop is put on a solid substrate, it will replace a portion of the solid-vapour interface by a liquid-solid and a liquid-vapour interface. The spreading of liquid will occur only if this results in a decrease in the free energy of the system. The work of adhesion, W_a , i.e. the bonding force between the liquid and the solid phase is defined in reference [205] as

$$W_a = \gamma_{lv} + \gamma_{sv} - \gamma_{sl} \quad (8)$$

Combining equation (7) and (8) gives

$$W_a = \gamma_{lv} (1 + \cos \theta) \quad (9)$$

The bonding force between the liquid and solid phase can be expressed in terms of the contact angle and surface tension of the liquid as shown in equation (8). The magnitude of the contact angle will describe the wettability,

- i $\theta = 0$, for perfect wetting
- ii $\theta = 180$, no wetting, and for
- iii $0 < \theta < 180$, there will be partially wetting

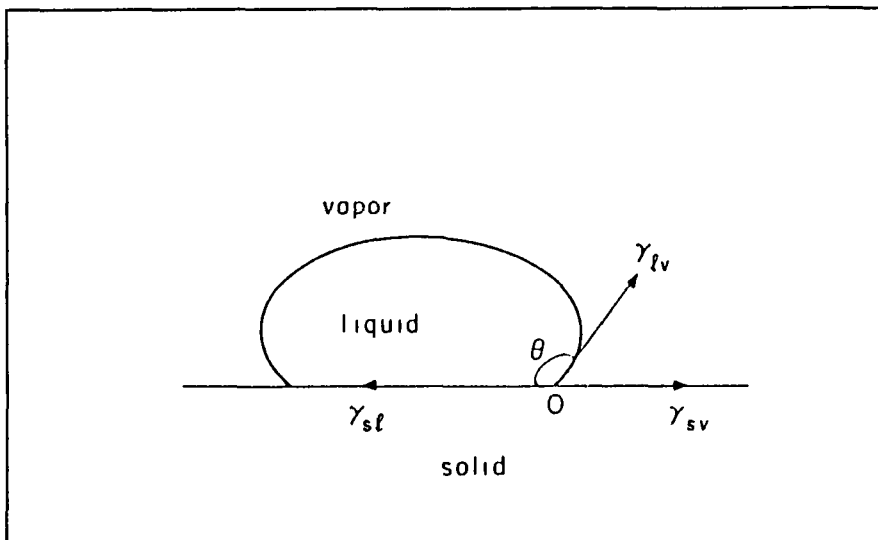


Figure 1 13 Sessile-drop test for contact angle measurement [154]

This means that a low contact angle will give good wettability. A liquid is said to wet a solid surface when $\cos \theta > 0$, i.e. when $\gamma_{sv} > \gamma_{sl}$. According to Dettlanch et al [161], in a vacuum, the driving force for wetting is affected by only two factors: the surface tension of the liquid and the strength of the solid-liquid interaction at the interface.

Usually wetting properties are measured by the Sessile Drop method, which is based on the measurement of the work of adhesion. Generally the sessile Drop technique

is used in the 400–2000°C temperature range [160,162-163] This technique involves the placing of a liquid drop of metal on a solid substrate

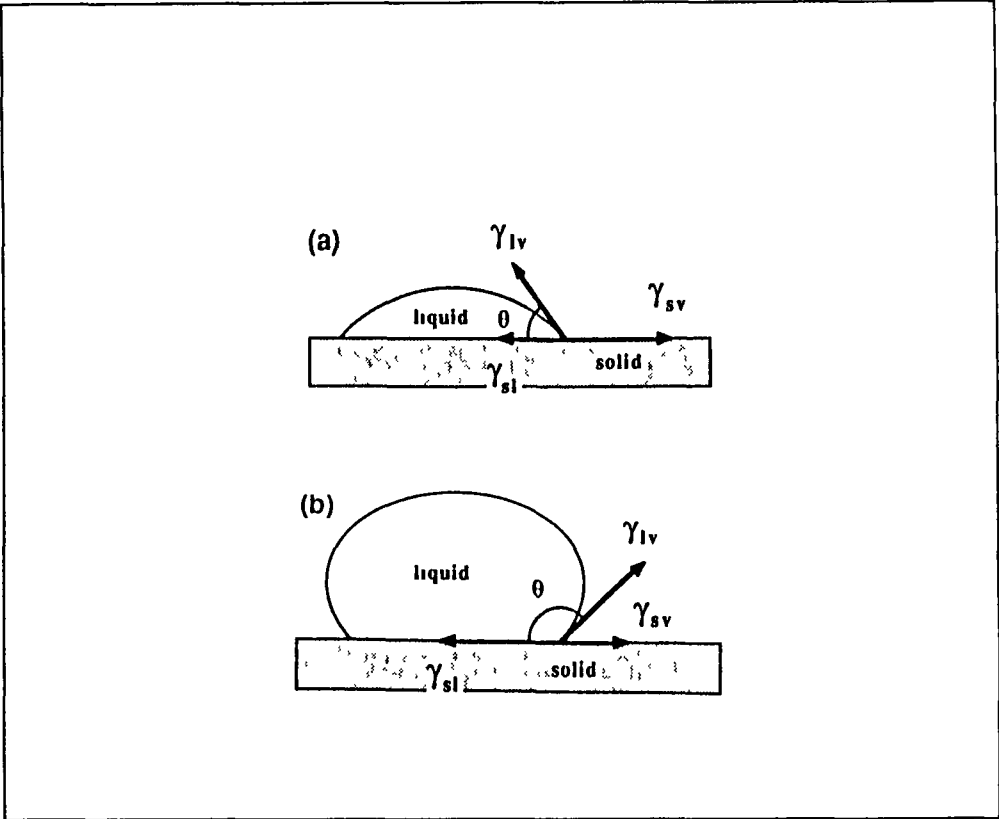


Figure 1 14 (a) Wetting and (b) non-wetting systems [160]

For the measurement of the dihedral angles, the system is rapidly cooled in order to freeze the equilibrium shapes. In measuring the contact angle θ , great care must be exerted to control several important parameters. These measurements require very precise control of experimental condition including the composition of the solid (particularly its surface), the melt, and the surrounding atmosphere. The chemical purity of all phases present must be tightly controlled. The composition and pressure of the vapor phase can exert a significant influence on θ as can deviations of the substrate geometry from a

plane, Also, oxide formation at the metal drop surface prevents proper contact between metal and substrate. Such control is often difficult to achieve and the literature contains many contradictions and inaccuracies attributable to error in experimental conditions.

Figure 1.14 shows wetting and non-wetting systems. The wetting or contact angle of various phases by liquid aluminium in a Sessile Drop test is summarised in Table 1.11. It shows that, in general, the value of contact angle decreases with the increase in aluminium liquid temperature, or in other words, the wettability is improved at a higher temperature, normally above 900°C.

1.8.2.2 Factors Which Retard Wettability

Generally the presence of oxides films on the melt surface or, adsorbed contaminants on the ceramic substrate, lead to non-wetting by molten alloys on reinforcement particles. This oxide layer also creates a resistance to reinforcement particles penetrating into the molten matrix, especially when the particles are added from the top of a cast. It is well known that aluminum has high oxygen affinity, and therefore, oxide formation in aluminum based systems is difficult to avoid without special treatment. For example at 400°C, a 50 nm thick layer is formed on aluminium alloy in 4 hours [174]. To ensure good wetting the contamination or formation of aluminium oxides on the surface of the ceramic should be minimized during the fabrication of a composite [160].

Table 1 11 Contact angles of aluminium liquid with ceramic

Ceramic Phase	Temperature [C°]	Angle [°] [o]	Vacuum [Torr]	Reference
SiC	900	150	2.7×10^{-4}	167
	1100	34	1.5×10^{-5}	168
	1100	42	2.7×10^{-4}	169
B ₄ C	900	135	$10^{-5} \times 10^{-6}$	170
	1100	120	$10^{-5} \times 10^{-6}$	170
	1100	119	1.5×10^{-4}	171
Al ₂ O ₃	900	90	2.6×10^{-5}	171
	900	120	10^{-5}	172
	1100	70	2.6×10^{-5}	171
	1100	80	10^{-4}	172
	1100	83	10^{-5}	173

Generally, it has been observed that the particle surface is normally covered with a gas layer. This prevents molten matrix coming into contact with the surface of the particle. In addition, when the particle concentration in the melt reaches a critical level, these gas layers can form a bridge, leading to total rejection of particles from the melt [175]. Hence it is essential that these gasses from the surface of the particles be dried off prior to composite synthesis. Zhao et al [176] have also proposed that the gas layer surrounding the particles might be the main reason for poor wettability. Therefore it is necessary to break the gas layers in order to achieve good wettability. When the gas layers are broken and the particles are wetted the particles will tend to sink to the bottom, rather than float to the surface.

Properties of the particle surface also affect wettability. The wetting of SiC by metals is often hindered by the presence of a layer of silicon oxide on the solid surface. As a result, a sharp transition from non-wetting to wetting is observed at a certain threshold temperature [177]. This transition temperature is determined by the kinetics of diffusion of the metal through the oxide layer. Wetting is not usually observed at below 900°C and this is also agreed with the data from Table 1.11. For example, the contact angle for Al-SiC system decreases significantly from 150° to 34° when the temperature of the melt is raised to 1100°C [168]. Eustathopoulos et al [166] showed that this phenomenon is due to the presence of the aluminium oxide layer preventing the direct contact of aluminium and carbon.

The attainment of complete wetting becomes more difficult to achieve as particle size decreases. This is due to the increase of surface energy required for the metal surface to deform to a small radius as the particles begin to penetrate through it. The smaller particles are also more difficult to disperse because of their inherently greater surface area. These finely divided powders show an increasing tendency to agglomerate or clump together as particle size decreases.

1.8.2.3 Methods Used to Promote Wettability

Several approaches have been taken to promote wetting of reinforcement particles with a molten matrix alloy, including [160, 178, 179]

- i Addition of alloying elements to the molten matrix alloy,
- ii Coating of the particles, and

The basic principles involved in improving wetting are increasing the surface energy of the solid, decreasing the surface tension of the liquid matrix alloy, and, decreasing the solid-liquid interfacial energy at the particle-matrix interface [180, 181]

Addition of an Alloying Element

The composites produced by liquid metallurgy techniques generally show excellent bonding between ceramic and molten matrix when reactive elements are added to induce wettability [89]. For example, the addition of magnesium, calcium, titanium, or zirconium to the melt may promote wetting by reducing the surface tension of the melt, decreasing the solid-liquid interfacial energy of the melt, or reducing wettability by chemical reaction.

It has been found that for aluminium based composites, magnesium has a greater effect in incorporating reinforcement particles in the melt, and improving their distribution, than other elements tested including cerium [181,182], lanthanum, zirconium and titanium [182], bismuth, lead, zinc, and copper [183]. The addition of magnesium to molten aluminium has been found to be successful in promoting wetting of alumina [89,184], and indeed it is thought that magnesium is suitable in aluminium with most reinforcements [185,186].

Magnesium is a powerful surfactant. The addition of magnesium to an aluminium melt improves wetting because of the lower surface tension of magnesium (0.599 Nm^{-1}) compared to that of pure aluminium (0.760 Nm^{-1}) or aluminium-11.8 wt % Si (0.817 Nm^{-1}) [187]. The addition of 3 wt % magnesium to aluminium reduces its surface tension from 0.760 to 0.620 Nm^{-1} at 720°C [189]. The reduction is very sharp for the initial 1 wt % magnesium addition. For example, with 1 wt % magnesium, the surface tension of an aluminium alloy has been found to drop from 860 dyn cm^{-1} to 650 dyn cm^{-1} [190]. In the work of Sukumaran et al [188] they concluded that the addition of magnesium is necessary during the synthesis of A356-SiC particle composites by a stir casting route, and found the optimum addition of magnesium for obtaining the best distribution and maximum mechanical properties to be around 1 wt %. The addition of magnesium lower than the optimum value results in the formation of agglomerates of reinforcement particles and their non-uniform dispersion in the melt.

Magnesium can also reduce the solid-liquid interfacial energy by aiding the reaction at the surface of the reinforcement particles and forming a new compound at the interface. Very small quantities of reactive elements may be quite effective in improving wetting since they can segregate either to the melt surface or at the melt-particle interface (simultaneously reducing the reactive element content in the matrix). Levi et al [185] found that the bonding of the reinforcement can be achieved by alloying aluminium with an element which can interact chemically with the reinforcement to produce a new phase at the interface which is readily wetted [186]. In the case of an Al-Mg alloy based

composite, they suggest that bonding was achieved through the formation of a MgAl_2O_4 layer, by reaction between the reinforcement and the magnesium in the aluminium melt

Magnesium is also a powerful scavenger of oxygen, it reacts with the oxygen present on the surface of particles, thinning the gas layer, and thus improving wetting and reducing the agglomeration tendency. Composite which is prepared by the liquid metal processing technique with 80-100 μm size silicon carbide particle in A356 alloy matrix showed that the addition of magnesium helped in thinning the gas layer which is present over the silicon carbide particles [187]

It can be concluded that the presence of magnesium in an aluminium alloy matrix during composite fabrication, not only strengthens the matrix but also scavenges the oxygen from the surface of the particle, leading to an increase in the surface energy of the particles. However, caution must be exercised in adding magnesium because the presence of excess magnesium in an aluminium melt will alter the microstructure of the matrix alloy by forming low-melting constituents, which deteriorate mechanical properties. The addition of 3 wt % magnesium to A356 alloy for example leads to a formation of a Mg_5Al_8 phase, having a low melting point of 450°C [188]. In addition, Korolkov [187] has warned that the addition of magnesium to molten aluminium will reduce its casting fluidity.

Particle Treatment

Heat treatment of particles before dispersion in the melt aids their transfer by causing desorption of adsorbed gasses from the particle surface. Agarwala and Dixit [191] observed the importance of preheating in the incorporation of graphite particles in aluminium alloy. There was no retention when the graphite particles were not preheated, whereas the particles were retained when preheated. Heating silicon carbide particles to 900°C assists in removing surface impurities, desorption of gasses, and alters the surface composition due to the formation of the oxide layer on the surface [192]. The ability of an oxide layer to improve the wettability of SiC particles by alloy melt has previously been suggested by other investigators [193,194]. The addition of preheated alumina particles in Al-Mg melt has been found to improve the wetting of alumina [195, 196].

A clean surface provides a better opportunity for melt-particle interaction, and thus enhances wetting. Ultrasonic techniques, various etching techniques and heating in suitable atmosphere could be used to clean the particle surface [160]. The silica layer grown naturally or artificially on the surface of SiC particles used in aluminium based matrix composites which is achieved through particle treatment, and has two functions: protection of the SiC from aluminium attack to form Al_4C_3 , and improvement of wettability of SiC by aluminium which results from the reaction between aluminium and SiO_2 [163].

Particle Coating

In general, the surfaces of some non-metallic particles are difficult to wet by metallic metal. Wetting has been achieved by coating the particles with a wettable metal. This is because liquid metals almost always-wet solid metals, and the wettability is the highest in the case of mutual solubility or formation of intermetallic compounds. Infiltration is thus made easier by desorption of a metallic coating on the surface of the reinforcing solid [161]. Nickel and copper are wet well by many alloys, and these metal have been used as a coating material. However, nickel is the most frequently used metal for coating reinforcement particles which are normally used for aluminium based composites [197-200]. Silver, copper and chromium coatings have also been proposed [199-201].

Metal coating on ceramic particles increases the overall surface energy of the solid, and improves wetting by enhancing the contacting interfaces to metal - metal instead of metal-ceramic. However, the interaction of coatings with a liquid metal during infiltration or stirring, and the influences of this interaction on the solidification microstructure and the mechanical properties of a coating are not well understood. Coating are applied in a variety of ways including CVD, several form of PVD, electroplating, cementation, plasma spraying [202] and by sol gel processes [203].

Other Methods

A mechanical force can usually be used to overcome surface tension to improve wettability. However, in the experimental work of Zhao et al [176], it was found that

mechanical stirring could not solve poor wettability, when the matrix alloy is in a completely liquid state. Stirring in a semi-solid state did help to promote wettability between SiC particles and Al-Si and Al-Mg alloys

Ultrasonic vibration was applied to liquid MMC processing to improve apparent wettability of Al_2O_3 particles with molten aluminium. Prior to the ultrasound-assisted processing, it was found that the application of ultrasonic vibration made the contact angle of the system change from non-wetting to a wetting system [175]

Mixing time is one of the important variables, which is often not adequately recognized or reported. Many of the metal-ceramic systems of commercial interest are made wettable by promoting interfacial reaction. Since these processes effecting with interfacial energy balance, progress with time, the contact angle, θ , is often a function of time. Therefore if the processing time is short, the particles may appear non-wetting but with an increase in time, these particles become wettable. For example, for Al-SiC composites, at the holding temperature of 800°C , the contact angle is 125° for a holding time of 125 minutes. This value drops to 55° for a holding time of 160 minutes. Similar time dependence of contact angle may also be observed for coated particles if the coating is soluble in the melt. The processing time should be controlled so that coating does not dissolve completely [88]

1.8.3 POROSITY

Porosity is one of the biggest problems in the production of aluminium casting. Defects such as porosity, inclusions and compounds formed by interfacial reactions will decrease the yield strength of any material, including composites. The volume fraction, size and the distribution of porosity in a cast MMC plays an important role in controlling its mechanical properties [78], and corrosion resistance. It is important therefore that the porosity level is kept to a minimum in order to produce a sound casting with optimum properties. Porosity cannot be fully avoided during the casting process, and so the mechanical properties of the cast materials are commonly correlated to the volume fraction of its porosity [209,210]. However, with some difficulty porosity levels can be controlled through an understanding of the main sources of this porosity.

In general porosity arises from three causes

- i Gas entrapment during stirring
- ii Hydrogen evolution,
- iii Shrinkage during solidification

According to Ghosh and Ray [261] the stirring parameters such as holding time, stirring speed, size and the position of the stirrer in the slurry will influence the formation of the porosity. Their experimental work showed that there is a decrease in porosity level with an increase in holding temperature. It has been recommended that the turbine stirrer should be so placed as to have 35% liquid below and 65% liquid above [51]. Ghosh and

Ray [74] concluded that porosity content in the composites have been found to increase initially up to a certain value. This phenomenon occurs with an increase in stirring speed, size of the impeller and its position as indicated by the distance from the bottom of the crucible, but decreases with a further increase in these process variables. According to Lloyd [133] and Samuel et al [206] structural defects such as porosity, particles clusters, oxide inclusion, and interfacial reactions are found arise from unsatisfactory casting technology. It was observed that the amount of gas porosity in casting depends more on the volume fraction of inclusions than on the amount of dissolved hydrogen [195]. This is because, in general composite casting will have a much higher volume fraction of suspended non-metal solid than even the most dirty conventional aluminium casting, so the potential for nucleation of gas bubbles is enormous. It has been observed that porosity in cast composites increases almost linearly with particle content.

Samuel et al [206] found that the porosity level decreases with increasing the mould temperature and that will improve the soundness of casting. The porosity shape and size were affected by the presence of the silicon carbide reinforcement particles through the tendency these particles display to block or restrict the growth of the pore [207]. As a result, a more uniform distribution of porosity was obtained compared to the un-reinforced matrix alloy, where the porosity was seen to occur in the inter-dendritic regions, spreading across several dendrites.

Cocen et al [208], producing aluminium-silicon alloy based composite containing different volume fraction of SiC particle, found that the volume fraction of porosity in all samples including the matrix alloy vary between 0.7% and 6.8%. These results are as shown in Figure 1.15. It was indicated that the porosity content increased with the total mixing time or with the volume fraction of SiC particle [208], or alumina [88].

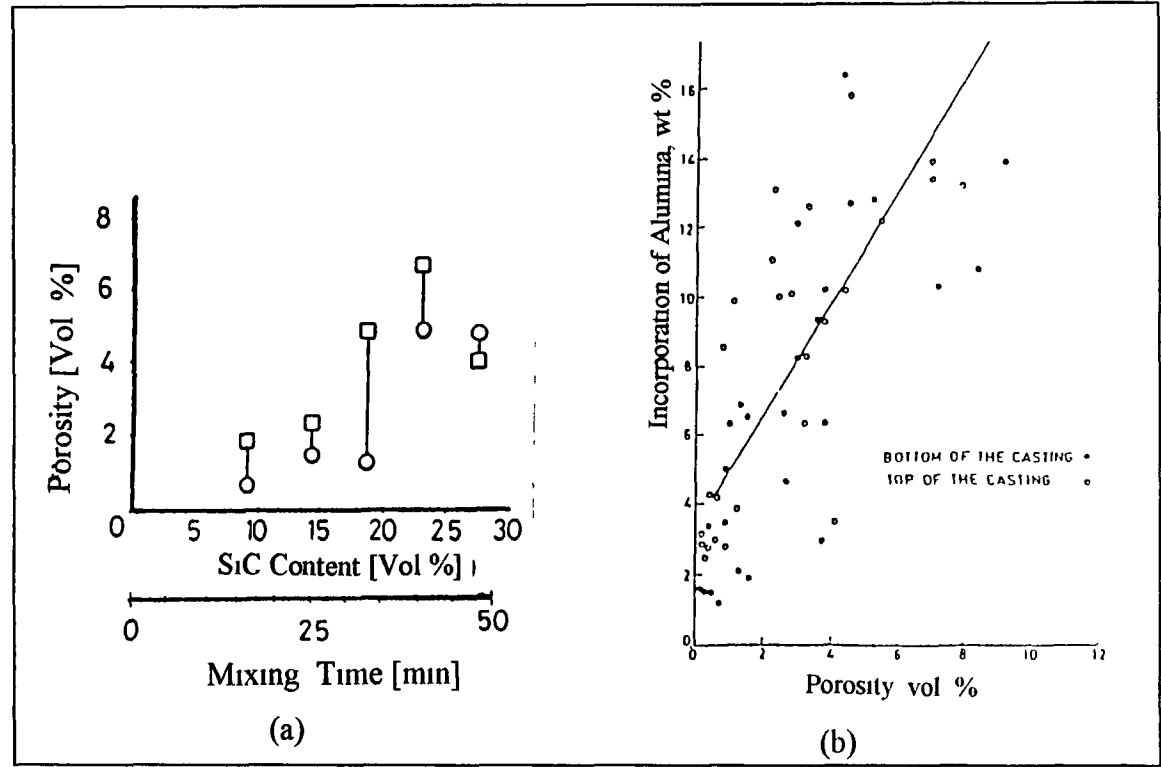


Figure 1.15 Porosity studies on (a) the effect of SiC particle content, and mixing time [208], (b) the effect of alumina particle incorporation [88]

The porosity of a composite primarily results from air bubbles which normally enter the slurry either independently, or as an air envelop to reinforcement particles [64]. The air trapped in a cluster of particles also contributes to porosity. Oxygen and hydrogen

are both source of difficulty in light alloy foundry process. The affinity of aluminium for oxygen leads to a reduction of the surrounding water vapor and the formation of hydrogen, which is readily dissolved in the aluminium.

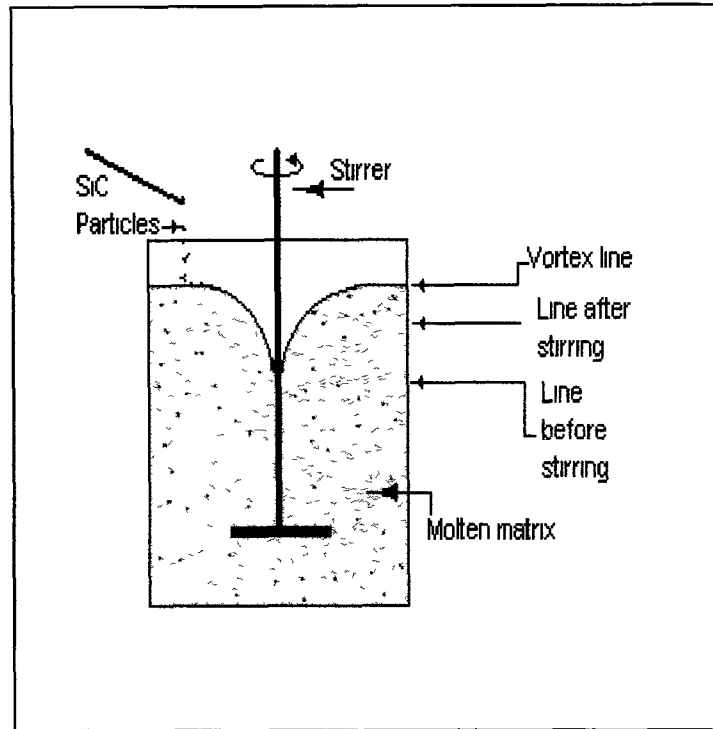


Figure 1 16 The effect of vigorously stirred melt to the incorporation of gas in the molten mixture [58]

There is a substantial drop in solubility as the metal solidifies, but because of a large energy barrier involved in the nucleation of bubbles, hydrogen usually stays in super saturated solid solution after solidification. The nucleation and growth of pores during solidification of A356-SiC particle reinforced composite is shown schematically in Figure 1 8. When solidification starts, a network of alpha-aluminum dendrites is developed. As solidification progresses, the silicon carbide particles that already exist in

the melt are rejected in front of the advancing alpha-aluminium dendrite network. At this stage there is an accumulation of hydrogen gas in a pocket of inter-dendritic liquid due to the decrease in solubility accompanying solidification. When the temperature reaches the eutectic temperature, the growth of the pores is limited by their abilities to expand in the remaining melt.

The occurrence of porosity can be attributed to the amount of hydrogen gas present in the melt, the oxide film on the surface of the melt that can be drawn into it at any stage of stirring, and gas being drawn into the melt by certain stirring methods. Vigorously stirred melt, or vortex tend to entrap gas and draw it into the melt. It has been found that the presence of a vortex inhibits wetting. An experiment performed to determine the extent of incorporation of gas in the molten mixture [58] is shown schematically in Figure 1.16. It shows that the level of the melt increase after stirring and this is because of the introduction of gases during high speed stirring. Introducing reinforcement particles by injection through an inert gas, and several degassing technique will increase the gas level in the melt. Pouring distance from the crucible to the mould should be as short as possible [109].

The shrinkage that occurs on solidification is the primary sources of porosity formation in solidifying casting. Shrinkage porosity also occurs on a micro level as micro-shrinkage, or micro-porosity, which is dispersed in the interstices of dendrite solidification region [98]. When the temperature reaches the eutectic temperature the

growth of the pores is limited by their ability to expand in a viscous media, by their edges being surrounded by the silicon carbide particle

There are several strategies that have been used to minimize porosity. These include

- i compocasting in vacuum,
- ii extensive inert gas bubbling through the melt,
- iii casting under pressure,
- iv compressing, extruding or rolling the materials after casting to close the pores

There are several methods which can be used to minimize the porosity in the cast MMCs, such as vacuum or inert atmosphere processing [64,195,212], purging the slurry by chlorine or nitrogen [213], or preheating of ceramic particles [191]. Most of the gas absorbed on the surface of the particles is in the form of H_2O . Miwa et al [67] found that the evolution process of H_2O gas with temperature is mostly finished at temperatures between 200°C to 600°C. Therefore it is suggested that most of the H_2O gas absorbed on the surface of the particles can be liberated by heat treatment at 600°C.

It is necessary to avoid gas pick-up during melting, since any gas taken into solution will be difficult to remove [74]. It is recommended to melt under a protective cover of dry argon or nitrogen to reduce significantly the possibility of oxidation, therefore degassing and fluxing are unnecessary [90]. This can be achieved by placing a fireproof

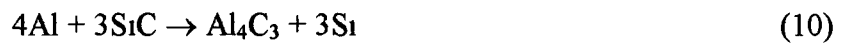
blanket such as kaowool, over the furnace or crucible, in which a small hole has been made for the reception of a simple piece of gas pipe. The protective gas is fed through a suitable flexible hose from a cylinder fitted with a pressure regulator and flow indicator. In order to get a clean melt, the matrix material must be well dried to over 200°C and added to a preheated crucible, and stirrer, ladles and sampling spoon must also be well preheated before being put into the melt. Richardson [90] recommended that any steel utensil introduced into the melt must be well coated with ceramic adhesive before use, to prevent iron contamination and must be well dried and preheated to prevent the possibility of hydrogen generation. The stirring action must be slow to avoid the formation of vortex in the surface of the melt. Care must be taken not to break the surface layer too often and take the surface skin into the melt. Porosity can also form in the mould during casting. Solidification shrinkage arises as a result of incorrect mould temperature and incorrect gating systems. It has been observed that increasing the mould temperature will improve the soundness of the casting, as shown by a decrease in porosity levels [21].

Degassing liquid aluminium alloy is a usual step in the casting procedure. When reinforcement materials are incorporated into a melt in air, molten compound must be treated to remove the dissolved gases. Although various out-gassing treatments are available (based on nitrogen gas, chlorine or vacuum treatment) it is difficult to reach a very low hydrogen content corresponding to the saturation of solid aluminium alloys. Girot et al [117] have developed a procedure for gas removal. In this process the usual cleaning, deoxidizing and refining treatments are applied before degassing. The

degassing is carried out in a vacuum chamber. At the end of the degassing step, the formation of bubbles is enhanced by an injection of nitrogen gas. However, the application of vacuum to the molten mixture of metal and particles during the mixing step can reduce the atmospheric gasses available for introduction into the melt, and also tend to draw dissolved, entrapped and adsorbed gasses out of the melt during mixing.

1.8.4 CHEMICAL REACTION

When metal matrix composite is produced by powder metallurgy, generally the reinforcement is not exposed to molten metal except for a short period of time during liquid phase sintering. However, in molten metal processing, the reinforcing particles are mixed directly into the liquid and exposure times to liquid metal are relatively long. As a result, the reinforcing particles may react with the liquid metal, which can degrade the reinforcement [133]. The main reaction between liquid aluminium and SiC is



The formation of aluminium carbide is bad for several reasons [75,133, 156,202,217,223]. Obviously it degrades the reinforcement, but Al_4C_3 is also susceptible to corrosion and its formation is accompanied by an increase in the Si level of the alloy, therefore modifying the composition and metallurgy of the matrix, which may be detrimental to the final composite properties. This formation may increase the viscosity

of the melt. In the casting fluidity test by Lloyd [214], it was found that, if the AA6061 composite is held for 30 min at 650°C it has zero fluidity. Associating the casting fluidity with Al_4C_3 formation is also consistent with the result for the A356 matrix composites.

Lloyd et al [152] studied the thermodynamic stability of the reinforcement in aluminium and magnesium alloy, and concluded that in a silicon free alloy, silicon carbide is thermodynamically unstable above the melting temperature of the matrix alloy, reacting to form aluminium carbide, Al_4C_3 and, a subsequent increase in the silicon level of the matrix occurs. The silicon that forms is relatively harmless, however the precipitation of aluminium carbide as crystals can substantially degrade the quality of the casting. For high Si content aluminium alloy, these phenomena can be easily prevented by keeping the melt temperature below 773°C at all the times, because below this value, the reaction proceeds too slow to be a problem [215]. Samuel et al [206] studied melt holding times and temperatures for aluminum and the A356 alloy-silicon carbide particle composite system, and found that Al_4C_3 forms rapidly at temperature above 790°C. The reaction can also occur below this temperature but at much lower rates, and in their study, no significant Al_4C_3 was formed, below this temperature (for holding times less than 30 minutes). Therefore, it is essential to be aware of the danger of overheating the melt. Good temperature control of the melt, and use of high silicon content aluminium alloy, can suppress unwanted chemical reaction between a molten aluminium and the silicon carbide particles [214].

The reaction between silicon carbide particles and liquid aluminium is believed to take place in several steps including the following [219,220]

- i Diffusion of silicon and carbon atoms away from the silicon carbide particle surface into the molten aluminium pool
- ii The formation of compounds when the aluminium and carbon concentrations exceed the equilibrium constants of Al_4C_3 , and/or
- iii Further precipitation of compounds on cooling due to a decrease in solubility

The carbon atoms go into solution and react with aluminium to form Al_4C_3 [221] Following the dissolution of silicon carbide, Al_4C_3 grows and silicon will diffuse into the melt around the Al_4C_3 . A layer of Al_4C_3 may form around the silicon carbide particle [222] and this layer act as a diffusion barrier for the further diffusion of silicon, carbon and aluminium

The aluminum carbide reaction can be avoided by using high silicon alloys for the matrix [133] but this restricts the choice of the matrix alloy. Increasing the amount of silicon in the matrix can reduce the dissolution of silicon carbide and prevent the formation of Al_4C_3 [152]. Usually 7-15 wt % silicon is necessary to prevent the reaction [46,152,219,224] as shown in Figure 1.17. Another method of controlling the aluminium carbide reaction is to oxidize the surface of the silicon carbide, forming an outer layer of SiO_2 . In this case the early stages of the reaction involves reducing the SiO_2 , rather than

dissolving the silicon carbide [225] According to Heuer et al [226] the SiO_2 layer on silicon carbide can easily be thickened by heating in air From their research, it is estimated that heating in air at 700°C for one hour increases the thickness of the oxide layer by between 30 and 50 nm from the original thickness of between 2 and 4 nm

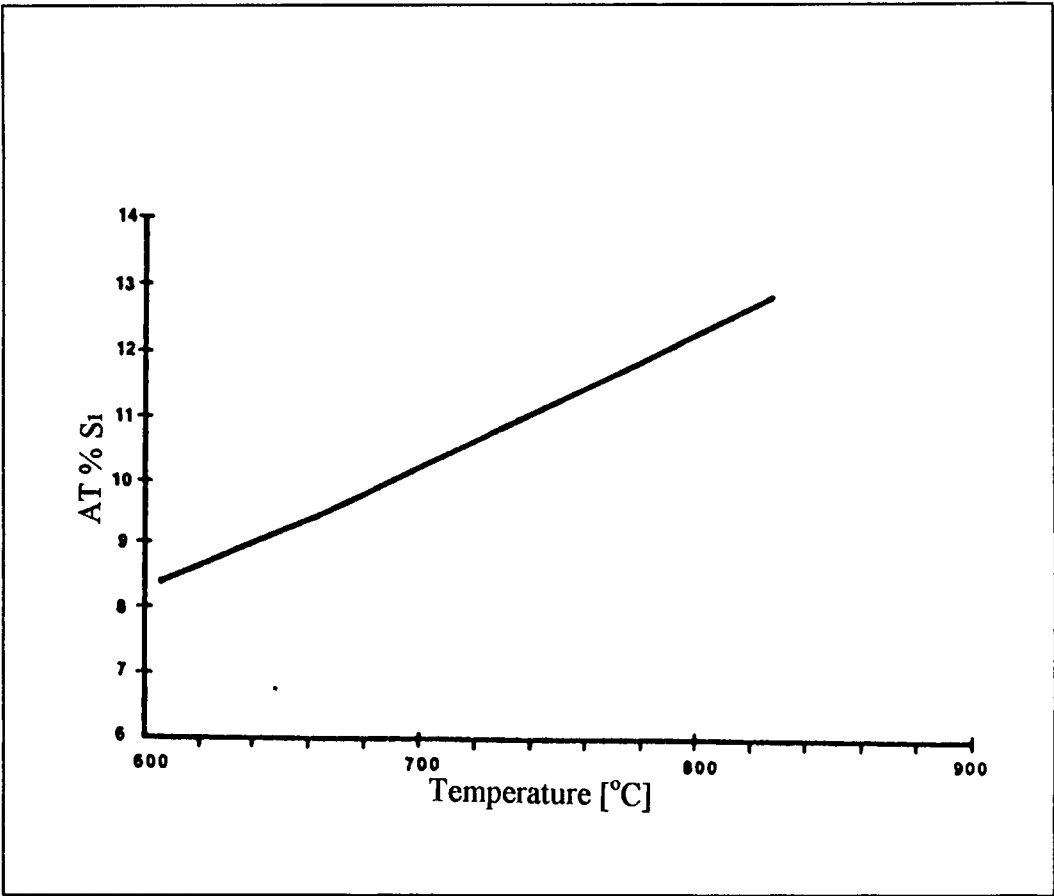


Figure 1 17 Silicon content level required preventing Al_4C_3 formation in aluminium melt at various temperatures [225]

Wang et al [227] studied the interfacial microstructure in a aluminum-silicon carbide system composite produced by molten mixing In their work, magnesium aluminate, MgAl_2O_4 was found at the interface as a reaction product after processing

Several studies of the aluminium alloy-alumina composite system also indicate that the MgAl_2O_4 spinel may be formed at the reinforcement-matrix interface [62,186] Levi et al [185] found that in the case of an aluminium-magnesium alloy based composite, the bonding between the reinforcement and the matrix metal is achieved through the formation of an MgAl_2O_4 (spinel) layer, by reaction between the reinforcement and the magnesium in the liquid aluminium. The chemical reaction between ceramic and metal, which occurs at the interface, generally improves the wetting and bonding, especially the spinel chemical reaction product.

1.9 HEAT TREATMENT OF METAL MATRIX COMPOSITE

The strength of the metal matrix can be improved by thermal treatments. These thermal treatments are similar to those ordinarily used as hardening treatments for aluminum alloy, namely a solution treatment and water quench, followed by room temperature aging (so called T4 treatment), or artificial aging which is performed at higher temperature (so called T6 treatment) [5, 245]. The treatment results in microstructural modifications only in the metal matrix, because reactions do not occur between aluminum and reinforcement materials at the treatment temperature [222]. The solution treatment of the casting produces three main effects: dissolution of Mg_2Si particles, homogenization of the casting, and changing the morphology of the eutectic Si .

1.9.1 Heat Treatment Procedure

Heat treatable aluminium alloys display appreciable solid solubility of the precipitating Mg_2Si phase at the solidus temperature. Under equilibrium conditions, solubility decreases with temperature and the second phase precipitates out as coarse particles. The decrease in solubility is a prerequisite to a significant response to heat treatment. In order to obtain a maximum concentration of Mg and Si particles in solid solution, the solution temperature should be as close possible to the eutectic temperature. In most cases, the A356, A357, A359 type alloys are solutionized at 540°C [246].

The solution treatment homogenizes the cast structure and minimizes segregation of alloying elements in the casting [245]. The eutectic Si morphology plays a vital role in determining the mechanical properties. Under normal cooling conditions the phase is present as coarse needles. The needles act as crack initiator and lower mechanical properties.

Following solution treatment, the casting is quenched in water. The purpose of quenching is to suppress the formation of equilibrium Mg_2Si phase during cooling and retain maximum amount in solution to form supersaturated solid solution at low temperatures. A rapid quench will ensure that all Mg_2Si is retained in solid solution, and the highest strength is obtained with fast quench rates. In most cases, the samples are quenched in water between 25 to 100°C.

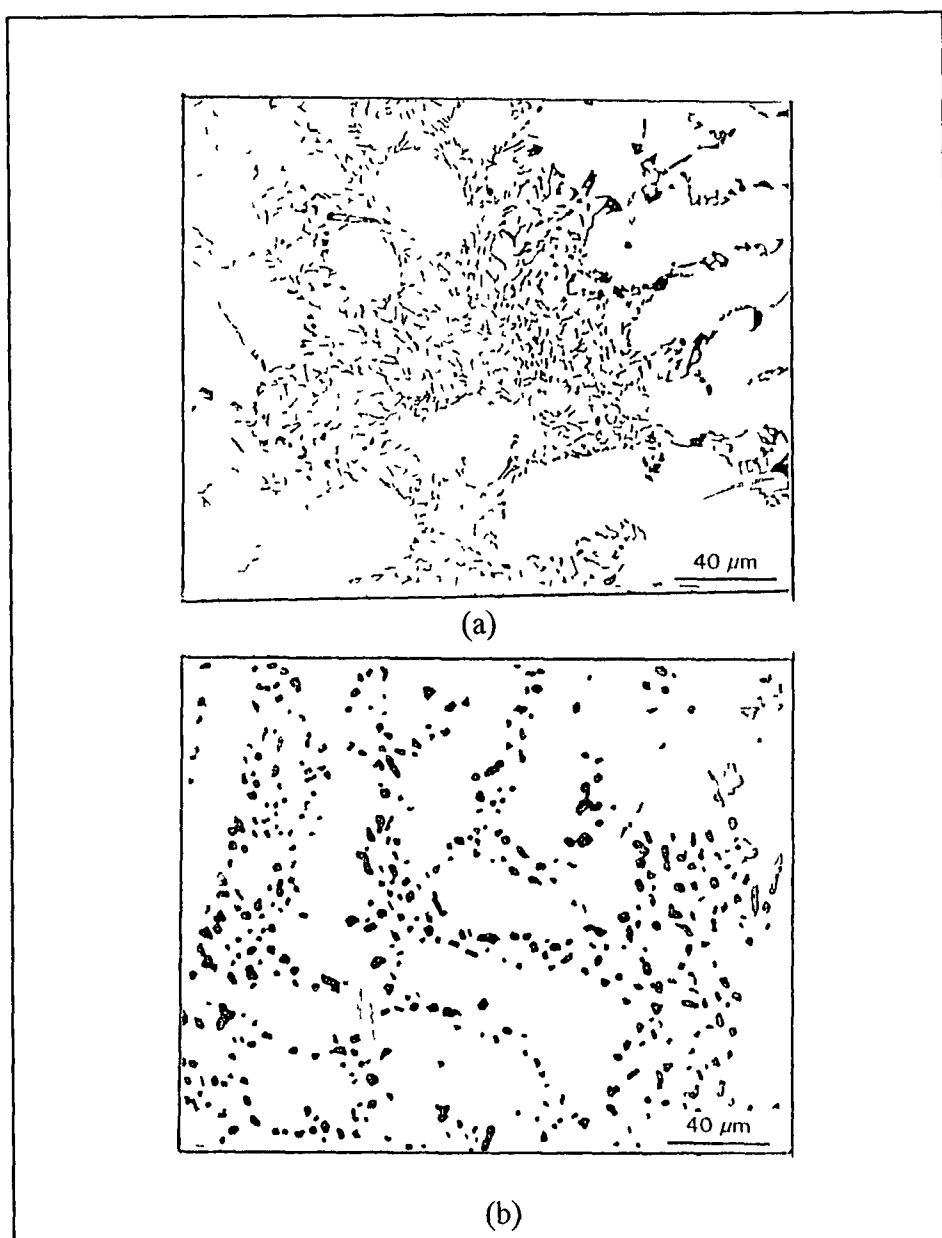


Figure 1 18 Microstructure depicting the morphology of eutectic Si1 as a function of aging time of 540°C (500X) (a) as cast (b) after 2 hrs [245]

Quenching is followed by aging treatment, either natural or artificial aging. The purpose of this treatment is to precipitate constituents, which were dissolved during solution treatment. The precipitation of very fine Mg_2Si during aging leads to pronounced improvements in strength properties. Both aging time and temperature effect the final properties. The microstructural changes occurring during heat treatment of A356 samples are shown in Figure 1.18 [245]. Initially Si broken down into smaller fragments and is gradually spheroidized. Prolonged solution treatment leads to coarsening of the particles and as the solution time is increased, there is coarsening of Si .

1.9.2 Effect of Reinforcement Particles

A number of investigators have reported that the presence of SiC particles accelerates the aging response in the matrix when compared to the un-reinforced alloy [241, 247]. Arsenault et al [241] found that the achievement of the solutionized state is more difficult for A6061- SiC particle composites than for AA6061 alloy, hence in the former case the solution treatment needs a higher temperature. Some of the studies [248-250] demonstrate that at low temperatures the aging kinetics slowed down, or unaffected by the reinforcement. Ribes and Suery [251] found that the addition of SiC particles to the Al-7Si-3%Mg alloy accelerates aging during thermal treatment at 185°C, and this is primarily due to the thermal mismatch between the reinforcement and the matrix. The aging behavior also depends on the nature of the surface of the particles. For oxidized particles, spinel forms at the interface leading to magnesium depletion in the matrix and subsequently to less age hardening.

Yamada et al [80] found that the addition of fibre or particles usually changes the aging response of the matrix due mainly to the presence of high dislocation densities and residual stresses generated close to the reinforcement-matrix interface. The addition of SiCp to Al-Si-Mg alloy accelerated their aging response during heat treatment. They also concluded that this is primarily due to the thermal mismatch between the reinforcement and the matrix. Salvo et al [252] investigated the effect of reinforcement on the age hardening of cast 6061-SiCp MMC, and found that precipitation sequence in the un-reinforced matrix and the composites are identical. The precipitation kinetics is accelerated in the composites by the higher dislocation density and enhanced nucleation, and this occurs at any aging temperature. The hardening behavior of the composites and un-reinforced 6061 seems to be identical when the aging temperature is below the critical temperature (the temperature when the phase transformation occurs). Composites reach their maximum hardness when the aging temperature is beyond the critical temperature.

The elastic-modulus is one of the properties that are improved in composites. Figure 1 19 [234] shows the effect of silicon carbide particle percentages on elastic-modulus. The silicon carbide particles cause an increase in Young-Modulus. Figure 1 20 [253], shows the effect of temperature on modulus. Table 1 12 shows the mechanical properties of SiC particles reinforced MMCs. It is obvious that it increases with the amount of the reinforcement over a large temperature range.

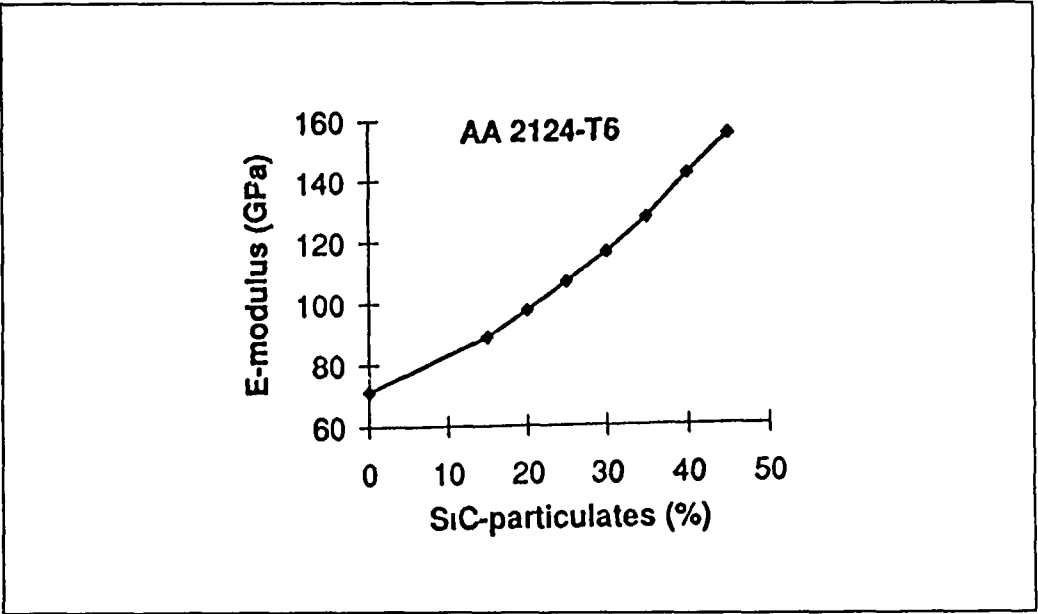


Figure 1 19 Elastic-modulus vs SiC particle content for A2124-T6 [234]

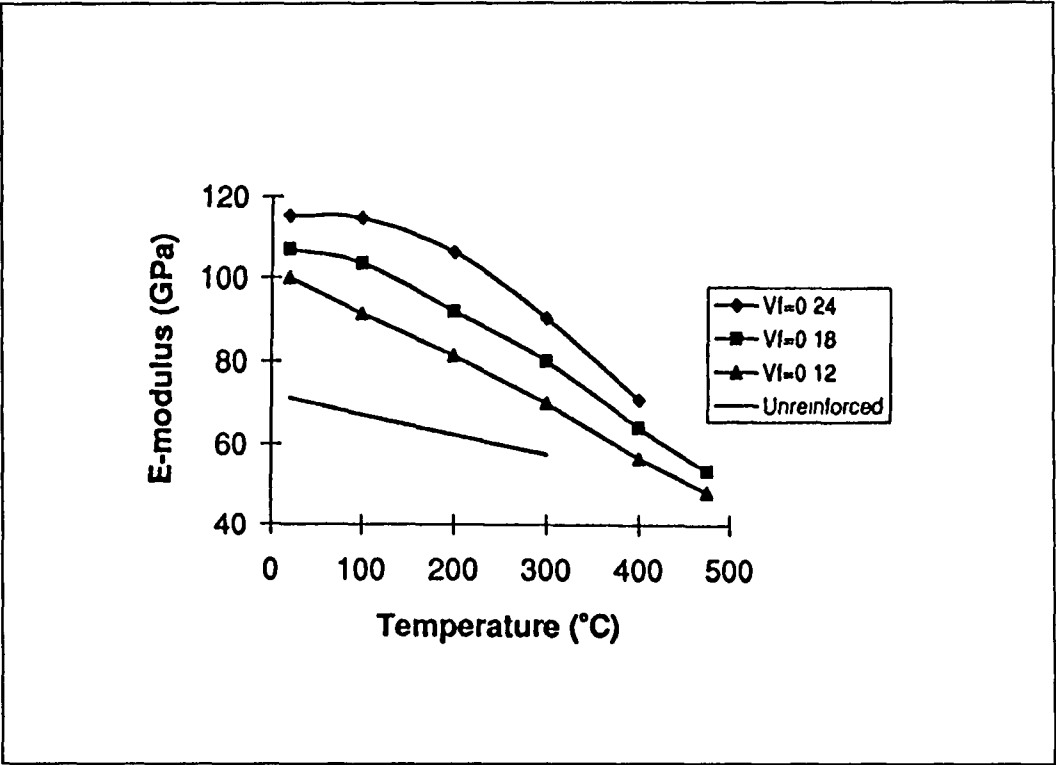


Figure 1 20 Elastic-modulus vs temperature for Al-9Si-3Cu alloy with varying quantity of alumina fibre [253]

In general the hardness of the MMC is better than un-reinforced matrix, and this is more pronounced in the heat-treated condition. The increase of hardness in heat treated MMCs, is primarily a result of precipitation microstructure changes, such as increase in dislocation density in the matrix, and the presence of the residual stress that is caused by the incorporation of reinforcement particles. The hardness in both matrix and composites are as shown in Figure 1.21. Dutta and Surappa [254] studied the effect of SiC particles on the age hardening and mechanical properties of aluminium based MMCs. They observed that the SiC particle reinforced composite is harder than the un-reinforced alloy.

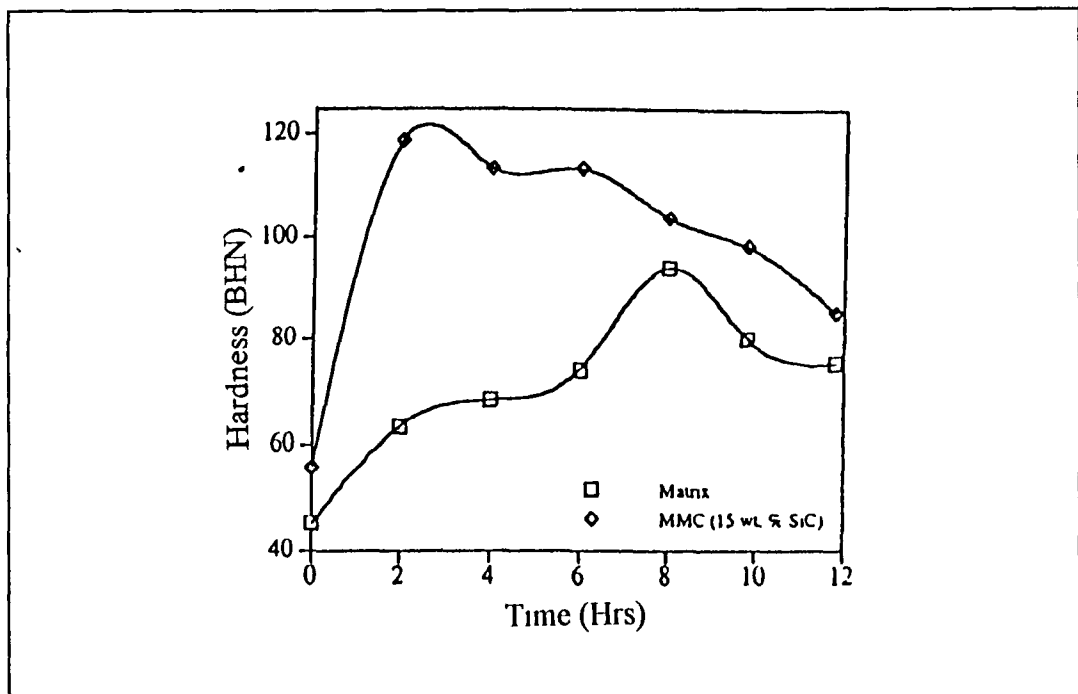


Figure 1.21 Aging studies conducted on Al-15%SiC materials [254]

The reinforcements increase the hardness of 8090 alloy approximately 120% and that of 2024 alloy by 45%. They also found that the maximum hardness in un-reinforced alloy as a result of aging is equal to, or less than the hardness of the composites in the

solution treated conditions Whereas Figure 1 22 shows the results of hardness measurement in Al-SiC particles composites by Gupta et al [255] Their results show that the heat treated sample and that with increased SiC particles content exhibit higher hardness

The tensile properties of sand-cast and permanent mould cast test bars of A356-SiCp composites are given in Table 1 12 It is clear that the addition of SiC particle results in substantial increase in the tensile yield strength, the tensile ultimate strength and the elastic modulus [115] These results also illustrate that as the strength and stiffness is improved, the tensile ductility is decreased with the addition of SiC

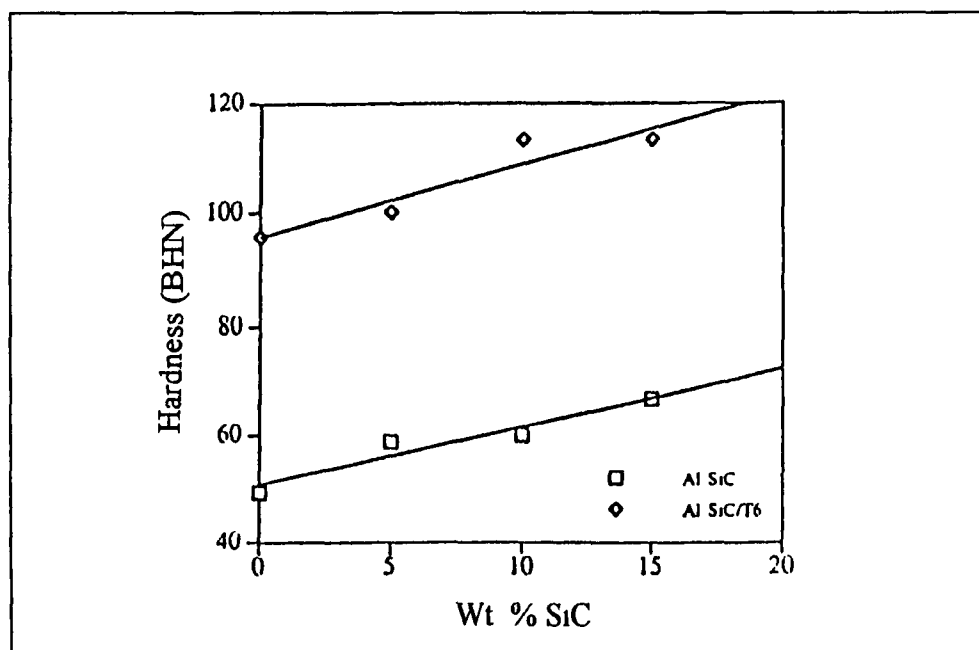


Figure 1 22 Effect of T6 heat treatment on the hardness of SiC particle reinforced Al based composite [255]

Table 1.12: Tensile properties of A356/SiC composite for different percentage of SiC.

At T6 condition (solutionised at 540°C, aging at 160°C) [115]

Volume percent of SiC	Ultimate Strength [MPa]	Yield strength [MPa]	Elongation
0	227.50	199.93	4.0
10	255.078	241.29	0.7
15	289.55	296.44	0.4
20	296.44	296.44	0.5

Table 1.13 : Mechanical properties of SiCp reinforced AMCs

Composite System	Yield strength [MN m ⁻²]	Ultimate Tensile strength [MN m ⁻²]	Percentage of elongation [%]	Elastic Modulus [GN m ⁻²]	Ref.
A359(as cast)	103.5	179.4	4-5	-	[258]
A356(as cast)	96.6	165.6	6-7	-	[71]
A356 – T6	205	280	6	76	[133]
A6061 – T6	275	310	20	69	[133]
A356/SiC/15p – T6	-	295	1.5	95	[214]
A2124/SiCp/17-T6	230	342	9.7	95	[259]
A6061/SiC/5 – T6	271.4	293.6	8.7	75.3	[255]
A6061/SiCp/20 – T6	415	498	6	97	[260]
T6 = Artifial Aging, T4 = natural Ageing.					

In general the strength of both matrix and composite drop remarkably at high temperature. At about 200–250°C, the strength of particle reinforced MMC is higher than fibre reinforced composites, but at higher temperature of about 450°C, the performance of both types of composites is almost the same [256-257]. Table 1.13 shows the mechanical properties of several silicon carbide particle reinforced aluminium matrix composites.

1.10 MECHANICAL PROPERTIES OF CAST, PARTICLE REINFORCED METAL MATRIX COMPOSITES.

Metals have a useful combination of engineering properties such as strength, ductility, toughness and high temperature resistance but they have low stiffness values. Ceramics are stiff and strong but are brittle. Aluminum and silicon carbide have very different mechanical properties, for example, Young moduli of 70 GPa and 400 GPa, CTEs of $24 \times 10^{-6}/^{\circ}\text{C}$ and $4 \times 10^{-6}/^{\circ}\text{C}$, and yield strengths of 350 MPa and 600 MPa respectively [238, 239]. The concept involved in the design of MMC materials is to combine the desirable attributes of metal and ceramic. The performances of several materials group are illustrated in strength-temperature diagram, shown in Figure 1.23.

In general the addition of reinforcement phase to the matrix material will give several advantages such as increases in elastic modulus, yield and tensile strength, creep and wear resistance, and also an increase in elevated temperature strength. If the elastic-moduli are increased, it is usually possible to decrease the component thickness and

therefore reduce of the weight for any given design. An increase in modulus indicates an increase in stiffness, and the specific stiffness for aluminium composite is high since the density is low.

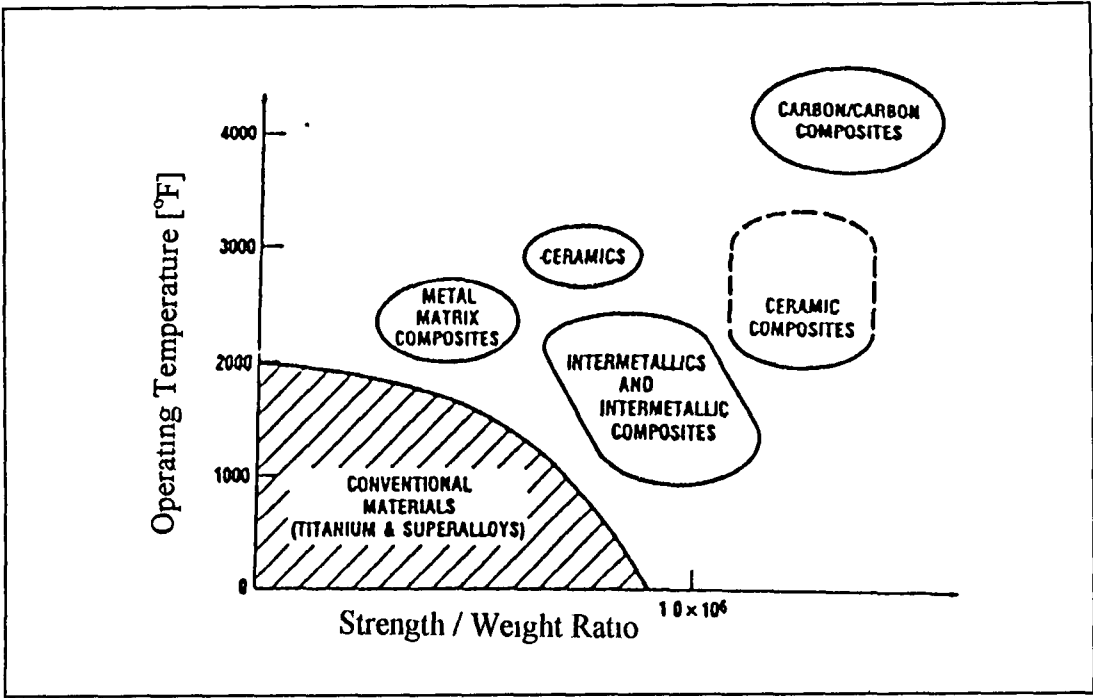


Figure 1.23 Strength-temperature map for classes of materials in terms of operating temperature and strength/weight ratio [239]

In general, with increasing volume fraction of reinforcement, the strength of the composite will increase. According to Mohn and Gegel [240] by increasing the content of SiC particles in composite materials, increases in tensile strength, yield strength and elastic modulus can be attained. Tensile tests [241] of Al- SiC particle MMC indicate that for high volume fraction samples (20%SiC p), the fracture process is very localized. As the volume fraction of the reinforcement decreases, the deformed region spreads out. For example in the case of 20 vol % of reinforcement, the reduction in area at the fracture

surface was only 3%, and 5 mm away from the fracture surface the reduction in area was zero Lim et al [242] studied the effect of volume fraction of reinforcement on the elastic response of Al-SiC composite They found that the elastic modulus of the composites increase with increasing content of the reinforcement, and the yield strength also increases with decreasing particle size [243], as shown in Figure 1 24

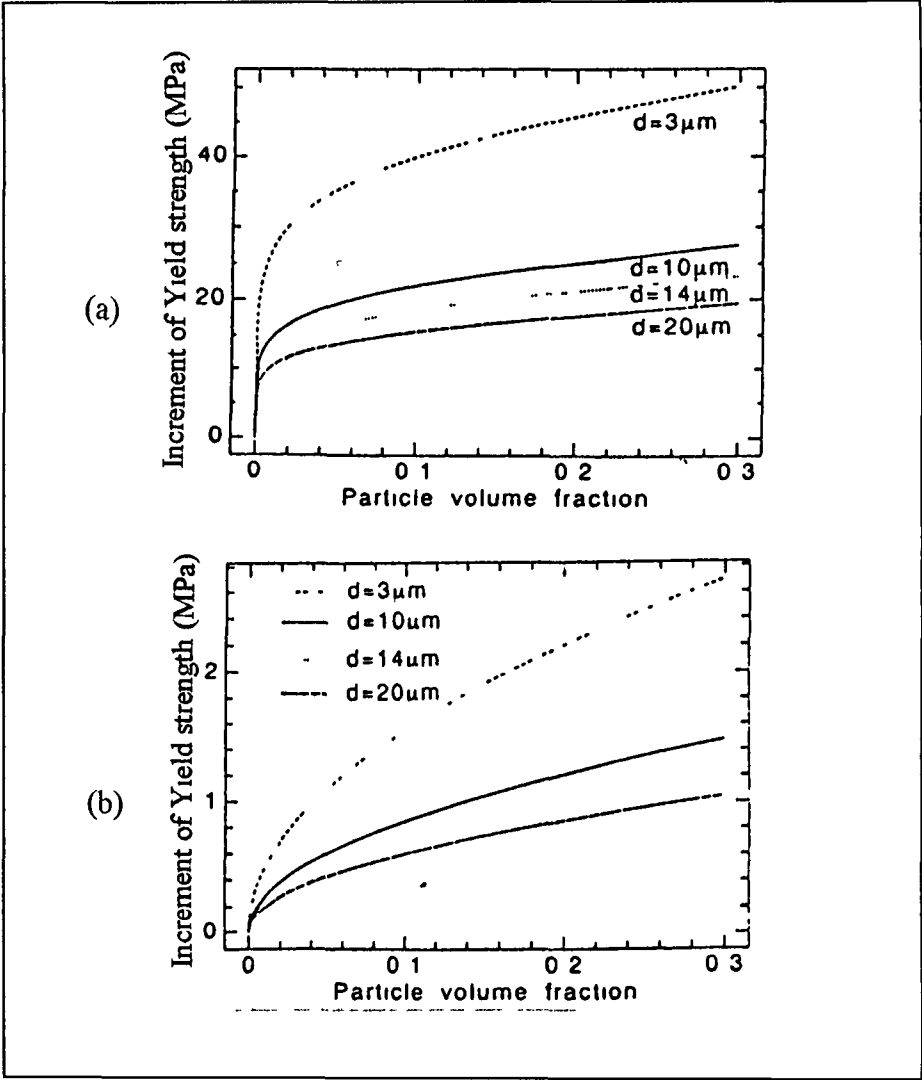


Figure 1 24 Increment of yield strength versus particle volume fraction (a) due to small sub-grain strengthening (b) due to dislocation strengthening for Al-SiC composites [243]

CHAPTER TWO

FEA SIMULATION OF PARTICLE DISTRIBUTION IN CAST METAL MATRIX COMPOSITE

2.1 INTRODUCTION

The production of metal matrix composites using a stir casting technique represents a potential means of producing complex shaped components. In the present research, an Aluminium based SiC particle reinforced MMC is being made using a stir casting technique. In this method the matrix material and the reinforcement particles are placed in a crucible, together with a wetting agent, and are subsequently heated under an inert gas atmosphere until the matrix material melts, as shown schematically in Figure 2.1. A stirrer is then applied after the matrix material is completely melted. A crucial part of this process is the efficiency of the mixing action to disperse the reinforcement particles, which are initially put at the bottom of the crucible.

The importance and difficulty of achieving a uniform distribution of particle reinforcement in the molten matrix, and also during solidification of the MMC, have been discussed in detail in Chapter I of this thesis. It is known that sufficient stirring action is necessary to control distribution from immediately after the addition of the particles into the melt, until pouring into a mould. However, in normal practice, the efficiency of the stirring action in the closed crucible cannot be seen, and the result of the stirring can only be deduced from the solidified MMC, using optical examination [261], and may not be clear due to solidification effects.

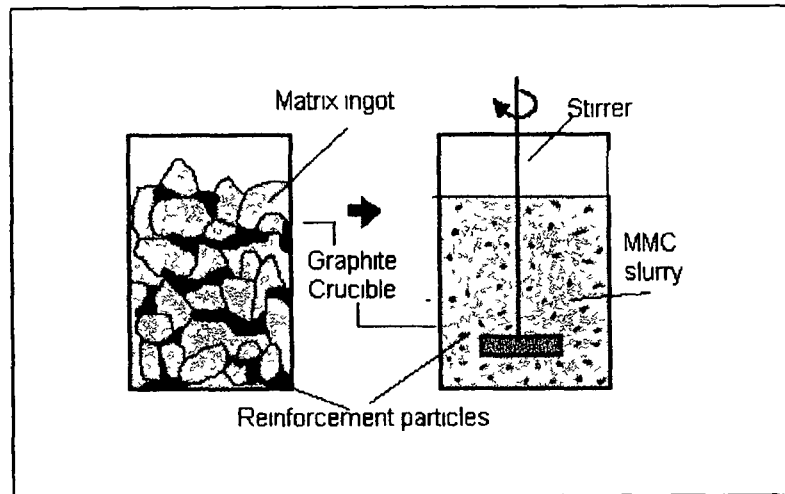


Figure 2 1 Schematic representation of MMC fabrication technique used

Actual measurement of fluid flow characteristics is expensive, time consuming, and in the case of molten metal may be dangerous. Also all relevant parameters may not be included. Additionally, the scale-up to industrial sized units is neither straightforward nor well established, since most stirrer-vessel systems perform several functions simultaneously (for example dispersion, reaction and heat transfer). In these situations Computational Fluid Dynamics (CFD) can provide a means for understanding the details of flow. In the past decade rapid progress has been made in numerical solution of turbulent mixing problems using CFD. However, application of this knowledge to mechanically stirred vessels is still in the early stages, because an impeller or stirrer induces a complex flow field. However, if the stirring action could be simulated, that would be very advantageous. In this research, flow generated by a stirrer in a cylindrical crucible is studied. CFD analysis using the Finite

Element Analysis (FEA) ANSYS® package is used to simulate the fluid flow representative of casting of an aluminium matrix composite.

The main focus of this simulation is to study the effect of stirrer position in the crucible and stirring speed on the flow pattern of particles. This computer simulation is then compared with visualisation experiment results using glycerol and polystyrene particles in a perspex crucible. The information derived from the computer model will be used quantitatively in subsequent MMC production by stir casting, in order to disperse reinforcement particles in the molten matrix as uniformly as possible. The use of glycerol and polystyrene is arbitrarily selected to just give some idea of the mixing flow pattern and does not directly relate to the molten aluminium and SiC particle combination.

2.2 STIRRING

In composites produced by a foundry technique, inhomogeneous distribution of ceramic particles in the casting has been identified as one of the primary problems. Mechanical stirring is usually used during melt preparation or holding and, in this context, the stirring condition, melt temperature, and the type, quantity and nature of the particles are some of the main factors to consider when investigating this phenomenon, [133, 134]. In general stirring helps in two ways: to transfer particles into the liquid metal, and to maintain the particles in suspension. Several types of stirrers are available for stirring purposes. In some cases, the stirrers are design in order to provide a high degree of axial flow, hence minimizing power requirements. This may be an important requirement in the chemical industry, where large vessels or long transport distances can be involved. In stir

casting for MMC fabrication, there are however other factors that need to be considered. As well as dispersing the solid particles uniformly, the stirring action must not be allowed to introduce gasses into the melt, which would be detrimental to the final product. A vortex created during stirring can suck in even non-wetting particles and also bubbles into a molten alloy. Particles often attached to the bubbles, counteracting the buoyancy, which would normally helps, them to float out of the melt. As a result, it has been observed that porosity content in a stircast composite varies almost linearly with particle content [88]. It is necessary to create turbulence during stirring, but it should be only in the bottom region of the fluid.

The stirrer diameter is also an important factor to be considered. When the stirrer diameter is too small, the solid particles remain suspended at the periphery of the vessel in spite of the lack of deposits at the center. When the diameter is too large, solid particles are remain un-dispersed in the center of the vessel bottom. Therefore the optimum diameter of the stirrer is that which result in solid particles being fluidized in both the central and peripheral part of the container at the same speed. It has been found that for a flat bottom vessel, stirrer diameter, d should be $= 0.4D$, where D is the diameter of the vessel, and the blade width b , should be $= 0.1-0.2D$ [263].

In case of agitation of solid particles in a liquid in a cylindrical vessel, a deposit of solid particles is observed on the bottom of the vessel at low agitator speeds, and all the particles are fluidized when the speed reaches a certain value [263]. This is a complex phenomenon dependent on stirrer design, shape and size of the vessel and particle properties. Two types of fluidization of solid particles are observed as shown in Figures 2.2

(a) and 2.2 (b). When the density of solid particles is small, and the impeller is set higher than 30% of liquid depth from the vessel bottom, pattern 1 is observed. When the impeller is set near the bottom, pattern 2 is observed.

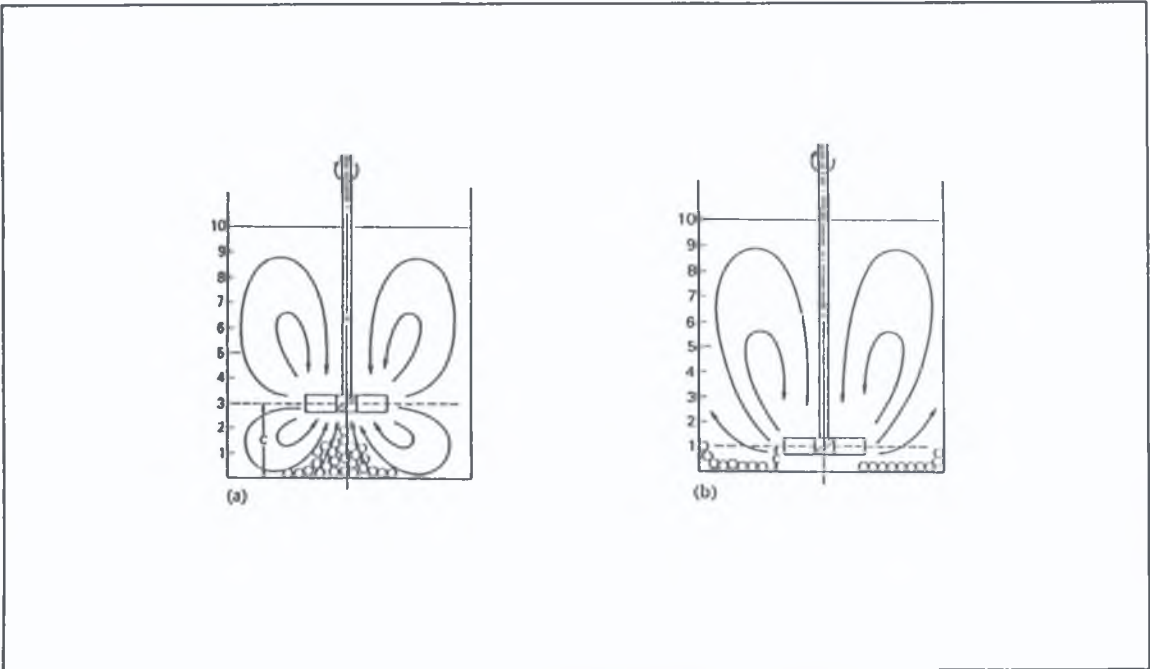


Figure 2. 2: Pattern of fluidization of solid particles
(a) Pattern 1 (b) Pattern 2 [263].

2.3 SIMULATION

In general, fluid flow can be approached in two different ways. One can choose to include the elementary flow units (for example molecules, particles, aggregates etc.) or to describe flow in macroscopic or continuum terms. The latter is used in this simulation to simplify analysis, but it is thought to be representative due to the fine nature of the particles involved in the casting of the particular composite being researched. Although this simulation studies the dispersion of the reinforcement particles in the molten aluminium

during stirring, no simulation of the solid particles was made. It is assumed that the particles are very fine ($<10\mu\text{m}$ average diameter). According to Thomas [131], the particles below $10\mu\text{m}$ in size are almost always carried fully suspended in the liquid and gravitational effects are negligible. From this assumption, if the wettability between the particles and the molten aluminium is good, it is expected that the particle will follow the fluid flow pattern, which is generated by the stirrer. The FEA package used also does not support multiphase flow analysis.

The application software ANSYS® Flotran-CFD types was used in this simulation, the model being built using two-dimensional elements. The simulation focuses on the fluid flow pattern for different positions of a stirrer in a crucible, and different speeds of stirring for two fluids: molten aluminium, and glycerol. The stirrer geometry was therefore kept as simple as possible and a flat blade stirrer was used. Due to the axisymmetrical shape of the crucible and the stirrer, only half of the real shape was included in the simulation, and the element coordinate system used was axisymmetric about the Y vertical axis.

The model was built by initially creating a rectangle, representing the shape of the crucible in 2-D. The simulation is representative of a fluid in a 80-mm diameter and 100 mm height graphite crucible. Meshing for the fluid in the crucible was carried out by assigning 50 grid points at the crucible wall in the vertical (y) direction, and 20 grid points for the crucible base in the horizontal (x) direction. The meshing was then replotted to generate thousands of nodes in a regular grid pattern. Boundary conditions were then applied to these nodes. The validity of a CFD prediction depends largely on the boundary conditions imposed. In this case the boundary representing the crucible wall was specified

as a solid surface which is smooth and frictionless. This is justified, as molten aluminium does not wet graphite [70,74,78,82], as was also demonstrated experimentally in this project. However the top surface was allowed a degree of freedom to displace, such that zero pressure would be maintained. The input viscosity of the fully molten aluminium was 1.0×10^{-3} Pa S, with density of 2.30 g/cm^3 which is assumed to be constant. The viscosity and density of glycerol are 1.15 Pa S and 1.20 g/cm^3 respectively.

Because of the fact that this CFD package does not support solid elements, another means of representing the stirrer, and its motion was required. The load was therefore considered as the velocity of a group of elements. These elements represented the shape and position of the stirrer. In the case of this 2-D simulation, the stirrer rotation speed is given as radial velocity. The rotation speeds used were in the range 50 rpm to 1000 rpm, for 4 different heights of 10%, 20%, 50% and 70% of the total height, as measured from the crucible base. The rotational speed range was chosen to encompass the lowest and highest speeds nominally being used in casting of MMCs. The position levels include those both above and below the 30% optimum indicated by other research [15], and also positions expected to cause a vortex on the melt surface.

The results from this simulation were compared with those from a visualisation experiment using glycerol. Streak photography of tracer particles in such a visualisation experiment is a good method for indicating the overall flow pattern, and existence of stagnant regions of fluid. However it was found that it is not suitable for showing the rate of mixing between different parts of a vessel. To physically simulate the molten aluminium and SiC particles, a 80mm diameter perspex vessel, filled to 100mm height with the transparent glycerol fluid was used. Particles of white polyethylene were added to the fluid,

and mixing was carried out using a digital control dc motor, connected to a flat stirrer blade (10mm height \times 2mm thickness) The stirrer speed was chosen in the range 50 rpm to 100 rpm, same as for some of the runs of the computer-based simulation The results of this visualisation test were recorded as follows The vessel was illuminated using a collimated light beam across a diametrical plane, and the backdrop darkened Using a suitable exposure time, a streak photograph of the polystyrene particles flow pattern was recorded, one of which is as shown in Figure 2 8

2.4 RESULTS AND DISCUSSION

Examples of the simulation results are shown in Figures 2 3 to 2 7, and the validity of the model predictions as found by comparison with the visualisation experiment results is indicated by Figure 2 8

Output from the simulation is given in the form of a flow pattern, indicated graphically by velocity vectors In interpreting the results it is important to keep in mind two requirements (1) turbulence at the base of the crucible which would give effective mixing (SiC particles are more dense than molten aluminium, and tend to settle, rather than float), and (2) the absence of a vortex at the surface (to avoid gas/impurity entrapment) It should be noted that to aid generalisation of interpretation of results, impeller position is given as a percentage of the total height of the fluid, h , and refers to the position of the lower edge of the impeller

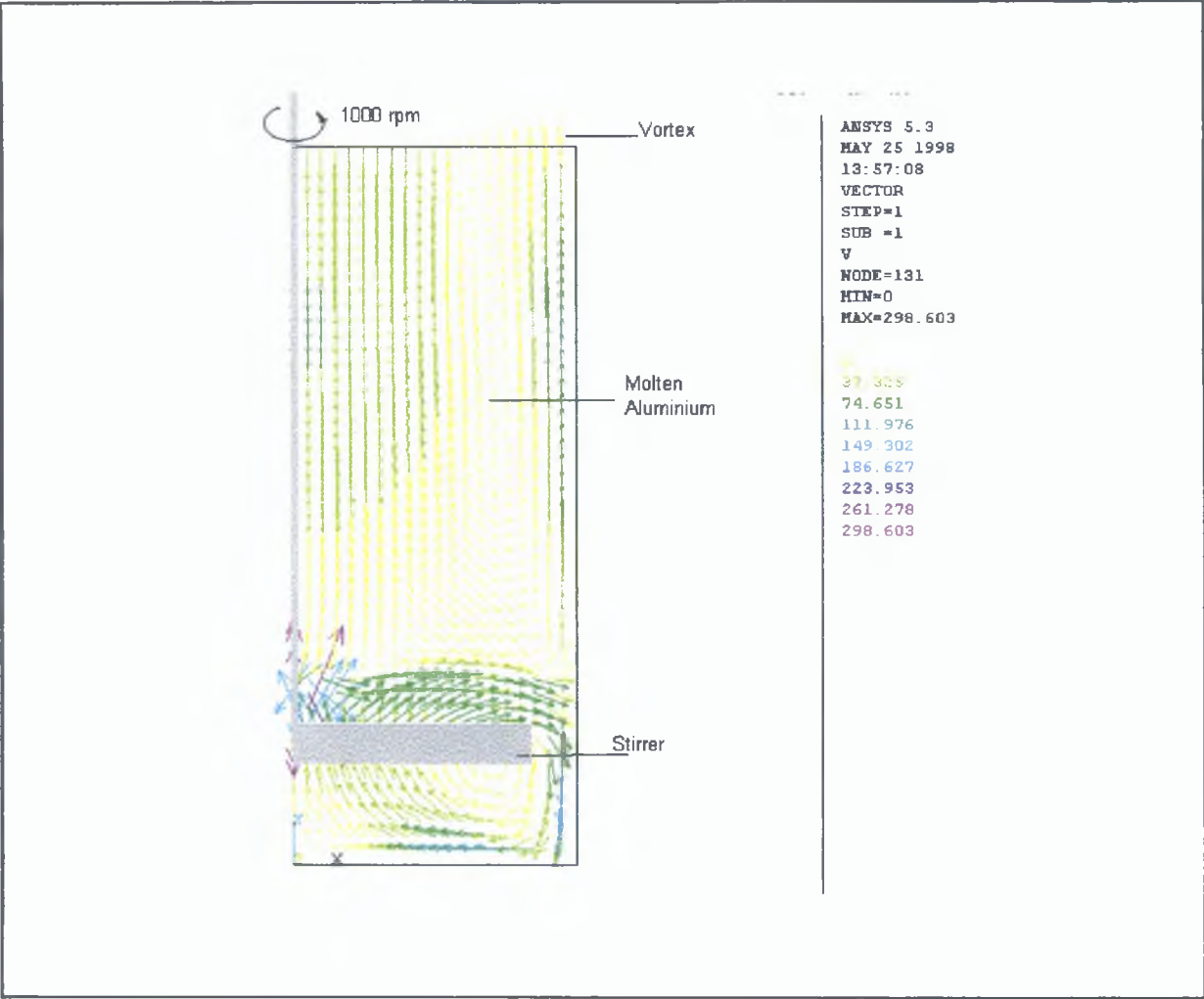


Figure 2.3 : The flow pattern for the position of the stirrer of 20 % from the crucible based, for 1000 rpm.

2.4.1 Effect of Stirrer Speed

The effect of stirrer speed is illustrated by taking the example of a case where the impeller is placed with its lower edge 20% h from the base of the crucible. The speed is then changed from 100 rpm to 1000 rpm. Figure 2.3 shows the flow pattern at the highest speed, and Figure 2.4 that at the lowest. At 100 rpm two well-defined circulation zones are apparent, one below the impeller, one above. Both zones reach the crucible wall. Under the

impeller the flow zone extends to the crucible base, but there is a ‘dead’ zone at the centre of the crucible. Above the impeller the circulation zone is centred 35% h from the crucible base, and extends vertically over a further height of 30% h . The region at the top of the vessel (constituting approximately 35% h) has little or no motion.

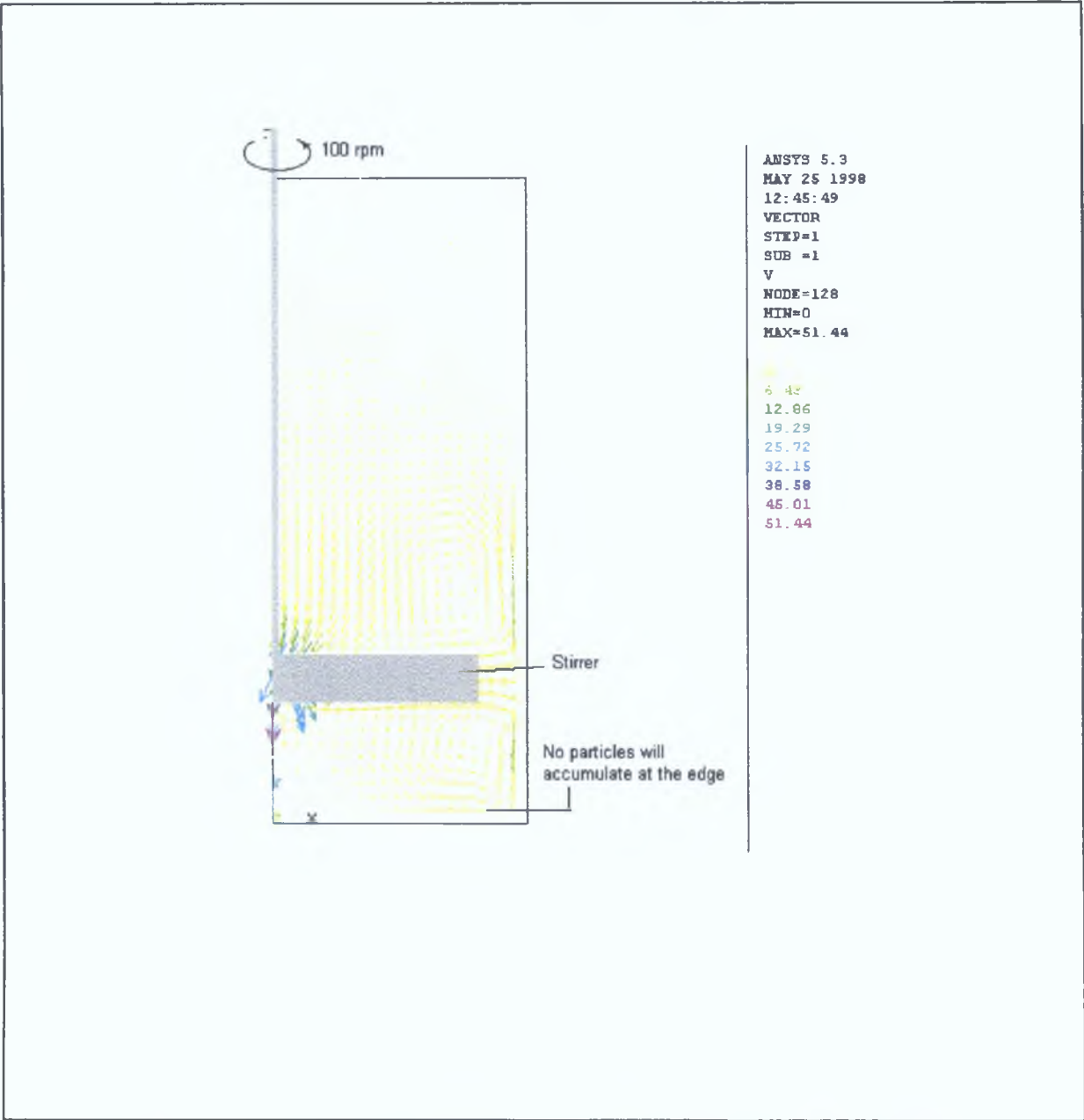


Figure 2.4: The flow pattern for the position of the stirrer of 20% from the crucible base for 100 rpm.

As speed increases the flow pattern below the impeller remains essentially the same. The difference lies only in the magnitude of the velocity of the fluid elements. At one sample position, 10mm from the crucible wall at the base, the velocity increases almost by 30 times from 6.4 rad/s to 186 rad/sec as impeller speed increases from 100 to 1000 rpm. This increase in speed causes fluid at the bottom centre of the vessel to be effected by the circulation region at the highest speeds. Above the impeller, at higher speeds the circulation is dominated by a vertical suction pattern, and a vortex has formed on the fluid surface, causing a maximum displacement of fluid elements of 3% h from their original position. From running the simulation at impeller speed values between those shown in Figures 2.3 and 2.4 it is clear that the transition to this type of flow occurs at very high speeds for this position. The flow pattern at 500 rpm for example is very similar to that shown for 100 rpm.

2.4.2 Effect of Position

According to experimental observation of Nagata [263] the stirrer should be placed no more than 30% of height from the base, to avoid accumulation of particles at the bottom of the mixture. The simulation results show good agreement with this statement. This is illustrated by Figures 2.5 and 2.6 in which rotor speed is maintained at 100 rpm, and the stirrer is located at 10% h and 70% h from the crucible base respectively.

At the lowest position the influence of the impeller is seen over the bottom half of the crucible. There is a circulation loop centred 25% h from the vessel base, and below the stirrer mainly horizontal velocity is seen, which does extend to the crucible wall, and to the

centre. At the highest position there are three distinct flow zones within the fluid. The first is a zone of little or no flow at the bottom of the crucible over 15% h , the second a circulation zone beneath the impeller, centred 50% h from the base, and the third, above the impeller, where a vortex has formed accompanied by strong vertical suction within the fluid. The transition to vortex formation occurs at positions higher than 50% h in the case of 100 rpm stirring speed.

2.4.3 Effect of Fluid Viscosity

The simulation was run for two different fluid types: the relatively low viscosity molten aluminium, and high viscosity glycerol. The effect of viscosity change on predictions was significant, as can be seen by comparing Figure 2.7 (aluminium) and 2. 8 (glycerol). In both figures stirrer speed and position are the same at 100 rpm and 20% h from the base respectively. In the higher viscosity fluid, the effect of stirrer rotation is more localised to the region of the impeller, and centered more toward the crucible centre. In addition, rather than two circulation tracks, in the more viscous fluid a single major circulation area is clearly identifiable. This area extends above and below its ‘eye’ to approximately 20% h . However there is a zone of no flow directly beneath the impeller, and another at the top of the vessel extending over 30% h of the fluid.

2.4.4 Interaction of Effects

It is obvious that as flow patterns are effected by both stirrer position and speed, and that several different combinations of these parameters could result in the desired

mixing conditions. Which combination of speed and position is chosen may depend on constraints to resources such as equipment, power or space. A systematic analysis of the combinations for the current application was not carried out, but should be part of further analysis.

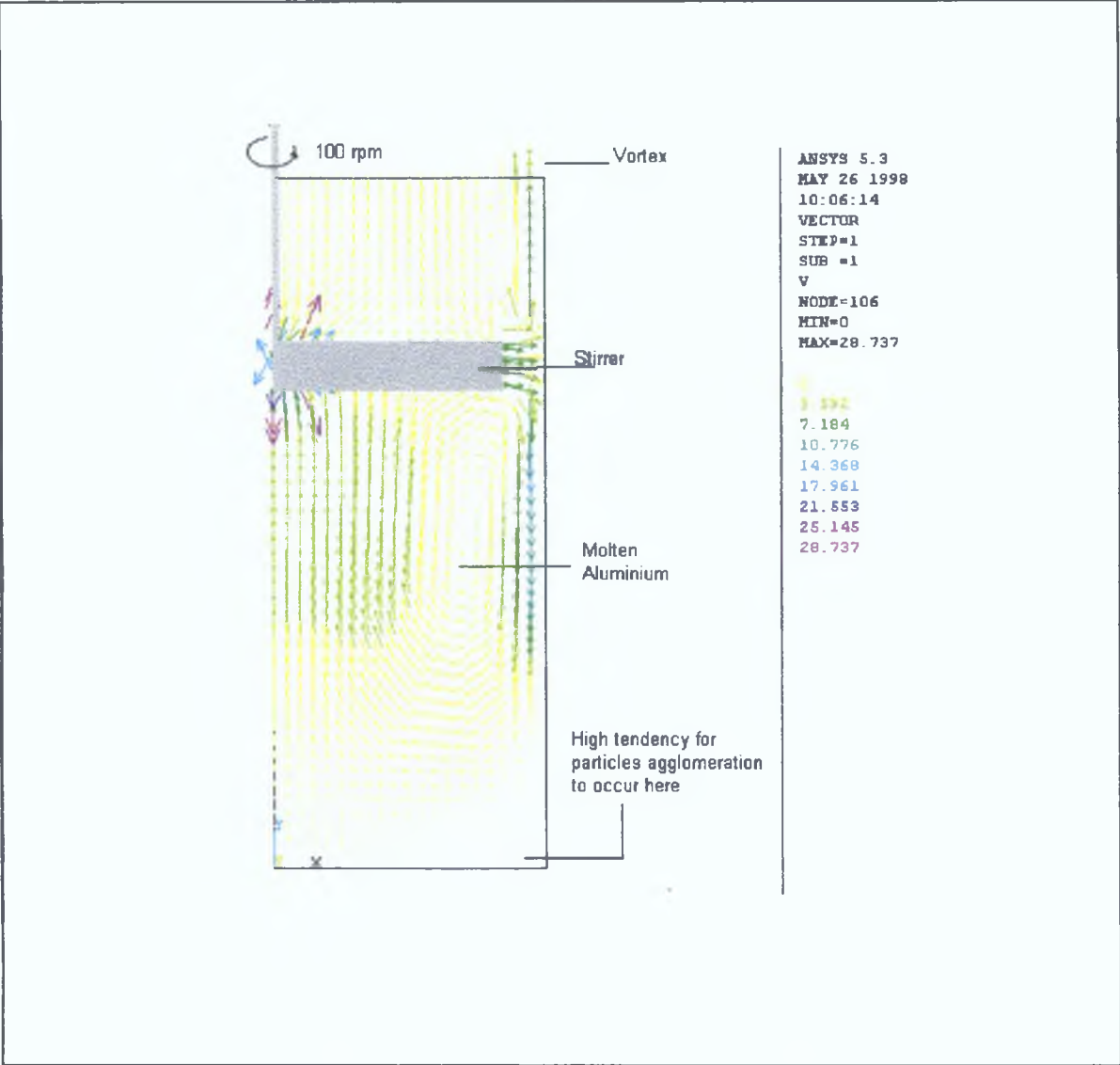


Figure 2.5: The flow pattern for the position of the stirrer of 70% from the crucible base for 100 rpm.

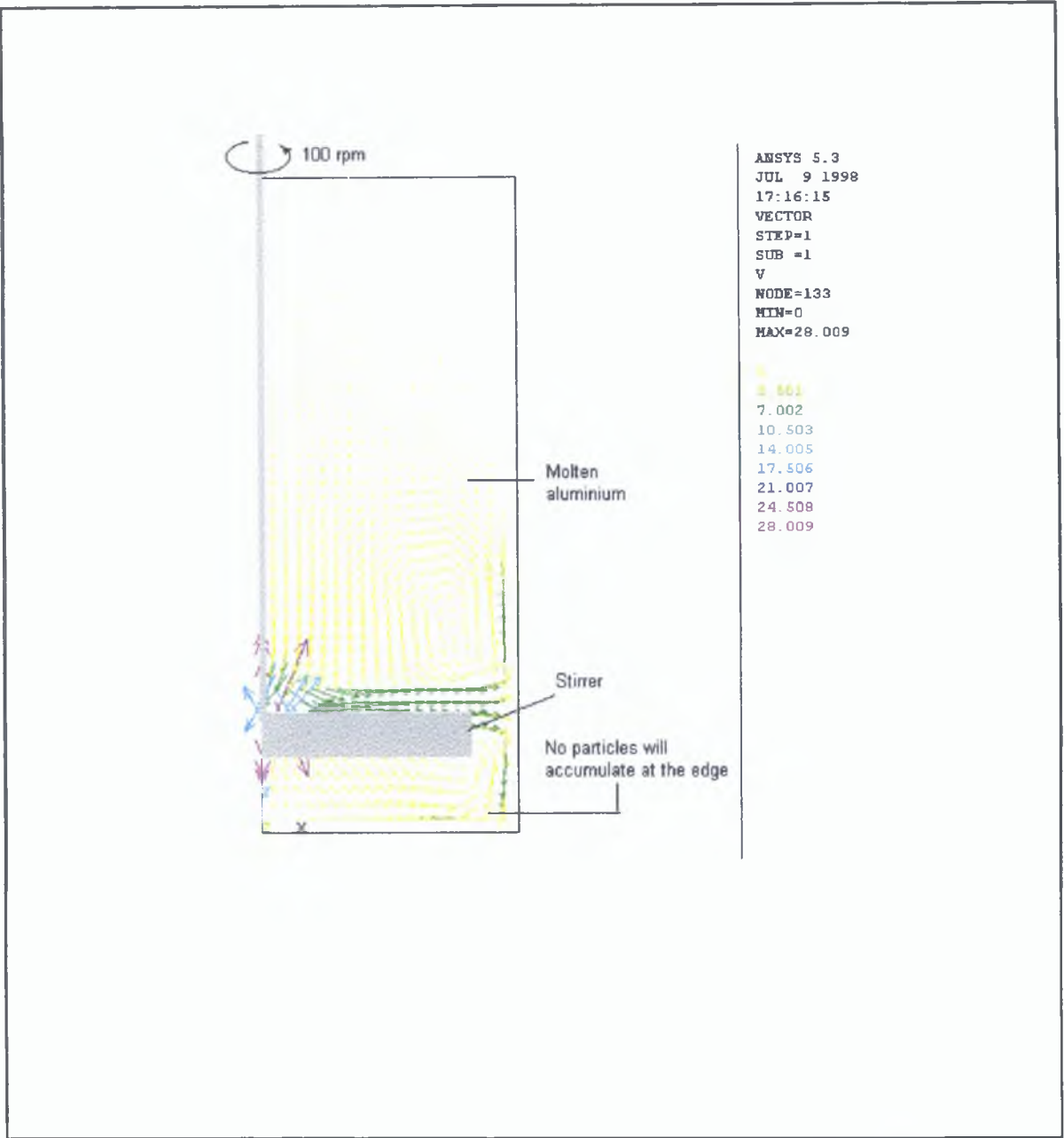


Figure 2.6: The flow pattern for the position of the stirrer of 10% from the crucible base for 100 rpm.

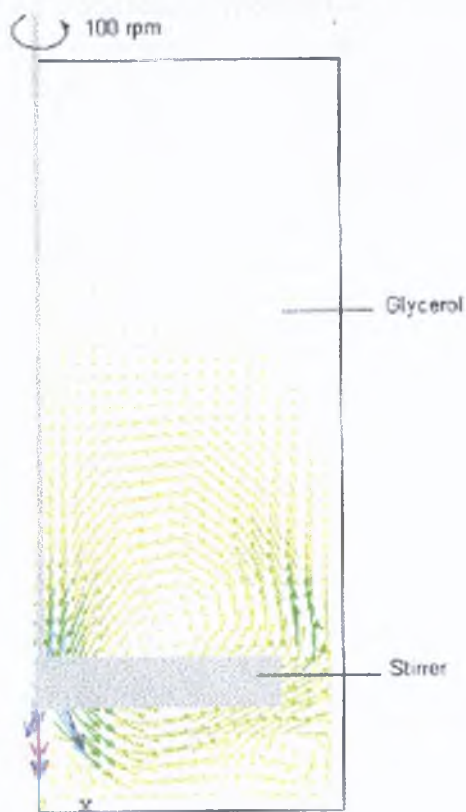
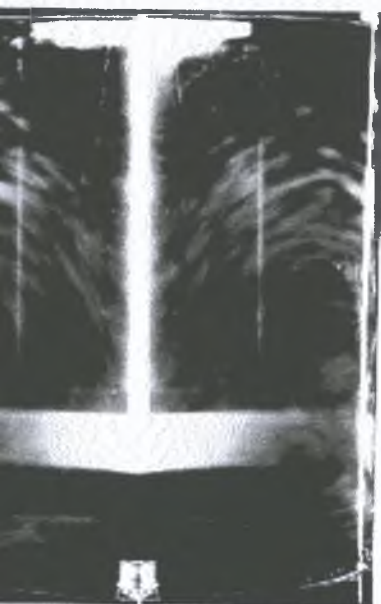


Figure 2.7 : The Flow pattern of glycerol at a stirrer
Position of 20% from the crucible base, 100 rpm.



Figure 2.8



Perspex container

Glycerol

Stirrer

Visualization experiment for glycerol at the stirrer
Position of 20% from the crucible base, 100 rpm.

2.4.5 Comparison with Visualisation Experiment

As it is not possible to experimentally validate the simulation using molten aluminium, and therefore the result from the FEA model was checked by comparing with experimental data. Figure 2.8 is a photograph of the visualisation experiment for the same stirring conditions as those for the simulation shown in Figure 2.7. The white lines in the photograph are the paths followed by the polyethylene particles through the fluid, and reflect the general fluid flow pattern. It can be seen that the predicted flow pattern in the simulation shows a very good agreement with the experimentally observed one. This lends some confidence to the validity of the model to predict optimum conditions for the aluminium casting situation.

2.4.6 Limitation of the CFD Model

While the model has been shown to represent the flow characteristics of stirred glycerol, it does have specific limitations in relation to simulating the stirring of aluminium and reinforcement particles. Firstly Newtonian flow has been presumed. This is not strictly valid for the real process, as discussed in [264]. In addition, no solid elements were used in the model, therefore it is not possible to account for variations in characteristics of the particles such as size distribution, and wettability for example.

2.5 CONCLUSION

A model of the stirring of molten aluminium containing fine SiC particles has been built using fluid elements in FEA. The model was applied to the case of the more viscous

glycerol fluid, and the results from this were compared with experimental results. The general flow patterns predicted by the model have been somewhat validated using this technique, indicating the usefulness of the model in parameter choice for casting aluminium based MMC's. The speed of rotation of the stirrer is shown to significantly impact on fluid flow characteristics, both velocity of flow, and direction. At higher speeds an undesirable vortex forms on the fluid surface. Stirrer location is also important. When the impeller is placed excessively high within the fluid, little flow occurs at the base of the vessel where it is required to lift particles into the melt. The model does have limitations, however is sufficiently representative of the process of stirring to inform decisions on process parameters for stirring of MMCs during the casting process.

CHAPTER THREE

EXPERIMENTAL EQUIPMENT AND PROCEDURE

3.1 INTRODUCTION

Considerable research all over the world has been devoted to MMCs over the past few decades. In any type of the fabrication method used, wettability and distribution of the reinforcement material in the alloy matrix are among the main problems, which still remain unsolved. In this research study, a new approach is proposed, to fabricate MMC using stir casting technique. The emphasis is given to the wettability and chemical reaction between substances. At the same time, the level of the porosity content and the distribution of the particle in the matrix are optimised.

In this approach of fabricating cast MMC, magnesium is used as a wetting agent, and two stirring steps in which the MMC slurry is in a semi-solid condition are applied in order to promote wettability between SiC particles and the matrix alloy. The two stirring steps are also used to disperse the SiC particles in the matrix alloy. In this technique, the slurry is stirred by using a stirrer which was especially design for this research. For the first step, the stirring takes place when the slurry is in semi-solid condition, and for the second step, the slurry is re-melted to a temperature 50-70°C above the liquidus, to make sure the slurry is fully liquid. The stirring is continued for another 2 to 3 minutes before the slurry is poured into a mould. A programmable temperature controller was attached to a heating element to control the temperature of the molten matrix. This is important in order to maintain the temperature below 750°C, as above this temperature the chemical

reaction between substances will rapidly occur. The main reason for choice of Aluminium-silicon alloy (A359) is to avoid this chemical reaction from developing. It is well established that, in A359 alloy, with the Si content between 8-9%, the chemical reaction between SiC particles and liquid aluminium will be delayed up to 780°C [214]. In order to minimise oxidation associated with this high temperature processing technique, the melting process was carried out in an inert nitrogen gas atmosphere.

3.2 DESIGN OF EXPERIMENTAL RIG

3.2.1 Preliminary Design

In order to fabricate cast MMC, the initial focus was placed on the design of an experimental rig. A number of ideas have been evaluated before a final design chosen. Several design rigs were tested. During the first stage of the experiment a stainless steel crucible and stirrer, with a bottom pouring mechanism was used. Bottom pouring was chosen in order to facilitate the casting, and also to prevent all the impurities (which normally float on the top of the melt), from flowing into the mould during pouring.

The reason why stainless steel was chosen was that this material proved easy to machine, and was readily available. The stirrer was connected to a DC motor, which was used to stir the molten matrix material. The crucible was a 100 mm diameter internal diameter x 150 mm height, and the stirrer was T-shaped, with a rectangular form of 70mm x 10mm x 3mm thick, which was screwed to the stirring rod. A heater band was placed around the crucible, and was connected to a control thermocouple. This is as shown in

Figure 3.1. The design was tested using A359 ingot, which was sectioned into small pieces of about 3-4 gram weight per piece. The temperature controller was set to 800°C, with the intention of melting the matrix alloy, and pouring it into a mould, using a bottom-pouring mechanism. It was found that the matrix alloy was not completely melted at this temperature. At the top and the middle part of the crucible, the matrix alloy was found to be in solid form, and material, which had melted, was subsequently stuck to the crucible wall. The alloy was not completely melted, due to heat lost during heating because the top part of the crucible was exposed to the room temperature. In addition, the room temperature at about 19°C was very low compared to the melting temperature of the A359 alloy, which is 560°C.

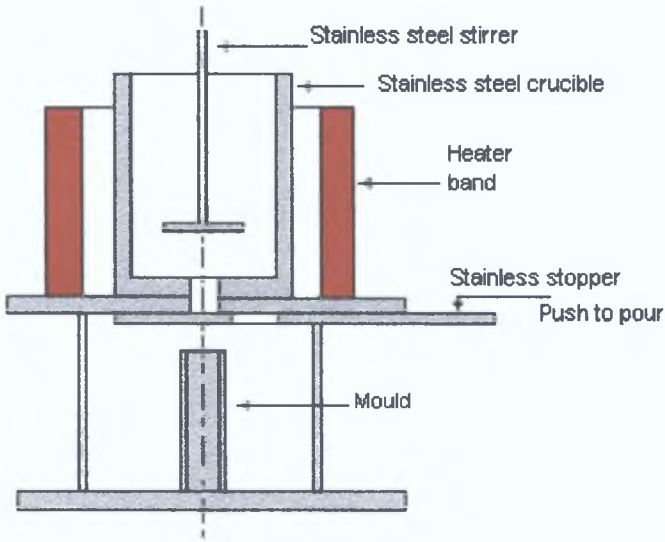


Figure 3.1 : The first design of rig using stainless steel as the material.

In order to minimise the heat loss during processing, a 50 mm thick kaowool insulator was placed around the heater band, as shown in Figure 3.2. In subsequent tests

the alloy was almost completely melted, however the top part was still in solid form. This may be due to an oxidation problem, because the top part of the material was exposed to air. When the molten matrix was poured into the mould, a few drops flowed, after that, the flow ceased. The molten matrix was solidifying during pouring, and it was sticking to the pouring mechanism. It was clear from this experiment, that stainless steel was not a suitable material to use with molten aluminium.

In literature, most researchers used graphite crucibles to melt aluminium alloy [60, 63, 67,73]. Based on this fact, it was decided to replace stainless steel by graphite. Nitrogen gas was used in order to minimize high temperature oxidation problems. The design in shown in Figure 3.3.

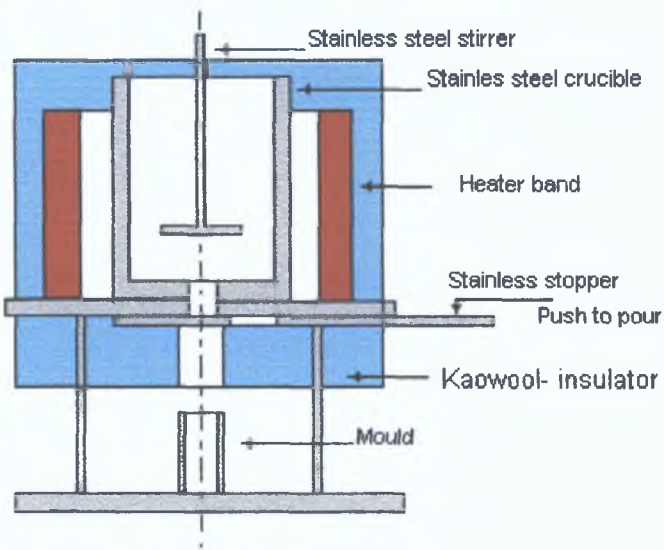


Figure 3.2: Kaowool insulator was used to minimised heat loss.

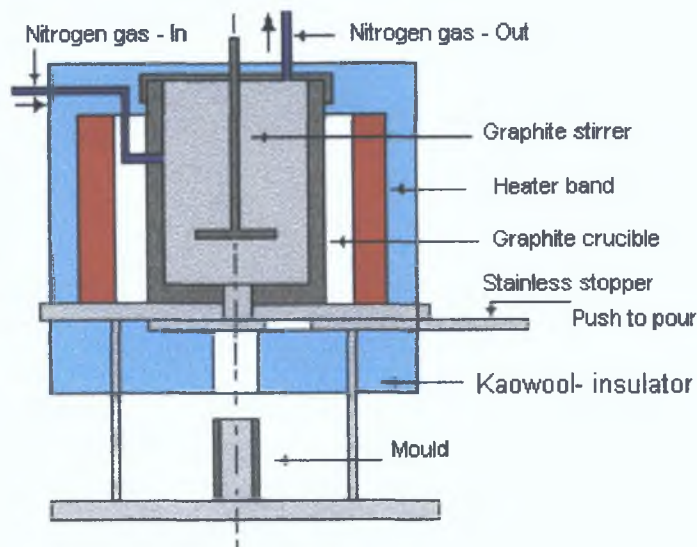


Figure 3.3: Casting rig incorporating a graphite crucible and nitrogen gas supply.

The size of the crucible was maintained as before, in order to suit the size of the heater band, and the main frame which was previously set-up. Nitrogen gas flow continuously with a flow rate of 3 cc/min. However, the pouring mechanism and stirrer used were still made of steel. This was because graphite was brittle and thought not strong enough to mix the composite slurry, particularly at high speed, and a graphite stopper was difficult to machine. With this type of arrangement the A359 alloy was melted and poured into a mould. During flow into the mould some of the melt solidified and stuck to the pouring mechanism. The tests showed that the pouring mechanism was still not functioning correctly.

The design of the pouring mechanism was modified and the new design is as shown in Figure 3.4. This new design functioned well. The aluminium melted easily, and poured into a mould. However during pouring of the molten alloy a droplet effect was noted because the distance between the stopper and the mould which was 120mm. Molten matrix was found to be leaking during pouring.

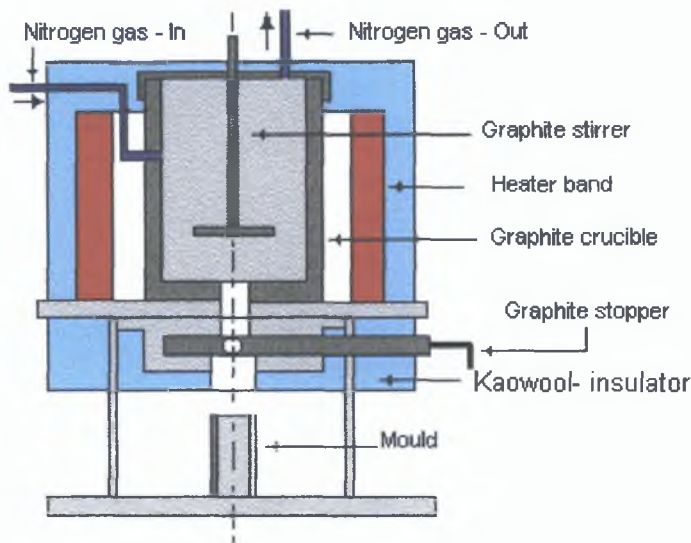


Figure 3.4: Rig with a new pouring mechanism, made of graphite.

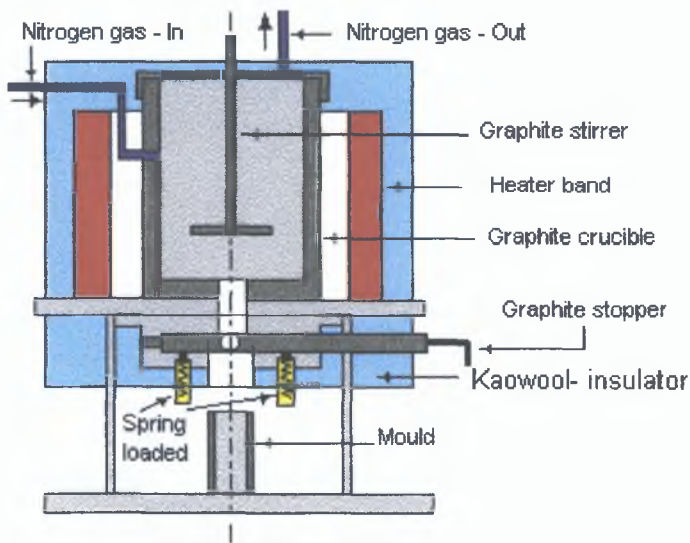


Figure 3.5: Modification to the pouring mechanism, using a spring loaded device.

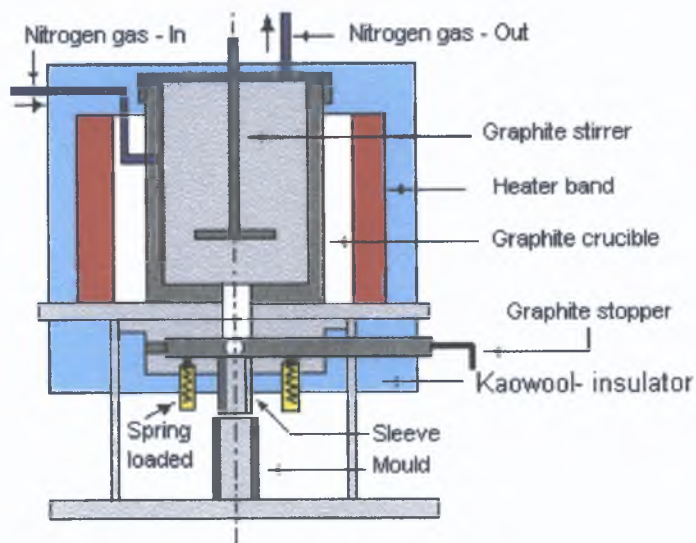


Figure 3.7 : Graphite sleeve have been used to avoid droplet effect.

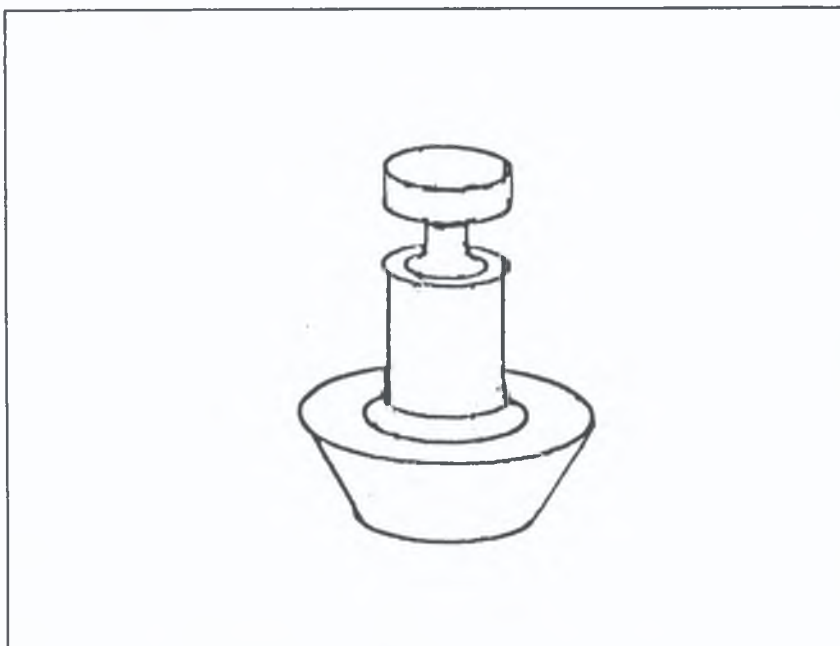


Figure 3.7 : Schematic Diagram of stopper

A series of experiments were run, however the leaking and sticking problems persisted. Several modifications were made to the pouring mechanism (Figure 3.5), and a graphite sleeve was designed (Figure 3.6) in order to minimise droplet effect of the MMC during casting. It was thought that the leaking problem may be due to the differences in thermal expansion of the stopper and the main frame which were made of graphite and steel respectively. Spring loading was used, in order to minimize this problem. It was also found that the graphite crucible was eroded at the outer wall while the inner wall remained in good condition. This was because the outer wall was exposed to air. The leaking problem may also be therefore have due to the fact that the graphite in the stopper was oxidised and eroded.

The basic insights gained from the above preliminary designs, and from a number of rig designs found during the literature review (as shown in Appendix A), resulted in a new design of rig. The emphasis of the new design of rig was on the pouring mechanism, and on providing an inert atmosphere for both the crucible and molten aluminium. AUTOCAD-14 was used to draw the components. For most parts of the design graphite was used as the main material. Detailed drawings of this rig are represented in Appendix B. 100-mm diameter graphite solid billet was used. Graphite is known to be a brittle material, and special attention is required during machining of this material. A lathe and CNC machine was used to fabricate the crucible, and to fabricate a specially designed stopper (Figure 3.7) and stirrer (Figure 3.8).

Difficulty in machining the graphite components was overcome by using ample coolant and suitable protective clothing. Changes were made to resolve the persistent pouring problems. The shape of the base of the crucible was changed, and a stopper incorporated into the stirring rod. A taper base shaped crucible was chosen in order to facilitate the flow of the slurry during pouring, and the stirrer shape was designed to suit this base.

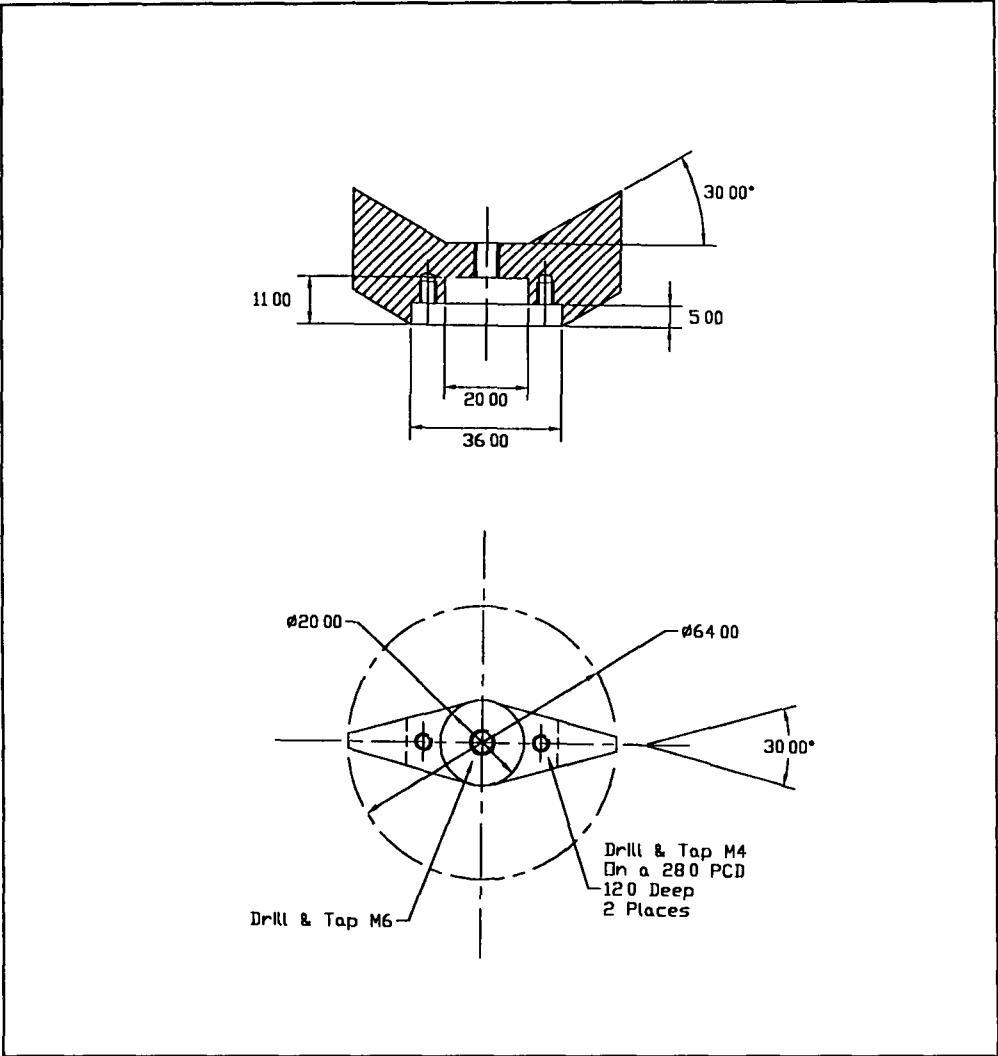


Figure 3.8 Schematic diagram of stirrer

In order to minimize the heat loss, a 50 -100 thickness kaowool insulator was placed around a heater band. A continuous purge of nitrogen gas at a flow rate of 3cc/min was used inside and outside of the crucible, in order to minimise the oxidation of molten aluminium and graphite parts. Figure 3.9 shows a schematic representation of the final rig design. A temperature controller was used to control the temperature inside the crucible. A K-type thermocouple was used and placed inside the crucible, in order to get a precise measurement of the molten temperature, and this thermocouple connected to a STUDIO 3000 temperature controller, and to the PICO data logger system. The temperature inside the crucible could either be displayed in the form of a temperature vs time graph, or in table form. A digital DC motor was used to stir the slurry. During loading, the top part of the rig was raised up, as shown in Figure 3.10. For pouring the stirring rod assembly needed to lift up about 5-10 mm. This opened the stopper and allowed the slurry to flow down into the mould, as shown in Figure 3.11, whereas Figure 3.12 shows a photograph of the rig.

Item No	Description
1	Digital DC Motor
2	Stirring Rod
3	Bearing Housing
4	Heater Band
5	Kaowool Insulator
6	Stirrer
7	Stopper
8	Steel Pipe (Nitrogen gas Input)
9	Graphite Crucible
10	Graphite Mould
11	Steel Pipe (Nitrogen Gas Input)
12	Steel Pipe (Charging)
13	Crucible Lid

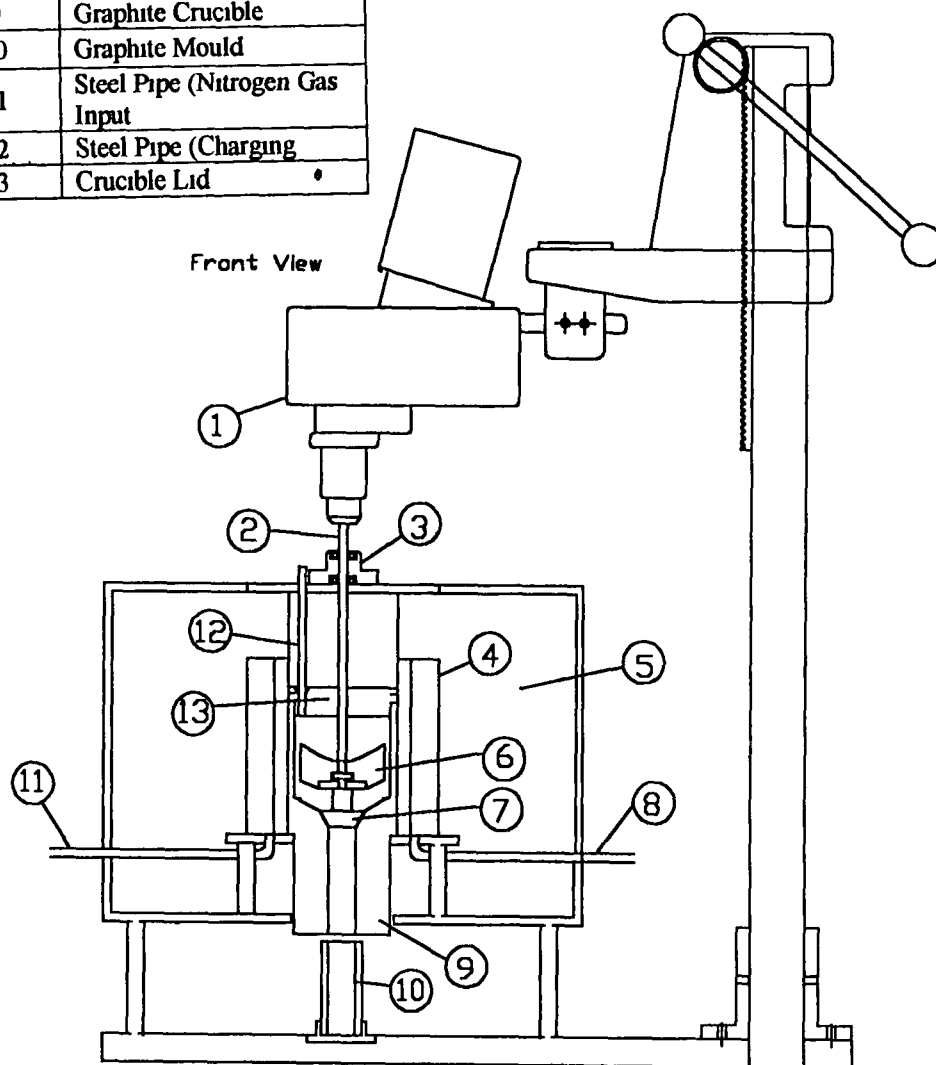


Figure 3 9 Schematic diagram of the final rig design

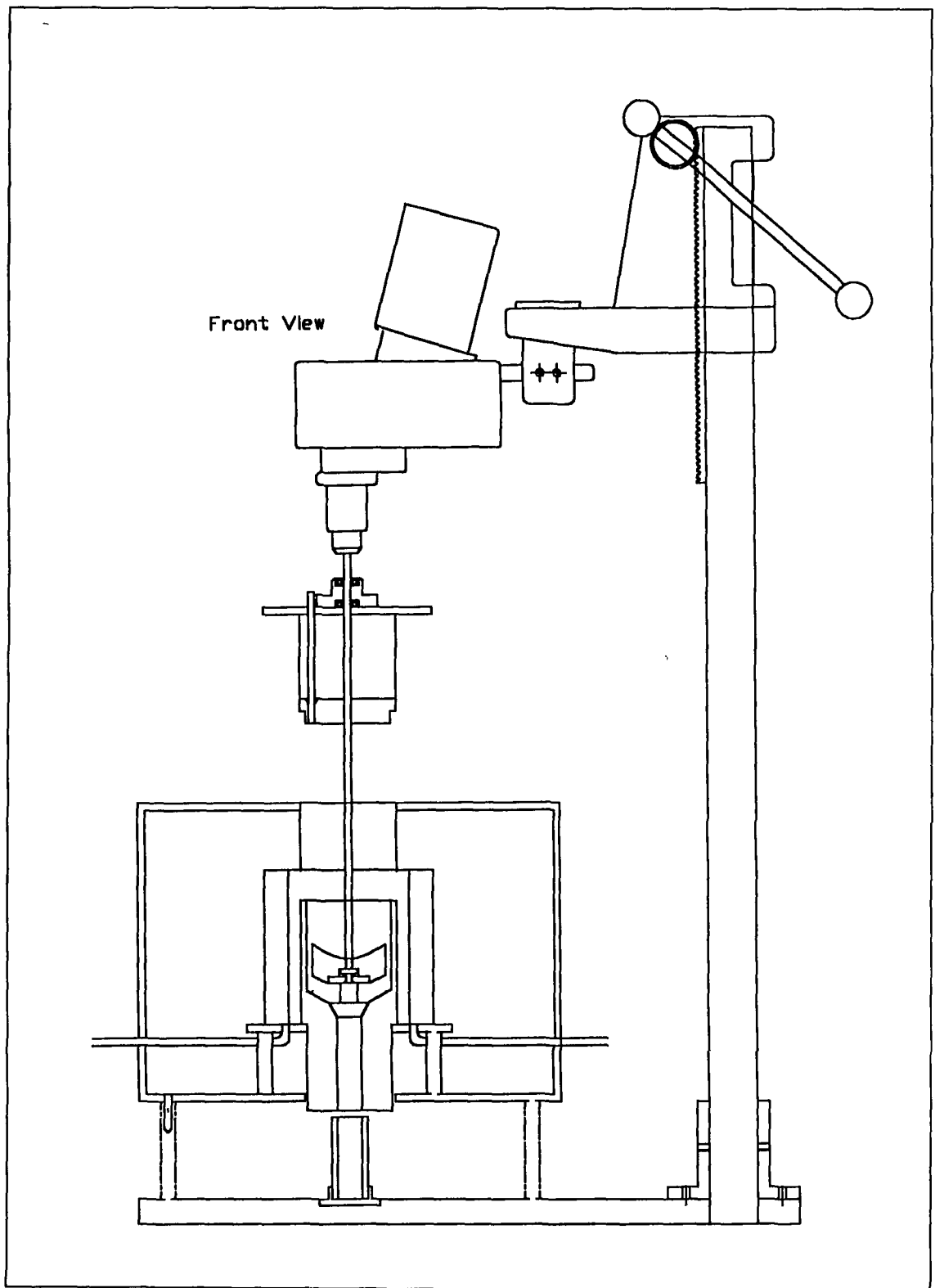


Figure 3 10 The position of top part of the rig is raised up during loading

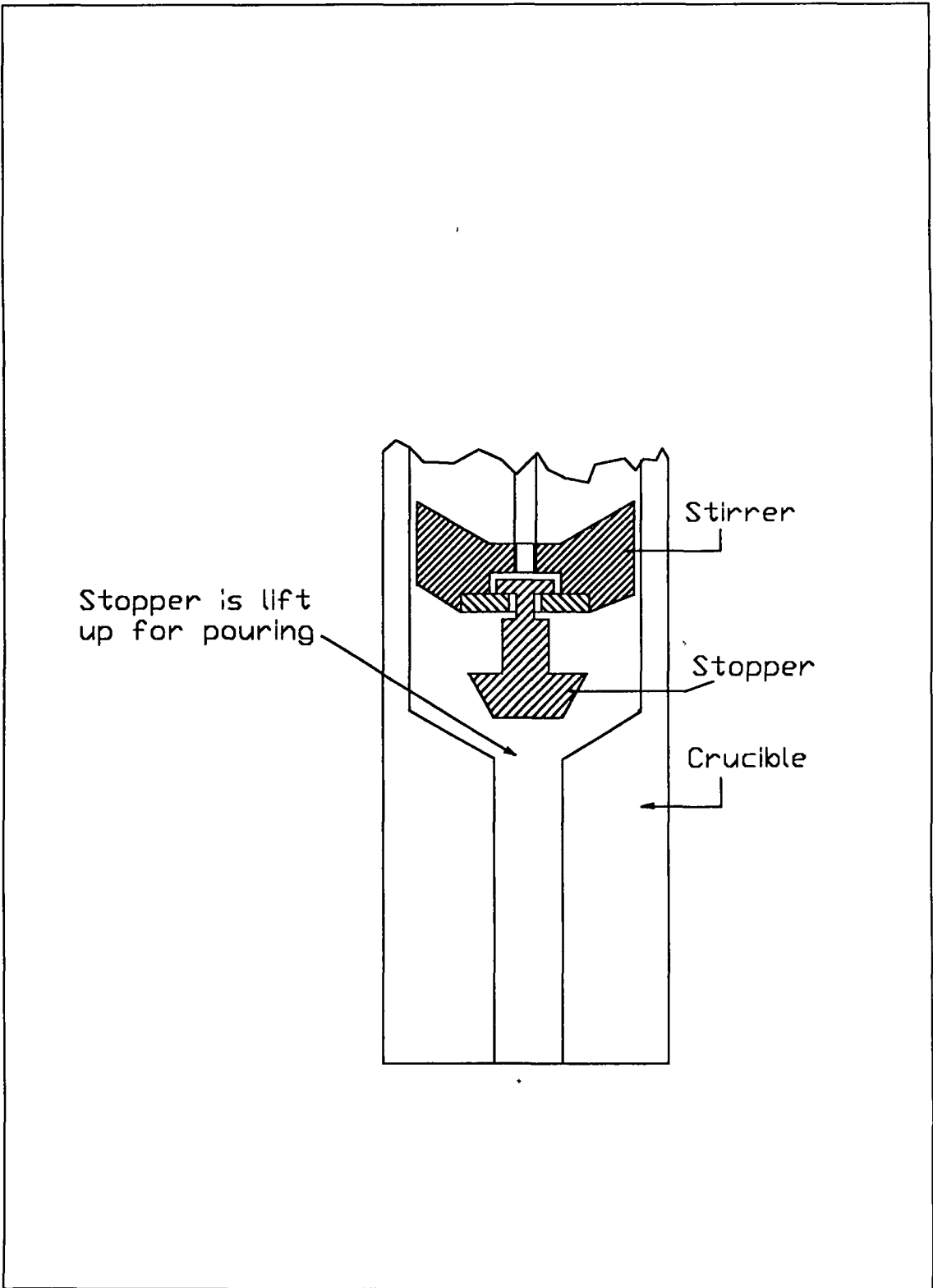


Figure 3 11 The position of the stirring rod assembly during pouring operation

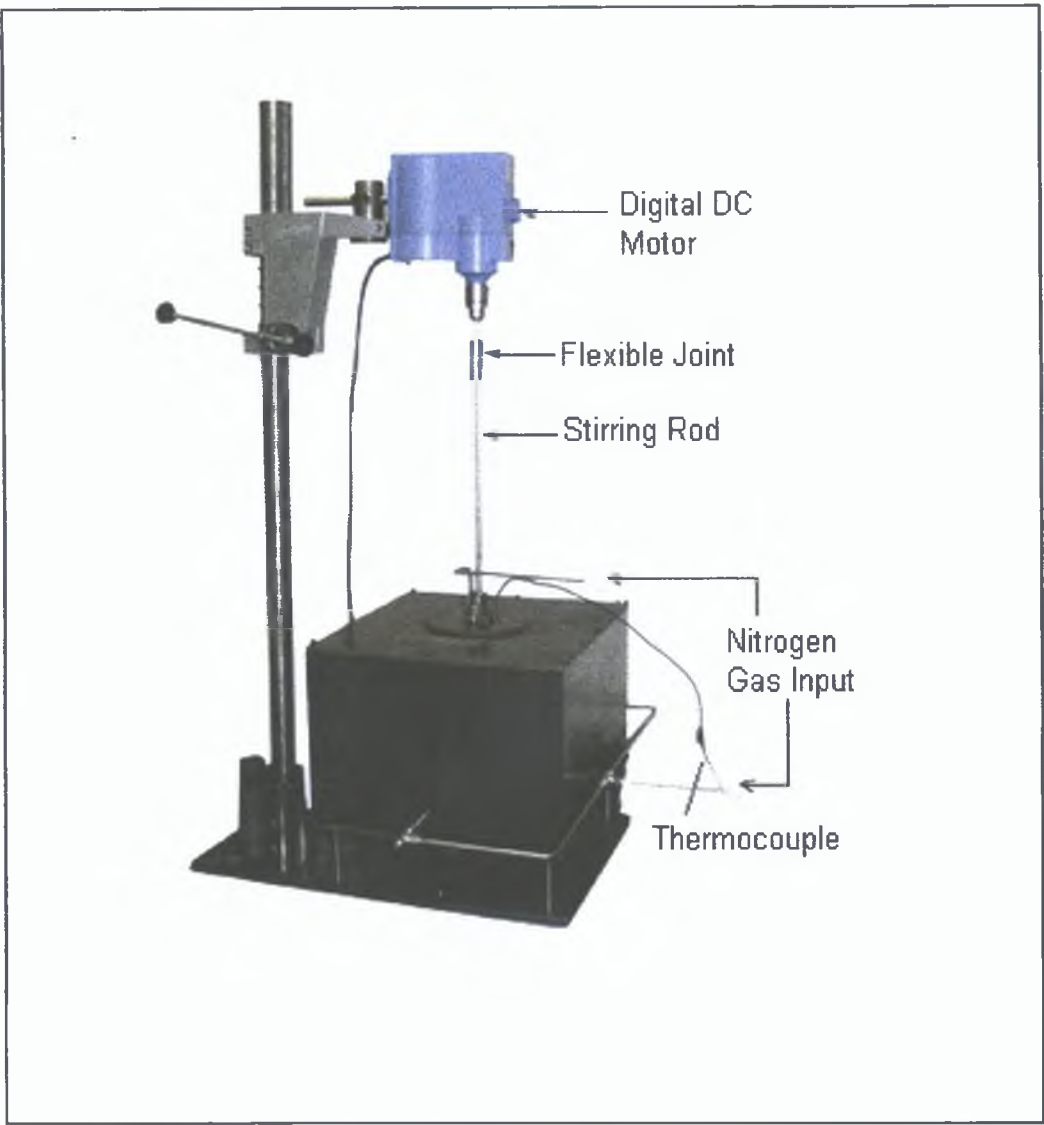


Figure 3.12: Photograph of the rig used.

3.3 WETTABILITY EXPERIMENTS

Several attempts were made to incorporate silicon carbide particles into a molten matrix. However, this has proved very difficult. SiC particles used were in as received condition. The silicon carbide particles remained at the bottom of the crucible, no matter how high the stirring speed. During stirring in a completely liquid condition, some of the particles tended to float to the top of the melt, and some accumulated at the base of the crucible. Microscopic observations showed that there are no SiC particles in the matrix alloy or in other words the wettability was zero. However, it is well documented in the literature how researchers tackle this wettability problem. Based on their experiences and the methods used to promote wettability between SiC and aluminium alloy, several experiments have been carried out. The main focus was to solve the problem of poor wettability between these two substances.

For the wettability experiments 1 to 4, a steel chamber was placed inside an electric furnace and a nitrogen gas atmosphere of flow rate of 3 cc/min used. The temperature of the furnace was raised to 700°C, and kept at that temperature for one hour to melt the matrix alloy. Stirring in fully liquid condition meant that, the slurry was stirred above the liquidus temperature of the A359 alloy, which is about 600°C. Conversely, stirring in semi-solid condition means that the stirring was performed at a temperature between liquidus (600°C) and solidus (565°C). The experimental set-up is as shown in Figure 3.13 (a) and (b). For experiment 5 a special design of rig was used, as shown in Figure 3.9. The advantage of using this rig is that, the temperature of the slurry, the stirring time and the oxidation of the melt can be controlled or minimised. For all

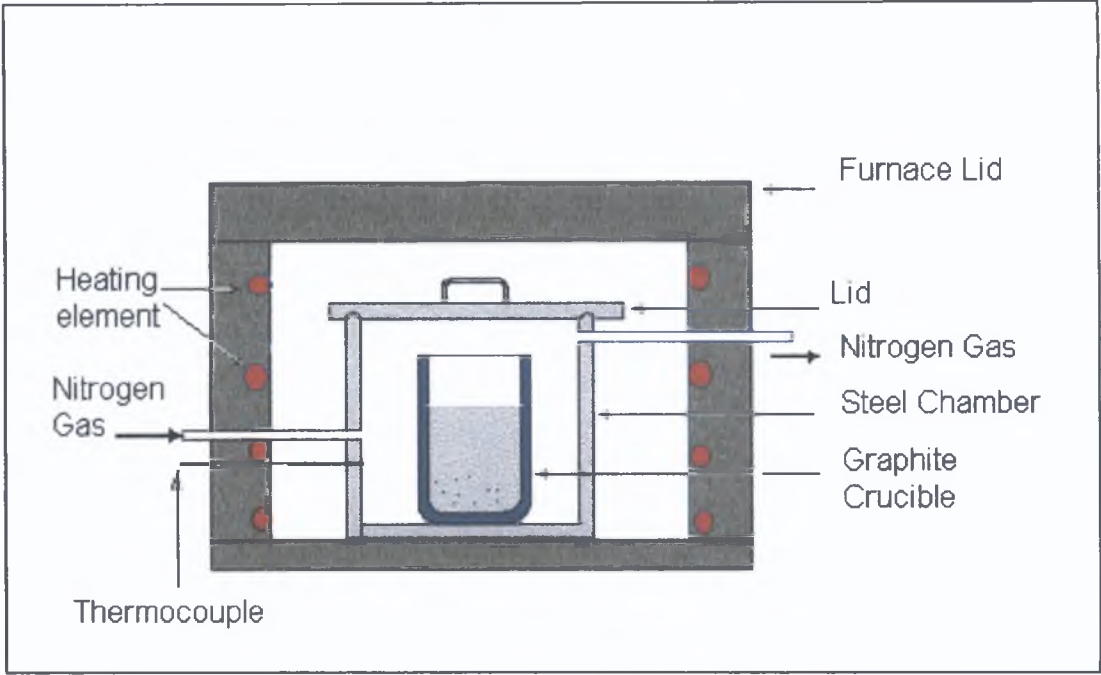


Figure 3.13: Wettability tests 1 to 4, using an electric furnace.

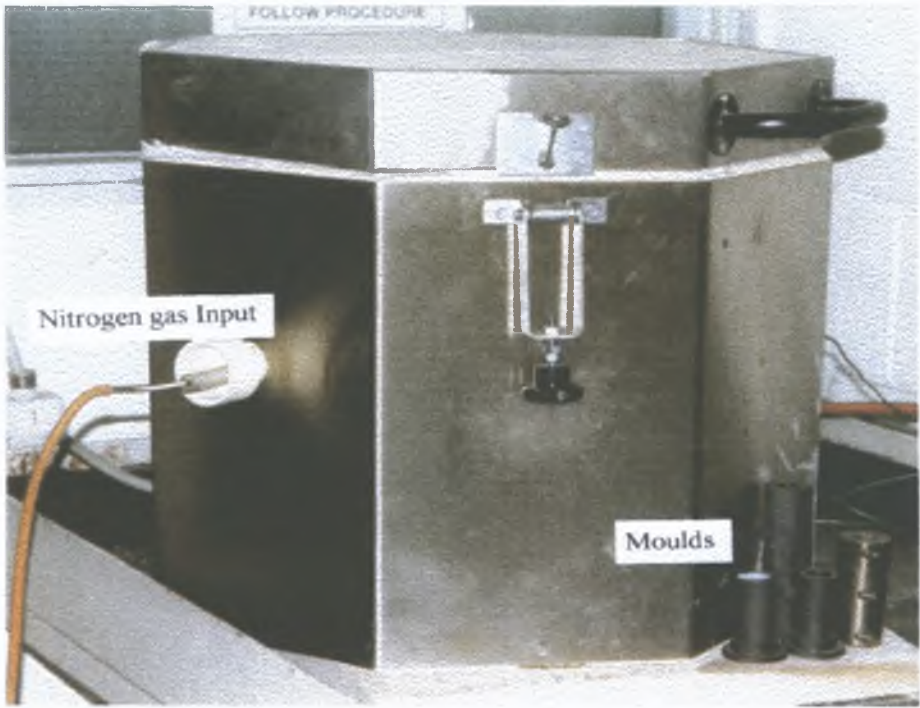


Figure 3.12(a) : Photograph of an electric furnace.

cases, the A359 matrix material was section into a small pieces of 3-5gram weight for each piece, in order to help it melt faster Magnesium used was in powder form

3.3.1 Wettability Testing

The wettability tests carried out mainly focused on the amount of particles, which can be incorporated into the matrix alloy, by considering several factors including

- Test 1 The effect of heat treated and non-heat treated SiC particles without the application of mechanical stirring
- Test 2 Stirring in fully liquid condition
- Test 3 Stirring in semi-solid condition
- Test 4 Varying magnesium content
- Test 5 Varying stirring temperatures, stirring conditions and volume fraction of SiC particles

The effect of heat-treated and non-heat treated SiC particles without the application of mechanical stirring (Wettability tests 1).

Initially the intention was to study the wettability of SiC particle with A359 matrix alloy without the application of any stirring Four sets of conditions were studied and are listed in Table 3 1 All the substances were placed in graphite mould, of 20-mm inner diameter and 20-mm height, which gives a cylindrical shaped mould cavity A nugget of A359 alloy was placed inside the mould first, and for mixture A, the SiC

particles were spread on the top the alloy without any pretreatment However for the mixture B and D, the SiC particles were oxidized at 900°C for 4 hours

In mixtures C and D, the SiC particles and the Magnesium powder were mixed thoroughly before being spread on the top of the alloy Because this is a very first stage of wetting test, the amount of SiC particles used was not given attention All the moulds were placed inside the gas chamber in the furnace and were brought together to 700°C over 4 hours, and soaked at that temperature for 1 hour Each sample was then taken out of the furnace and left to cool slowly in air at room temperature

Table 3 1 Materials for wettability test 1

Sample	Composition
A	A359 + SiC particles (as received)
B	A359 + SiC particles (oxidized at 900°C
C	A359 + SiC particles (as received) + 1%Mg
D	A359 + SiC particles (oxidized) + 1% Mg

Stirring in fully liquid condition (Wettability test 2)

A second series of experiments was carried out, in order to study the effect of stirring in fully liquid condition on the wettability between silicon carbide and the A359 matrix alloy The same types of material combinations were used, but this time with 10-volume percentage SiC particle content A 80 mm diameter graphite crucible was used as

the container. These experiments were repeated four times. The mixture was heated up to 700°C and soaked at that temperature for about 1 hour, to make sure that the mixture was in a fully melted state before stirring. The crucible was taken out from the furnace, and manually stirred. For all cases the stirring was carried out for about 2-3 minutes only to avoid solidification. The molten matrix was stirred manually and then poured into the cylindrical mould. This experiment was repeated by varying the stirring speed, qualitatively.

Stirring in semi-solid condition (Wettability test 3).

In order to study the effect of stirring the mixture in a semi-solid condition, experiments were conducted with the same components and procedures as in wettability tests 2. However the stirring of the molten mixture was continued until the slurry became viscous and the stirring became difficult. For this, the stirring was carried out for about 4-5 minutes. The crucible was then placed back inside the furnace, to re-melt the slurry at 700°C, and it was soaked at that temperature for 30 minutes. It was removed from the furnace and stirred again for about 2-3 minutes before being poured into the cylindrical mould.

Varying magnesium content (Wettability test 4)

Further tests were done to study the effect of magnesium content on the enhancement of wettability between silicon carbide and A359 matrix alloy, under both conditions of stirring. Four different types of mixture were tested. Each mixture contained 10-volume percent of SiC particles and A359 matrix alloy, with weight

percentages of magnesium content of either 0, 1, 2, or 3 The SiC used was in as-received condition

The experiments were divided into two sets For the first set, the mixture was heated to 700°C until it melted The stirring was carried out in a fully liquid condition, and for the second set, the stirring was carried out on semi-solid slurry and was followed by a second stage of mixing in a fully liquid condition before being poured into the mould

Varying stirring temperature, stirring conditions and volume fraction of SiC particles (Wettability testing 5).

The wettability tests 1 to 4 were repeated using the specially designed rig This was because the testing which was done initially did not have facilities to record the temperature of the slurry during stirring, and the stirring was also done manually The oxidation problem could also be minimised by using this rig

From the wettability testing 1 to 4, it was found that the use of magnesium as a wetting agent can promote the wettability between SiC particle with A359 matrix alloy Therefore, for the test 5 series, only the effect of the stirring condition was repeated For this purpose, the mixture of A359 matrix alloy with 10 volume percent of SiC particle and 1 wt % magnesium was used The stirring speed used was 100 rpm Three stirring conditions were investigated

- i The mixture was heated to its fully liquid temperature, which is about 700°C, and stirring was applied for 10-15 minutes, before the stirring rod assembly was lifted up to pour the slurry into the mould. The temperature profile used is as shown in Figure 3 14
- ii The mixture was heated to a temperature between the solidus and liquidus of the matrix alloy, which was 590°C, and the stirring was applied for 10-15 minutes, then the slurry heated to 700°C and soaked for 30 minutes, and re-stirred for 5 minutes before poured into the mould. Figure 3 15 shows the temperature profile used
- iii The mixture was heated to 700°C and soaked for one hour, then the heating was stopped, and the temperature allowed to drop to 550°C. The stirring was carried out during the temperature drop, until the slurry almost fully solidified. Then the temperature was increased to 700°C and held for 30 minutes, and re-stirred before pouring into the mould. The temperature profile used is shown in Figure 3 16
- iv By using the temperature profile type such as in Figure 3 16, a series of experiments were carried out to study the effect of reducing the solidification time during stirring and also, to study the effect of volume fraction of silicon carbide particles, on wettability enhancement. In order to reduce the cooling time, the flow rate of the nitrogen gas inside the

crucible to the melt surface, and to outside the crucible, has been increased. The detail of temperature measurement data is as shown in Appendix C.

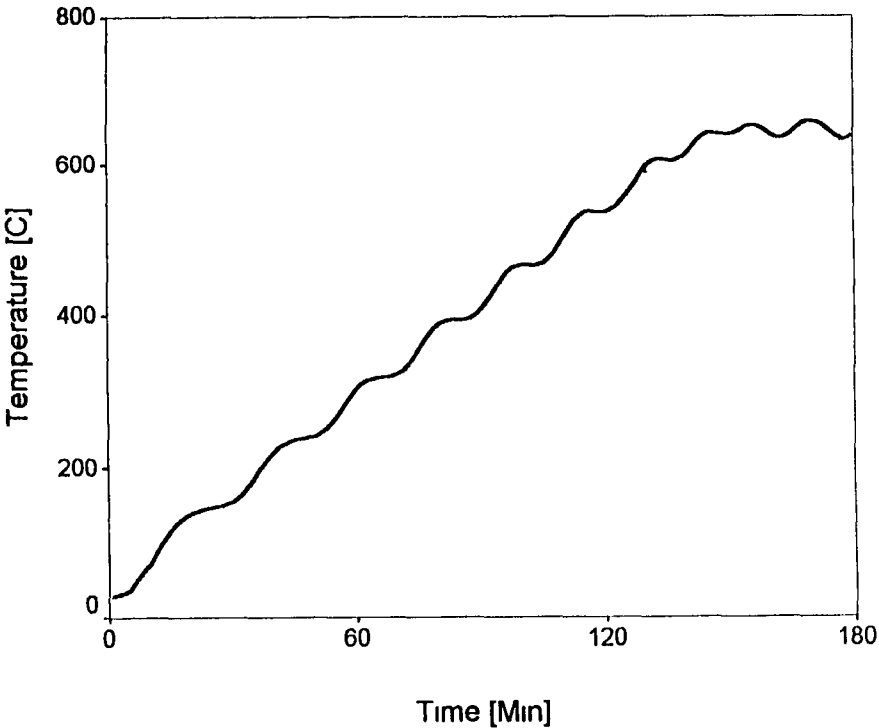


Figure 3 14 Temperature profile for stirring in fully liquid condition (1)

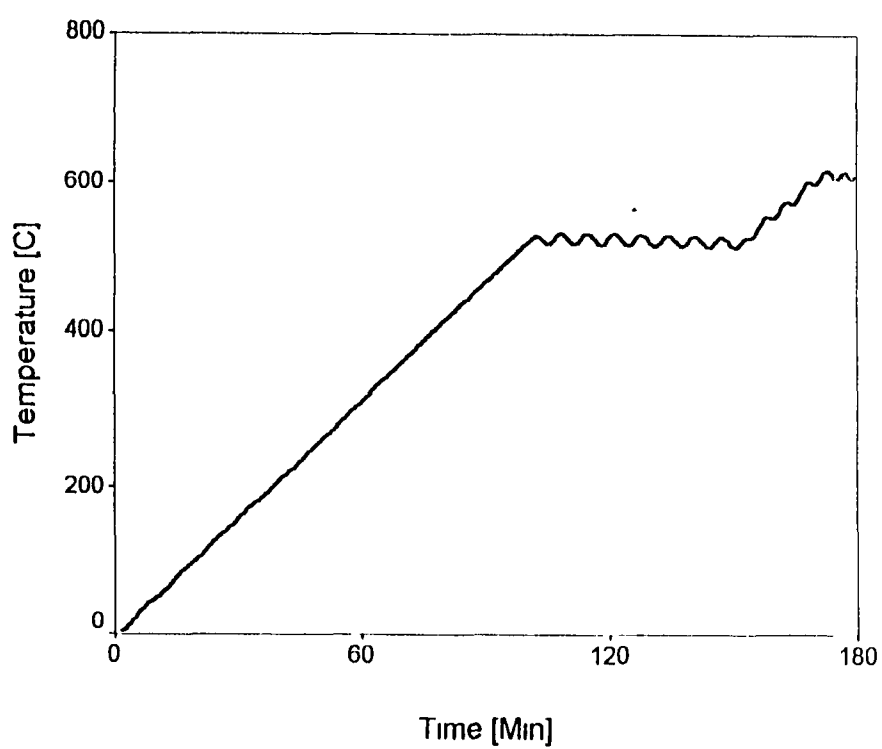


Figure 3 15 Temperature profile for stirring in semi-solid condition -(11)

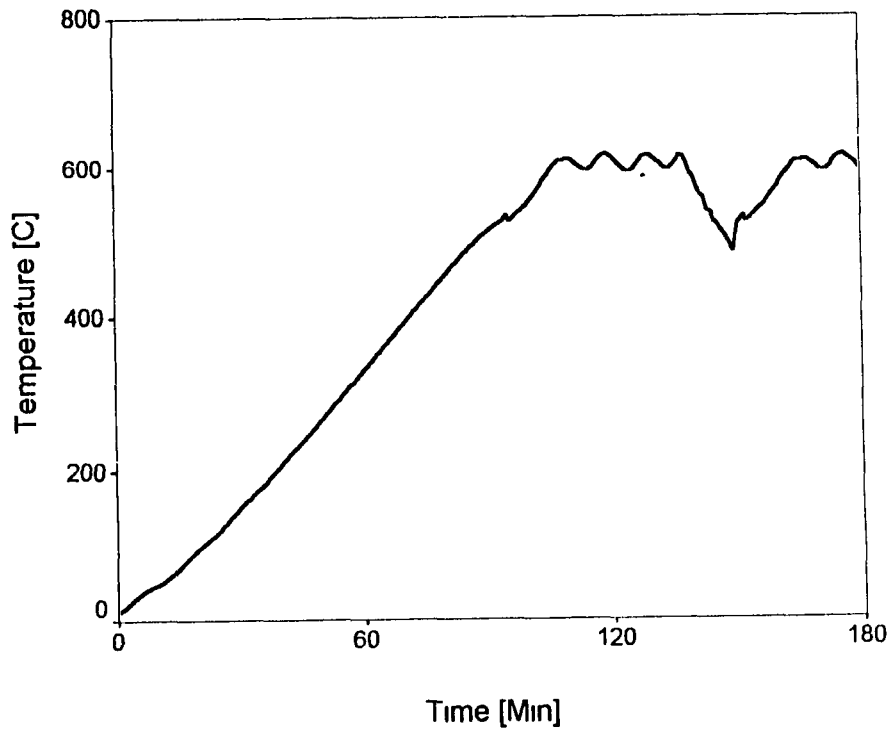


Figure 3 16 Temperature profile for stirring in semi-solid condition –III

All the samples from the wettability tests 2 to 5 were sectioned at three different locations 5 mm from the top, at the middle, and 5 mm from the bottom. For wettability tests 1, all the samples were sectioned vertically. For each specimen, four samples of micrographs were taken for analysis and for point counting to measure wettability percentage.

3.3.2 Wettability Measurement Method

It is proposed that the percentage of SiC incorporated within the solidified composite is indicative of the success with which wetting was achieved.

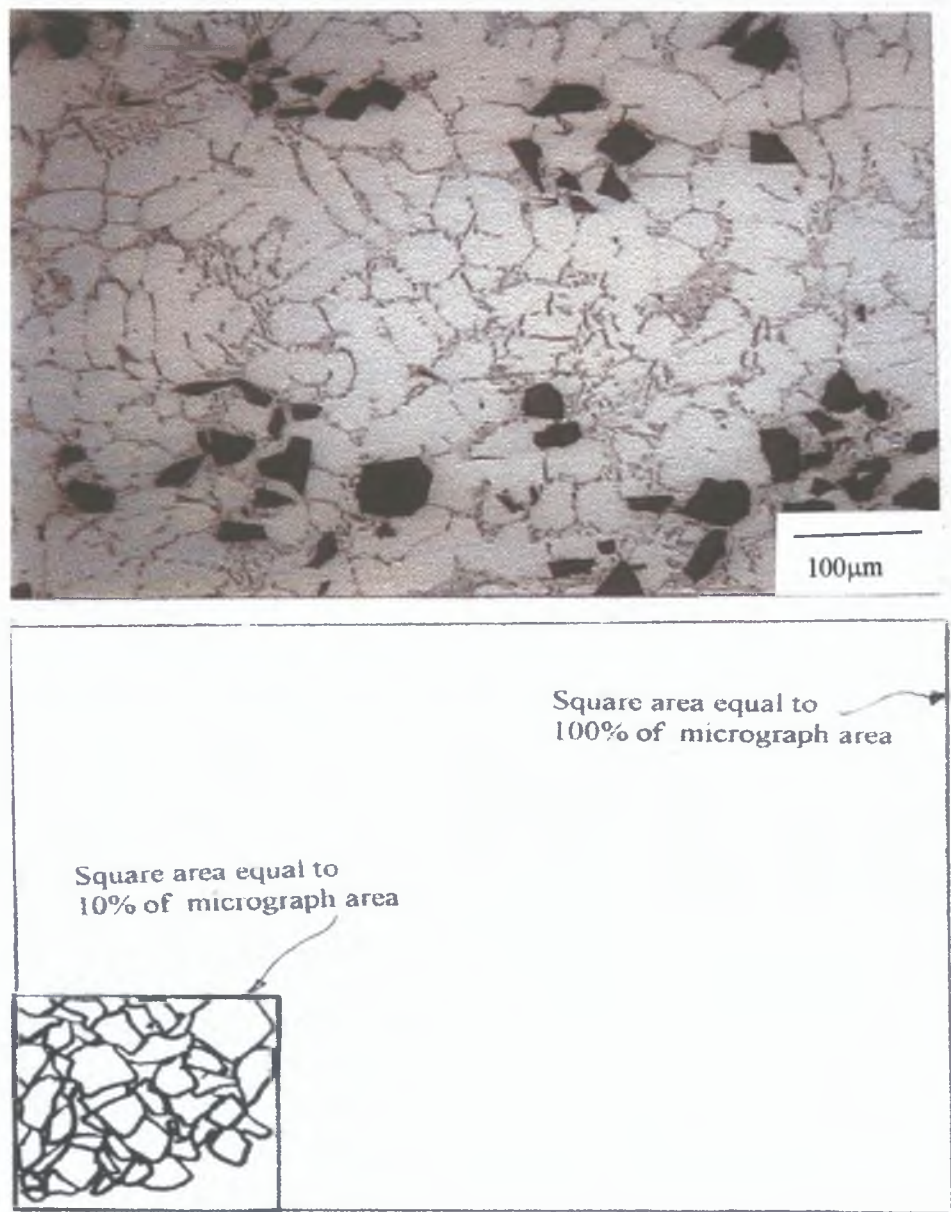


Figure 3.17: Wettability Measurement

Therefore measuring the amount of SiC is necessary. This was done using a graphical method based on 2 dimensional micrograph of the composites, Specifically the total area of SiC as compared to the total micrograph area. The micrographs used were at 80 X magnification, and 8 samples were investigated for each cast MMC sample, which were section at the middle of 150mm long ingot. To determine the total area of SiC particles, which occupied a particular micrograph, tracing paper was used. For example, to calculate wettability percentages for A359/SiC/5p cast MMC samples, the area size of 5 % of the total micrograph area was drawn on tracing paper. In order to facilitate the process, a square shape is used. Then tracings were made of individual particles, into the square. The wettability percentage for each micrograph is evaluated approximately, based on the total area of the SiC particles in square are. If the area of the SiC particles fully occupies the square, that means that the wettability is 100 percent. Figure 3 17 shows an example of Wettability Measurement Method used for A359/SiC/10p cast MMC. Detail results of these wettability measurements are shown in Appendix D. This method of measuring wettability is subject to error as it relies upon a two dimensional section to evaluate a three dimensional parameter. In addition, errors may occur in tracing out individual particles, and for this reason a high number of samples were taken.

3.4 MMC FABRICATION

A series of wettability tests were carried out, before the method to improve the wettability between silicon carbide particles with A359 matrix alloy was identified. From these tests, it was found that using 1 wt % of magnesium, coupled with the semi-

solid stirring method, promoted wettability This information was used to fabricate cast MMC The MMCs were produced using an electric furnace, while waiting for the rig to be manufactured The intention was to produce cast MMC, by stir casting and evaluated this casting using optical microscope and a mechanical testing device The fabrication process is summarised in the flow chart in Figure 3 18

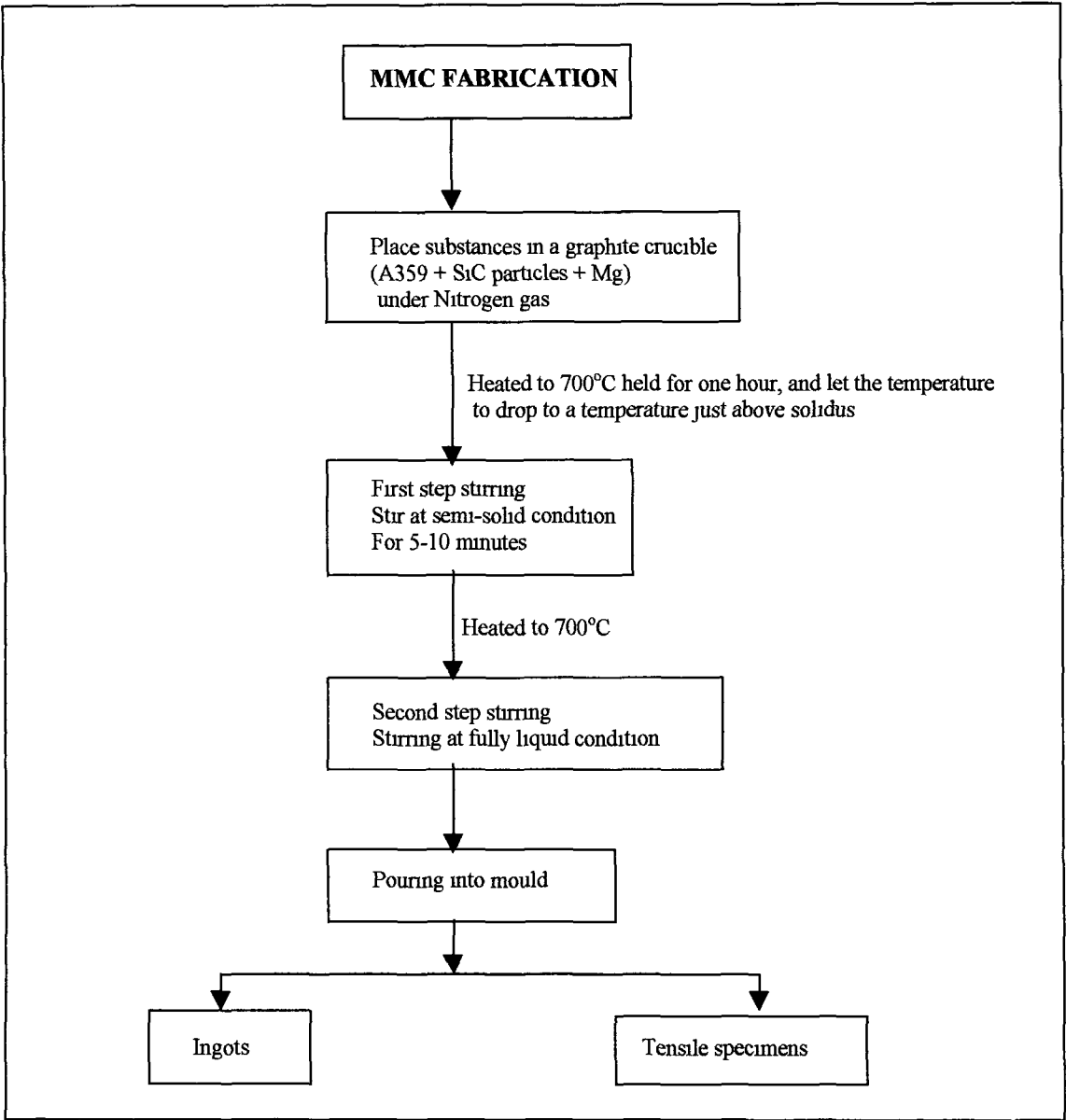


Figure 3 18 Flow chart of flow process of MMC fabrication method used in this study

3.4.1 Materials

The aluminium alloy used was A359 as a matrix material, and SiC particles were added as reinforcement particles. A359, silicon carbide particles and magnesium were supplied by the Aluminium Powder Company limited, UK. The properties of these materials are shown in Table 3.2 and 3.3 respectively, whereas the thermal properties are shown in Table 3.4. This type of aluminium alloy was chosen because increasing the silicon content in the matrix reduces the dissolution of SiC and prevents the formation of chemical reaction product Al_4C_3 . Usually 7-15wt% Si was used [68,205]. A359 aluminium alloy has the following characteristics: good castability and mechanical properties, light weight and excellent oxidation resistance, and is widely used. A359 alloy reinforced with particles or short fibers of SiC are employed in the fabrication of castings for automotive and aerospace applications. Silicon carbide particle was chosen as reinforcement material because it is the most used of the particle material for aluminium alloy matrix composites. This is because of combination of mechanical properties, density and costs [47]. The silicon carbide particle's size of 29.2 μm was the only size of the particle, which is available from the supplier. However, this size is not much different from those used for most molten metal process involving ceramic particles, which tend to be in the range of 10 - 20 μm [46].

Table 3.2 Chemical analysis A359 alloy matrix - wt % (from supplier)

Si	Mg	Cu	Al
8.5-9.5	0.55 – 1.2	< 0.03	Balance

Table 3 3 Properties of SiC particles and Mg powder used (from supplier)

Material	Hardness [Vickers]	D ₅₀ APS* [Microns]	Chemical analysis [wt %]					
			SiC	SiO ₂	Si	Fe	Al	C
SiC	2800-3300	29.2	98.73	0.48	0.3	0.09	0.1	0.3
Mg	-	256	Mg	O ₂				
			99.79	0.1				

* D₅₀APS = Average Particle Size which is based on the cumulative frequency size distribution

Table 3 4 Thermal properties of A359 alloy and SiC [246]

Properties	A359	SiC
Thermal conductivity [W/m ² K]	152.0	83.6
Specific gravity [g/cc]	2.68	3.21
Liquidus temperature [°C]	600	-
Solidus temperature [°C]	565	-
Coefficient of Thermal Expansion [$\times 10^{-6}/K$]	20.9	4

These composites have received a considerable amount of attention because of their much lower costs of fabrication compared to their continuous fibre-reinforced counterparts. The lower cost of the silicon carbide particle, is also the main reason why this reinforcement was chosen. Continuous forms of reinforcement materials are not suitable to the stir casting method. This is because the stirring action is found to cause the reinforcement to fracture. Magnesium is a well-known wetting agent, used to improve the wetting of the ceramic by the liquid alloy.

3.4.2 FABRICATION METHOD

The A359 matrix material was received in the form of 1 2-kg ingot. The ingots were cut into smaller pieces of about 3 to 5 grams weight for each piece. The reason for this was to minimise the dwelling time, or in the other words, to make the alloy melt faster. Another benefit of using smaller pieces is to help to give more precise reading during weight them. The ingots were cut to the small pieces by using a cut off machine, with a cutting wheel of grade HH especially for non-ferrous metal, with a continuous flow of coolant, to avoid any overheating of the ingot and also the cutting wheel. After cutting, the ingots were washed using warm water, then dried at about 70°C for about 1 hour, before being weighted. For one experiment, about 200 gram of the A359 was placed into a graphite cylindrical 80-mm diameter x 100mm long crucible. The weighing of the matrix alloy, silicon carbide and magnesium were carried out using an analytical balance with an accuracy of 0.01 grams. 1 wt % of magnesium particles were used as a wetting agent, and the amount of SiC particles used was varied from 5 to 25 vol %. The graphite crucible was placed inside a steel chamber. This method was almost similar to the method used in wettability test 1 to 4. A J-type thermocouple was inserted into the steel chamber to give a feedback of the temperature inside the chamber to the temperature controller of the furnace. Special computer software, namely PICO with thermocouple data logger facilities was used to read the temperature and display it on a computer monitor.

The furnace was preheated to 100°C, and the nitrogen gas set to flow continuously at a rate of 3cc/min. All the substances, A359 alloy, SiC particle, and magnesium were

placed inside a graphite crucible. The crucible was then placed in a stainless steel chamber inside the furnace, and the chamber closed. In order to get a controlled temperature inside the chamber and inside the crucible, the temperature of the furnace was increased step by step, to reach to the temperature of 700°C (took about 4 hours period). This temperature was raised in steps to 200°C, 500°C and 700°C with a ramp time of 2hrs, 1 hr, and 1 hr respectively. This heating procedure was slightly different to that used during wettability test because the quantity of the mixture used was higher, and required additional time to melt. Although the thermocouple was not attached to the crucible, it was expected that there was a very small difference between the temperature inside the chamber with the temperature inside the crucible as 1-hour soaking time was used. In any event, it is expected that the temperature inside the crucible was not more than 700°C. The experiment set-up using an electric furnace is as shown in Figure 3.13.

Theoretically the A359 matrix alloy melts completely at about 600°C. The temperature inside the chamber can be obtained from the thermocouple in the crucible, sending a signal to computer monitor screen of data logger system. After soaking for one hour at 700°C, the crucible with molten metal was taken out of the furnace, and before the stirring started the top layer of the melt was skimmed off. This is because the top surface always contains an oxidation and slag layer. The slurry was stirred thoroughly for about 4-5 minutes, until the slurry became partly solidified because of the dropping temperature. The stirring was stopped when the slurry became viscous making further stirring difficult. The crucible was then placed back inside the chamber, in the furnace, then heated back to 700°C for another half an hour. The melt was re-stirred for 2-3

minutes before being poured into a graphite mould. The pouring temperature of the mixture was found to be below 700°C, but above the liquidus temperature (600°C).

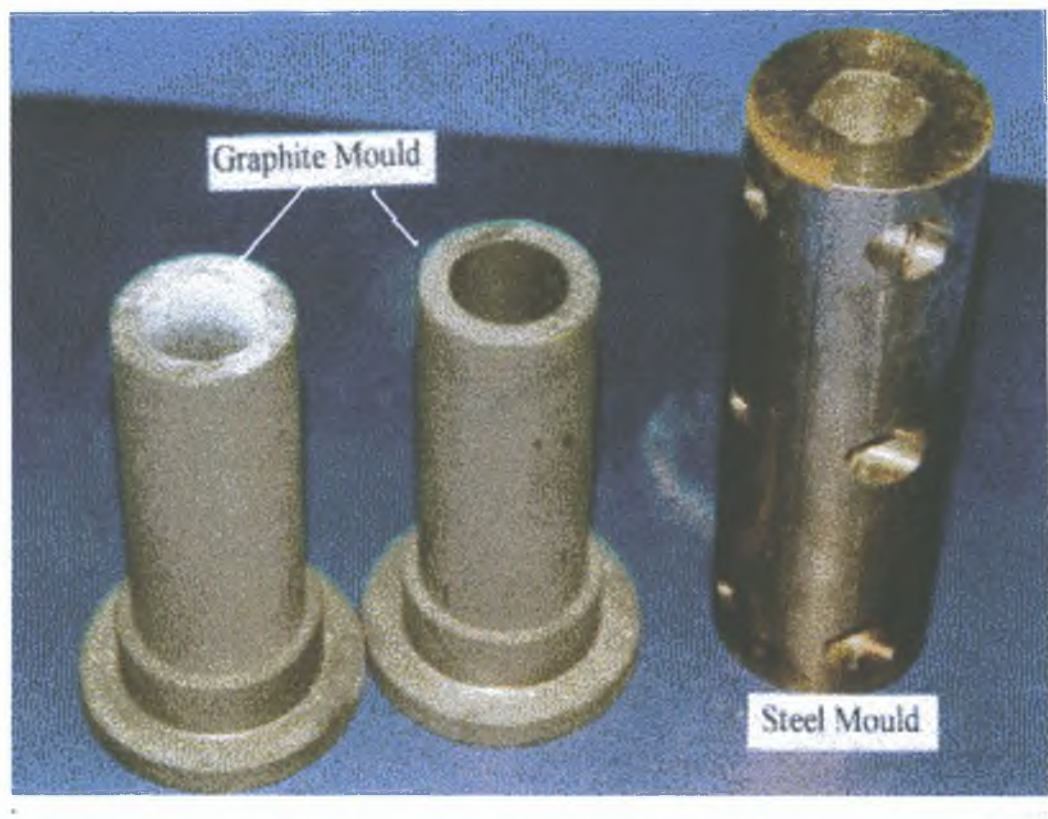


Figure 3.19: Moulds used to cast MMC ingots.

The resultant mixture was then cast into a steel and graphite cylindrical mould, of two different sizes but with same configuration. The smaller one was 10-mm diameter (ingot A) and the bigger mould was 18-mm diameter (ingot B). The mould was in a vertical position during pouring. Figure 3.19 shows the moulds used to produce ingot of cast MMC. The labeling system used to identify the cast MMC samples produced is based on the percentage of silicon carbide contained in the sample, and the type of mould used. For example for samples with labels such as 15G and 10 S: 15 and 10 indicate the

percentage of silicon carbide in the matrix during initial fabrication process; G and S stand for graphite and steel mould used to cast the MMC.

3.5 SAMPLE PREPARATION

MMC was produced in the form of cast ingots as shown in Figure 3.20. Ingot A was cut into samples of 7-9mm height, while the ingot B was cut into samples of 10-14 mm height, and these are shown in Figure 3.21 and 3.22 respectively. The samples from ingot A were used in porosity measurements, and in compression testing, whereas the samples from ingot B were used in porosity and micro hardness measurements. Both types of samples were also used in microscopic examination.



Figure 3.20: Cast MMC ingots produced.



Figure 3.21: Specimens from ingot type A, 10mm diameter.



Figure 3.22 : Specimens from ingot type B, 18 mm diameter.

3.5.1 Metallographic Preparation

MMC ingots were cut into smaller pieces. Cutting a material always causes a deformation of the surface, and often other types of damage, such as pull-out of silicon carbide particles. Therefore, during cutting, it is essential to reduce the damage of the

surface to a minimum. It is believed that to minimise this damage, a very low feeding speed, but constant pressure need to be used. For this purpose a HHH grade cutting wheels was used. A diamond cut-off wheel would give a better result, but these cutting wheels are very expensive, and were not available.

Metallographic preparation of particle-reinforced MMC was quite a challenge, as the reinforcement particles are very hard and fragile compared to the matrix materials. This combination of respectively hard and soft materials makes it difficult to avoid damages like cracks and broken reinforcement particles, and relief between the particles and the soft matrix during preparation.

A Struers Prestopress-3 was used to make specimen mounting. A Struers DAP-V grinding machine was used for the grinding and polishing operation to prepare samples for micro hardness testing and for microstructure analysis. Grinding is a very important step in the preparation process, as the surface damage done by the cutting are removed by this step. Grinding is divided into two steps: plane grinding and fine grinding.

The objective of the plane grinding is to make the sample surface plane, whereas fine grinding must reduce the surface damage introduced by plane grinding to a level to make polishing possible. SiC paper is often used for grinding of metal, and this must be avoided when the MMC is reinforced with SiC particles. This is because the soft matrix will quickly be removed whereas the SiC particles will in general remain intact. Plane grinding was performed, on a TEXMET grinding disc with 30µm diamond. This

grinding was done manually and only very light pressure was applied. The plane grinding took about 5-10 minutes. This was followed by fine grinding using TEXMET grinding disc with 9 μm , 6 μm , 3 μm and 1 μm diamond suspended in water as a lubricant. Scratches as a result of silicon carbide particles during polishing sometimes are unavoidable. The optical microscope Reichert MeF3 was used for the microstructure observation. This microscope was attached to a video printer which has facilities to print a photograph.

3.5.2 Preparation for Porosity Measurement

Samples used for porosity measurement needed to be grinded in order to make sure the top and the bottom surface of the sample is flat, and to minimise error because of the surface roughness. Density measurements were carried out in order to ascertain the volume fraction of porosity in the samples. Two different sizes, and two different mould materials were chosen in order to investigate the effect of size and mould material, or solidification rate on the density. The densities of cast MMC produced, containing different amounts of SiC particles were calculated by measuring the volume of a known weight of composite. From this data, calculations were made to evaluate the percentage of porosity in the cast MMC produced. To minimise the effect of surface irregularities, or the effect of the shrinkage and pores on the surface of the ingot, the average of the diameter of the sample was used. Three readings were taken at three different places on the sample using a digital Vernier caliper. The actual density of each sample was then directly evaluated from mass/volume. The value of density was then compared with theoretical data [265]. This data is shown in Appendix E.

3.5.3 Micro hardness and Compression Testing

A micro hardness tester of types LEITZ MINILOAD 2 (Figure 3 21(a)) was used to measure the micro hardness of the specimens. This tester is capable of measuring two kinds of hardness, Vickers and Knoop. In this study, Vickers hardness was employed. According to the indentation diameter of the diamond indenter (pyramid shape) made on the surface of the samples, the value of the microhardness can be read directly from a conversion tables provided by the manufacturer. For this microhardness measurement, the indentation load used was 100g. The main objective of this was to study the effect of SiC addition, and to measure the hardness of the matrix alloy. For microhardness testing, it is easier to find the suitable place or space for indenter that is in the matrix, but not on the particles. This is difficult to achieve if doing macrohardness such as Brinnell and Rockwell hardness testing. For micro hardness testing, all the sample used need to be fine polished in advanced. In this study, hardness of as-cast and after heat-treatment was tested. For as-cast specimens, the hardness was measured as a function of the distance from the top to the bottom of the ingot, referring to the original position of the ingot during pouring. The results of those measurements are shown in Appendix F. Hardness was also measured for each specimen after being heat treated, and the result of these microhardness tests are shown in Appendix G. A minimum of 4 hardness measurement were made on each sample.

Ingot A with a diameter of 10 mm was used for compression testing. The ingots were cut into small pieces, with lengths between 10-15mm. In order to avoid buckling during testing, a teflon layers were placed at both sides of the sample. The samples also

need to be grinded on both sides in order to make sure of flatness at both sides. The dimensions of the sample (initial diameter, and thickness) were recorded before testing. This information was used for the calculation to get the compression strength of the sample. Compression testing be carried out on as cast and heat-treated condition for various percentage of SiC content. The data result from this testing as shown in Appendix H.



Figure 3.21(a): LEITZ MINILOAD 2 Micro hardness Tester.

3.5.4 Tensile Testing

Normally tensile specimens may be produced by machining or turning on a lathe from ingot to the desirable shape or dimension, by following a certain standard. However for MMC materials, machining is a great challenge. The surface finish of the machined

MMC was not good, and a special tool has to be used. A good surface finish is important for tensile testing, because tensile properties are very sensitive to surface discontinuities. Therefore it is advantageous if this tensile specimen of MMC is fabricated directly from casting, so machining process can be minimised.

The dimension of the samples used in the present work followed MPIF Standard No 10, which is comparable to ASTM B783, ASTM E 8 and ISO 2740. The dimensions of the sample are shown in Figure 3.22. A pattern sample was first machined using a lathe, and this pattern was used in order to produce a steel mould, using an EDM machine. A metal or steel mould was chosen as mould materials in order to achieve the advantages of a faster cooling rate offered by this material, compared to graphite. The MMC slurry prepared was then poured into the mould. Several different volume fraction of SiC were used. The mould used is shown in Figure 3.23.

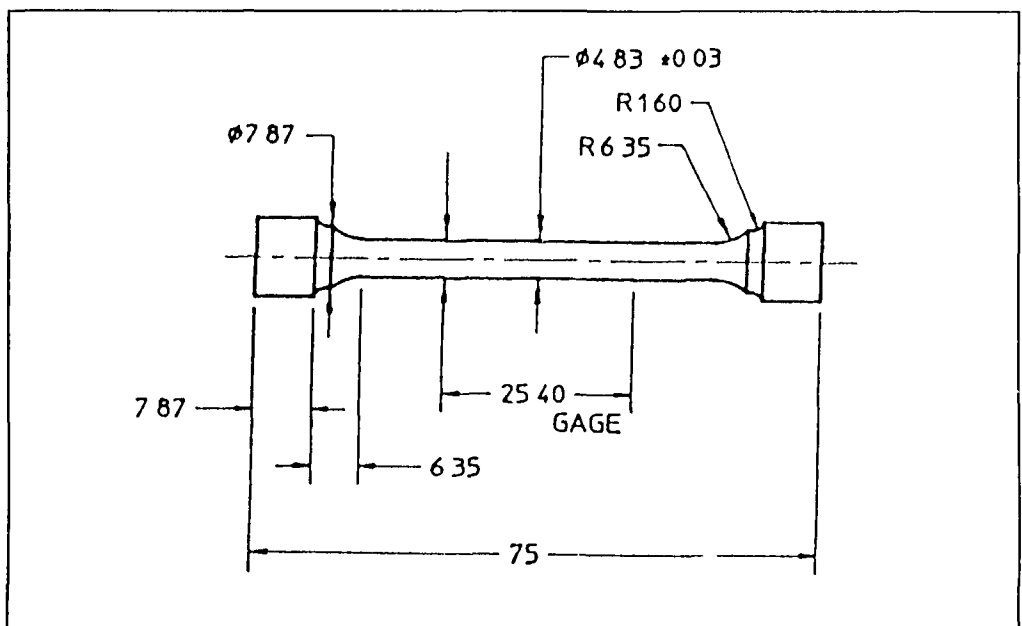


Figure 3.22 Dimensions of tensile specimen

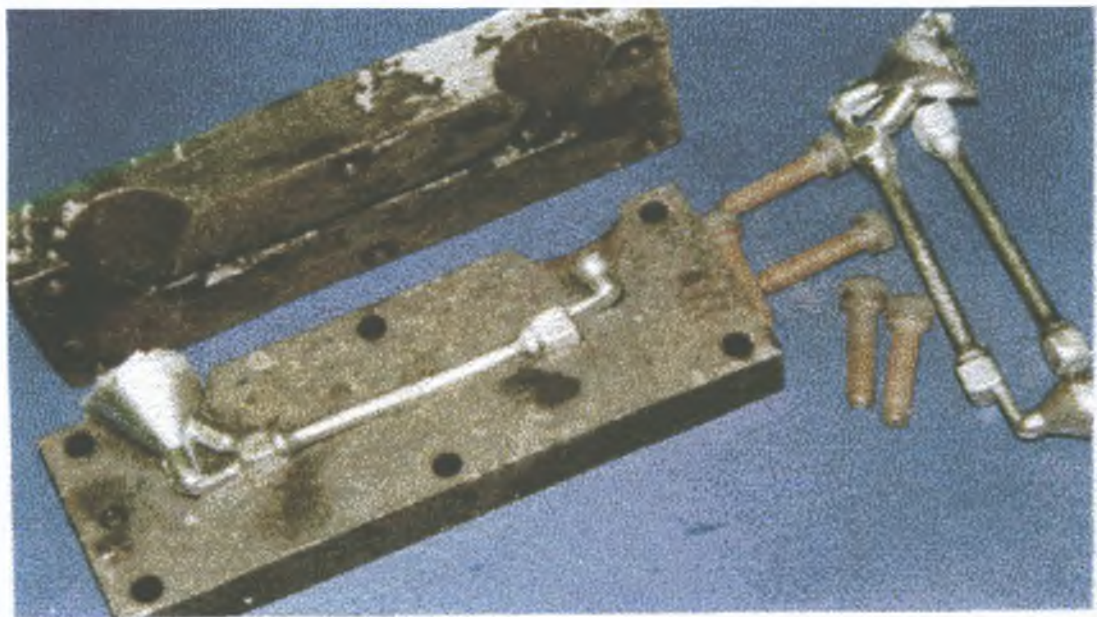
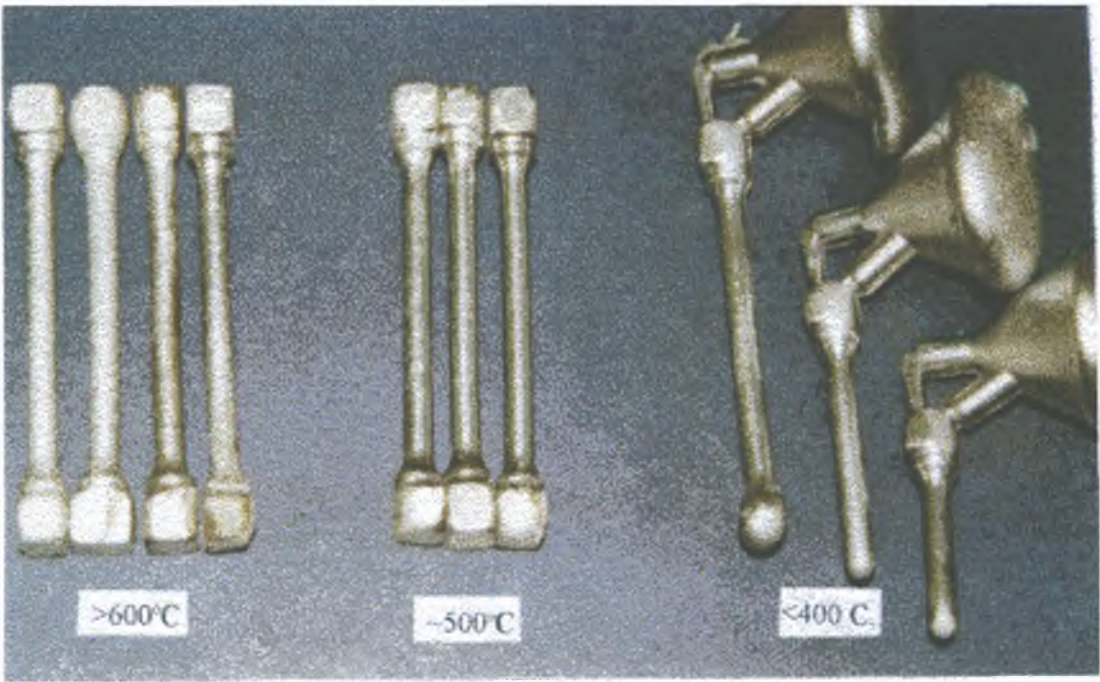


Figure 3.23 : Mould used to produce tensile specimens



(c)

(b)

(a)

Figure 3.24 : Tensile specimen produced from different mould temperatures.

It is quite difficult to produce tensile specimen directly by using this casting method. This is because the size of the mould cavity to produce the sample is quite small, and the ability of the MMC slurry to flow and fill the mould cavity is a very important factor, in order to give a good sample. It was found that the mould should be preheated, and the temperature of the MMC's slurry also needs to be controlled. If the temperature is not right, the slurry cannot flow into the mould cavity. If the temperature is too low, for example below 400°C, the slurry is only able to flow to halfway of the mould cavity. This is because the slurry will solidify very fast, and produce a sample as shown in Figure 3.24(a). It was found that the mould temperature should be preheated to a temperature in the range of 500°C in order to get a good sample with a better surface finish. This is shown in Figure 3.24(b). However, if the mould temperature was too high, for example exceeding 600°C, the sample produced has a very poor surface finish, this is most likely because of high temperature oxidation, and this is shown in Figure 3.24(c).

It was also found that a good tensile specimen can be produced if the mould temperature is in between 400-450°C, however, the slurry temperature should be above 700°C. Unfortunately, the temperature of the slurry should not be too high, in order to avoid the chemical reaction between SiC and aluminium. Figure 3.25 shows tensile specimens produced. The tensile tests were carried out on cast and heat-treated samples.

A 50 kN INSTRON universal testing machine (model 4204) was used for tensile testing. The Instron machine consists of a loading frame, and a controller and a plotter. The basic operation of the instrument consisted of selecting a load cell for a particular

testing application, mounting the load cell in the moving crosshead within the loading frame, then setting a specimen in position so that the load applied could be measured.

Cylindrical tensile specimens of 4.83-mm diameter were used. This machine was equipped with extension meter with a gauge length of 25 mm as shown in Figure 3.26. The strain rate used was 1mm/min. All samples were tested for tensile properties in longitudinal direction. Tests were performed using ASTM Standard E8. Tests were conducted under constant speed control. Loads versus strain were recorded automatically using a plotter. The tensile strength and, 0.2% proof stress were determined for cast and heat-treated conditions. Detail results are detailed in Appendix I.



Figure 3.25: Tensile specimens produced.

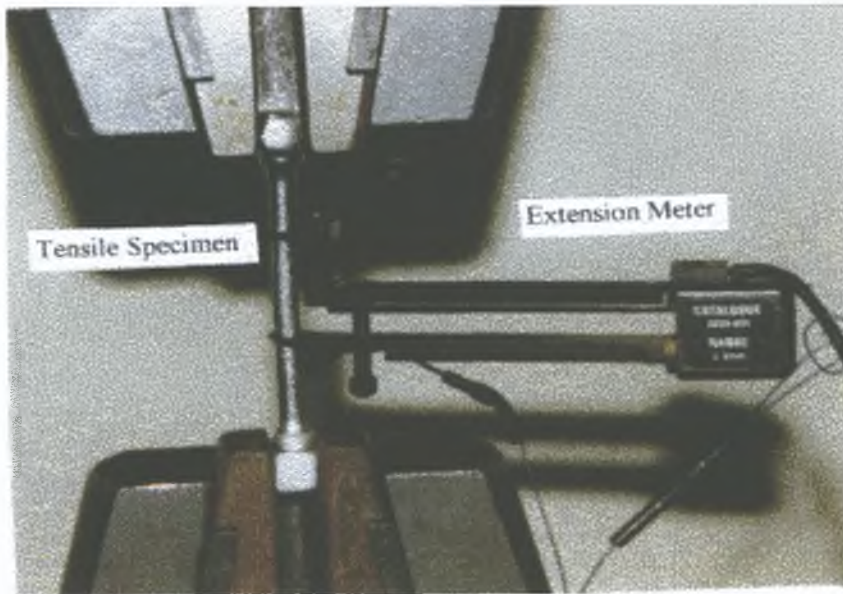


Figure 3.26 : Tensile testing

3.6 HEAT TREATMENT

Aging studies were carried out in order to obtain the effect of aging time on hardness and tensile properties of the cast composites samples produced. Age hardening or precipitation hardening is a versatile method used to strengthen certain metallic alloy. It is an especially popular technique for aluminium alloys, and is discussed in greater detail in Chapter 4. This heat treatment consists of solution treatment at high temperature follow by quenching. Aging treatment is done either by natural aging (T4) or artificial aging (T6). The temperature used for solution treatment and artificial aging varied with the type of matrix alloy used. Normally the solution treatment temperature is in the range of 450°C to 550°C and following by quenching. In most cases samples were quenched in

water at temperatures between 25 to 100° C and the aging temperature in the range of 80°C to 230°C [244 - 246] In this experiment, for A359 alloy, the solution treatment was carried out at 540°C for about one hour It followed by quenching in 40°C water Artificial aging (T6) was carried out at the temperature of 170°C

CHAPTER FOUR

RESULTS AND DISCUSSION

4.1 INTRODUCTION

The foundry technique is seen to be the cheapest method of producing MMC, and the size of the product limited to 500 kgs [57]. However, the main MMC fabrication problems such as wettability between substances, the chemical reaction between them, the distribution of the reinforcement particles in the matrix and also the porosity content in the matrix, still remain and research continues to aim to solve them. In normal practice of stir casting technique, cast MMC is produced by melting the matrix material in a vessel, then the molten metal is stirred thoroughly to form a vortex and the reinforcement particles are introduced through the side of the vortex formed. Research related to this type of cast MMC producing method is broad, and is still going on. However, the main approach used remains the same as mentioned above. From some points of view, this approach of producing MMC by stir casting has disadvantages, mainly arising from the particle addition and the stirring methods. During particle addition, there is undoubtedly local solidification of the melt induced by the particles, and this increases the viscosity of the slurry. A top addition method also will introduce air into the slurry, which appears as air pocket between particles. The rate of particle addition also needs to be slowed down, especially when the volume fraction of the particles to be used increases. This is time consuming for a bigger product, and there may be a chemical reaction if the temperature of the slurry is not well controlled.

Wettability between ceramic reinforcement particles and aluminium alloy as a matrix material is considered as a key factor, controlling the success of MMC fabrication. Without solving this problem, MMC can not be fabricated. Therefore in this study, wettability testing was given priority.

4.2 WETTABILITY

Several series of wettability experiment have been carried out, considering the effect of stirring action, the treatment of the silicon carbide particles, the use of wetting agent and the temperature of the slurry. This wettability testing can be divided into two categories: Those carried out using an electric furnace and those carried out using a specially designed rig. The difference between the two categories is that in the first case, melting was achieved by using an electric furnace and then the stirring was carried out manually outside the furnace. Whereas, in the second case melting was done within the rig, the stirring time was monitored, the temperature of the slurry was controlled, and the oxidation level was minimised. Except in wettability test 1, all the slurry was cast into cylindrical ingots, 19mm diameter x 150mm long. The ingot was sectioned at three different parts: at the top, at the middle and at the bottom, All the samples were prepared for metallography examination.

From the wettability test 1, where no stirring was applied, all the samples were sectioned vertically, and were prepared for microscopic examination. The results show that for all cases, no particles got into the matrix alloy, that means the wettability was zero. The micrographs of these samples is as shown in Figure 4.1.

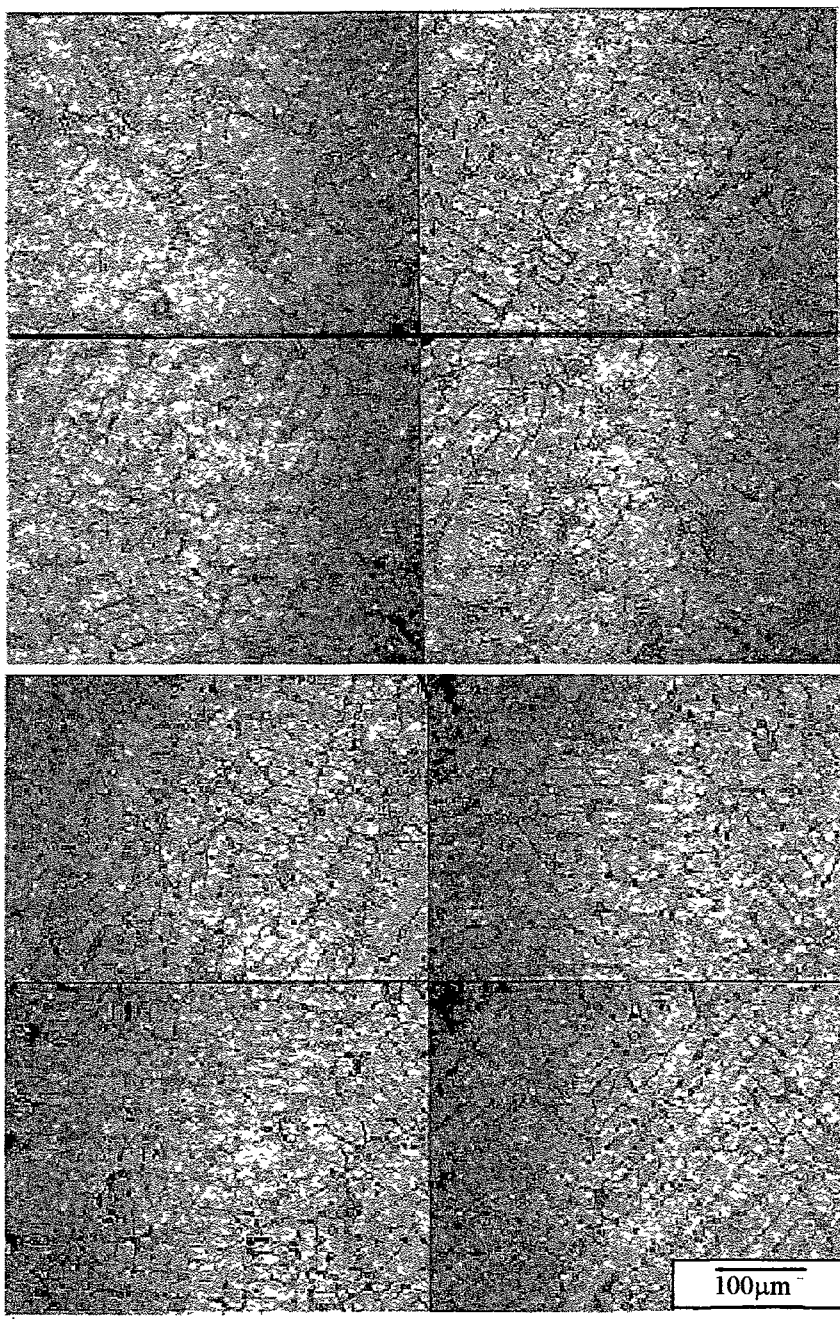
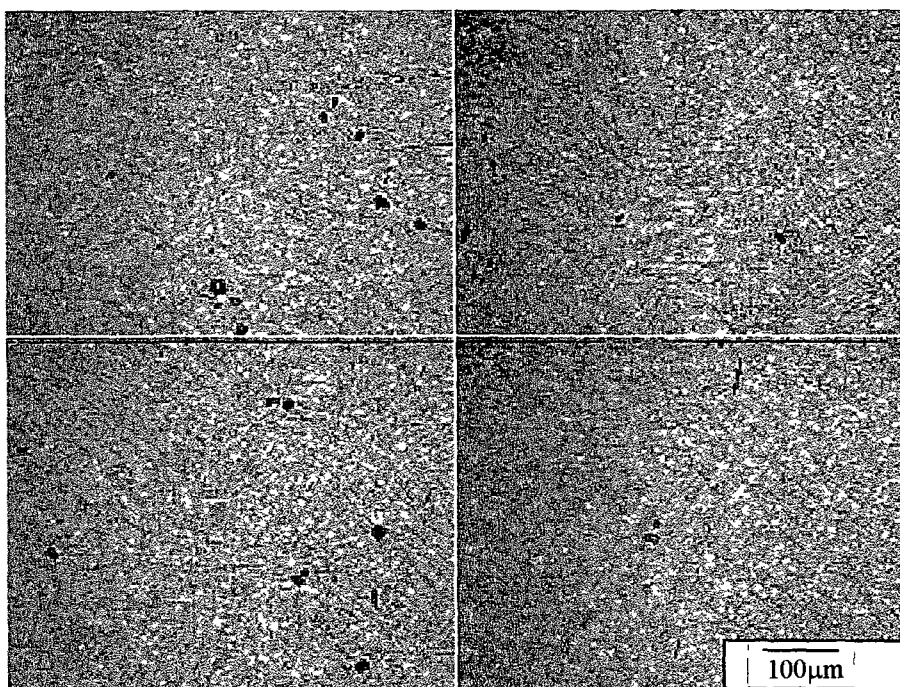


Figure 4 1 Micrograph from wettability test 1 - no stirring action, failed to incorporate any SiC particles

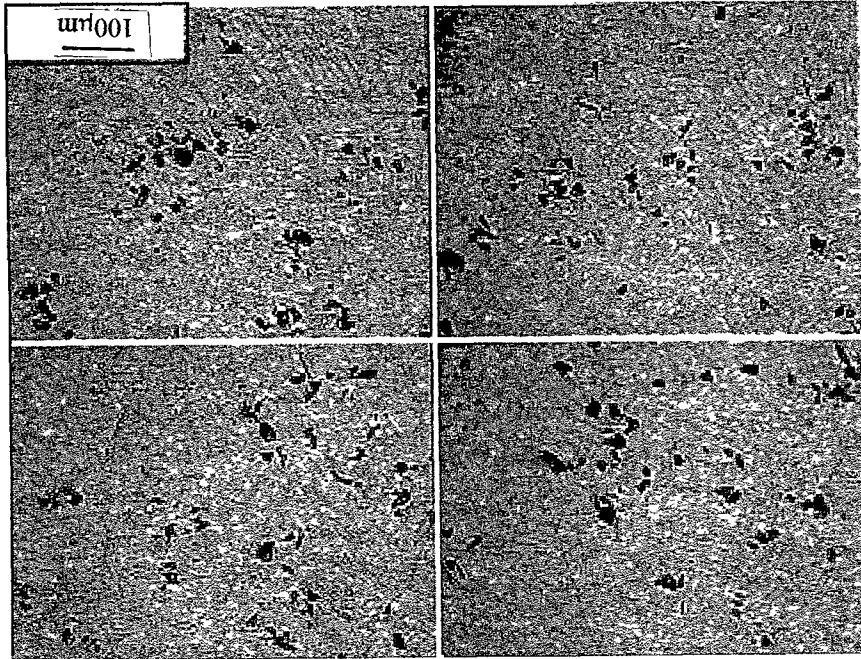
From wettability test 2, where stirring was applied to slurry in a fully liquid condition, it was found to be very difficult to incorporate particles into the molten matrix. During stirring, some of the particles tended to float on the top of the molten alloy. After pouring, it was found that most of the particles still accumulated at the bottom of the crucible. Microscopic examination shows that without any magnesium addition as in mixtures A and B, the wettability is virtually zero. However with the addition of 1 wt % magnesium as in mixture C and D, some particles got into the matrix. The wettability for mixture C and D is about 30 percent and 40 percent respectively. These can be seen in Figure 4.2.



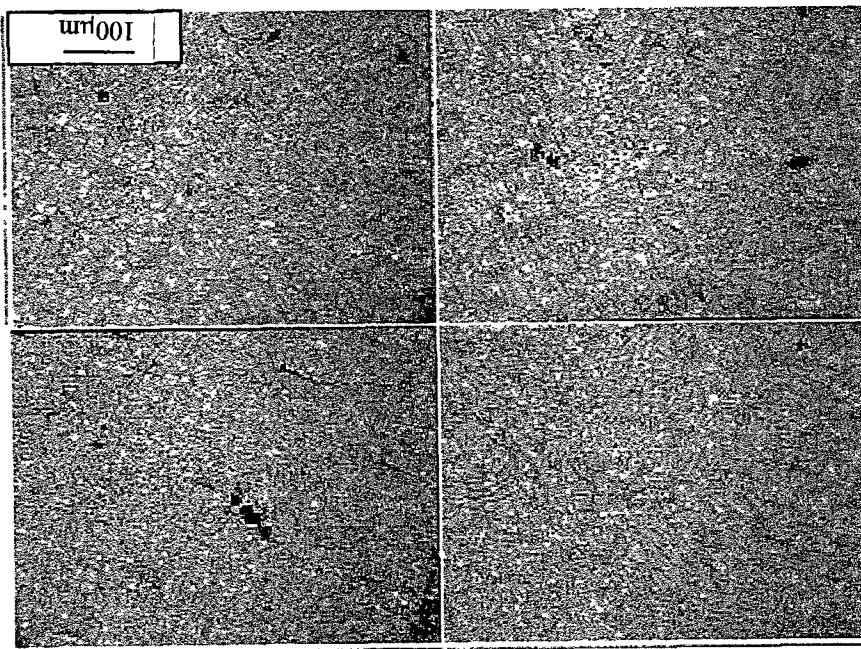
(a)

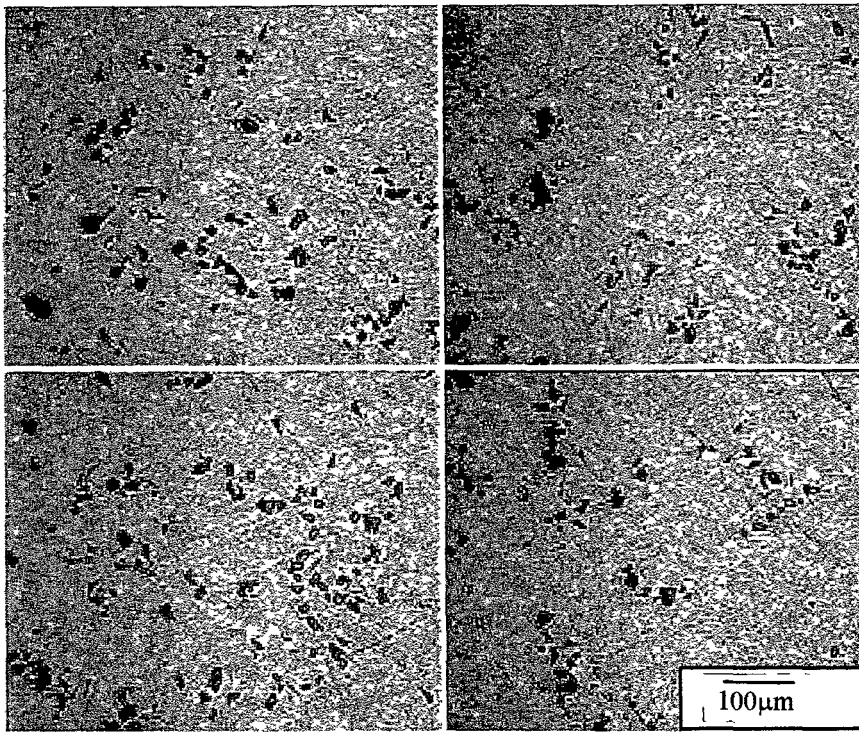
Figure 4.2 Micrograph from wettability test 2 (a) Mixture A, (b) Mixture B, (c) Mixture C (d) Mixture D

(c)



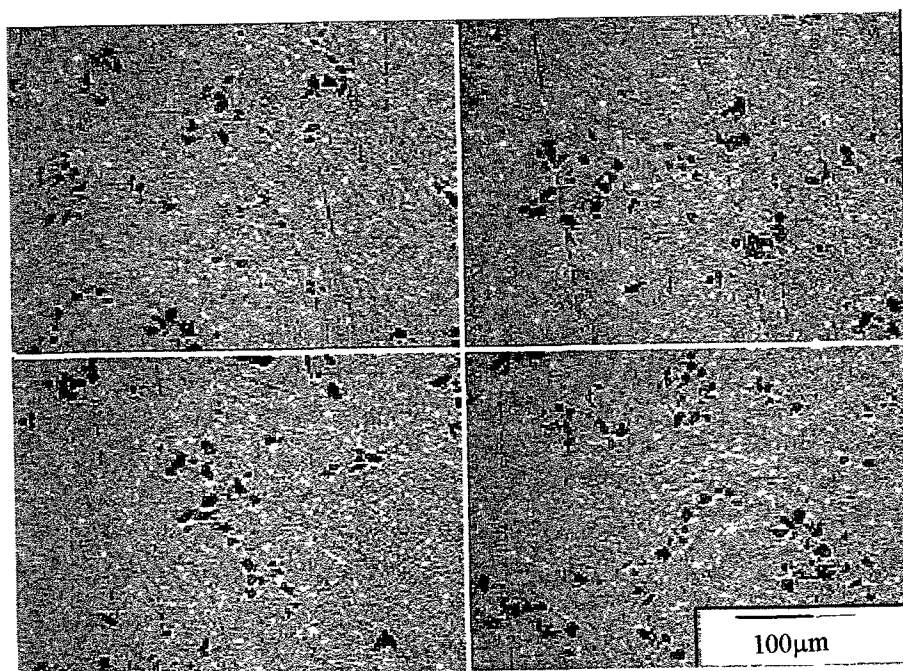
(q)



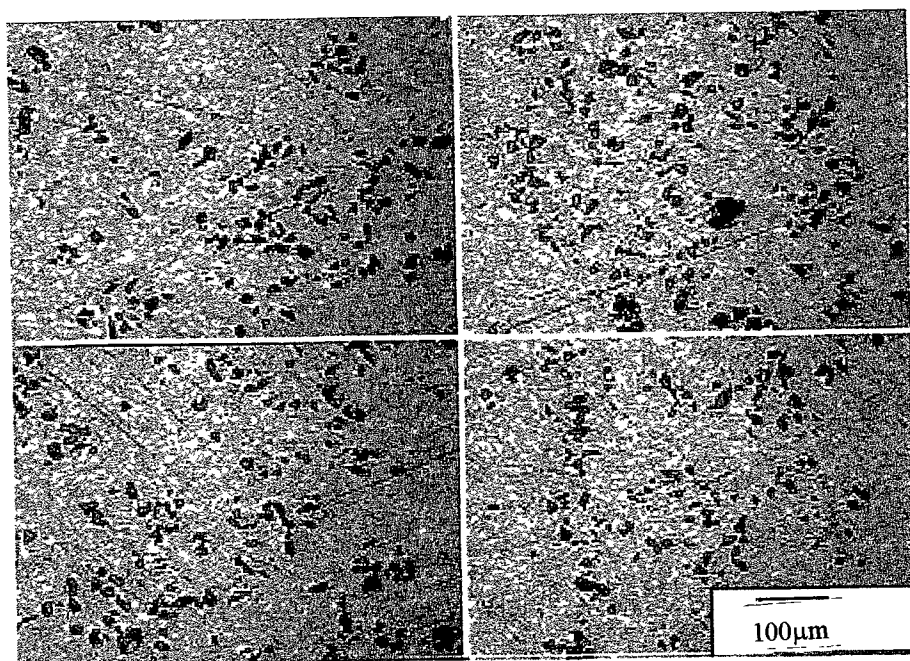


(d)

Stirring the slurry in semi-solid condition as was carried out in wettability testing 3 gave a positive result. It was found that it was easier to incorporate the particles into the matrix alloy while stirring in a semi-solid state. After pouring, it was found that only a little of the particles were left behind, or accumulated at the crucible base. This means that a lot of the particles got into the matrix. The microstructure observation shows that, all the samples contained a large number of particles especially with the addition of 1 wt % magnesium, in mixtures C and D, with the wettability of about 60 percent and 95 percent respectively, as shown in Figure 4 3



(a)



(b)

Figure 4 3 Micrograph from wettability testing 3 (a) Mixture C,
(b) Mixture D,

Experimental work to study the effect of magnesium carried out in wettability test 4, gave two different results. Stirring in fully liquid condition did not help to incorporate silicon carbide particles into the matrix, no matter what percentage of magnesium was added. Stirring in semi-solid condition gave a positive result. All the samples contained 0, 1, 2, and 3 percent of magnesium, and contained a large number of particles in the matrix alloy. However, metallography shows that increasing the magnesium content increases the tendency for the particles to agglomerate or clump together. These can be seen in Figure 4.4. According to Sukumaran et al [188] increasing the magnesium content more than 1 wt percent, will increase the viscosity of the A356 matrix alloy significantly.

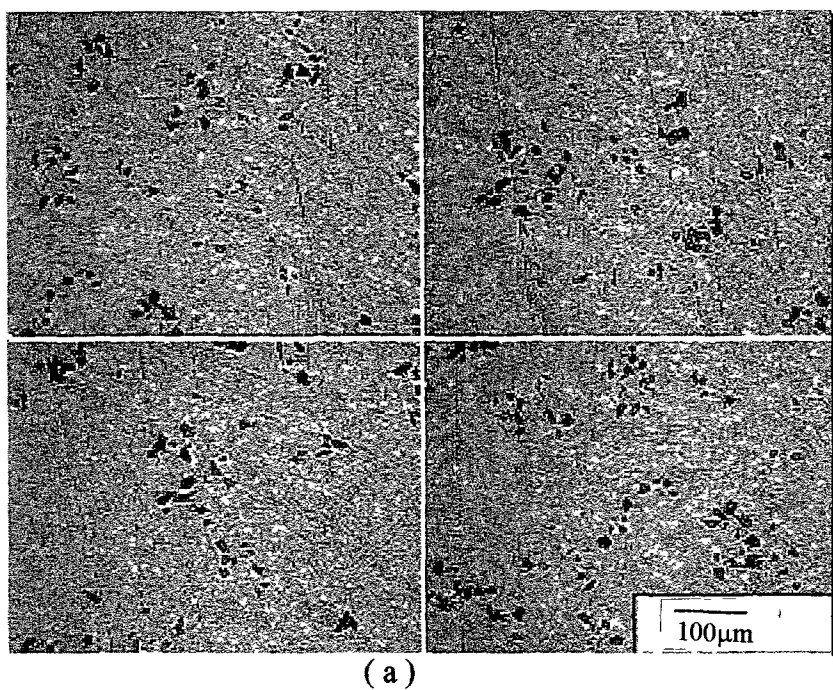
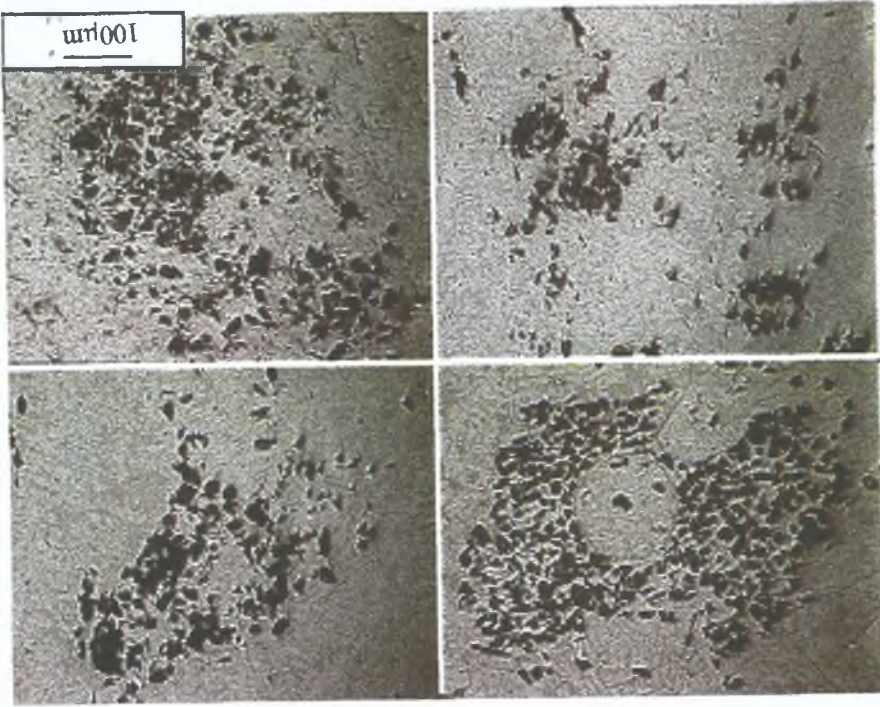
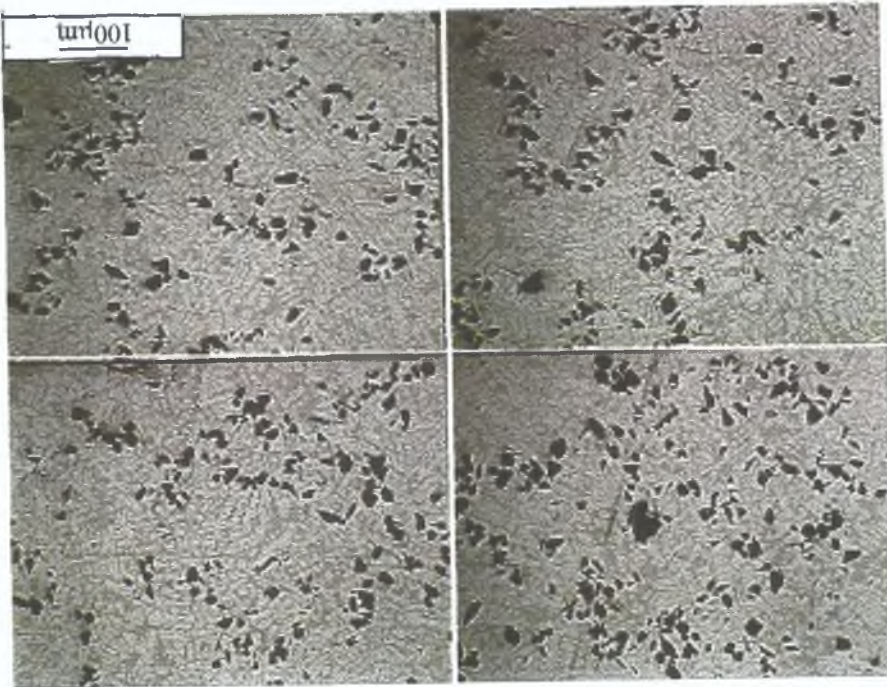


Figure 4.4 Micrograph from wettability test 4 for the mixture contained
(a) 0% wt Mg, (b) 1wt % Mg, (c) 3wt % Mg

(c)



(p)



In wettability test 5, an attempt was made to study effect of the stirring conditions on the wettability of silicon particles by A359 alloy, with 1 wt % magnesium as a wetting agent This test gave three different results

- i Stirring in fully liquid condition gives zero wettability
- ii Isothermal stirring in semi-solid condition at a temperature in the solidification range (590°C), then re-stirring in a fully liquid condition before pouring, also gives zero wettability For both case (i) and (ii), high level of porosity resulted as shown in Figure 4 5 and Figure 4 6 respectively
- iii Stirring continuously while the slurry become semi-solid from a liquid condition give good wettability However, comparing to the result from wettability test 4, it was found that some of the silicon carbide particles were broken (Figure 4 7), because of increasing shearing action

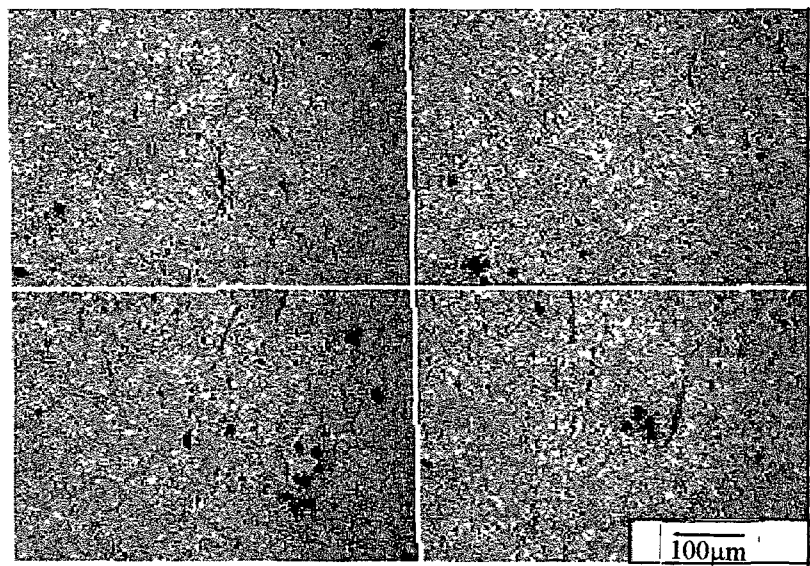


Figure 4 5 Micrograph for wettability test 5 (i)- stirring in fully liquid condition, no particle incorporation

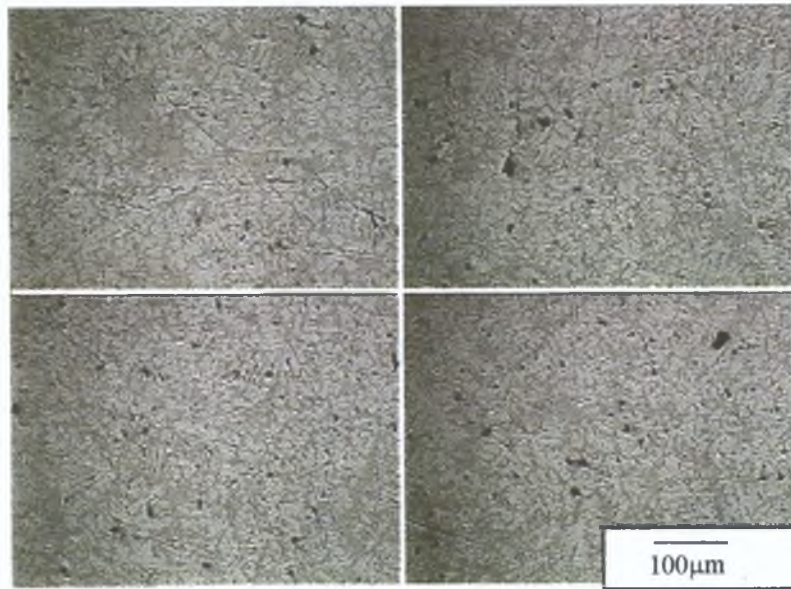


Figure 4.6 : Micrograph for Wettability test 5 (ii) - Isothermal stirring at semi-solid condition, no particle incorporation.

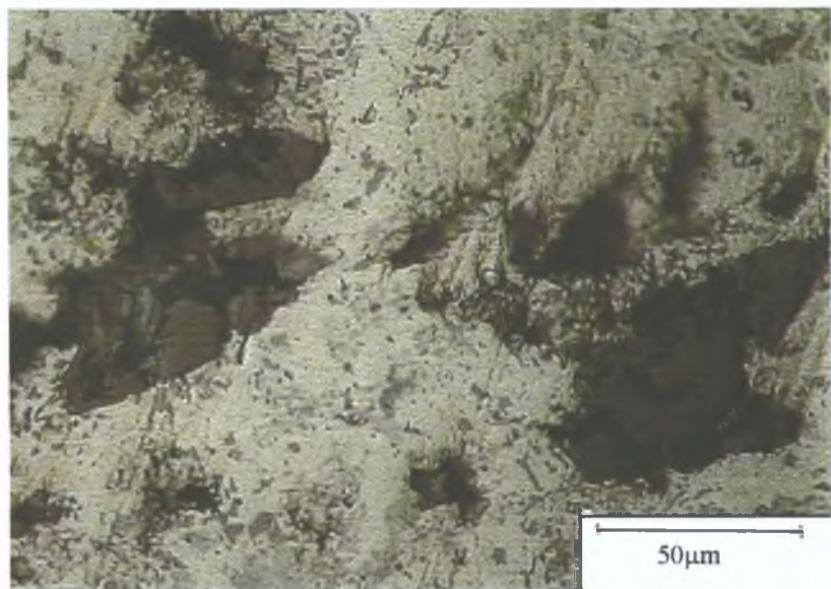


Figure 4.7 : Micrograph for Wettability test 5 (iii)- stirring in semi-solid condition while the melt solidifying give good wettability, but there is some particle fracture because of increasing shearing action.

iv Varying the cooling time and volume fraction of SiC gave two different results a fast temperature drop into the solidification temperature range, improved wettability This is shown in Figure 4 8 Conversely, increases in volume fraction of SiC, gave the opposite effect This is shown in Figure 4 9

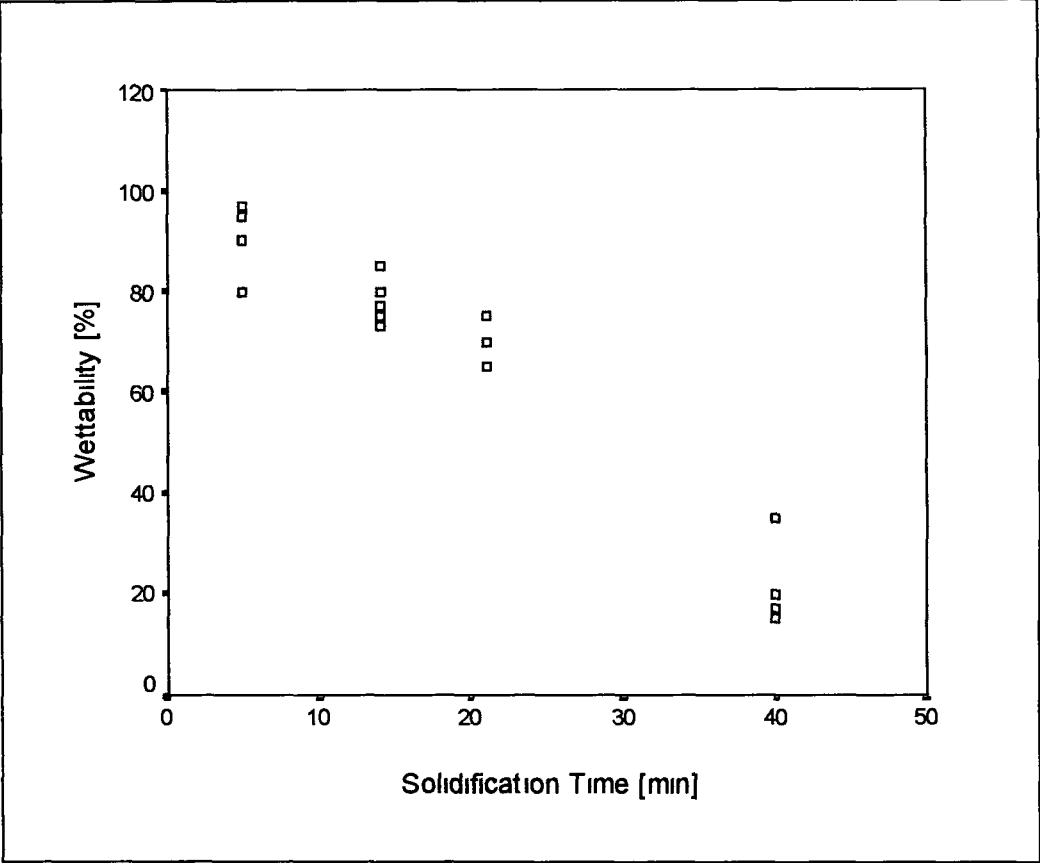


Figure 4 8 Effect of decrease in solidification time during stirring on wettability enhancement

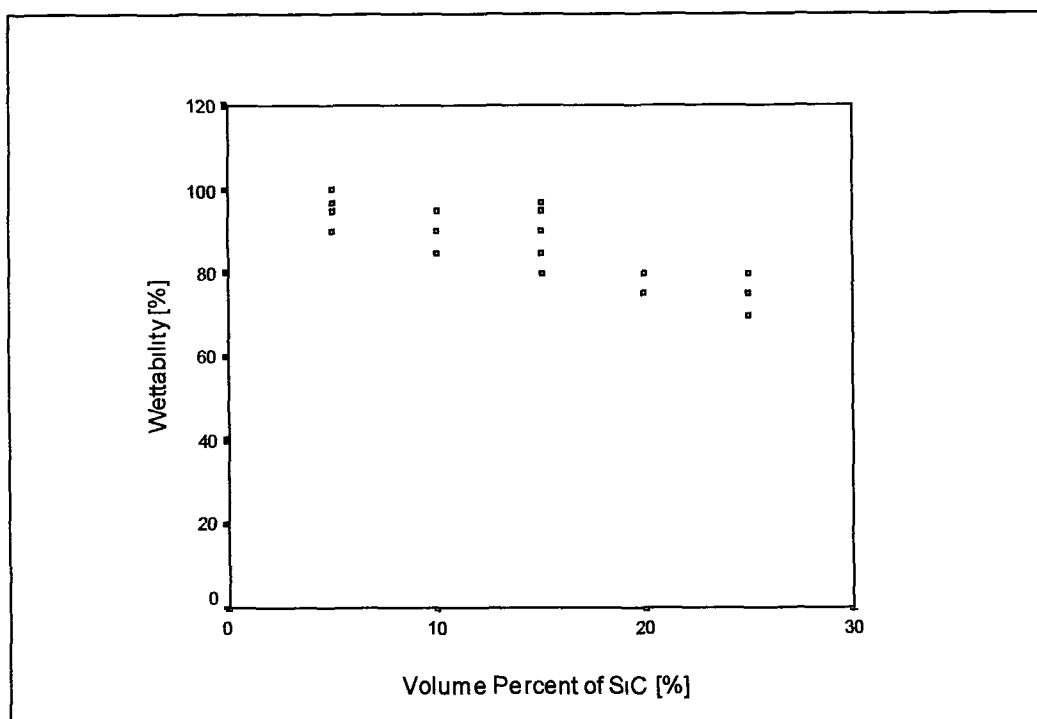


Figure 4.9 Effect of volume fraction of silicon carbide particle on wettability enhancement

Table 4.1 The summary results from the wettability tests

Test	Conditions	Results
Test series 1	No stirring	The wettability is zero for all cases
Test series 2	Stirring in liquid state	Only mixture C and D give a little wettability, which is about 30 percent and 40 percent respectively
Test series 3	Stirring in semi-solid state	All mixture shows a good wettability, especially for mixtures C (with Mg) and, mixtures D (with Mg and treated SiC). The wettability is 60 percent and 95 percent respectively
Test series 4	Stirring in both liquid and semi-solid state	Stirring in fully liquid condition gives zero wettability. Stirring in semi-liquid condition gives a good wettability, but increasing Mg content increases agglomeration of particles
Test series 5	Stirring during solidification	Decreasing solidifying time increases the wettability. Increasing volume fraction of SiC particles decreases the wettability

Results from the wettability tests 1-5 are summarized in Table 4.1. Initial tests showed that stirring is essential for any incorporation of particles to occur. Particles in test series 1, where there was no stirring, simply remained floating on the top of melted alloy, irrespective of the presence of magnesium or heat treatment of particles.

With stirring in the liquid condition, poor wetting was also seen when SiC particles were used in an as-received condition, without magnesium. Microscopic observations show no SiC particles within the matrix alloy or, in other words, zero wettability. This was also the case for treated particles, without magnesium. During stirring, some of the particles tended to float to the top of the melt, and others accumulated at the base of the crucible. This occurred irrespective of speed of stirring. After pouring, it was found that most of the particles still accumulated at the bottom of the crucible. However, microscopic examination shows that some particles were incorporated in the matrix for mixtures C and D, to which magnesium had been added. The wettability is limited, at 30 and 40 percent for mixtures C and D respectively.

Stirring the slurry in a semi-solid condition in wettability tests 3 gave a positive result. It was easier to incorporate the particles into the matrix alloy. After pouring, no particles were left behind in the crucible, indicating that they all were incorporated in the matrix. The microstructure observation shows that in all samples contained a lot of particles, with wettability at a maximum of about 95 percent for composition D containing oxidized particles and 1wt% Mg. It was less, at 66 percent, for untreated particles and magnesium (mixture C).

Experimental work to study the effect of magnesium (wettability test 4) gave two different results. Irrespective of the weight percentage magnesium, SiC particles were not incorporated into the matrix when stirring took place in fully liquid condition. However, stirring in a semi-solid condition gave a positive result. All of the samples, either contained 0, 1, 2, or 3 percent magnesium, contained a high proportion of particles within the matrix alloy. The addition of 1 wt % magnesium is known to improve wettability [269, 270] by reducing the surface tension of the liquid melt, and by promoting chemical reaction at the solid-liquid interface [269, 271-274]. However, metallographic investigation shows that increasing the magnesium content increases the tendency for the particles to agglomerate or clump together. According to Sukumaran et al [188] increasing the magnesium content over 1 wt %, increases the viscosity of the A356 matrix alloy significantly. The increase in viscosity makes it more difficult to get uniform distribution of the SiC particles. This was previously proposed by Mondolfo [186], whose experimental result also showed that the addition of 3 wt % Mg to Al-Si alloy leads to the formation of a Mg_5Al_8 phase, which has a low-melting point and deteriorates the mechanical properties of the MMC. Therefore, the amount of Mg used needs to be carefully controlled.

Wettability tests 5 show that stirring the melt, while the slurry is solidifying, or when the melt is in the semi-solid state improves the incorporation of the SiC into the matrix. In a semi-solid state, primary alpha-Al phase exists, so agitation can apply large forces on the SiC particles through abrasion and collision between the primary alpha-Al

nuclei and particles. The SiC particles are mechanically entrapped and prevented from agglomeration by the presence of the primary alloy solid phases. This process also can help to trap the SiC particles and stop them from settling, thus helping to achieve good wettability. It was also found that decreasing the cooling time helps trap more particles. Decreasing the cooling time increases the volume fraction of primary α -Al nuclei, improving the possibility to trap more particles into the matrix. The second step of stirring is important in order to disperse the particles throughout the matrix. This is because, the particles (more dense than aluminium) which are already incorporated into the matrix during semi-solid stirring, will tend to settle to the bottom of the molten matrix during soaking in fully liquid state.

It was also found that the tendency to incorporate the SiC into the matrix alloy reduced with increasing of volume fraction of SiC. This is because by increasing the volume fraction of SiC particles, the viscosity of the slurry is increased, thus creating greater difficulty and less chance for more particle to be embedded into the melt. According to Moustafa [267], for Al-Si alloy reinforced SiC particles, the percentage of the particle addition to the melt can be as high as 20 wt %. If the addition is higher than that, the mixture will become very viscous and will become difficult to stir or cast. Caron and Masounave [268] also concluded that a large amount of particles are difficult to incorporate by foundry processes to fabricate cast MMCs.

In the early stages of research into semi-solid behavior, it was recognized that the viscosity of semi-solid slurries provides an attractive opportunity to incorporate ceramic

particles and produce MMCs [51] It was found that even in cases where the ceramic is not wetted by the matrix, the ceramic particles are prevented from settling, floating or agglomerating by the partially solidified matrix In addition it has also been noted that increasing the mixing times promote metal-ceramic bonding Cheng and coworkers [276] reported the reduced in grain size and segregation in structure, relative to those of the conventional processed casting

It can be concluded that to fabricate aluminium MMCs by using stir casting technique, with this proposed approach, some important factors need to be considered such as

- i Mechanical stirring is necessary to help to promote wettability
- ii Stirring in a fully liquid condition does not help to incorporate particles into the matrix The particles tend to float to the top of the molten alloy, regardless of the speed of stirring
- iii Stirring while the slurry is solidifying improves incorporation of the particles into the matrix alloy However the slurry then must be re-melted to a fully liquid condition in order to enable pouring into a mould Decreasing the solidifying time during stirring increases the percentage wetting
- iv Using magnesium enhances wettability, however increasing the content above 1-weight percent magnesium increases the viscosity of the slurry to the detriment of particle distribution
- v Increasing the volume percentage of SiC particles in the matrix alloy decreases the wettability

4.3 MMC FABRICATION METHOD

This research is proposing a new method of casting MMC. The main focus was to solve the problem of wettability between Silicon carbide particles and the matrix materials. Attempts were also made to eliminate the other three problems: non- uniform distribution of silicon carbide particles in the matrix, chemical reaction between these two substances and porosity. Placing all substances in a graphite crucible, and heating in an inert atmosphere until the matrix alloy is melted, has advantages in terms of promoting wettability between Silicon carbide particles and the matrix alloy.

The success of the incorporation of Silicon carbide particles into the matrix alloy showed that the wettability between Silicon carbide particles and the matrix alloy could be adequate. During the initial stage of the experiment when the as-received silicon carbide particles were added to the matrix alloy, without the use of any wetting agent, the particles settled at the bottom of the crucible. This may be because of the contamination of silicon carbide particles, or due to an air envelope between the particles, which prevents contact between silicon carbide particles and the matrix melt, and the fact that the wettability between ceramic and metallic melt is poor. In normal practice, this wettability problem has been solved either by coating the ceramic particles, heat treating the particles, or by using a certain wetting agent or alloying element. The addition of magnesium to aluminium improves wetting by reducing the surface tension of the liquid melt and by promoting chemical reactions at the solid-liquid interface. Silicon carbide particles was heat treated, by preheating the particle to a certain temperature for a certain period of time, between 1-2 hours, in order to burn out all the impurities and water vapor,

and provided a clean particle surface. This clean surface helps to give good contact between matrix melt and the Silicon carbide particles, and improves the wettability between them [270]

In this research, the wettability enhancement was done by using magnesium as a wetting agent, and the silicon carbide particle was also heat treated during fabrication process. These two combined methods for enhancing the wetting seem to give a very good wettability between silicon carbide particles and matrix alloy due to the reasons mentioned above. The presence of excess reactive element such as magnesium in aluminium melt will alter the microstructure of the matrix alloy by forming a low-melting constituent and will deteriorate the mechanical properties. The addition of 3 wt % of magnesium to A356 alloy leads to the formation of Mg_5Al_8 phase, having a low melting point of 450°C, in addition to the formation of strengthening phase, Mg_2Si [186]. According to [158, 187], the enhancement in porosity content with higher magnesium content may be attributed to the presence of extra magnesium, which is known to increase the solubility of hydrogen in the melt, as well as decreasing the fluidity of the melt.

Mechanical stirring mixed the particles into the melt, but in a completely liquid state, and when stirring stopped, the particles returned to the surface. Most of these particles stuck to one another in clusters. Gas layers or air pockets between particles can cause the buoyancy migration of particles, making it difficult to incorporate the particles into the melt. In a completely liquid melt, single particles and particle clusters can flow easily and this gas layer facilitates their flow. When the gas layers were broken, the

contact surface between Silicon carbide particles particle and matrix alloy increased, and the particles were wetted. However, the particles will tend to sink to the bottom (due to higher specific weight) rather than float to the surface.

4.4 METALLOGRAPHY AND MICROSTRUCTURAL ANALYSIS

In aluminum-silicon alloy system, alloys with less than 12% Si, such as the A359 being used in this research study (8.5 wt %Si, 0.5 wt %Mg, 0.03 wt %Cu), are referred to as hypoeutectic. In A359, the microstructure is composed of an aluminium matrix containing eutectic Si. In general the eutectic Si is not uniformly distributed, but tends to be connected at inter-dendritic boundaries. Optical microscopy was carried out on the as-cast and heat treated samples. Figure 4.9 shows the microstructure of A359 alloy as-cast condition. It can be seen that the eutectic Si is not uniformly distributed, and most of Si accumulated at the grain boundaries. Eutectic Si is present in the form of needles or flakes shaped.

In the specimen produced by using a smaller size mould, however, the grain size is finer, and this is attributed to the faster cooling rate. This can be seen in Figure 4.10. By adding silicon carbide particles to this matrix, the eutectic structure appears to be gradually modified. This can be seen in the A359/SiC/5p and A359/SiC/20p in Figure 4.11 (a) and (b). It was found that the particles showed a strong tendency to accumulate in the colonies, which froze in the last stage of solidification and usually contain eutectic phases. This is most clearly seen in A359/SiC/5p microstructure.

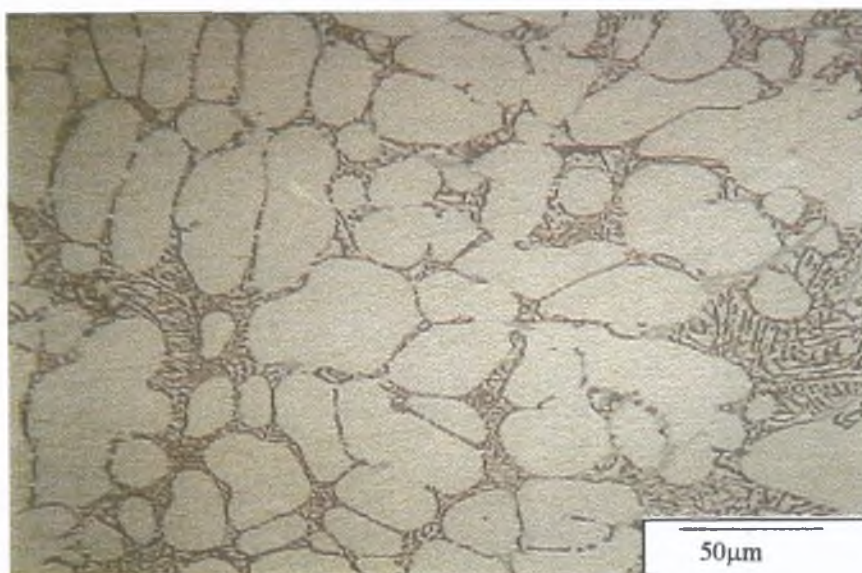


Figure 4.9: Microstructure of A359 matrix alloy as cast condition (ingot B) showing eutectic Si between grain of α -Al.

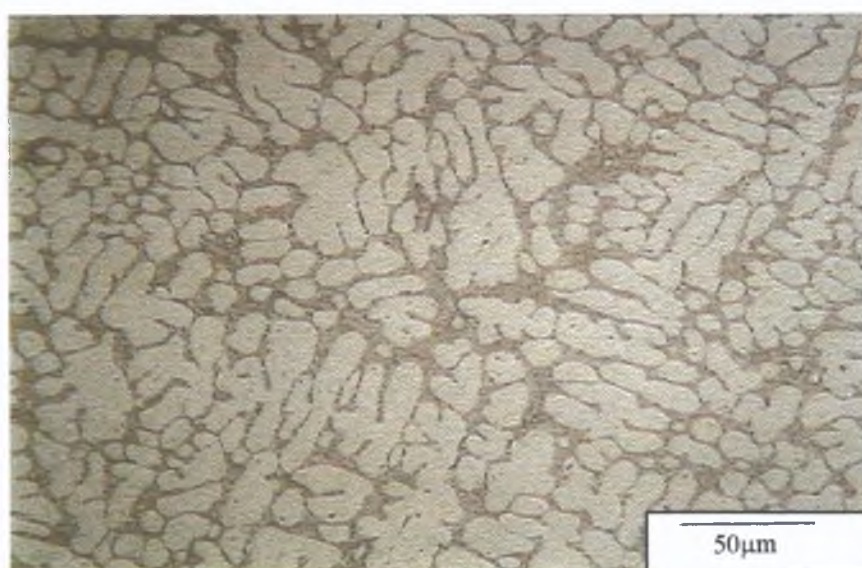
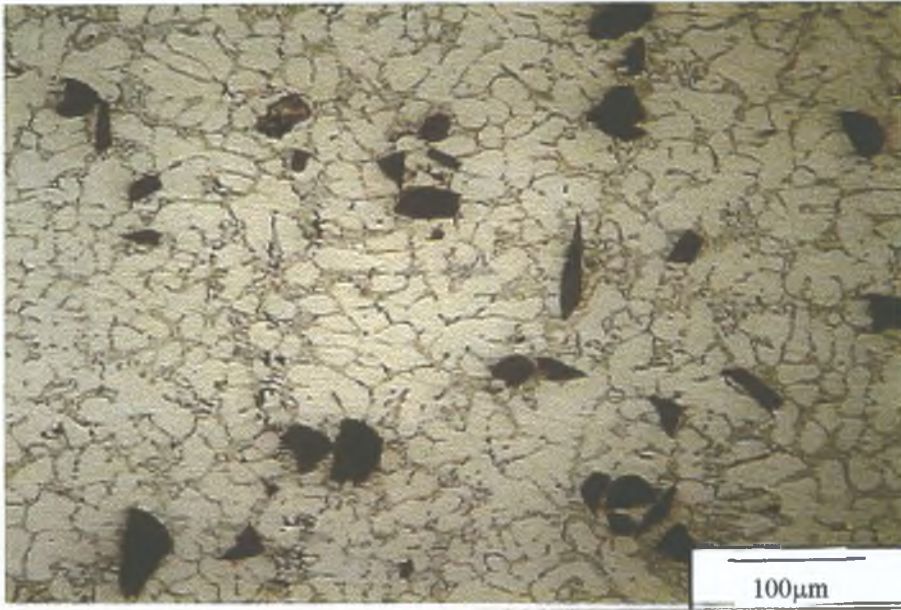


Figure 4.10: Microstructure of A359 matrix alloy as cast condition, (ingot A)-refined grain due to faster cooling.



(a)

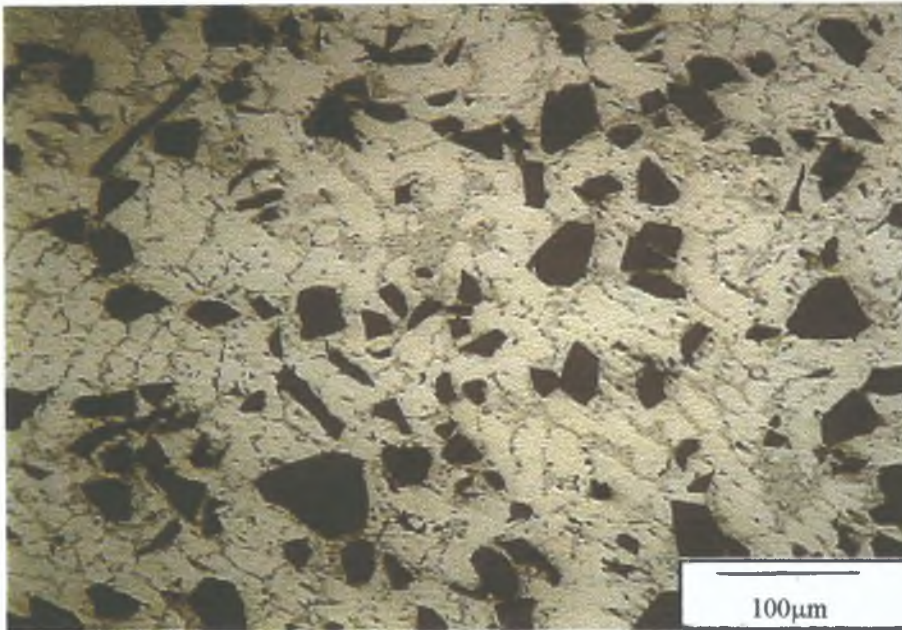


Figure 4.11: The microstructure of (a) A359/SiC/5p and (b) A359/SiC/20p, as cast condition.

The silicon carbide particles were also observed to be accommodated on the grain boundaries. It can be seen that, the aluminium grain structure is equiaxed shape. This is attributed to the effect of stirring action at semi-solid condition. This stirring action breaks the dendritic shaped structure, and leaves the structure in equiaxed form. The same effect also can be seen when the specimen is cast by using a smaller mould of the same material.

Another important aim of microstructural observation in the case of non-reinforced and reinforced samples, investigated in the present study, was to quantify particle distribution in-homogeneities. The simplest approach was to consider the number of particles in fixed test area [10,216, 238]. Another method involves measurement of inter-particle separation, although it is important to define clearly which inter-particle separation is being considered. Often the most useful approach is to measure distances to nearest and/or near neighbours. For this analysis, it is necessary to identify clearly the neighbours of each particle. Some researchers have attempted to do this by visual inspection [244]. In this study, visual inspection method was used to quantify the rate of distribution of Silicon carbide particles in the matrix alloy. It can be seen that the composite materials made by the investigated processing technique had a cast microstructure of the matrix accompanied with particles, distributed homogeneously throughout the casting. Relatively uniform distribution was observed in almost all the composites produced. However, there are some particles-free zones due to particle pushing effects during solidification.

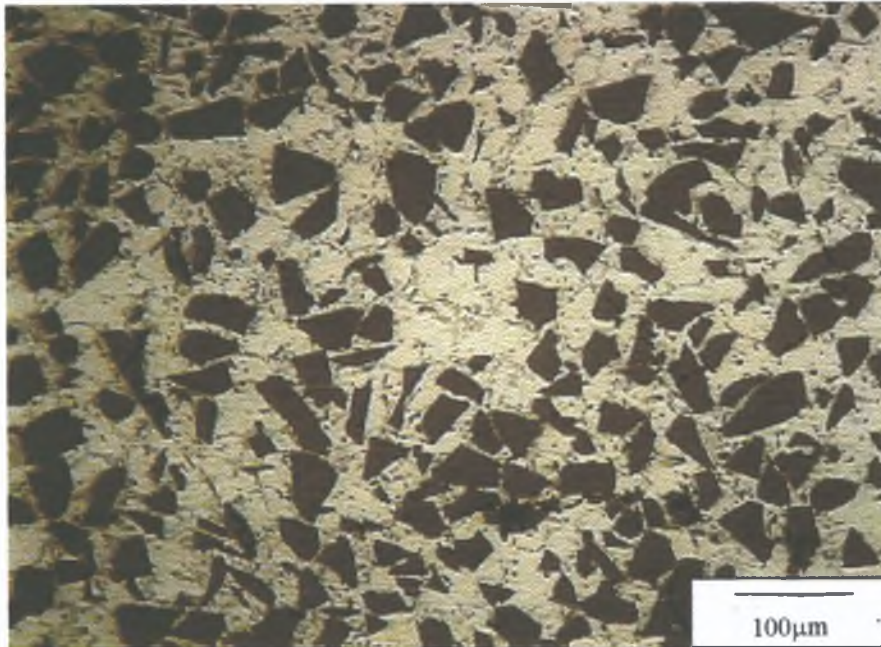


Figure 4.12: The microstructure of A359/SiC/25p, as cast condition.

In present experiments, the directionality of the microstructures also observed to be disrupted by the presence of silicon carbide particles. It is apparent from the microstructure that the distribution of reinforcement particles become more uniform in the matrix as their weight percentage increases. Figure 4.12 shows the distribution of silicon carbide particles in matrix alloy with 25 % volume fraction of silicon carbide particles. Comparing to the distribution of silicon carbide particles in 5 volume percent (Figure 4.11(a)), the 25 volume percent give a more uniform dispersion. However, the tendency for particle to clump together also increases when the volume fraction of the silicon carbide increased.

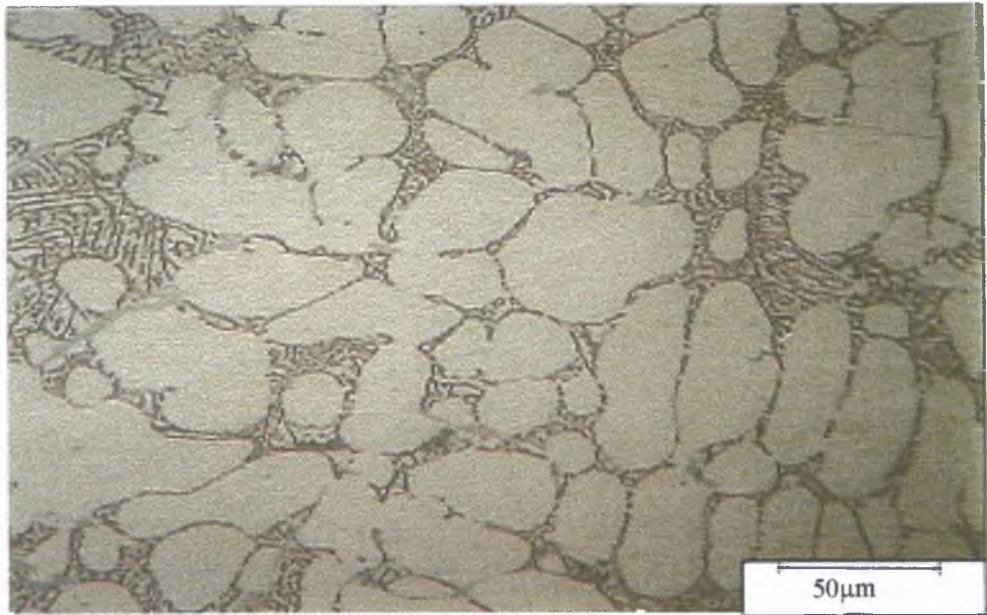


Figure 4.13 : Photograph of A359, as-cast condition

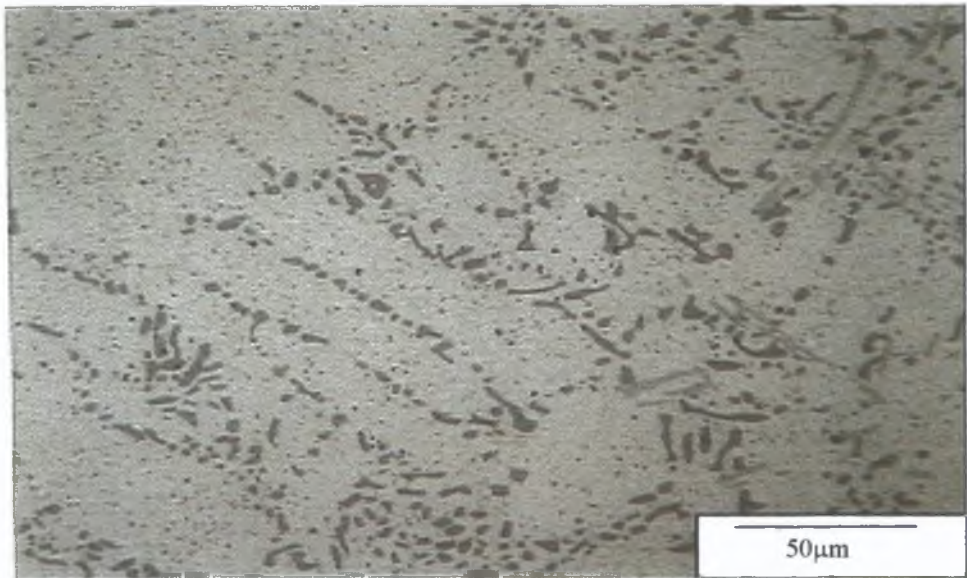


Figure 4.14 : A359 after 2 hours aging at 170°C, T6 treatment.

It has been reported that the presence of foreign particles, fibres, or other constraints, significantly affects the solid-liquid interface morphology and microstructure [51,71, 266] For example, the cellular-dendritic solid-liquid interface of an Al-2%Mg alloy was highly disturbed by the presence of silicon carbide [71], and the orderly directional microstructures of Al-Si alloy were also disrupted by the entrapment of silicon carbide [57]

Aluminium-silicon alloys are widely used for the casting of high strength components, because they offer a combination of high achievable strength and good casting characteristics. However the strength of this alloys as-cast condition is very low. A significant increase in strength can be achieved through precipitation hardening by a T6 heat treatment. The microstructure of A359 as-cast condition is shown in Figure 4 13

The dark particles are eutectic structure. According to Zhang et al [277], the microstructure of the solution treated A359 alloy, consists of alpha-Al dendrites and large number of rounded eutectic Si particles distributed in the inter-dendritic regions. Figure 4 14 shows the microstructure of A359 matrix alloy after 2 hours aging, under T6 treatment condition. It can be seen that there are some changes in the microstructure between as-cast and after-aging treatment. After aging, the needle or flake shaped Si eutectic structure was transformed to the spheroid shaped Mg_2Si precipitation structure. This transformation is responsible for the changing or improvement of the mechanical properties of the alloy. It can be seen that the size of this precipitation becomes finer when the aging time increases. This is shown in Figure 4 15

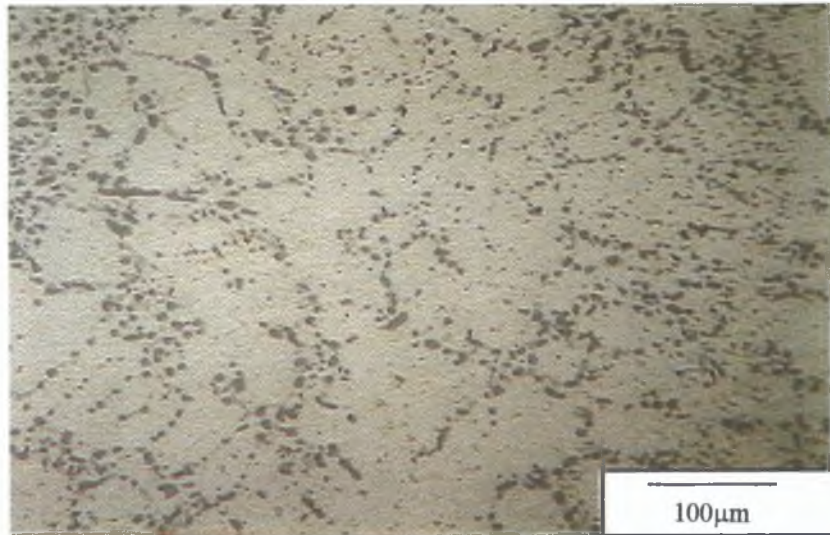
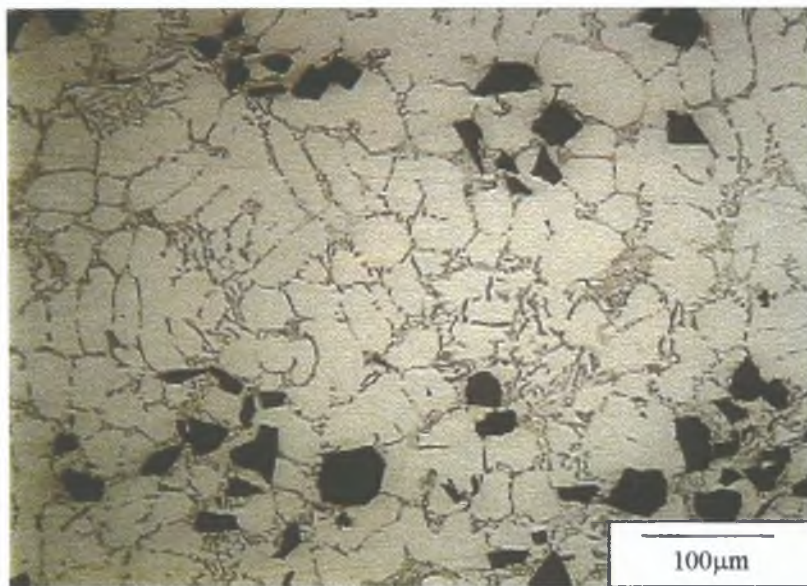


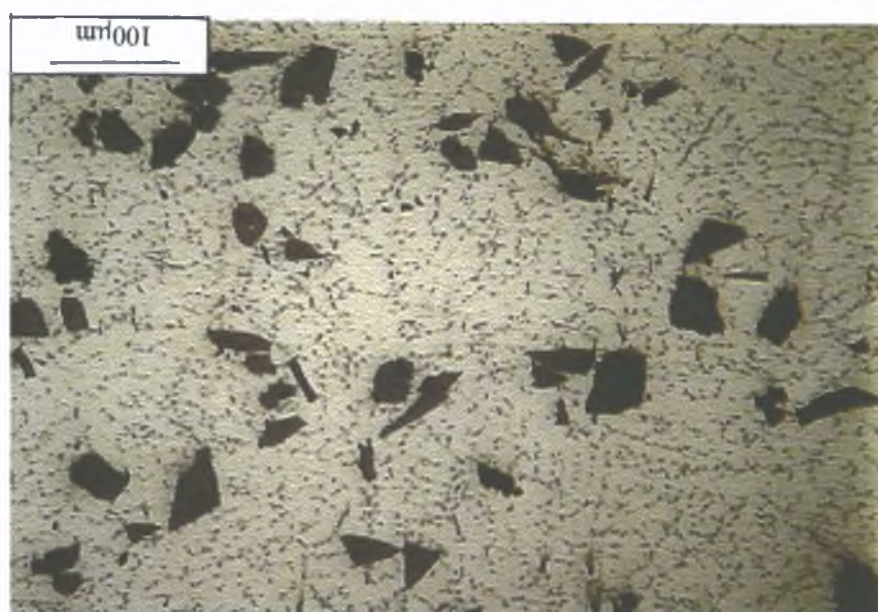
Figure 4.15 : The microstructure of A359 alloy, after 8 hours aging, at 170°C.



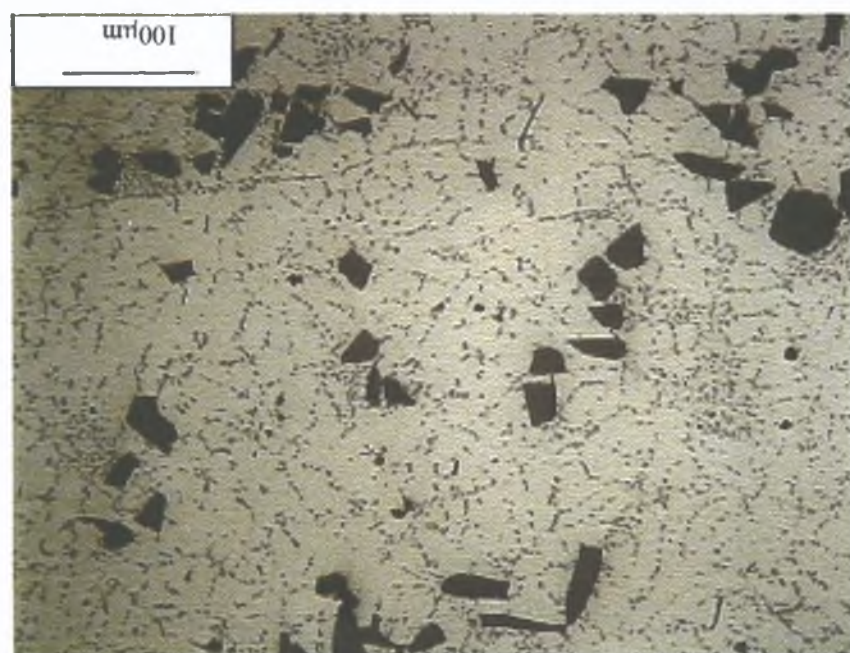
(a)

Figure 4.16: The microstructure of A359/SiC/10p (a) as cast condition, (b) after 2 hours aging at 170°C, (c) after 6 hours aging at 170°C.

(c)



(q)



The same changes in microstructure occur when silicon carbide particles are added to A359 alloy. The T6 treatment does not change the distribution of the silicon carbide particles in the matrix alloy, because the treatment is done in solid state condition, below solidus temperature. This is shown in Figure 4.16(a)(b) and (c). However, the addition of silicon carbide particles to aluminium alloy accelerates aging during thermal treatment, and this is due to the thermal mismatch between the reinforcement and the matrix.

4.5 POROSITY

Another point of concern with respect to casting is porosity. Particle-reinforced MMCs are invariably associated with this problem, although the presence of the reinforcement particles has been seen to be beneficial in some respects. Usually it is porosity measurements, which are used as a measure of casting quality in fabrication environments. In general, a good quality casting practice will keep the porosity level to a minimum. Porosity is a void or cavity that arises in the interior of a casting during mixing and solidification, and is the cause of lowering the mechanical properties of the casting.

In general, there are two basic mechanisms, which produce porosity: precipitation of hydrogen gas and the density change of the alloy upon solidification. Porosity tends to decrease the mechanical properties of a casting by reducing the amount of material that can carry the applied load; further, the voids often act as stress raisers and preferred nucleation sites for cracks.

From the porosity measurement in this study, it was found that porosity content is increased with increasing volume fraction of silicon carbide. The results reveal that the volume percent of porosity is less than 1.85 percent in the case of non-reinforced matrix material, when compared to about 4.39 percent determined for A359/SiC/10p, as cast composite samples. This is as shown in Figure 4.17. The addition of silicon carbide particles decreased the density of the casting significantly. However it was observed that the value of porosity content for A359/SiC/20p samples, produced by using graphite mould, were higher than other samples.

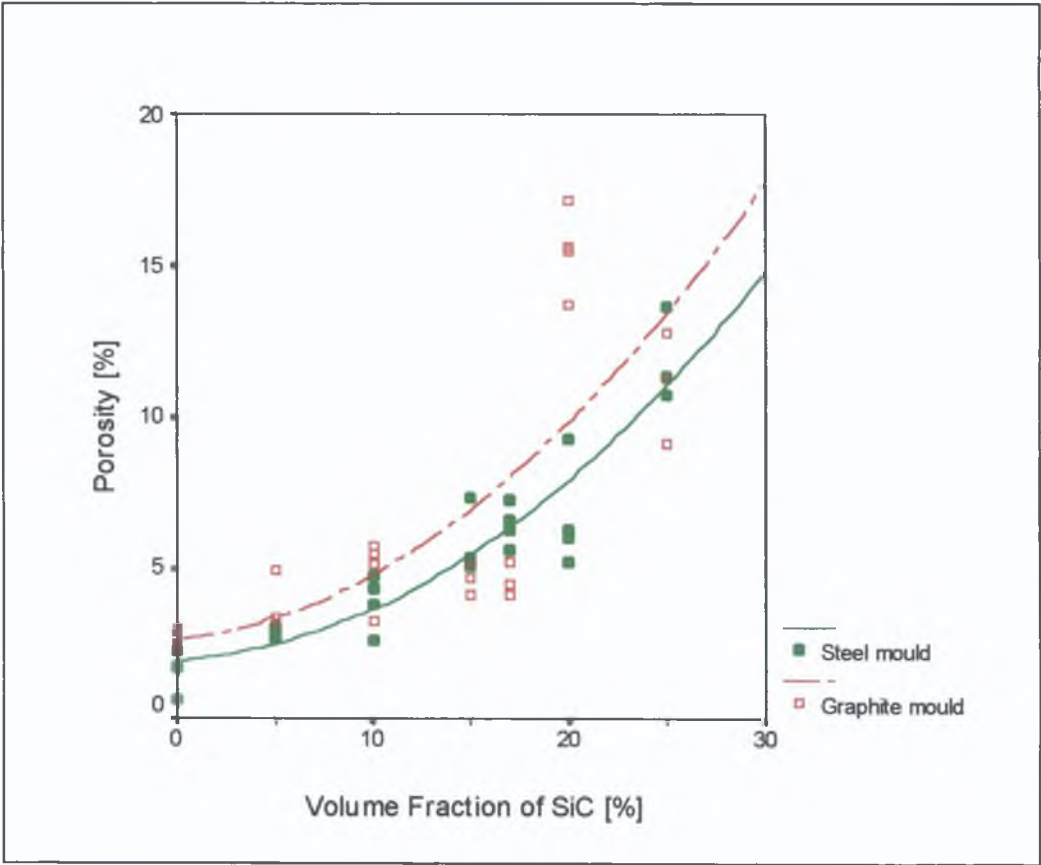


Figure 4. 17: Porosity as a function of silicon carbide content.

Porosity seems to increase with the increase of Silicon carbide particles in the matrix. This is supported by the fact that when the volume fraction of silicon carbide particles increases, the tendency for them to agglomerate or clustering will increase. There are also air pockets between the particles, and these air pockets tend to become bigger when the Silicon carbide particles content increases. As shown in Figure 4.18 a void or pore is always surrounded by silicon carbide particle clusters. The percentage porosity decreases with the size of the ingot, and decreases of porosity when using a steel mould is mostly attributed to the faster rate of cooling of the ingot. Theoretically, the faster the cooling rate, the more uniform the distribution of Silicon carbide particles in the matrix, and the finer will be the grain size, and hence the possibility of void formation is reduced.

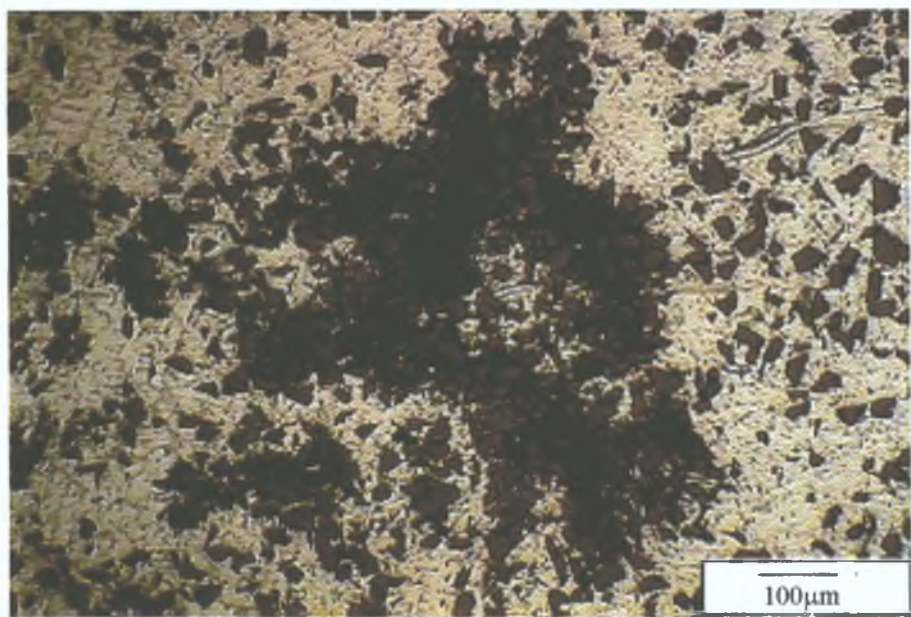


Figure 4.18: Porosity is always within a silicon carbide particles cluster..

In this study, the level of the porosity in the cast composites is determined comparing with theoretical density, and the % of the porosity is calculate from the

equation (12) [265] by assuming the distribution of silicon carbide particles in the matrix is uniform, and the wettability is 100 percent

$$\% \text{ Porosity} = \frac{\text{Theoretical density} - \text{Measured density}}{\text{Theoretical density}} \quad (12)$$

The theoretical value of density of A359 matrix alloy is 2.68 g/cm^3 , and in the MMC samples which have been produced, it was found that the density of A359 matrix alloy was 2.63 g/cm^3 (samples A) and 2.62 g/cm^3 (samples B). Smaller size of ingot seems to give a higher value of density. This may be because of the faster cooling rate. In general, the density of the MMC samples decreases with the increase of volume percentage of silicon carbide particles. In the sample studied, the trend of this change varies with the cooling rate. This is shown in Figure 4.19 for different mould material: graphite and steel, which give different values of cooling rate. Steel mould gives faster cooling rate than graphite, which is 1.475°C/s for steel mould, and 0.803°C/s for graphite mould. Detailed of these data can be seen in Appendix C.

It was also found that the value of porosity increases with the increase of volume percentages of silicon carbide particles. For example, the percentage of porosity in A359/SiC/5p is 2.90 percent (sample A) and 3.85 percent (sample B), compared to the porosity content in A359/SiC/25p, which is about 7.82 percent (small samples) and 11.05 percent (for bigger samples). It was also found that the porosity content decreases in the ingot, which was produced by using steel mould. The porosity content was also decreased with the ingot size.

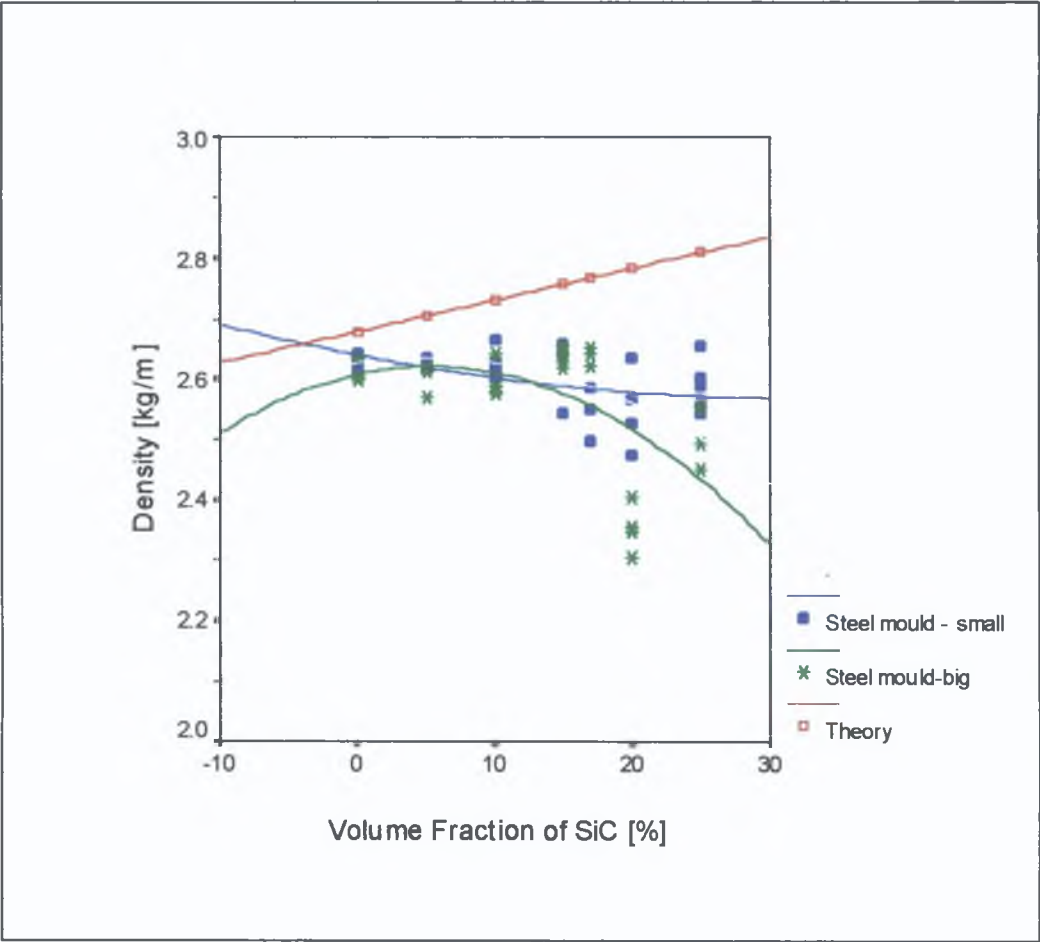


Figure 4.19 : The effect of silicon carbide particles particle content to the density

4.6 COMPRESSION TESTING

Compression tests were carried out on MMC samples containing different percentages of SiC, in the range from 5-25%, both in as cast and after heat treatment conditions. The T6 heat treatment procedure was used as described previously in section 3.5. Figure 4.20 shows the result of the compression tests for MMC samples, as-cast condition. Equation (13) was used to calculate the rupture strength [278]:

$$\sigma = \frac{2 P}{\pi D t} \tag{13}$$

where, P applied load at fracture, D and t is the diameter and length of the sample.

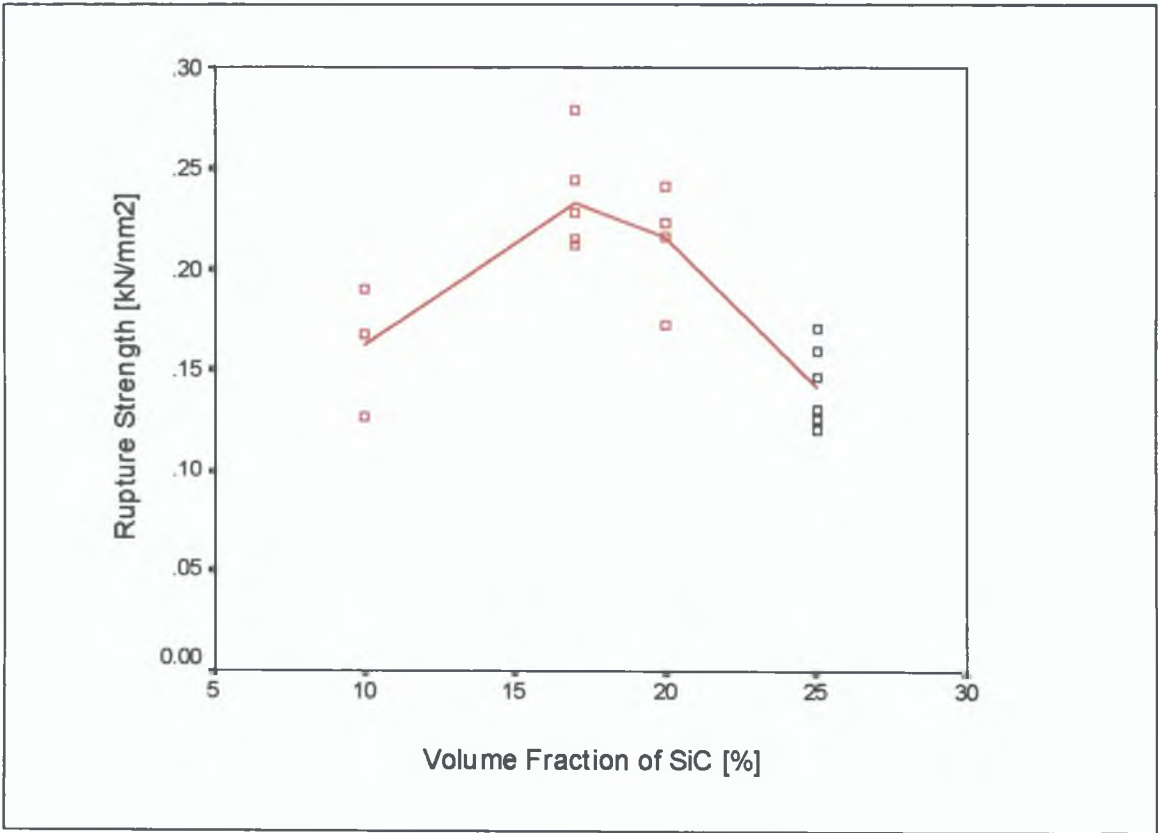


Figure 4.20 : Compression strength as a function of SiC content.

Based on the experimental results, initially the compression strength increases with volume fraction of silicon carbide. For example, from Figure 4.20, the rupture strength for A239/SiC/10p is about 0.16 kN/mm², and this value increases to about 0.22 kN/mm² for A359/SiC/17p. However, the value decreases with further increase of silicon carbide content. This is following the fact that, increasing the silicon carbide content in the alloy matrix decreases the ductility of the alloy, therefore lowering the rupture strength of the samples. The increase of porosity content is also the reason why the rupture strength lowers at higher silicon carbide content. The result from porosity study shows that, increasing the silicon carbide content in the matrix will increase the porosity content significantly. Some of the scatter arises from the irregularities of the sample, such as the flatness of the samples, the surface finish on the surface of the sample. Another important reason for scatter results is the non-uniform distribution of the silicon carbide particles in the matrix alloy. According to several researchers [23,279-281] clustering of reinforcement particles can result in an inhomogeneous distribution of the particles in the matrix. Such regions promote damage due to increased constraint of the matrix within the cluster, resulting in low ductility. It was reported in references [44, 281, 282] that clustered regions were preferred sites for damage initiation and that damage accumulation ahead of a propagating crack also tends to occur in cluster regions.

4.7 MICROHARDNESS

Theoretically, the hardness of the cast ingot should be uniform from the top to the bottom of the ingot. This is, if the distribution of the particles throughout the ingot is

uniform. However, other factors such as the cooling rate, the gravity effect and the non-uniform distribution of the particles in the ingot will give a different value of hardness. The experimental data shows that the hardness of the ingot is lower at the top and at the bottom of the ingot, and it is higher in the middle. 13 ingots have been tested, and all of them give identical trend. The result of Vickers microhardness tests are shown in Figure 4.21, as a function of distance from the top to the bottom, referring to the original position of the ingot during pouring.

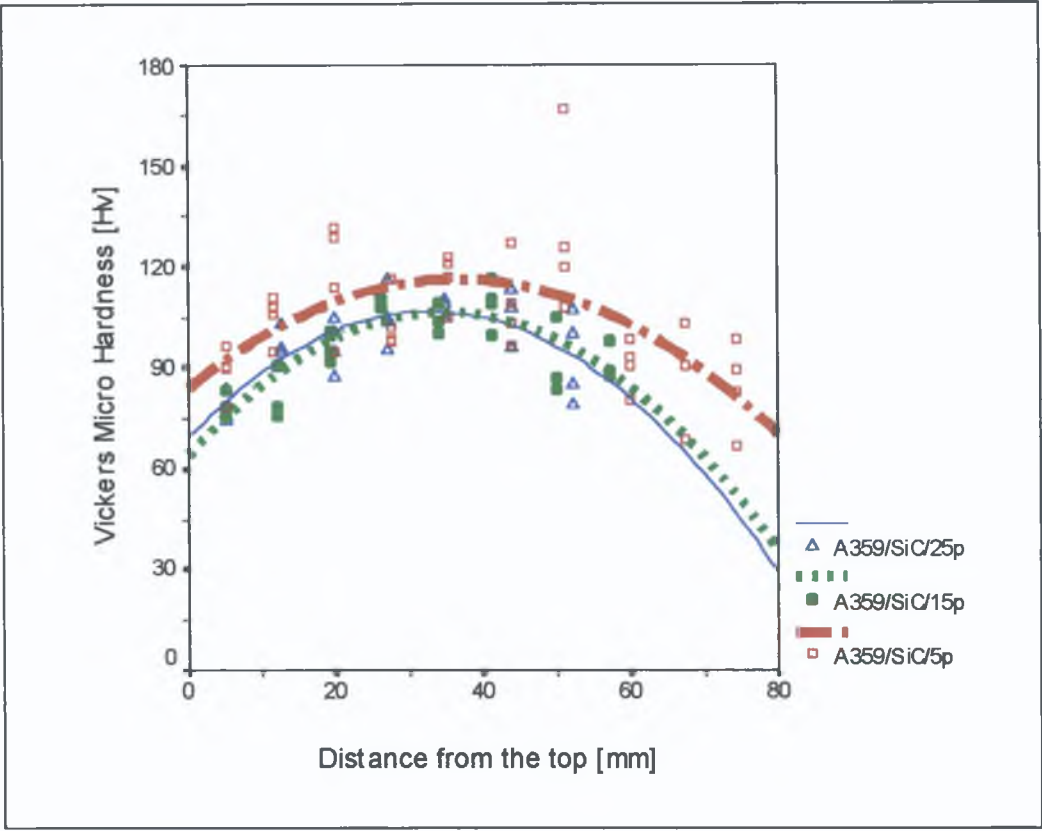


Figure 4.21: Micro hardness as a function of ingot’s distance from the top.

In this experiment it was found that, the value of hardness of A359 matrix alloy as cast condition is 68.22 Hv, as shown in Appendix F. Comparing the hardness between three

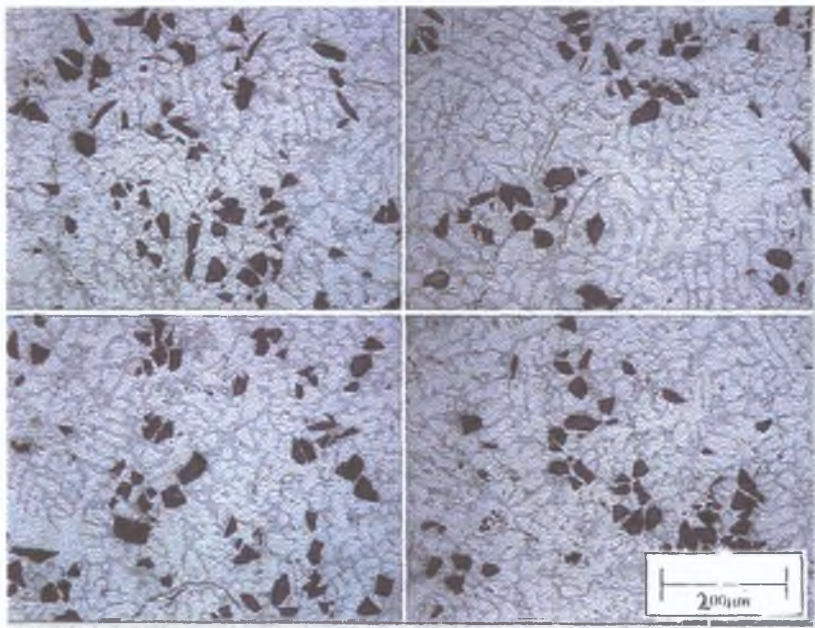
different composite ingots as shown in Figure 4 21, it was found that the maximum value is at the middle part of composite For example, the hardness for A359/SiC/5p and A359/SiC/25p, at the top, middle and bottom of the ingot is shown in Table 4 2 and are presented in a graph form as in Figure 4 21

Table 4 2 Micro hardness value as cast condition for three MMC ingots

Position in ingot	Hardness [Hv]		
	A359/SiC/5p	A359/SiC/15p	A359/SiC/25p
Top	88 9	75 4	79 5
Middle	116 5	104 3	90 2
Bottom	84 45	87 6	82 1

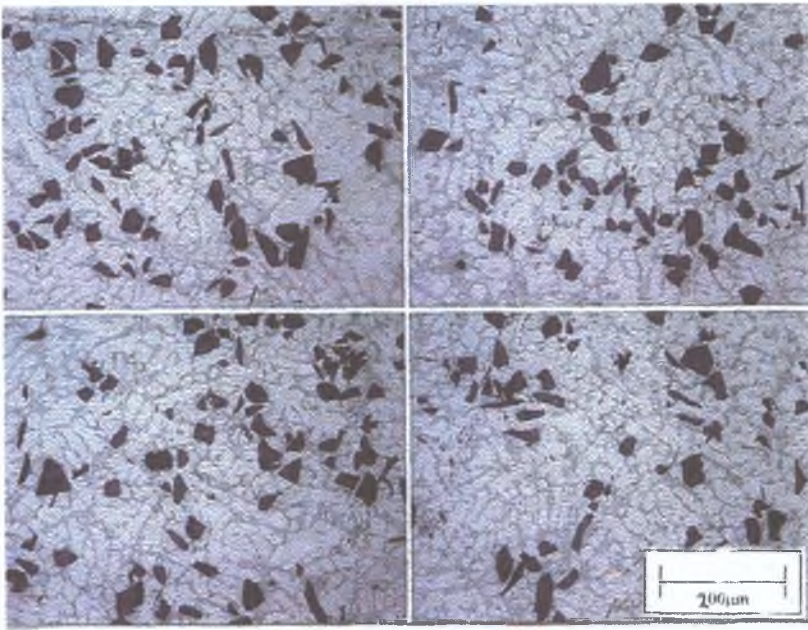
The variation of the hardness values in the ingots possibly attributes to the non-uniform distribution of the SiC in the ingot Because of the pouring method used in this experimental rig, the first drop of slurry was occupied the bottom part of the mould, and therefore, contains less particles Because the size of the mould was not too big, this part of ingot will also solidify first and prevent the SiC particles from settling to the bottom The settlement of the SiC particles occurs in the middle part of the ingot The top part contains less SiC particle than in the center part The high concentration of the SiC particles in the centre part of the ingot, may be the reason why the hardness at this part in maximum comparing to a very top or bottom part of the ingot This is as shown in Figure 4 21(a)(b) and (c), for A359/SiC/10p The concentration of the silicon carbide particles at the top, middle and the bottom of the ingot is 60, 95, and 50 percent respectively

The settlement of particles in the melt is already start to occur when the melt is still in the crucible. This is because the specific gravity of the reinforcements is higher than that of the molten aluminium, which leads to settling or sedimentation of the particle reinforcements. Sedimentation of the SiC particles from the top part of the crucible normally occurs when the stirring is stopped, leaving the upper regions of the melt become devoid of the reinforcement. This phenomenon can result in less particle contained in the first drop of slurry which was occupied the bottom part of the mould.

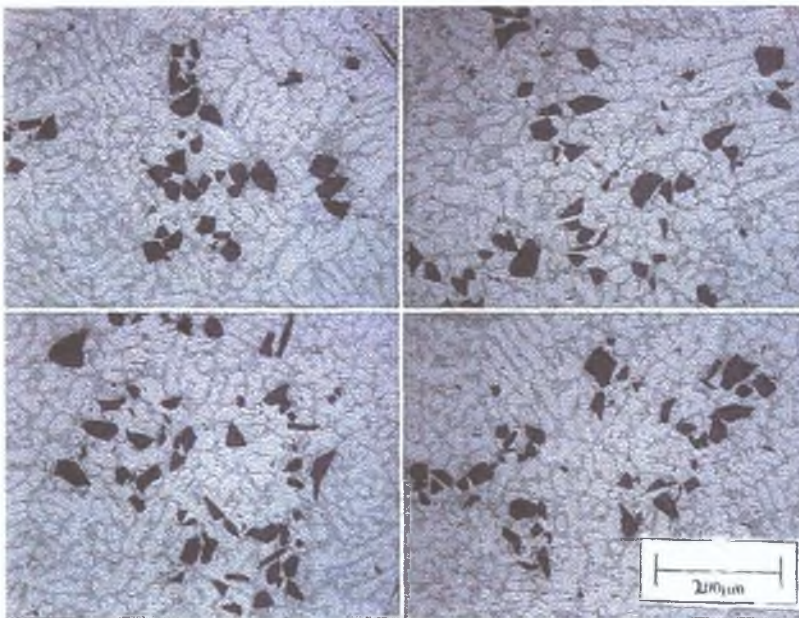


(a) Concentration of silicon carbide particle is 60 percent

Figure 4.21 : The variation of distribution of silicon carbide particles in 150mm long ingot. (a) 5 mm from the top, (b) at the middle, and (c) 5 mm from the bottom of the ingot.



(b) Concentration of silicon carbide particle is 95 percent



(c) Concentration of silicon carbide particle is 55 percent

4.7.1 Effect of Heat Treatment on Micro hardness

The results of the vickers microhardness measurement as a function of aging time are shown in Figure 4 22 (a) and (b). The result shows that the MMC samples after being heat-treated exhibit higher hardness when compared to the non-heat treated samples. For example, the hardness for A359/SiC/5p is 106 417 Hv, as cast condition, and this value of hardness increases to 119 67 Hv, if T6 procedure is applied, after aging for 8 hrs, at 170°C. The results also indicate that the hardness of the samples increases with aging time. The results obtained so far, are not unusual and can be attributed to the increase in strength of the composites primarily as a result of precipitation of Mg_2Si phase during T6 heat treatment. Figure 4 22 (b) also indicated that the strengthening metallic matrix (in non-heat treated condition) due to the incorporation of SiCp. Therefore the increasing in hardness of the composite samples in both non-heat treated and heat treated conditions, with an increase in the volume fraction of SiC may be attributed to the microstructural changes, and also because of an increase in the dislocation density in the matrix, and the presence of residual stress brought by the incorporation of SiC particles, in the metallic matrix.

It is a well known phenomenon in monolithic alloys that aging kinetics decreases with decrease in aging temperature, and the hardness peaks at lower aging temperatures are more flat [284]. This essentially means that peak hardness is retained for a much longer duration of time during low temperature aging. As a result of this, during low temperature aging, the interfaces retain the peak hardness for a long time and a

considerable area of the matrix also reaches the same level of hardness by this time, leading to the occurrence of flat peaks in hardness versus distance plot. Thus the occurrences of flat peaks at lower aging temperatures is merely a manifestation of slower aging kinetics at these temperatures. The mechanism of aging for an aluminium MMC is similar to the alloy, except that the MMC requires less time to attain peak hardness. . The accelerated aging response in MMC has been attributed to the presence of excess dislocations in the matrix which are generated due to the differential thermal contraction between the particles and the matrix during cooling rate of the composite from the solutionizing temperature [285, 259, 286-288].

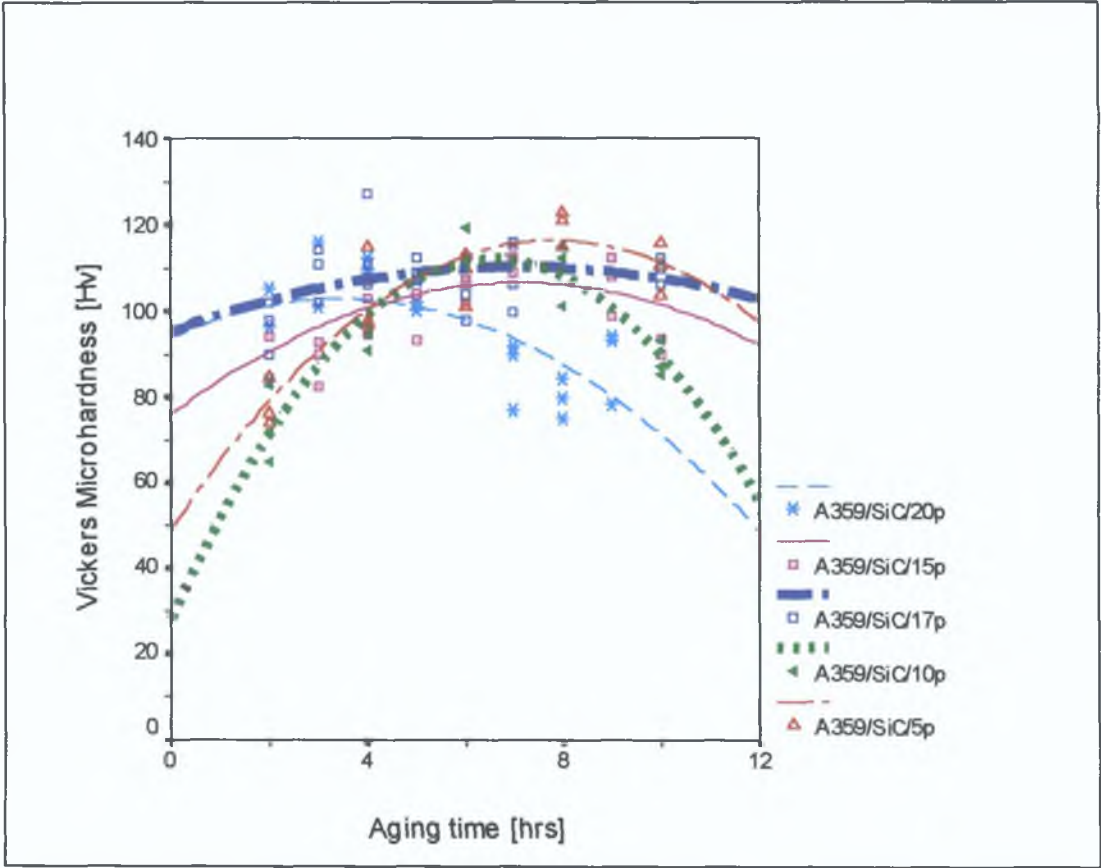


Figure 4.22: Micro hardness as a function of Aging time.

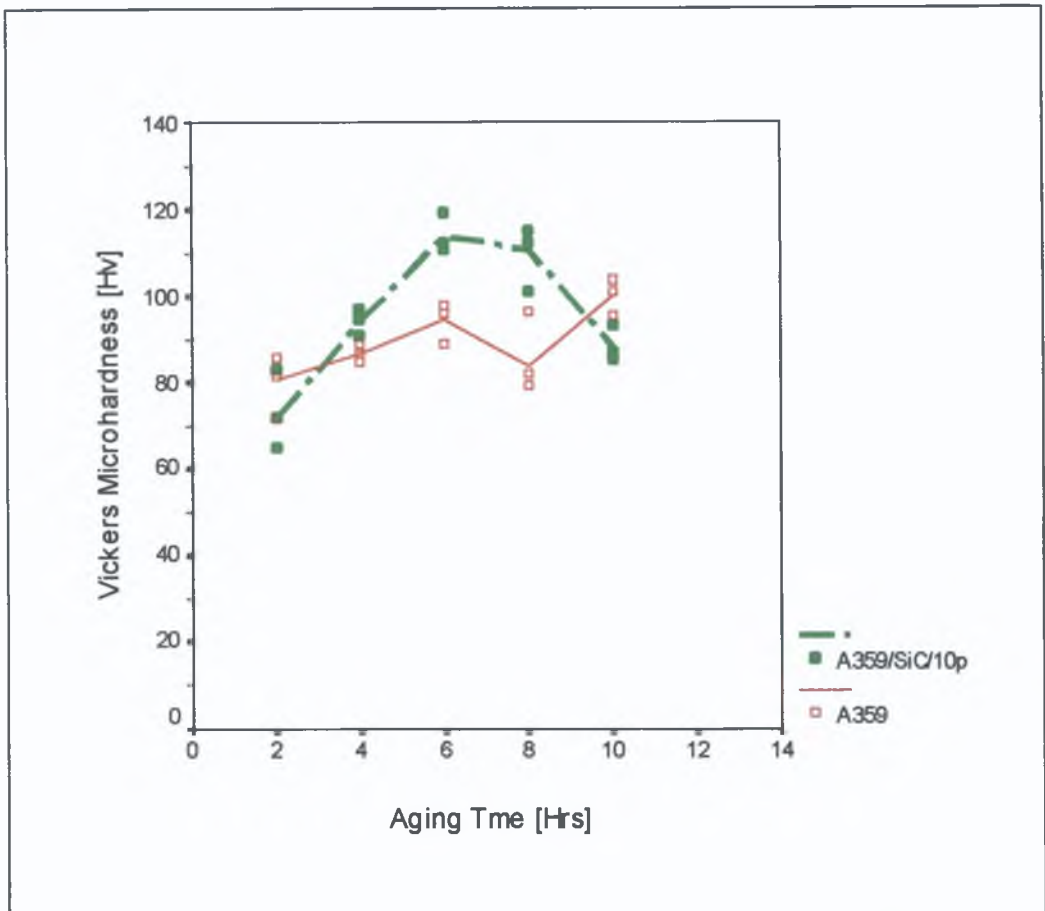


Figure 4.22(a): Micro hardness as a function of aging time, for matrix alloy and cast MMC (A359/SiC/10p)

Theoretical [289-292] as well as experimental [257] studies have shown the existence of a gradient in dislocation density at the particles/matrix interface in composites containing a low volume fraction of reinforcement. Suresh et al [293] measured the dislocation density and showed that it is approximately $6 \times 10^9 \text{ cm}^{-2}$ in non-reinforced alloy, whereas in the composite it can be as high as $2 \times 10^{10} \text{ cm}^{-2}$.

It can be seen in Table 4 3, that the time to reach peak hardness of every composite ingot is different In general, this time decreases with the increase of SiC volume fraction This result is mainly attributed to the accelerated aging response due to the increase of silicon carbide particles content in the matrix material

Table 4 3 Time to reach peak hardness value after T6 treatment

Ingot	Time to reach peak hardness value [Hrs]
A359/SiC/5p	8
A359/SiC/10p	7 30
A359/SiC/15p	7
A359/SiC/17p	6
A359/SiC/20p	3

4.8 TENSILE PROPERTIES

In this study, the experimental results show that in general, the tensile strength of the MMC's produced are somewhat higher than that obtained for the non-reinforced A359 alloy It can be noted that the addition of silicon carbide particles improved the tensile strength of the composites It is apparent that an increase in the volume fraction of SiC results in an increase in the tensile strength Figure 4 23 shows the effect of volume fraction on the tensile strength The tensile strength of the A359 alloy in non-reinforced

condition is 103.75 N/mm², and this value increases to a maximum of 150 N/mm², for A359/SiC/5p, which is about 65% improvement on that of the non-reinforced matrix material.

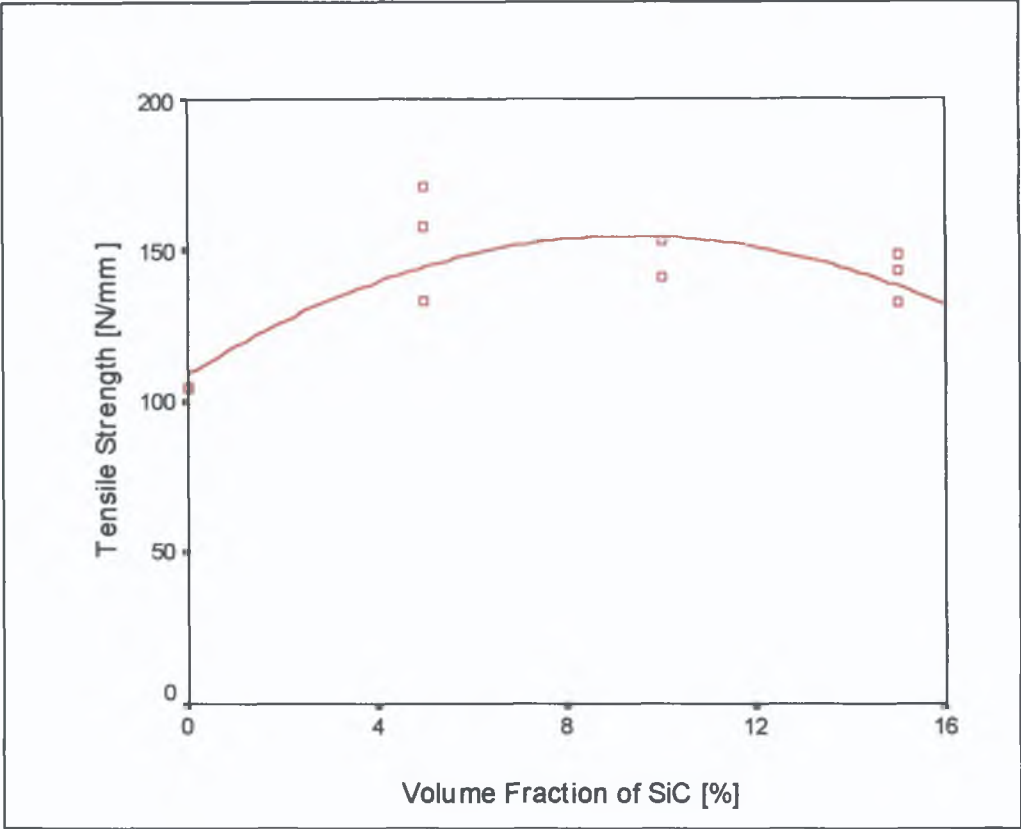


Figure 4.23: Tensile strength as a function of volume fraction of SiC particles.

Figure 4.24 and Figure 4.25 show the surface topography viewed from scanning electron microscope of the tensile fracture surface. It shows that the main reasons for the fracture occurring at that specific location was agglomeration of the silicon carbide particles and porosity. Agglomeration of particles reduced the strong bond between matrix alloy and silicon carbide particles. In the study of McDanel [295], it was found that in the SiC particle reinforced Al alloy, containing beyond approximately 30-40-

volume fraction of SiC, the rate of increase in strength with volume fraction decreases. Moreover, when the reinforcements cluster, the matrix material between individual reinforcement does not bond well. During subsequent deformation these interfaces are likely to separate.

The embedded hard particles in the matrix act as a barrier that resists the plastic flow of composites when it is subjected to strain. This can explain the improvements of the tensile properties in SiC composites, and other mechanical properties such as compression strength and hardness. The presence of hard particles in a soft matrix increases the dislocation density. It was reported that SiC/Al composites have higher dislocation density than those of Al₂O₃/Al composite [296]. The low ductility of the investigated composites could be attributed to the susceptibility to the effect of stress-raiser.

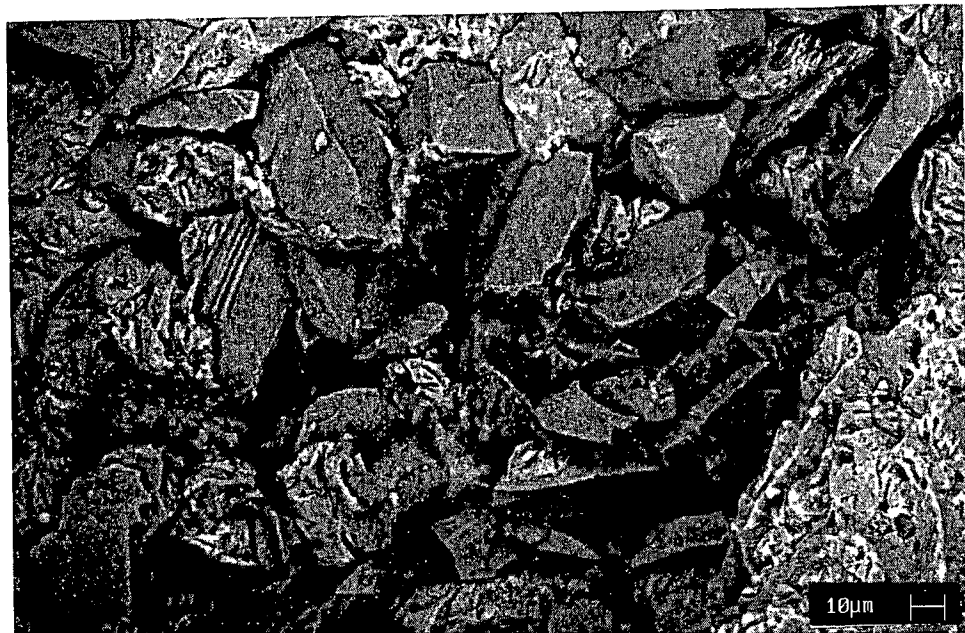


Figure 4.24 Tensile fracture surface topography showing agglomeration of SiC particle (from SEM)



Figure 4 25 Tensile fracture surface topography showing porosity content (form SEM)

An inhomogeneous distribution of silicon carbide particles in the matrix is always associated with the formation of particle cluster. Such cluster region promotes damage due to increased constraint of the matrix within the cluster, resulting in low ductility. Lewandowski et al [281] found that cluster regions were preferred sites for damage initiation and that damage accumulation ahead of a propagation crack also tended to occur in cluster regions. Present experimental results agree well with these facts.

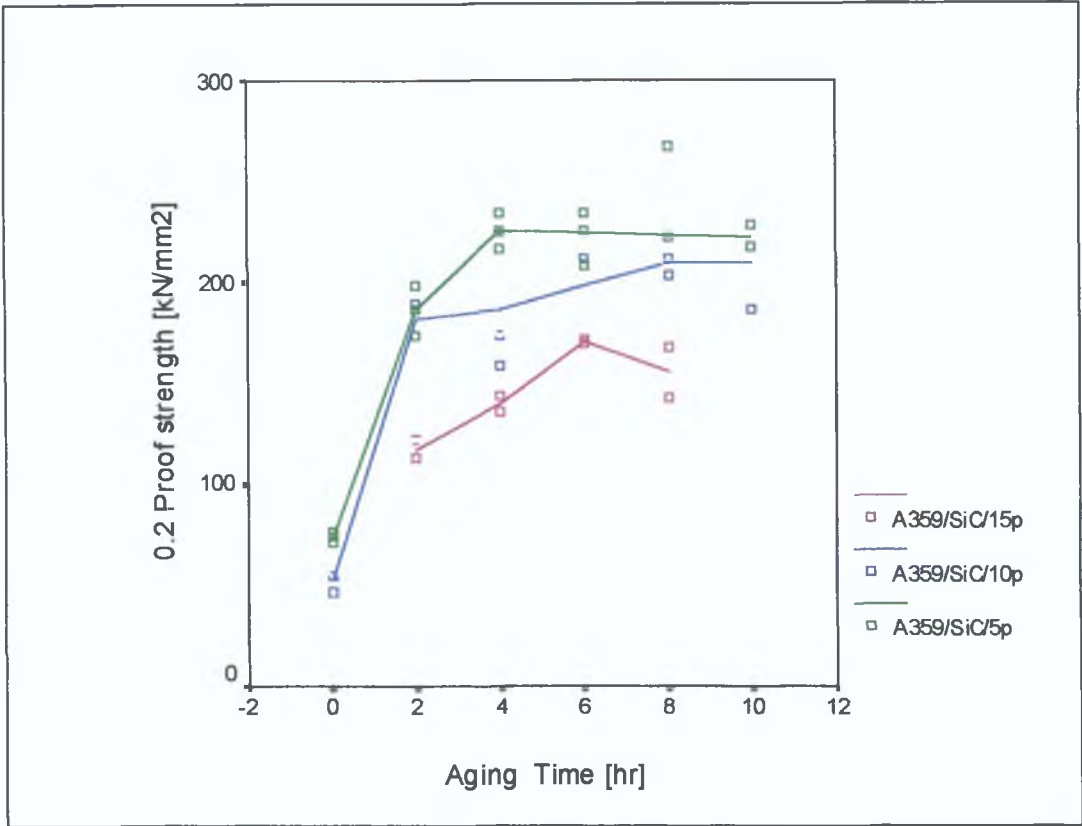


Figure 4.27: Proof Stress as a function of aging time.

The result of aging studies and the effect on 0.2 proof stress conducted on the samples is shown in Figure 4.26. In general, the tensile strength increases with aging time. The majority of the increase in tensile properties that accompany most heat-treatment is due to the formation of non-equilibrium precipitates during aging [1,2]. Precipitates interfere with the movement of dislocations through the matrix. Thus the degree of strength depends upon precipitates size, spacing and coherency. It can be seen that the introduction of SiC particles into Al alloy results in a significant reduction in their ductility. Flom and Arsenault [218] relate such a reduction in ductility to an

inhomogeneous distribution of SiC particles and void initiation at the reinforcement matrix interface

The tensile strength obtained in this study is comparable to results from other researcher This is summarised in Table 5 1

Table 5 1 Tensile strength for some aluminium-silicon alloy based MMC produced by casting technique

Researcher	MMC System	Tensile Strength [MPa]	
		As-Cast	After Heat Treatment
Present study	A359/SiC/5p	102 75	150 50
Samuel et al [33]	A359/SiC/10p	115 00	185 00
Paray et al [204]	A356/SiC/10p	105 00	200 00
Shivkumar et al [262]	A356/SiC/10p	95 70	115 70

CHAPTER FIVE

CONCLUSION AND RECOMMENDATIONS

5.1 CONCLUSION

Conclusions, which can be made from this research, are

- 1 Stirring the MMC slurry in semi-solid state, at a temperature in the solidification range of the alloy matrix, during the solidification process, helps to incorporate ceramic particles into the alloy matrix. In the semi-solid state, primary alpha-aluminium phase exists, and the stirring action assists this solid phase to trap the silicon carbide particles between the dendrite arms, thus stopping them from settling. In other words, the growing solid phases help to drag the ceramic particles into the alloy matrix. However, in semi-solid state, the slurry cannot be poured into a mould, because at this stage, its viscosity is very high, and the fluid flow is very low. Therefore, before pouring the slurry into the mould, it is necessary to re-melt it to a fully molten condition, and re-stir before pouring. The re-stirring process will help to disperse the silicon carbide particles to a more uniform distribution.

- 2 A new approach of fabricating cast Aluminium Matrix Composites by using the stir casting method has proved to be successful. Placing all substances together for melting is experimentally a very convenient process. During the initial stage of heating to about 600°C, any moisture in the ceramic particles, and the matrix materials is burnt off and thus reduces the level of porosity. This advantage cannot be achieved by other methods in which the ceramic particles are introduced in the molten matrix materials from the top.
- 3 The addition of silicon carbide particles to the matrix alloy improves the mechanical properties such as compression, hardness and tensile strength of the matrix alloy. However, the presence of these particles introduced more porosity to the casting. Precipitation hardening, (T6 treatment) applied on the MMC samples was found to improve its mechanical properties. In this case, the precipitation phase formed during the heat treatment was responsible for this positive result. In general, these properties increase with aging time, until reaching its optimum level, then decrease gradually with increasing aging time.
- 4 Microstructural observation suggests that the stirring action of the slurry produces cast MMC with smaller grain size compared to an unstirred one. Stirring breaks the dendrite structures into a small equiaxed or chilled-type structure. The addition of ceramic particles, coupled with the smaller grain size are factors that strengthen the alloy matrix.

The main contributions of this research are:

- 1 A new stir casting rig has been designed, manufactured and commissioned The rig enables
 - i Melting of aluminium in an inert atmosphere
 - ii Casting using a bottom pouring mechanism
 - iii Control of stirring time and temperature of the molten metal
- 2 A new method of wettability enhancement between silicon carbide particle and A359 matrix alloy has been developed This involves the use of 1 wt % Mg , combined with the use of clean silicon carbide particles and stirring continuously at a temperature in the solidification range of the alloy matrix during solidification
- 3 A new approach of fabricating cast MMC using stir casting technique has been proposed This involves placing all substances together in the graphite crucible, at the start of the process, thus avoiding problems associated with particle addition
- 4 A variation in hardness of the cast ingot from the top to the bottom surface has been identified The hardness is maximum at the middle This mainly because of the distribution of the reinforcement particles, which is concentrated in the middle part of the ingot

5.2 RECOMMENDATIONS FOR FUTURE WORK.

Research areas in cast MMC are broad. Several areas regarding the proposed fabrication method which merit study, or development in more detail, include

1 The effect of different size of stirrer and stirring speeds

It may be feasible to reduce particle fracture, further improve wetting, and minimise porosity through improved understanding of the process of mechanical stirring

2 Modification of the rig

Examples include the addition of a controllable cooling system, which could provide greater control of temperature during stirring

3 The microstructure and phase composition of the composite produced

Variations in stirring and casting temperature can influence chemical reactions, and solidification mechanisms during composite production. Conditions could be tailored to optimise properties

References

REFERENCES

- [1] Chou T W , Microstructural Design of Fibre Composites, Cambridge University Press, Cambridge, United Kingdom, 1992
- [2] Ishikawa T and Chou T W , Stiffness and Strength Properties of Woven Fabric Composites, Journal of Materials Science, 17, 1982, pp 3211-3220
- [3] Skolianos S , Mechanical Behaviour of Cast SiC_p-Reinforced Al-4 5%Cu-1 5%Mg, Materials Science and Engineering, A210, 1996, pp 76-82
- [4] Clyne T W and Whithers P J , Introduction to Metal Matrix Composites, Cambridge University Press, Cambridge, 1993
- [5] Ibrahim I A , Mohamad F A and Lavernia E J , Particulate Reinforced Metal Matrix Composites - A Review, Journal of Materials Science, 1991, pp 1137-1156
- [6] Russel K C , Oh S-Y and Figueredo A , Theoretical and Experimental Studies of Ceramic Metal Wetting, MRS Bulletin, April 1991, pp 46-52
- [7] Warren R , Proceedings of the 9th Riso International Symposium On Mechanical and Physical Behavior of Metallic and Ceramic Composite , Eds Andersen S I , Riso Press, Denmark, 1988, p 233
- [8] Abis S , Characteristics of an Aluminium Alloy-Alumina MMC, Composite Science and Technology, 35, 1989, pp 1-11
- [9] Eliasson J and Sandstrom R , Applications of Aluminium Matrix Composites, Key Engineering Material, 104-107, 1995, pp 3-36

- [10] Mohr W R and Vukobratovitch D, Recent Applications of Metal Matrix Composites in Precision Instruments and Optical System, Key Engineering Material, 10, 1988, pp 225-235
- [11] Lilholt H , Aspect of Deformation of Metal Matrix Composites, Materials Science and Engineering, A135, 1991, pp 161-171
- [12] O'Donnell G , Process Optimisation and Numerical Modeling of Powder Metallurgical Aluminium Matrix Composites, Ph D Thesis, Dublin City University, Ireland, 1999
- [13] Ling C p , Bush M B and Perera D S , Effect of Fabrication Techniques On the Properties of Al-SiC Composites, Journal of Materials Processing Technology, 40, 1995, pp 325-331
- [14] Girod F A , Quenisset J M and Naslain R , Mechanical Behaviour of Aluminium Matrix Composites Reinforced by Short Fibres and Processed by Compocast, Composites Science and Technology, 30, 1987, p 155
- [15] White J and Willis T C , Materials and Design, 10, 1989, p 121
- [16] Divecha A P , Fishman S G and Karmarkar S D , Silicon Carbide Reinforced Aluminium - A Formable Composites, Journal of Metals, 9, 1981, p 12
- [17] Smith P R and Froes F H , Journal of Metal, 19, 1984
- [18] Erich D L , Metal Powder Report, 43, 1988, p 418
- [19] Hagstrom J and Sandstrom R , Pre-selection of Materials Groups Using Property Database System, 3rd International Conference On Aluminium and Aluminium Alloy, Trondheim, Norway, 1992

- [20] Savage W , Proceedings of 2nd International Conference on Cast Metal Matrix Composite , Eds Stefanescu D M and Sen S , Des Plaines, IL, USA, 1994, p 100
- [21] Feest E A , Exploitation of the Metal Matrix Composites Concept, Metals and Materials, 4, 1988, pp 273-278
- [22] Thaw C , Minet R , Zemaný J and Zweben C, Metal Matrix Composites For Microwave Packing Components, Electron Packaging Product, 27, August 1987, pp 27-29
- [23] Lloyd D J , Particle Reinforced Aluminium and Magnesium Matrix Composites, International Materials Review 39, 1994, pp 1-23
- [24] Huda M D , Hashmi M S J and El-Baradie M A , MMCs Materials, Manufacturing and Mechanical Properties, Key Engineering Materials, 104-107, 1995, pp 37-64
- [25] Taya M and Arsenault R J , Metal Matrix Composites-Thermomechanical Behaviour, Pergamon Press, Oxford, 1989, pp 41-156
- [26] Trumper R L , Metal Matrix Composites - Application and Prospects, Metal and Materials, 3, 1987, p 662
- [27] Lindroos V K and Talvitie M J, Recent Advances In Metal Matrix Composites, Journal Materials Processing Technology , 53, 1995, pp 273-284
- [28] Schoutens J E , Hand Book of Ceramics and Composites, Vol 1, p 495
- [29] Vedula K and Stephens J R , Proceeding of Materials Research Society Symposium, 81, 1987, p 381

- [30] Bendixen J and Mortensen A , Particle/Matrix Bonding In Alumina-Steel Composites, *Scripta Metallurgica et Materialia* v 25 n 8 August, 1991 p 1917-1920
- [31] Talvitie M J and Lindroos V K , Proceedings of Powder Metallurgy World Conference , 2, 1994, p 1465
- [32] Kainer K U , PD-Vol-37, Composite Materials Technology, 37, 1991, p 191
- [33] Samuel F H and Samuel A M , Solution Treatment of Permanent Mold Castings of an A359/SiC/10p Composites, *AFS Transaction*, vol 102, 1994, pp 387-395
- [34] Nutt S R *Journal of American Ceramic Society*, 71, 1988, p 149
- [35] Bonfield W , *Interfaces in Metal Matrix Composites*, Ed Metcalfe A G , Academic Press, New York, 1974, p 363
- [36] Vinson J R and Chou T W , *Composite Materials and Their Use In Structures*, Applied Science Publishers Ltd, London, 1975
- [37] Odorio J , Use of Composite Materials For Aeronautical Structure, Proceedings of the 1st France-Japan seminar On Composite Materials, Paris, France, March 13-14, March, 1990,
- [38] Johnson W S , Metal Matrix Composites-Their Time to Shine?, *ASTM Standardization News*, October, 1987, pp 36-39
- [39] Hunt W H , Proceedings of the International Conference on Powder Metallurgy Aerospace Materials, Lausanne, Switzerland , Nov, 1991
- [40] Makamoto K and Takao C , *Journal of Materials Science* , 28, 1993, p 684
- [41] Hunt W H Jr , Cook C R and Sawtell R R , Cost Effective High Performance Powder Metallurgy Aluminium Matrix Composites for Automotive Applications,

- International Congress and Exposition, Detroit, Michigan, USA, SAE Technical Paper Series, 910834, March, 1991, pp, 1-11
- [42] Odorico J , Proceedings of the 1st France-Japan Seminar on Composite Materials, Paris-Le Bourget, March 1990
- [43] Kamat S V ,Hirt J P and Mehrabian R , Acta Metallurgical, 37, 1989, p 2395
- [44] Lloyd D J, Aspect of Fracture in Particulate Reinforced Metal Matrix Composites, Acta Metallurgical Materials , 39, 1991, pp 59-71
- [45] Watt D F Xu X Q and Lloyd D J , Effect of Particle Morphology and Spacing on the Strain Fields In a Plastically Deforming Matrix, Acta Material , 44, 1996, pp 789-799
- [46] Lloyd D J and Chamberlain B , Properties of Shape-Cast Al-SiC Matrix Composites, In Cast Reinforced Metal Composites, World Mater Congress, Chicago, September, 1988, pp 263-269
- [47] Hunt J R , International Conference on Powder Metallurgy Aerospace Materials, MPR Publication, Laussane, Switzerland, 1991, pp 32 1-32 15
- [48] Kahl W and Leupp J , High Performance Aluminium Produced by Spray Deposition, Metal Powder Rep , 45, 1990, pp 274-278
- [49] Ghosh P K and Ray S , Fabrication and Properties of Compocast Aluminium-Alumina Particulate Composite, Indian Journal of Technology, February 1988, 26, pp 83-94
- [50] Mehrabian R, Sato A and Fleming M C , Light Metal, 2, 1975, p 177
- [51] Mehrabian R , Rich R G , and Fleming M C , Metallurgical Transaction, 5, 1974, p 1899

- [52] Skibo D S and Schuster D M , Process For Preparation of Composite Materials Containing Non-Metallic Particles in a Metallic Matrix, and Composite Materials Made Thereby, United State Patent Number 4, 786,467, Nov 1988
- [53] Rohatgi P K , Foundry Processing of Metal Matrix Composites, Modern Casting, 78, 1988, pp 47-50
- [54] Srivatsan T S , Ibrahim I A , Mohamed F A and Lavernia E J , Processing Techniques For Particulate Reinforced Metal Aluminium Matrix Composites, Journal of Materials Science, 26, 1991, pp 5965-5978
- [55] Clegg A J Cast Metal Matrix Composites, Foundryman, 84, 1991, pp 312-319
- [56] Lloyd D J , Factors Influencing the Properties of Particulate Reinforced Composites Produced by Molten Metal Mixing, in 12th Riso International Symposium In Materials Science , Roskilde, Denmark, 1991, pp 81-99
- [57] Surappa M K , Microstructure Evolution During Solidification of DRMMC (Discontinuously Reinforced Metal Matrix Composites) State of Art, Journal Materials Processing Technology, 63, 1997, pp 325-333
- [58] Bonollo F , Guerriero R , Sentimanti E , Tangerini I and Yang V L , Effect of Quenching on the Mechanical Properties of Powder Metallurgy Produced Al-SiC Particles, Metal Matrix Composites, Material Science and Engineering , A144, 1991, pp 303-310
- [59] Skibo M , Morris P L and Lloyd D J , Structure and Properties of Liquid Metal Processed SiC Reinforced Aluminium, World Materials Congress, Chicago, 1988, pp 257-262

- [60] Surappa M K and Rohatgi P K , Preparation and Properties of Cast Aluminium Ceramic Particle Composites, Journal of Materials Science , 16, 1981, p 983
- [61] Maruyama B and Rabenberg L , Interfaces In Metal Matrix Composites , Proceedings Conference, Eds Dhingra A K and Fishman , S G New Orleans, TMS-AMIE, 1986, pp 233-238
- [62] Quigley B F , Abbaschian G J , Wunderlin R and Mehrabian R , Metallurgical Transaction A, 13A, 1982, p 93
- [63] Khrishnan B P , Surappa M K and Rohatgi P K , Journal of Material Science, 16, 1981, pp 1209-1216
- [64] Fleming M C and Mehrabian R , Transaction American Foundrymen's Soc , 81, 1973, p 81
- [65] Fleming M C Rich R G and Young K P , AFS International Cast Metal, 1, 1976, p 11
- [66] Ghosh P K Rays S , and Rohatgi P K , Transaction of Japan Institute of Metal, 25, 1984, p 440
- [67] Miwa K , Fabrication of SiCp Reinforced Aluminium Matrix Composites by Compocasting Process , Journal of Japan Foundryman's Society, 62, 1990, pp 423-428
- [68] Lee H C and Kim M S , A Fabrication Method of Aluminium-Short Fibre Alumina Matrix Composites by Compocasting, Proceedings of the KSME-JSME Joint Conference, 1990, pp 471-475

- [69] Salvo L Esperance G L , Suery M, and Legoux J G , Interfacial Reaction and Age Hardening in Al-Mg-Si Metal Matrix Composites Reinforced with SiC Particles, *ibid*, A177, 1994, pp 173-183
- [70] Yilmaz M and Altintas S , Properties of Al-Mg-SiC Composites Produced by a Modified Compocasting Technique, Proceedings of the 2nd Biennial European Joint Conference On Engineering Systems, London, ASME New York, 1994, pp 119-124
- [71] Labib A , Liu H and Samuel F H , Effect of Solidification Rate (0.1-100C/s) On the Microstructure, Mechanical Properties and Fractography of Two Al-Si-10 Volume % SiC particles Composite Castings, *Materials Science and Engineering*, A160, 1993, pp 81-90
- [72] Zhong W M , Esperance G L and Suery M , Interfacial Reaction in Al-Mg/SiCp Composites During Fabrication and Remelting, *Metallurgical and Materials Transactions A*, 26A, 1995, pp 2637-2649
- [73] Milliere C and Suery M , Fabrication and Properties of Metal Matrix Composite Based On SiC Fibre Reinforced Aluminium Alloys, *Materials Science and Technology*, 4, 1988, p 41
- [74] Ghosh P K and Ray S , Fabrication and Properties of Compocast Aluminium-Alumina Particulate Composites, *Indian Journal of Technology*, 26, 1988, pp 83-94
- [75] Miwa K , Takashi I And Ohashi T , Fabrication of SiC Whiskers Reinforced Aluminium Matrix Composites by Compocasting Process, Proceedings of the 2nd

- International Conference On The Semi Solid Alloys and Composites, Eds Brown S B and Fleming M C , MIT, Massachussets, 1993, p 398-405
- [76] Wang W and Ajerch F , Particle Interaction of Melt-Stirred Al-Si/SiCp Composites, Proceedings of International Symposium in Production & Fabrication of Light Metal & Metal Matrix Composites, Edmonton Alberta, 1992, pp 629-641
- [77] Gupta M and Surappa M K , Processing-Microstructure-Mechanical Properties of Aluminium-Based Metal Matrix Composites Synthesis Using Casting Route, Key Engineering Materials, 104-107, 1995, pp 259-274
- [78] Ghosh P K and Ray S , Effect of Porosity and Alumina Content On the High Temperature Mechanical Properties of the Compocast Aluminium Alloy-Alumina Particulate Composite, Journal of Materials Science, 22, 1987, pp 4077-4086
- [79] McCoy J W , Jones C and Wawner F E , Preparation and Properties of Cast Ceramic/Aluminium Composites, SAMPE Quarterly, Jan 1988, pp 37-50
- [80] Yamada K , Sekiguchi S and Matsumiya T , The Optimum Condition of Compocasting Method For Particulate Metal Matrix Composites, 34th International SAMPE Symposium, 1989, pp 2266-2277
- [81] Young R M K and Clyne Y M , Journal of Materials Science, 21, 1986, pp 1057-1069
- [82] Yarrandi F M , Rohatgi P K and Rays S , Two Phase Flow Behaviour and Microstructure in Aluminium Alloy-SiC Particulate Composite, Proceedings of 2nd International Conference On Processing of Semi Solid Alloy & Composites, 1993, pp 447 - 465

- [83] Narciso J , Alonso A , Pamies A , Cordovilla C G and Louis E , Wettability of Binary and Ternary Alloys of the System Al-Si-Mg with SiC Particulate, Scripta Metallurgical, 31, 1994, pp 1495-1500
- [84] Wang W and Ajersch A , Silicon Phase Nucleation On SiC Particulate Reinforcement In Hypereutectic Al-Si Alloy Matrix, Materials Science and Engineering, A 187 1994, pp 65-75
- [85] Surappa M K and Rohatgi P K , Materials Technology, 5, 1978, pp 358-361
- [86] Ray S , M Tech Dissertation, ITT Kanpur, India, 1969
- [87] Gibson P R , Clegg A J and Das A A , Foundry Trade Journal, 152, 1982, pp 253-256
- [88] Ray S , Casting of Composite Components, Proceeding of the 1995 Conference On Inorganic Matrix Composites, Bangalore, India, 1996, TMS, pp 69-89
- [89] Hanumanth G S , Iron G A and Lafremer S , Metal Transaction, 23B, 1992, p 753
- [90] Richardson I F , Casting of Silicon Carbide Reinforced Aluminium Alloys, Foundryman, 82, 1989, pp 538-542
- [91] Ribes S K and Suery M , Effect of Particle Oxidation On Age Hardening of Al-Si-Mg/SiC Composite, Scripta Metallurgy, 23, 1989, pp 705-709
- [92] Morita M , Metal Matrix Composites, Advances Composite Materials, 4, 1995, pp 237-246
- [93] Lloyd D J , The Solidification Microstructure of Particulate Reinforced Aluminium/SiC Composites, Composites Science and Technology, 35, 1989, pp 159-179

- [94] Mortensen A , Cornie J A and Fleming M C , Columnar Solidification In a Metal Matrix Composites, Metallurgical Transaction A, 19A, March 1988, pp 709-721
- [95] Uhlmann D R , Chalmers B and Jackson K A , Journal of Applied Physics, 35, 1964, p 2986
- [96] Chernov A and Melnikova A M , Soviet Physics – Crystallography, 10, 1966
- [97] Bolling G F and Cisse J , J Crystall Growth, 10, 1971
- [98] Samuel A M , Gotmare A and Samuel F H , The Effect of Solidification Rate and Metal Feedability On Porosity and SiC/Al₂O₃ Particle Distribution In an Al-Si-Mg (A356) Alloy, Composite Science and Technology, 53, 1995, pp 301-315
- [99] Rohatgi P K , Asthana R and Das S , Solidification, Structure and Properties of Cast Metal-Matrix Composites, International Metal Review, 31, 1986, p 115-139
- [100] Geiger G H and Dorrer D R , Transport Phenomena in Metallurgy, Addison Wesley Publication, Co , 1973
- [101] Sekkar J A and Trivedi R , Materials Science and Engineering, A147, 1991, p 9
- [102] Hunt W H , Interfaces in Metal Matrix Composites, Eds Dhingra A K and Fishman S G , TMS-AIME, 1986, pp 3-25
- [103] Kang C G , Ray S and Rohatgi P K , Micromechanical Solidification Heat Transfer In One Dimensional Al-Al₂O₃ Composites and Its Consequences On Microstructure Evolution, Materials Science & Engineering A Structural

- Materials Properties, Microstructure and Processing, 188, Nov 30 1994, pp 193-199
- [104] Fukunaga H , Komatsu S and Kanoh Y , Bulletin of Japan Society Mechanical Engineering, 26, Oct 1983, p 1814
- [105] Abe Y , Nakatani M , Yamatsuta K , and Horikiri S , Developments In the Science and Technology of Composite Materials, Proceedings of the 1st European Conference On Composite Materials , ECCM-1, Bordeaux, France, Eds Bunsell A R Lamicq P and Massiah A , September, 1985, pp 604-609
- [106] Jeng S C and Chen S W , The Solidification Characteristic of A6061 and A356 Aluminium Alloys and Their Ceramic Particles Reinforced Composites, Acta Materials , 45, 1997, pp 4887-4899
- [107] Backerud L , Chai G and Tammiren J , American Foundrymen's Soc , Skan Aluminium De Plaines, IL, 2, 1990
- [108] Kaufmann H , Neuwirth E , Larsher J and Pacyna H , Aluminium Alloys, Eds Arnberg A , Lahne O and Ryum N , NTH and SINTEF Trondheim, Norway, 1992, p 81
- [109] Ray S , Cast Metal Matrix Composites - Challenges In Processing and Design, Bulletin Materials Science , 18, 1995, pp 693-709
- [110] Moon H K , Ito Y , Cornie and Flemings M C , Key Engineering Materials, 15, 1993, pp 79-80
- [111] Carotenuto G , Gallo A and Nocolais L , Degradation of SiC Particles In Aluminium-Based Composites, Journal Materials Science, 29, 1994, pp 4967-4974

- [112] Mummery P and Derby B , Influence of Microstructure On the Fracture Behaviour of Particulate Metal matrix Composites, Materials Science & Engineering A Structural Materials Properties, Microstructure and Processing Papers on Metal Matrix Composites, A135, 1991, pp 221-224
- [113] Milliere C and Suery M , Advanced Materials Research and Developments For Transport, Edn Lamicq, Paris, 1985, pp 241-24
- [114] Mada M and Ajers F , Trixtropic Effect in Semi-Solid Al-6%Si Alloy, Metal and Ceramic Matrix Composite , Ed Bhagat R B , TMS Publication , 18, 1990, pp 337-350
- [115] Hoover W R , Recent Advances In Castable Metal Matrix Composite, in Proceedings of International Conference " Fabrication of Particulates Reinforced Metal Matrix Composites", Montreal, Canada, 1990, pp 115-123
- [116] Hoover W R , Die Casting of Duralcan Composites, Proceedings of the 12th Riso International Symposium on Materials Science Metal Matrix Composites - Processing, Microstructure and Properties, Riso Natl Lab Roskilde Denmark, 1991, p 387
- [117] Girot F A , Albingre L , Qeunisset J M and Naslain R , Rheocasting Aluminium-Matrix Composites, Journal of Metal, 39, 1987, pp 18-21
- [118] Fleming M C , Behaviour of Metal Alloys In the Semi-Solid State, Metallurgical Transaction, 22A, 1991, pp 957-981
- [119] Moon H K , Materials Science & Engineering, 144A, 1991, pp 253-265

- [120] Asthana R , and Tewari S N , Interfacial and Capillary Phenomena In
Solidification Processing of Metal Matrix, Composites Manufacturing, 4, March,
1993, p 3-25
- [121] Sekkar J A , Material Science & Engineering, 147, 1991, pp 9-21
- [122] Krishnan B P Surappa M K and Rokatgi P K , Journal of Materials Science,
16, 1981, pp 1209-1216
- [123] Lajoye L and Suery M , Solidification Processing, Proceedings Conference
Sheffield, September, 1987, pp 473-476
- [124] Krishnan B P and Rohatgi P K , Metal Technology, February, 1984, p 41
- [125] Yarrandi F , Ph D Thesis, University of Wisconsin-Milwaukee, 1991
- [126] Geiger J F and Zaki W N , Chemical Engineering Science, 3, 1954, p 65
- [127] Laffreniere S and Iron G A , Sedimentation During Liquid Processing of Metal
Matrix Composites, Proceedings of International Symposium ' Production,
Refining, Fabrication and Recycling of Light Metals', Eds Boushard M and
Tremblay P , Pergamon Press, 1990, pp 177-186
- [128] Richardson F J and Zaki W N , Transaction International Chemical Engineering,
32, 1954, pp 35-53
- [129] Hanumanth G S and Iron G A ,Particle Incorporation By Melt Stirring For the
Production of Metal Matrix Composites, Journal of Materials Science, 28, 1993,
pp 2459-2465
- [130] Mirza S and Richardson J F , Chemical Engineering Science, 34, 1979, pp 447-
454
- [131] Thomas D G , A I C H E J , 1, 1962, p 373

- [132] Ray S Casting of Metal Matrix Composites, Key Engineering Materials, 104-107, 1995, pp 417-446
- [133] Lloyd D J , Particle Reinforced Aluminium and Magnesium Matrix Composites, Journal of International Materials Review, 39, 1994, pp 1-5
- [134] Mortensen A and Jin I , Solidification Processing of Metal matrix Composites, International Materials Review, 37, 1992, pp 101-128
- [135] El-kaddah N E and Chang K E , The Dispersion of SiC-Al Slurries in Rotating Flows, Materials Science & Engineering A Structural Materials Properties, Microstructure and Processing, A144, Oct 1 1991, p 221-227
- [136] Stefanescu D M and Dhindaw B K , Kakkar S A and Moitra Q , Behavior of Ceramic Particles at the Solid-Liquid Metal Interface In Metal Matrix Composite, Casting Handbook (ASM), 15, 9th Edition, 1988, pp 142-147
- [137] Xiao K and Lyons J S , On the Distribution of Particulate In Cast MMCs, Journal of Reinforced Plastic and Composites, 15, 1996, pp 1131-1148
- [138] Stefanescu D M , Moitra A , Kacar A S and Dhindaw B K , The Influence of Buoyancy Force and Volume Fraction of Particles On the Particles Pushing/Entrapment Transition During Directional Solidification of Al/SiC and Al/Graphite Composites, Metallurgical Transaction A, 121A, 1990, p 231-239
- [139] Rohatgi P K , Yarrandi F M and Liu Y , Influence of Solidification Conditions On Segregation of Aluminium-Silicon Carbide Particle Composites, ASM International Conference On Cast Reinforced Metal Matrix Composites Eds, Fishman S G , and Dhingra A K , 1988, p 249

- [140] Asthana R and Tewari S N , Engulfment of Foreign Particles By a Freezing Interface, *Journal of Materials Science*, v 28, 1993, p 5414-5425
- [141] Han N , Pollard G , Stevens R , Interfacial Structure and Fracture of Aluminium Alloy A356-SiC Particles Metal Matrix Composite, *Materials Science and Technology*, 8, 1992, pp 184-187
- [142] Han Q , and Hunt J D , Redistribution of Particles During Solidification, *ISIJ Int* , 35, 1995, pp 693-699
- [143] Han Q D , M Phil Thesis, Department of Materials , University of Oxford, 1994
- [144] Jin I And Lloyd D J , Solidification of SiC Particulate Reinforced Al-Si Alloy Composites, *Fabrication of Particulate Reinforced Metal Composites*, Eds Massounave J , and Hamel F G , *ASM Int* , 1990, pp 47-52
- [145] Kennedy A R McCartney D G and Wood J V , Homogeneous Metal Matrix Composites Produced By a Modified Stir Casting Technique, *Synthesis/Processing of Lightweight Metallic Materials*, Eds Froese F H , Suryanarayana C and Ward C M , *TMS*, 1995, pp 261-174
- [146] Patton A M , *Journal Institute of Metal*, 100, 1972, p 197
- [147] Biswas P K , PhD Thesis, Indian Institute of Science, Bangalore, 1981
- [148] Deonath R T and Rohatgi P K , *Journal of Materials Science*, 15, 1980, p 1241
- [149] Krishnan B P et al , *Transactions AFS* , 84, 1976, P 73
- [150] Surappa M K , PhD Thesis, Indian Institute of Science, Bangalore, 1979
- [151] Deonath R T and Rohatgi P K , *Journal of Composites*, 12, 1981, p 124

- [152] Lloyd D J , Lagace H , Mcleod A and Morris P L , Microstructural Aspect of Al-SiCp Composites Produced By Casting Methods, *Materials Science & Engineering*, A107, 1989, pp 73-80
- [153] Lewandowski J J , Liu C and Hunt W H , Microstructural Effects On the Fracture Micromechanisms in 7XXX Al P/M-SiC Particulate Metal Matrix Composites, *Processing and Properties for Powder Metallurgy Composites*, Eds Kumar P , Vedula K , and Ritter A , TMS-AIME, Warrendale, 1987, pp 117-137
- [154] Oh S Y , Cornie J A and Russell K C , Wetting of Ceramic Particulate With Liquid Aluminium Alloys, Part II Study of Wettability, *Metallurgical Transaction A* , 20A, 1989, pp 533-541
- [155] Kelly A and Macmillan N H , *Strong Solid*, Clarendon, Oxford, 3rd Edn 1986, pp 258-318
- [156] Chawla K K , *Composite Materials-Science and Processing*, Springer, Berlin, 1987, pp 79-86
- [157] Taya M and Arsenault R J , *Metal Matrix Composites-Thermo Mechanical Behavior*, Pergamon, Oxford, 1989, pp 41-156
- [158] Mortensen A , *Proceedings of the 9th Riso International Symposium On Metal and Materials Science*, Riso National Lab , Riso, Roskilde, Denmark, September, 1988, pp 141-155
- [159] Blackmun E V , *AFS Transaction*, 57, 1971, p 63

- [160] Russel K C , Cornie J A and Oh S Y , Particulate Wetting and Particle Interfaces in Metal Matrix Composites, Eds Dhingra A K and Fishman S G , Proceedings Conference, New Orleans, TMS-AIME, 1986, pp 61-91
- [161] Delannay F , Froyen L and Deruyttere A , The Wetting of Solid by Molten Metals and Its Relation to the Preparation of MMCs, Journal of Materials Science, 22, 1987 pp 1-16
- [162] Pai B C , Ramam G , Pillai R M and Satyanarayana K G , Role of Magnesium In Cast Alummum Alloy Matrix Composites, Journal of Materials Science, 30, 1995, pp 1903-1911
- [163] Laurent V , Chatain D and Eustathopoulos N , Wettability of SiO_2 and Oxidised SiC by Aluminium, Materials Science & Engineering, A135, 1991, pp 89-94
- [164] Widdows N and Nicholas M G , Report AERE R5265, United Kingdom Atomic Energy Authority, Harwell, 1967
- [165] Manning C R and Gurganus T B , Journal of American Ceramic Society, 52, 1969, p 115
- [166] Eustathopoulos N , Joud J C , Desre P and Hicter J M , Journal of Material Science, 9, 1974, p 1233
- [167] Warren R and Anderson C H , Silicon Carbide Fibres and Their Potential For Used in Composite Materials, Part II, Composites, April, 1984, pp 101-111
- [168] Naidich Y U , Solid-Melts Interfaces, Nankova Dumba, Kiev, 1972
- [169] Kohler W , Untersuchungen Zur Benetzung Von Al_2O_3 -und SiC -Kristallen Durch Aluminium und aluminium- Legierungen, Aluminium, 51, 1975, pp 443-447

- [170] Halverson D C , Pyzik A J and Aksay I A , Processing and Microstructural Characterization of B₄C/Al Cermet, Preprint UCRL-91305, 1985
- [171] Brennan J J and Pask J A , Journal of American Ceramic Society, 51, 1968, pp 569-573
- [172] Wolf S M , Levitt A P and Brown J , Chemical Engineering Progress, 62, 1966, pp 74-78
- [173] Champion J A , Keene B J and Sillwood J M , Journal of Materials Science, 4, 1969, pp 39-49
- [174] Wefer K , Aluminium, 57, 1981, pp 722-726
- [175] Ramani G , Ramamohan T R , Pillai R M and Pai B C , Scripta Metallurgical Materials, 24, 1990, p 1419
- [176] Zhou W and Xu Z M , Journal of Materials Processing Technology, 63, 1997, pp 358-363
- [177] Himbeault D D , Varin R A and Piekarski K , Proceedings International Symposium On Advanced in Processing of Ceramic and Metal Matrix Composites, Halifax, NS, Canada, August, 1989, pp 312-323
- [178] Taftø J , Kristiansen K , Westengen H , Nygård A , Borradaile J B and Karlsen D O , Proc International Symposium On Advances in Cast Reinforced Metal Composites, Chicago, IL, September, 1988, pp 71-75
- [179] Pai B C , Satyanarayana K G and Robi P S , Journal of Materials Science Letter, 11, 1992, p 779
- [180] Tracey M H , Materials Science and Technology, 4, 1986, pp 227-230

- [181] Raman G , Pillai R M , Pai B C , and Satyanarayana K G , *ibid*, 12, 1993, p 117
- [182] Kobashi M and Choh T , *Journal of Materials Science*, 28, 1993, p 684
- [183] Agarwala V and Dixit D , *Fabrication of Aluminium Base Composites by Foundry Techniques*, *Transactions of Japan Institute of Metal*, 22, 1981, pp 521-526
- [184] Oh S Y , PhD Dissertation, Department of Materials Science & Engineering , Massachusetts Institute of Technology, 1987
- [185] Levi C G , Abbashian G J and Mehrabian R , *Metallurgical Transaction A* , 9A, 1978, pp 697-711
- [186] Mondolfo L F , *Aluminium Alloy Structure and Properties*, Butterworth, London, 1976
- [187] Korolkov A M , *Casting Properties of Metal and Alloys*, Consultant Bureau, New York, 1963, pp 26-27
- [188] Sukumaran K , Pillai S G K , Pillai R M , Kelukutty V S , Pai B C , Satyanarayana K G and Ravikumar K K, *The Effect of Mg Addition On the Structure and Properties of Al-7Si-10SiCp Composites*, *Journal of Materials Science*, 30, 1995, pp 1469-1472
- [189] Kimura Y et al , *Journal of Materials Science*, 19, 1984, p 3107
- [190] Milliere A P and Suery M , *Fabrication and Properties of MMCs Based On a SiC Fibre Reinforced Aluminium Alloys*, *Materials Science and Technology*, 4, 1988, p 41

- [191] Agarwala V and Dixit D , Fabrication of Aluminium Base Composites by Foundry Technique, Transaction Japan Institute of Metal, 22, 1981, pp 521-526
- [192] Ribes H , Dasilva R , Suery M and Breteau T , Materials Science & Technology, 6, 1990, p 621
- [193] Thanh L N , and Suery M , Scripta Metallurgy, 25, 1991, p 2781
- [194] Clyne T W , ICCM-VI and ECCM-2, Elsevier Applied Science , 2, 1987, pp 275-286
- [195] Namai T , Osawa Y and Kikuchi M , IMONO, Journal of Japan Foundryman's Society, 56, 1984, pp 604-609
- [196] Lignon R , Research Aerospace, 1, 1974, p 49
- [197] Amateau M F , Journal of Composites, 10, 1976, p 279
- [198] Aggour L, Fitzer E , Heym M and Ignatowitz, Thin Solid Films, 40, 1977, p 97
- [199] Ishikawa T , Tanaka J , Teranishi H , Okamura T and Hayase T , United State Patent Number US440571, 1981
- [200] Goddard D M , Metal Progress, 1984, p 49
- [201] Pai B C and Rohatgi P K , Materials Science & Engineering, 21, 1975, p 161
- [202] Chou T W , Kelly A and Okura A , Fibre Reinforced Metal Matrix Composites, Composites, 16, 1985, p 187
- [203] Landis H , Unnam J , Naidu S V N and Brewer W , SAMPE Q, July 1981, p 19
- [204] Paray F and Gruzleski J E , Cast Metal, vol 5, 1993, p 187
- [205] Young T , Transaction of Royal Society, 95, 1805, p 65

- [206] Samuel A M and Samuel F H , Foundry Aspect of Particulate Reinforced Aluminium MMCs-Factors Controlling Composite Quality, Key Engineering Materials, 104-107, 1995, pp 65-98
- [207] Samuel A M and Samuel F H Metallurgical Transaction A, 24A, 1993, pp 1857-1868
- [208] Cocen U and Onel K , The Production of Al-Si Alloy SiCp Composites Via Compocasting, Materials Science & Engineering, A221, 1996, pp 187-191
- [209] Cohen J and Ishai O , Composite Materials, 1967, p 390
- [210] Christman T, Needleman A and Suresh S , An Experimental and Numerical Study of Deformation In Metal -Ceramic Composites, Acta Metallurgica, 37, 1989, pp 3029-3050
- [211] Badia F F and Rohatgi P K , Transactions AFS, 76, 1969, pp 402-406
- [212] Appendino P and Badini C , 6061 Aluminium Alloy-SiC Particulate Composites A Comparison Between Aging Behaviour in T4 and T6 Treatment, Materials Science & Engineering, A135, 1991, pp 275-279
- [213] Maruyama B and Rabenberg L , Interfaces In Metal Matrix Composites, Eds Dhingra A K , and Fishmann S G , Proceedings of Conference New Orlean, TMS-AIME, 1986, pp 233-238
- [214] Lloyd D J , The Solidification Microstructure of Particulate Reinforced Alumimum/SiC Composites, Composite Science & Technology, 35, 1989, pp 159-179
- [215] Hammond D E , Foundry Practice For the First Castable Aluminiun/Ceramic Composite Materials, Modern Casting, 79, 1989, p 29

- [216] Waechter A and Windelberg D , Acta Stereol, 5, 1986, pp 29-36
- [217] Piggot M R , Load Bearing Fibre Composites, Chapter 9, Pergamon Press, 1980
- [218] Flom Y and Arsenault R J , Interfacial Bond Strength In an Aluminium Alloy 6061-SiC Composites, Materials Science & Engineering, 77, 1986, pp 191-197
- [219] Lin C-Y , McShane H B and Rawling R D , Structure and Properties of Functionally Gradient Aluminium Alloy 2124/SiC Composites, Materials Science and Technology, 10, 1994, pp 659-664
- [220] Kannikeswaran K and Lin R Y , Journal of Materials, 9, 1987, p 17
- [221] Selvaduray G , Hickman R , Quinn D , Richard D and Rowland D , Interfaces in Metal-Ceramic Composites, Anaheim, CA, Eds Lin R Y and Arsenault R J , IBID, 1989, p 271
- [222] Clyne T W and Mason J F , Metallurgical Transaction A, 18, 1987, p 1519
- [223] Viala J C , Fortier P and Bouix J , Stable and Metastable Phase Equilibria In the Chemical Interaction Between Aluminium and Silicon Carbide, Journal of Materials Science, March, 1990, p 1842-1850
- [224] Legoux J G , Lesperance G L, Salvo and Suery M , Proceedings of Fabrication of Particulate Reinforced Metal Composites, Eds Massounave and Hamel F G , Materials Park, OH, ASM Int , 1990, pp 31-39
- [225] Heuer A H , Ogbuji I U and Mitchell T E , The Microstructure of Oxide Scale On Oxidised Si and SiC Single Crystals, Journal of American Ceramic Society, 63, 1980, pp 354-355

- [227] Wang N , Wang Z and Weatherly G C , Formation of Magnesium Aluminate In Cast SiC Particulate-Reinforced Al(A356) Metal Matrix Composites, Metallurgical Transaction A, 23A, May 1992, pp 1423-1430
- [228] Hille V D , Bengtsson S and Warren R , Composite Science & Technology, 35, 1989, pp 195-206
- [229] Kendall E G , Composite Materials, Volume IV, Metallic Matrix Composites, Eds Broutman and Krock, Acad Press , 1974, p 319
- [230] Nakata E and Kagawa Y , Journal of Materials Science Letter, 4, 1985, pp 61-62
- [231] Vedula M and Queey, Interfaces In Metal Matrix Composites, Eds Dhingra A K , and Fishman S G , Proceedings Conference, New Orleans, 1988, TMS-AIME, pp 227-231
- [232] Portnoi K I , Zabolotskii A A and Timofeeva N I , Materials Science and Heat Treatment, 22, 1980, pp 813-815
- [233] Viala J C Bossellet F , Fortier P and Bouix J , Proceedings of the 6th International Conference On Composite Materials, ICCM VI, London, Eds Matthews F L , Buskell NCR, Hodginsin J M and Morton J , Elsevier Applied Science, London, 1987, pp 2 146-2 155
- [234] Stone I C and Tsakiroopoulos P , Materials Science & Technology, 11, 1995, pp 222-227
- [235] Champion A R , Krueger W H , Hartmann H S and Dhingra A K Proceedings of the 1978 International Conference On Composites Materials, ICCM II, AIME, 1978, p 883

- [236] Hall I , and Barailler V , Developments In the Science and Technology of Composite Materials,, Proceedings of the 1st European Conference On the Composite Materials, ECCM-1, Bordeaux, France, Eds, Bunsell A R , Lamicq P , and Massiah A , 1985, pp 589-594
- [237] Dinwoodie J W and Horsfal I , Proceedings of the 6th International Conference On Composite Materials, ICCM-VI, Eds Buskell N C R , Hidginson J M and Morton J , Elsevier Applied Science , London, 1987, pp 2 390-2 401
- [238] Lilholt H , Aspects of Deformation of Metal Matrix Composites, Materials Science & Engineering, A135, 1991, pp 161-171
- [239] Eliasson J and Saandstrom R , Applications of Aluminium Matrix Composite, Key Engineering Materials, 104-107, 1995, pp 3-36
- [240] Mohn W R and Gegel R A , Diensionally Stable Metal Matrix Composites For Guidance Systems and Optics Applications, ARCO Chemical Advanced Materials, USA, 1987
- [241] Arsenault R J , Shi N , Wang I And Feng C R , Localized Deformation of SiC-Al Composites, Materials Science & Engineering, A131, 1991, pp 55-68
- [242] Lim L G and Dunne F P E , The Effect of Volume Fraction of Reinforcement On the Elastic-Viscoplastic Response of Metal Matrix Composites, International Journal of Mechanical Science, 38, 1996, pp 19-39
- [243] Sekine H and Chen R , A Combined Microstructure Strengthening Analysis of SiCp/Al Metal Matrix Composites, Composites, 26, 1995, pp 183-188
- [244] Werlefors T , Esklisson C and Ekelund S and Scand J , Metallurgy, 8, 1979, pp 221-231

- [245] Apelian D , Shivkumar S and Sigworth G , Fundamental Aspects of Heat Treatment of Cast Al-Si-Mg Alloys, AFS Transactions, 1989, pp 727-742
- [246] Properties and Selection Non-Ferrous Alloy and Special Purpose Materials, ASM Handbook, ASM International, Vol 2, 1992
- [247] Arsenault R J and Pande C S , Scripta Metallurgy, 18, 1984, p 131
- [248] Rack H J , Age Hardening Behaviour of SiC Whiskers Reinforced 6061 Aluminium, Proceedings of the 6th International Conference On Composite Materials, ICCM-VI, Eds Mathews F L et al, Elsevier Applied Science, 1987, pp 2 382-2 389
- [249] Pragnell P B and Stobbs W M , Proceedings of the 7th International Symposium On Composite Materials-ICCM-VII, Eds Yunshu et al, Oxford, Pergamon Press, 1989, pp 573-578
- [250] Hunt E , Pitcher P D and Gregson P J, Precipitation Reactions In 8090 SiC Particulate Reinforced MMC, Scripta Metallurgica et Materialia, v 24, May 1990 pp 937-941
- [251] Ribes H and Suery M , Effect of Particle Oxidation On Age Hardening of Al-Si-Mg/SiC Composites, Scripta Metallurgical, 23, 1989, pp 705-709
- [252] Salvo L and Suery M , Effect of Reinforcement On Age Hardening of Cast 6061 Al-SiC and 6061 Al-Al₂O₃ Particulate Composites, Materials Science & Engineering, A177, 1994, pp 19-28
- [253] Dinwoodie J , Moore E , Langman C A J and Symes W R , The Properties and Applications of Short Staple Alumina Fibre Reinforced Aluminium Alloys, 5th Chemical International Conference On Composite Materials, 1995

- [254] Dutta B and Surappa M K , Studies On Age-Hardening Characteristics of Ceramic Particle/Matrix Interfaces In Al-Cu-SiCp Composites Using Ultra Low-Load-Dynamic Microhardness Measurements, Journal Materials Research, 12, 1997, pp 2733-2778
- [255] Gupta M and Surappa M K , Processing -Microstructure-Mechanical Properties of Aluminium-Based Metal Matrix Composites Synthesis Using Casting Route, Key Engineering Materials, 104-107, 1995, pp 259-274
- [256] Arsenault R J , Strengthening and Deformation Mechanisms of Discontinuous Metal Matrix Composites, International Conference On Advanced Composite Materials, TMS, 1993, pp 19-27
- [257] Vogelsang M , Fisher R and Arsenault R J , In situ HVEM Study of Dislocation Generation at Al/SiC Interfaces In Metal Matrix Composites, Metallurgical Transactions, 17A, 1986, pp 379-389
- [258] Stefanescu D M , Dhindaw B K , Kacar S A and Moitra A , Metallurgical Transactions A, 19A, 1988, p 2847
- [259] Harris S J , Cai H W and Weatherburn P C , Structure-Properties Relationships in Al₂O₃ Short Fibre and SiC Particle Reinforced Aluminium Alloys, International Conference On Advanced Composite Materials, TMS, 1993, pp 1301-1307
- [260] Nair S V , Tien J K and Bates R C , International Metal Review, 30, 1985, p 275
- [261] Ghosh, P K and Ray, S , Zeitschrift Fuer Metallkunde, 80, 1989, pp 53-59
- [262] Shivkumar S , Keller C and Apelian D, AFS Transactions, Vol 98, 1990, p 905

- [263] Nagata S , Mixing Principles and Applications, John Wiley & Sons, 1975, pp 250-258
- [264] Hashim J , Looney L and Hashmi M S J , Proceeding Advanced Materials Processing Tehnology Conference, Kuala Lumpur, 1998, pp 349-358
- [265] Liaw P K , Hsu D K , Yu N , Miriyala N, Saini V and Jeong H , Investigation of Metal and Ceramic-Matrix Composites Modulı Experiment and Theory, Acta Materialia, 44, 1996, pp 2101-2113
- [266] Rohatgi P K , Pasclak K , and Narendranath C S , Evolution of Microstructure and Local Thermal Conditions During Directional Solidifications of A356-SiC Particles Composites, Journal of Materials Science, 29, 1994, pp 5357-5366
- [267] Moustafa S F , Casting of Graphite Al-Si Base Composites, Canadian Metall Quarterly, 33, 1994, pp 259-264
- [268] Caron S and Masounave J , A Literature Review On Fabrication Techniques of Particulates Reinforced Metal Matrix Composites, Proceeding of International Conference ' Fabrication of Particulate Reinforced Metal Matrix Composites, Montreal, Canada, 1990, pp 79-85
- [269] Pai B C , Pillai R M and Satyanarayana K G , Role of Magnesium In Cast Aluminium Alloy Matrix Composites, Journal of Materials Science, 30, 1995, pp 1903-1911
- [270] Kobashi M and Choh T , Journal of Materials Science, 28, 1993, p 684
- [271] Rohatgi P K , Asthana R and Das S , Solidification, Structure and Properties of Cast Metal-Ceramic Particles Composites, International Metal Review, 31, 1986, pp 115-139

- [272] Han N , Pollard G and Stevens R , Interfacial Structure and Fracture of Aluminium Alloy A356-SiC Particle Metal Matrix Composite, Material Science and Technology, 8, 1992, p 184-187
- [273] Henriksen B R , Composites, 21, 1990, p 333
- [274] Salvo L , Suery M , Legoux J G and Esperance G , Material Science and Engineering, A135, 1991, p 29
- [275] Fabietti L M , Seetharaman V and Trivedi R , Metallurgical Transaction A, 19, 1988, p 284
- [276] Cheng J A , Apelian D and Doherty R D , Metallurgical Transaction, 17A, 1986, pp 2049-2062
- [277] Zhang D L and Zheng L , Metallurgical and Materials Transaction A, 27A, 1996, pp 3983-3991
- [278] Bonolla F , Molinas B , Tangerini I and Zambon A , Diametral Compression Testing of Metal Matrix Composites, Materials Science and Technology, 10, 1994, pp 558-564
- [279] Wilkinson D S and Embury J D , Role of Heterogeneity On the Flow and Fracture of Two-Phase Materials, Materials Science & Engineering A Structural Materials Properties, A233, 1996, pp 145-154
- [280] Osman T M , Lewandowski J J , Hunt W H , Fabrication of Particulate Reinforced Metal Matrix Composites (1990), Montreal, J Masounave and F G Hamel (Eds), Vol 1, ASM Int, pp 209-216
- [281] Lewandowski J J , Liu C, and Hunt W H , Materials Science & Engineering, A107, 1989, pp 241-255

- [282] Hunt W H , Richmond O and Yound R D , Proceedings of ICCM6/ECCM2 (1987), London, Eds F L Matthew N C R Buskell, J M Hodgkinson and Morton J , Vol 2, pp 209-223
- [283] Payne R D , Moran A L and Cammarata R C , Relating Porosity and Mechanical Properties In Spray Formed Tubular, Scripta Metallurgical Materials , 29, 1993, pp 907-912
- [284] Rack H J , Dispersion Strengthened Aluminium Alloys, Eds Y W Kim and W M Griffith, TMS, Warrendale , PA, 1988, p 649
- [285] Chawla K K , Esmaeili A H , Datya A K , and Vasudevan A K , Effect of Homogeneous/Heterogeneous Precipitation On Aging Behaviour of SiC/Al 2014 Composite, Scripta Metallurgica et Materialia , 25, 1991, p 1315-1319
- [286] Song Y and Baker T N , Materials Science Technology, 10, 1994, p 406
- [287] Thomas M P and King J E , Comparison of the Ageing Behaviour of Powder Metallurgy 2124 Alloy and Al-SiC Metal Matrix Composite, Journal of Materials Science, 29, 1994, p 5272-5278
- [288] Dutta B and Surappa M K , Age-Hardening Behaviour of Al-Cu-SiCp Composites Synthesized by Casting Route, Scripta Metallurgica et Materialia, 32, March, 1995, pp 731-736
- [289] Christman T and Suresh S , Acta Metallurgical , 36, 1988, p 1691
- [290] Arsenault R J and Shi N , Dislocation Generation Due to Differences Between The Coefficients of Thermal Expansion, Materials Science & Engineering, 81, 1986, pp 175-187

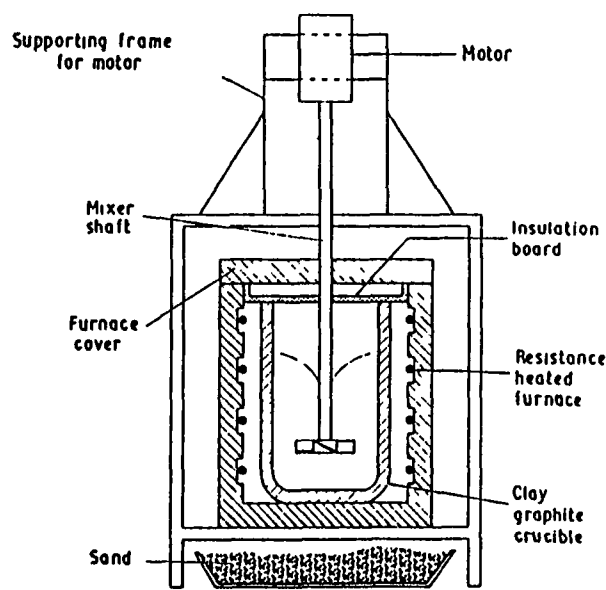
- [291] Taya M , Lulay K E and Lloyd D J , Strengthening of Particulate Metal Matrix Composites by Quenching, *Acta Metallurgical Material* , 39, 1989, p 73
- [292] Kim C T , Lee J K and Plichta M R , Plastic Relaxation of Thermoplastic Stress In Aluminium/Ceramic Composites, *Metallurgical Transactions A (Physical Metallurgy and Materials Science*, 21A, 1990, pp 673-682 IS
- [293] Suresh S , Christman T and Sugimura Y , *Scripta Metallurgical Material* , 23, 1989, p 1599
- [294] Humphrey F J , Basu A and Djazed M R , *Proceeding of 12th Riso International Symposium*, Ed, Hansen N , Riso Nat Lab , Denmark, 1991, p 51
- [295] McDanel D L, *Metal Transaction*, 16A, 6, 1985, p 1105
- [296] Arsenault R J , Wang L and Feng C R , Strengthening of Composites Due to Microstructural Changes In the Matrix, *Acta Metallurgica et Materialia*, 39, 1991, pp 47-57
- [297] MPIF, *Standard Test Method for Metal Powders and Powder Metallurgy Product*, ISBN 0-07007280-9
- [298] Klimowicz T F , *Fatigue Behaviour of Cast 359/SiC/20p Aluminium Composite*, AFS Transaction, 1994, pp 965-970
- [299] Samuel A M ,Samuel F H , Analysis of the Tensile Properties and Fractography of As-Cast and Heat Treated A359-SiC-20p Composite, *Journal of Materials Science*, 30, 1995, pp 3098-3110
- [300] Hallen J M , Balmori H M , Jaramillo D and Estrada J L , Influence of Mg and Stirring on the Strength of an Aluminium Matrix Composite Obtained by Compocasting, *Key Engineering Materials*, 121-131, 1997, pp 495-502

- [301] Miwa K and Ohashi T , Preparation of Fine SiC Particles Reinforced Aluminium Alloy Composites by Compocasting Process, Proceedings of the 5th Japan-US Conference on Composites Materials, Tama City, Tokya, Japan, 1990, pp 335-362
- [302] Suery M , Fabrication and Properties of Metal Matrix Composites Based on SiC Fibre Reinforced Aluminium Alloys, Materials Science & Technology, 4, 1988, pp 41-51
- [303] Nunes P C R and Ramanathan L V , The Influence of Processing Parameters on the Structure of Particles Reinforced Al Base MMC, Proceedings of Interternational JSYMP production Refining Fabrication and Recycling of Light Metals, Pergamon Press, 1990, pp 187-198
- [304] Caron S and Masounave I , A Literature Review on Fabrication Techniques of Particulates Reinforced Metal Composites, Proceedings of the International Conference on Fabrication of Particulate Reinforced Metal Composites, Montreal, Quebec, Canada, 1990, pp 79-85
- [305] Gilliland R G , Symposium on Fracture, Industrial Technology, Kobe, Japan, March, 1988
- [306] Ichikawa K and Kinoshita Y , Refinement of Microstructures and Improvement of Mechanical Properties in Intermetallic Ti Al alloy by Rheocasting, Materials Transaction, Vol 37, 1996, pp 1311-1318
- [307] Terry B and Jones G , Metal Matrix Composites, Elsevier Science Publisher Ltd , Oxford, England, 1990

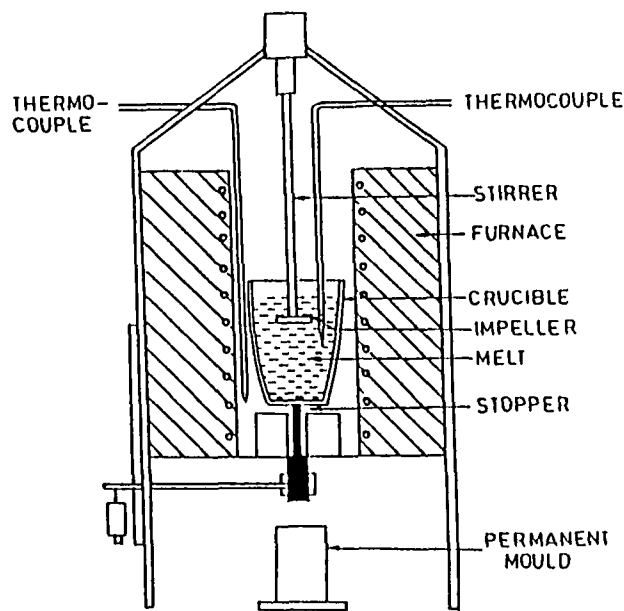
- [308] Kahl W Leupp J , High Performance Aluminium Produced by Spray Deposition,
Metal Powder Rep , 45, 1990, pp 274-278
- [309] Powder Metallurgy, Vol 7, ASM Metals Handbooks, American Society for
Metals, Metal Park, Ohio, IBSN 0-87170-013-1, 1990
- [310] Technical File no 144, Metal Matrix Composites, Engineering, London, 4, April,
1986, p 226

Appendix A

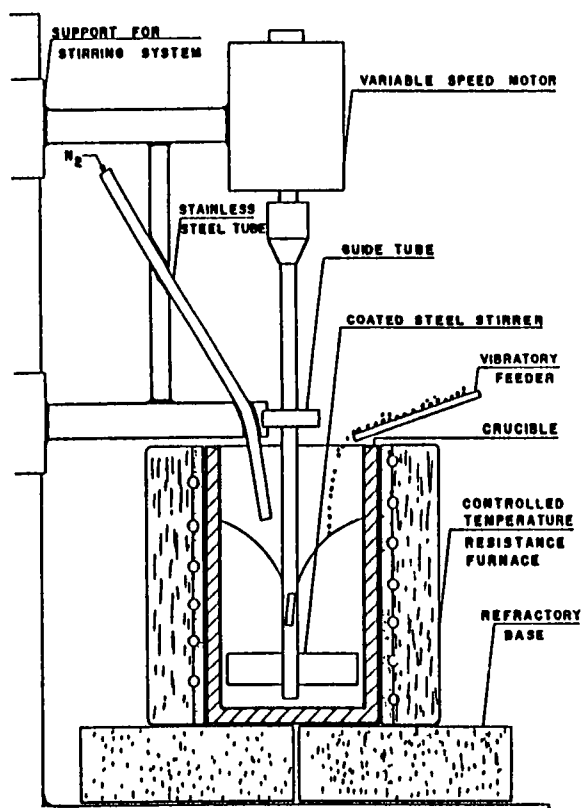
Schematic Drawings of Casting Equipment Found In the Literature



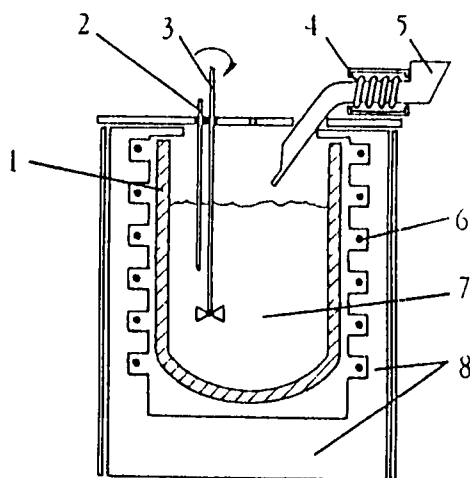
Rig designed by Hanumanth and Irons [129]



Rig designed by Ghosh and Rays [74]

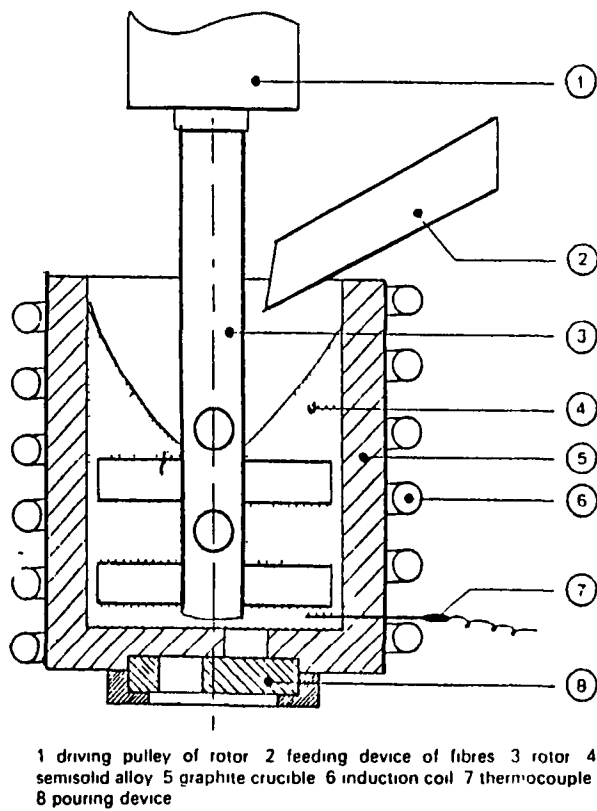


Rig designed by Nunes and Ramanathan [303]

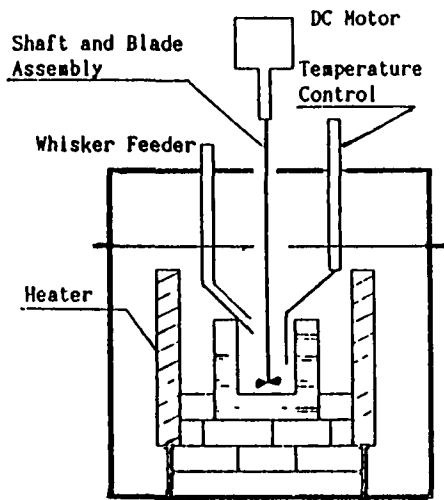


Rig designed by Abis [8]

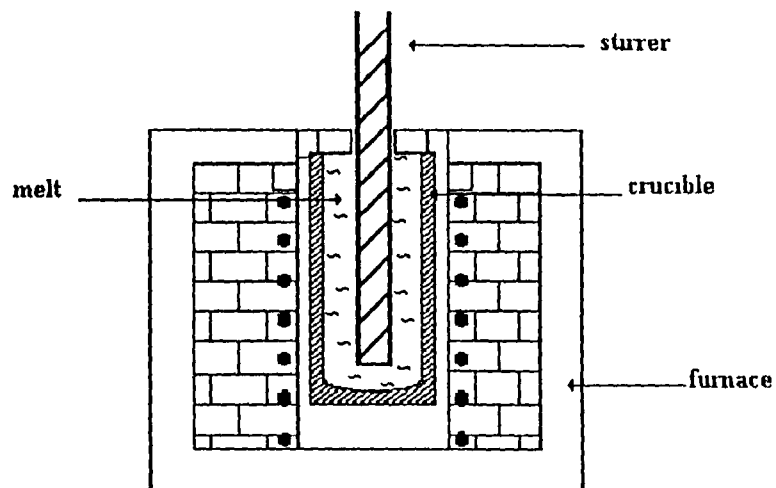
(1 crucible, 2 Thermocouple, 3 Stirrer, 4 Heater, 5 Fibre feeder, 6 Electric resistance, 7 Semi-solid bath, insulating refractory)



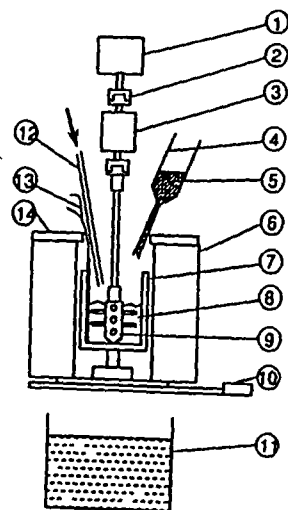
Rig designed by Suery [302]



Rig designed by Lee and Kim [68]

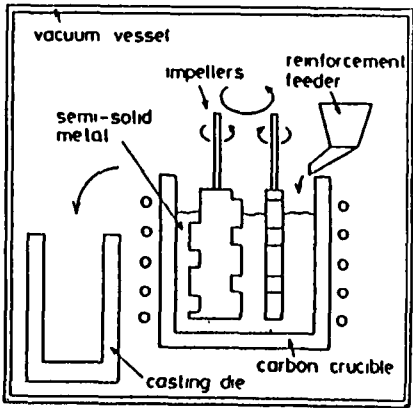


Rig designed by Hallen et al [300]

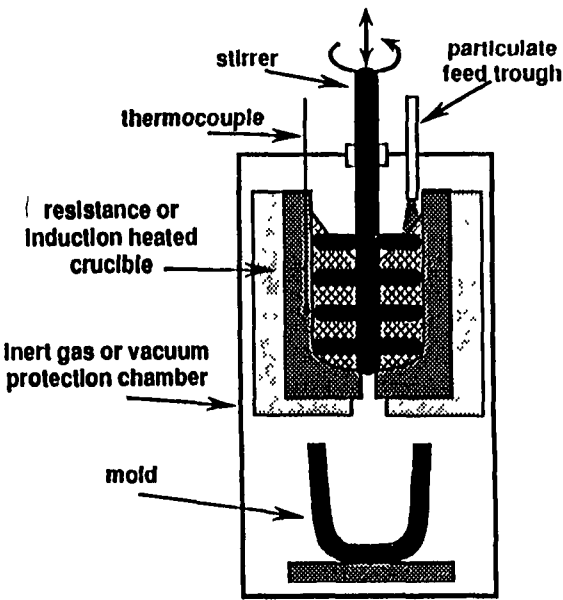


Rig designed by Miwa and Ohashi [301]

(1 motor, 2 Joint, 3 Roecque meter, 4 Argon gas, 5 SiCp, 6 Glass funnel,
7 Thermocouple, 8 Rotor, 9 Crucible, 10 Sample, 11 Furnace, 12 Support, 13 Water bath)



Rig designed by Yamada et al [80]



Rig designed by Caron and Masounave [304]

Appendix B

Detailed Drawing of Present Rig

(All dimensions are in mm)

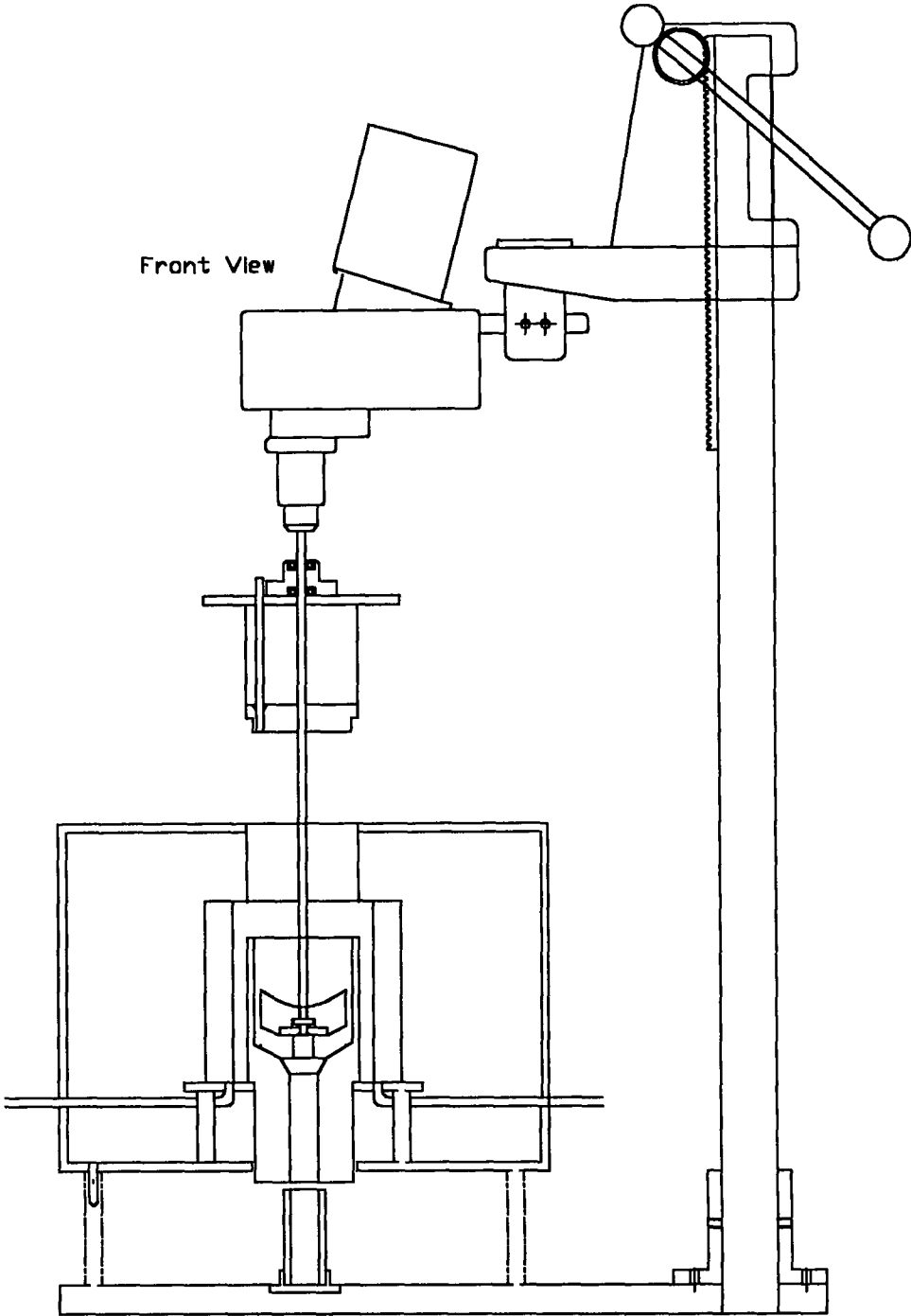
2

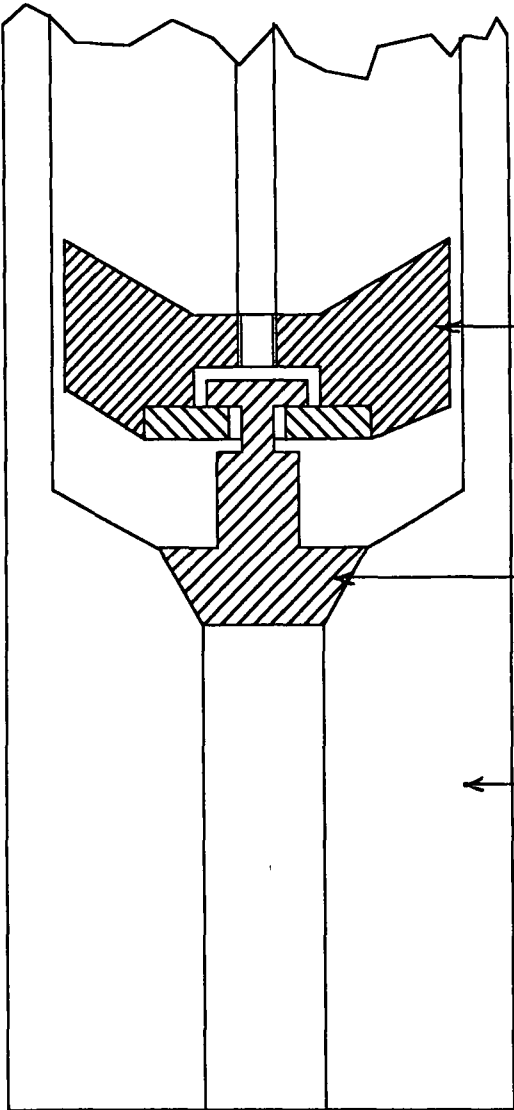
Item No	Description	REV	DESCRIPTION	BY	DATE
1	Digital DC Motor				
2	Stirring Rod				
3	Bearing Housing				
4	Heater Band				
5	Kaowool Insulator				
6	Surrer				
7	Stopper				
8	Steel Pipe (Nitrogen gas Input)				
9	Graphite Crucible				
10	Graphite Mould				
11	Steel Pipe (Nitrogen Gas Input)				
12	Steel Pipe (Charging				
13	Crucible Lid				

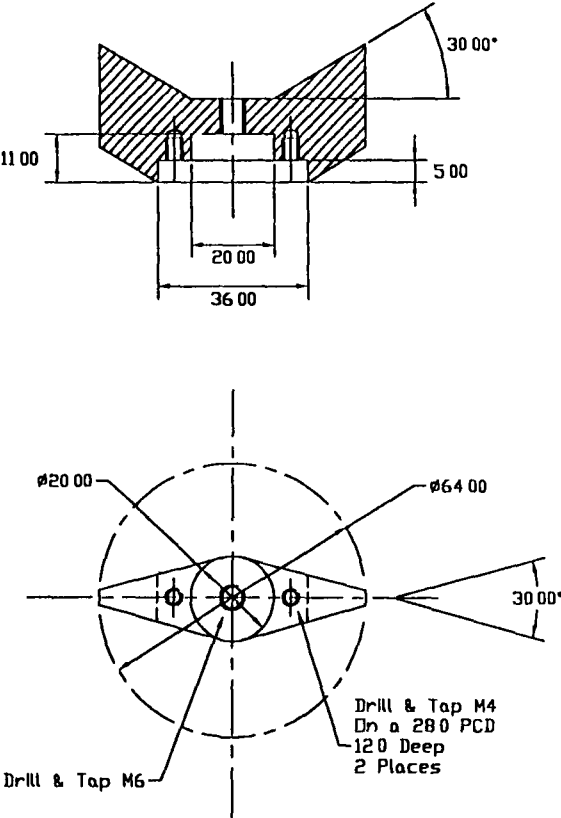
Front View

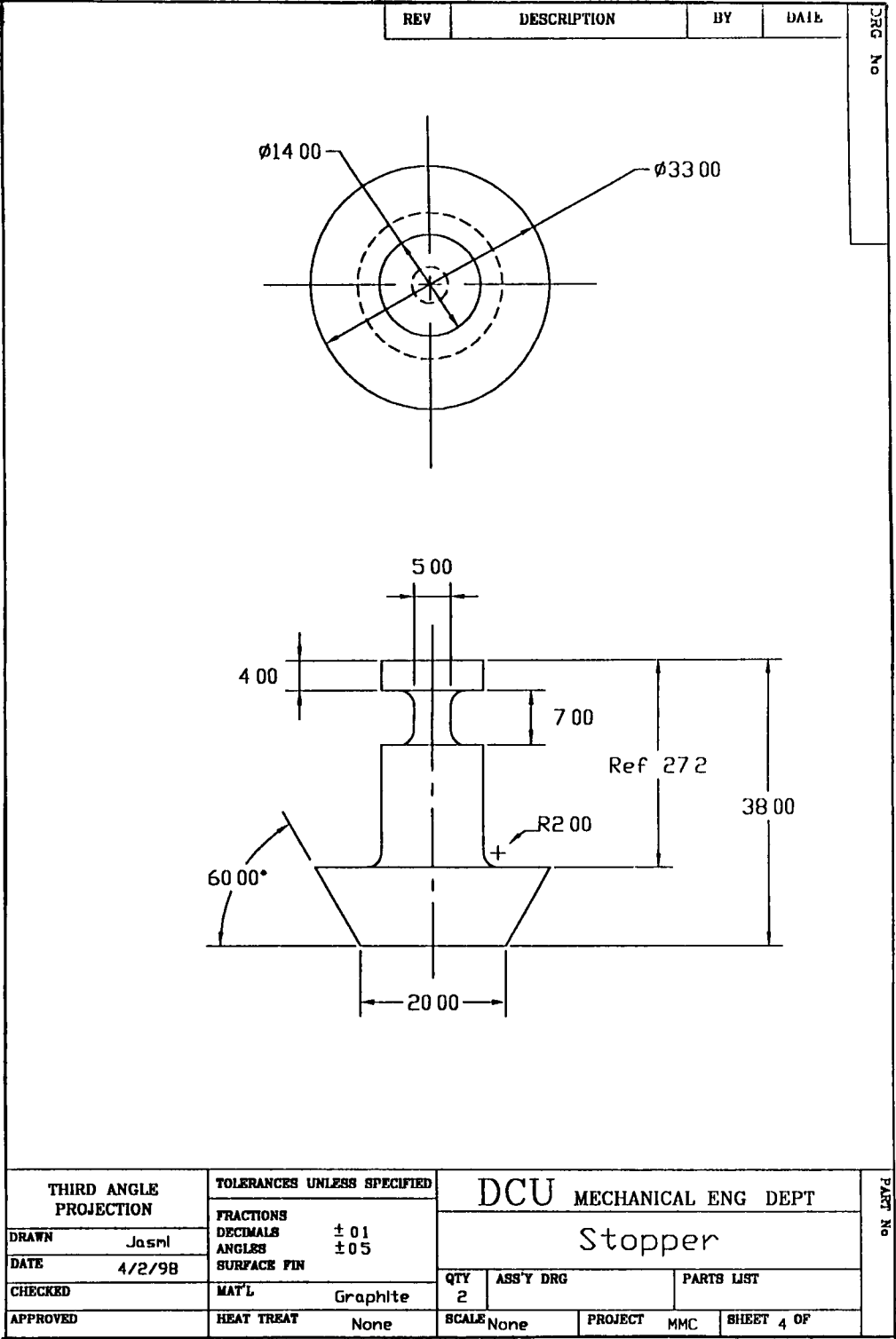
THIRD ANGLE PROJECTION		TOLERANCES UNLESS SPECIFIED		DCU MECHANICAL ENG DEPT		
DRAWN	Jasmi	FRACTIONS		Rig Assembly		
DATE	4/2/98	DECIMALS	± 0.1			
CHECKED		ANGLES	± 0.5	QTY	ASS'Y DRG	PARTS LIST
APPROVED		SURFACE FIN		2		
		MAT'L	Graphite	SCALE	None	PROJECT MMC SHEET 5 OF
		HEAT TREAT	None			

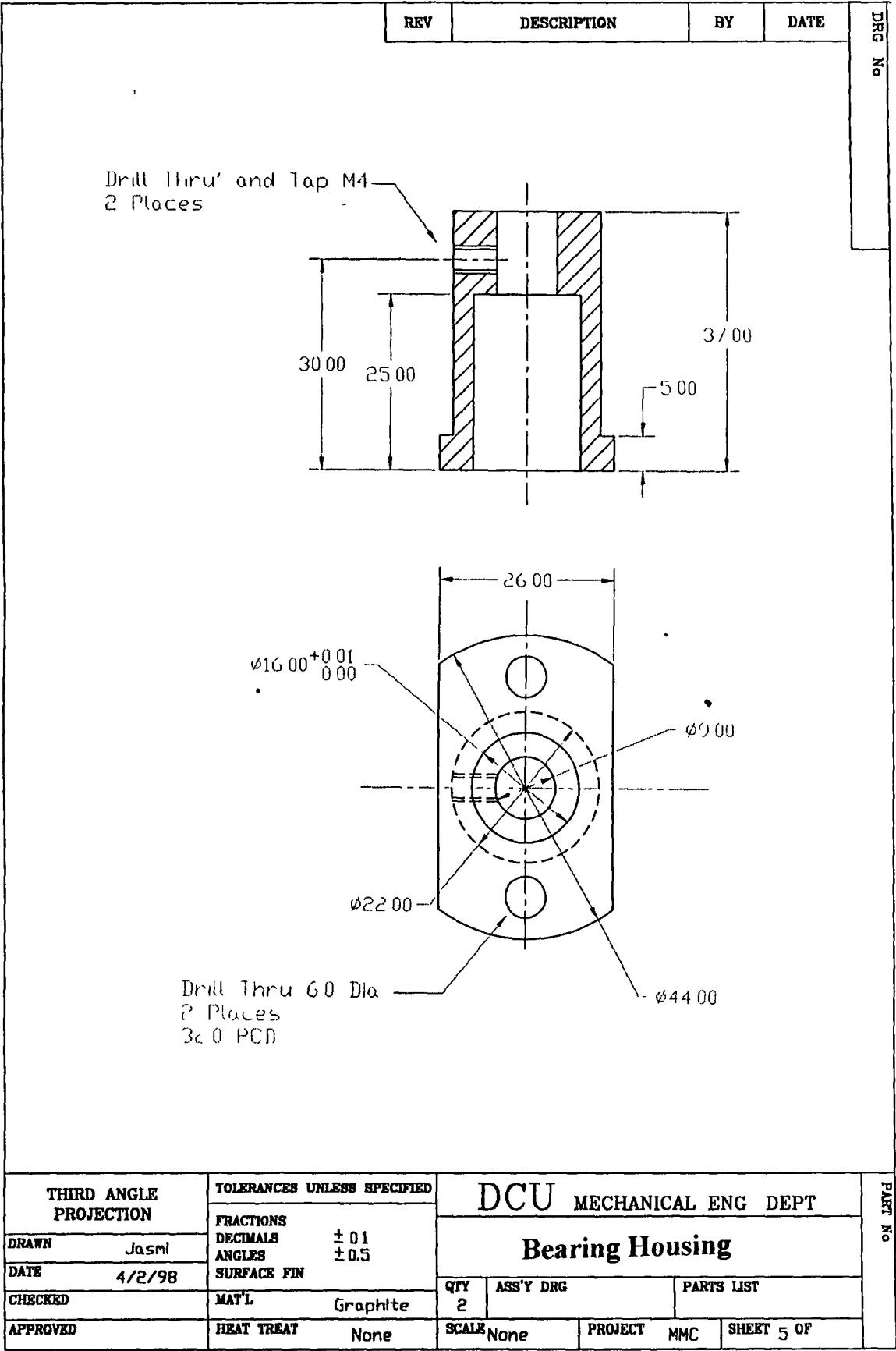
PART No

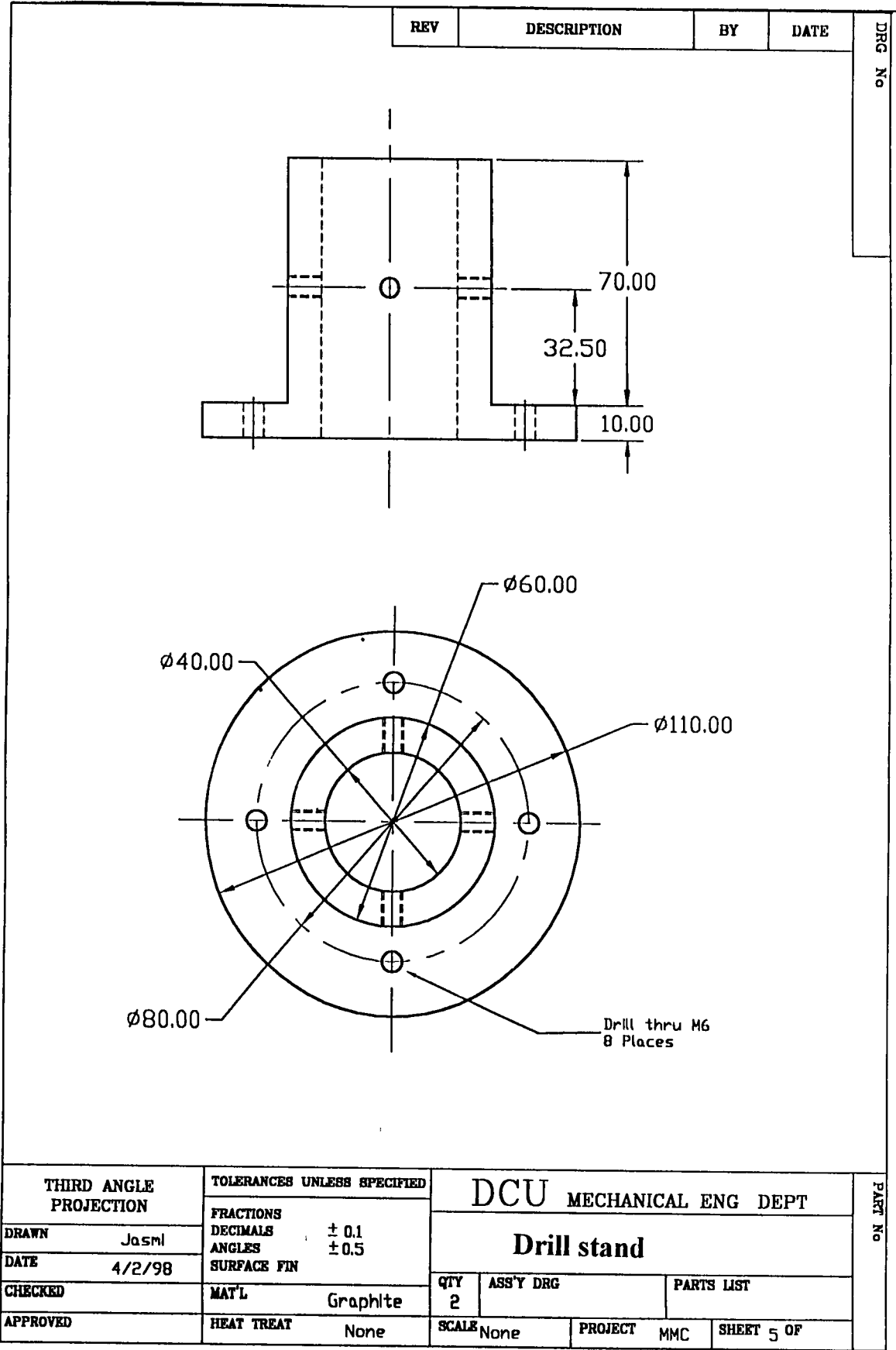
REV		DESCRIPTION		BY	DATE	DRG No	
 <p>Front View</p>							
THIRD ANGLE PROJECTION		TOLERANCES UNLESS SPECIFIED		DCU MECHANICAL ENG DEPT			PART No
DRAWN Jasml		FRACTIONS		Loading Operation			
DATE 4/2/98		DECIMALS ± 01		QTY 2			
CHECKED		ANGLES ± 05		ASS'Y DRG			
APPROVED		SURFACE FIN		PARTS LIST			
		MAT'L		SCALE None			
		HEAT TREAT None		PROJECT MMC			SHEET 5 OF

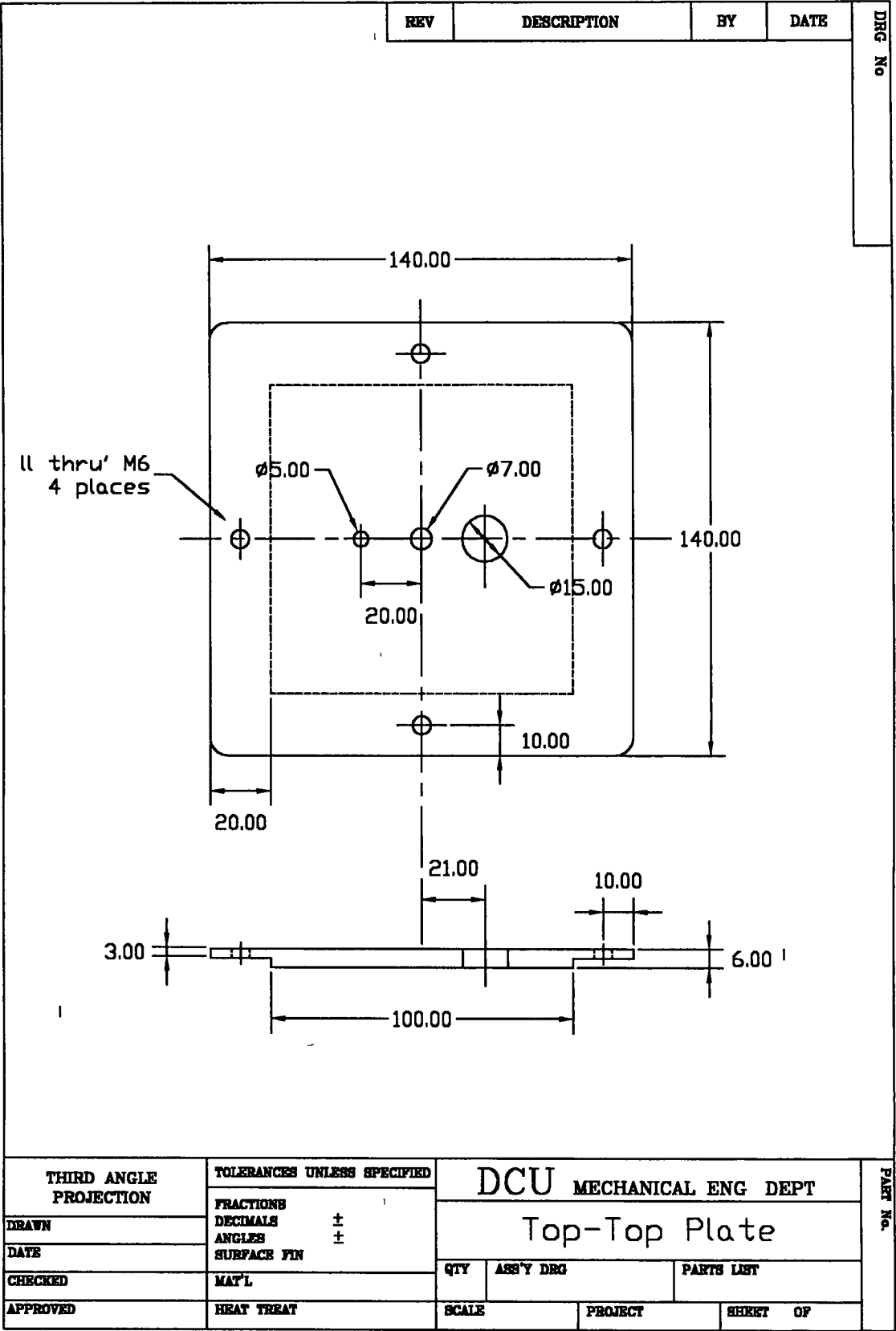
REV		DESCRIPTION		BY	DATE	DRG No	
							
THIRD ANGLE PROJECTION		TOLERANCES UNLESS SPECIFIED		DCU MECHANICAL ENG DEPT			PART No
DRAWN Jasm		FRACTIONS		Stirrer Assembly			
DATE 19/1/98		DECIMALS ±		QTY ASS'Y DRG PARTS LIST			
CHECKED		ANGLES ±		SCALE PROJECT MMC SHEET OF			
APPROVED		SURFACE FIN					
		MAT'L Graphite					
		HEAT TREAT					

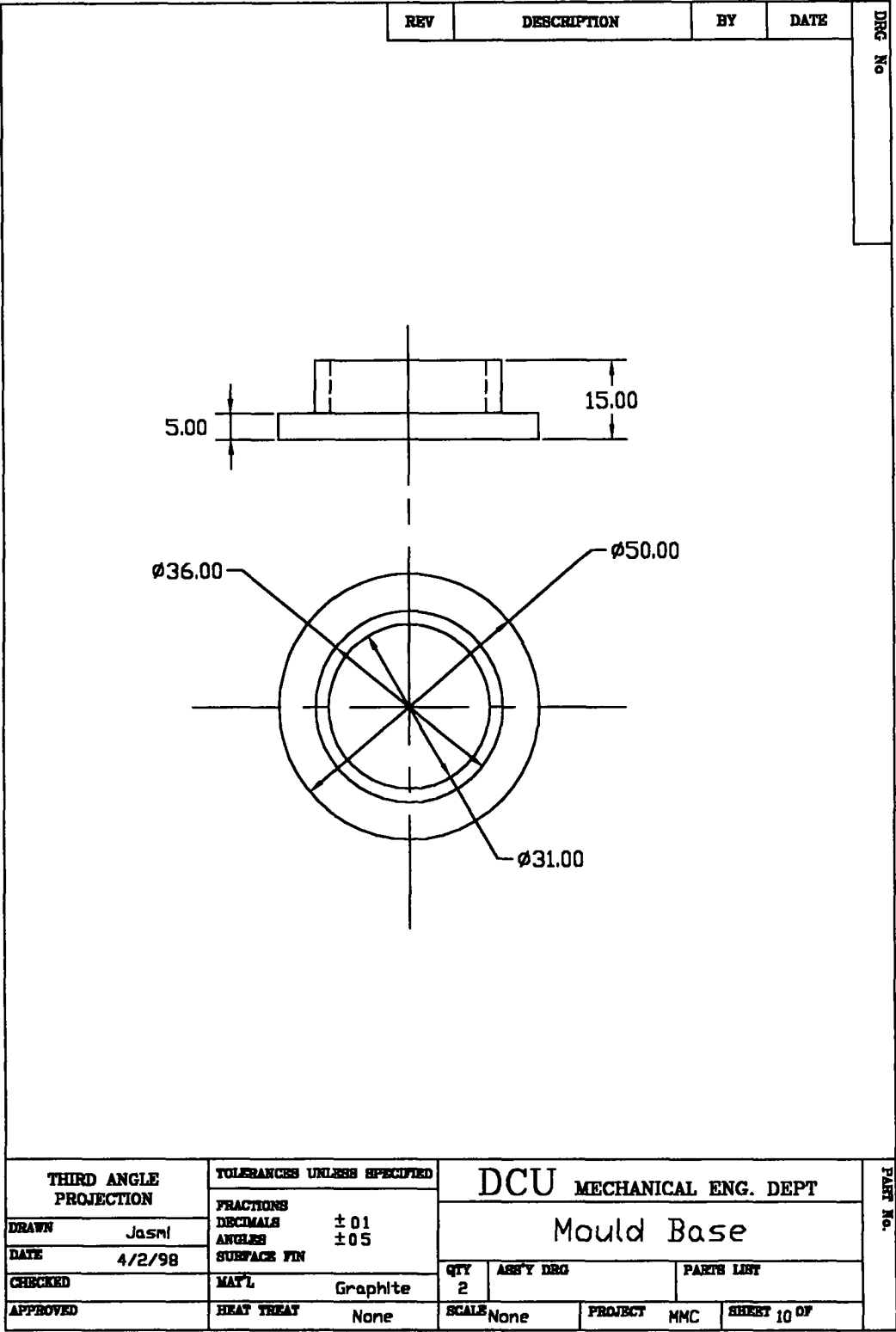
REV		DESCRIPTION		BY	DATE	DRG No	
<div></div>							
THIRD ANGLE PROJECTION		TOLERANCES UNLESS SPECIFIED		DCU MECHANICAL ENG DEPT			PART No
DRAWN Jasmi		FRACTIONS		Stirrer			
DATE 4/2/98		DECIMALS ± 01		QTY 2 ASS'Y DRG PARTS LIST			
CHECKED		ANGLES ± 05		SCALE None PROJECT MMC SHEET 5 OF			
APPROVED		SURFACE FIN					
		MAT'L Graphite					
		HEAT TREAT None					

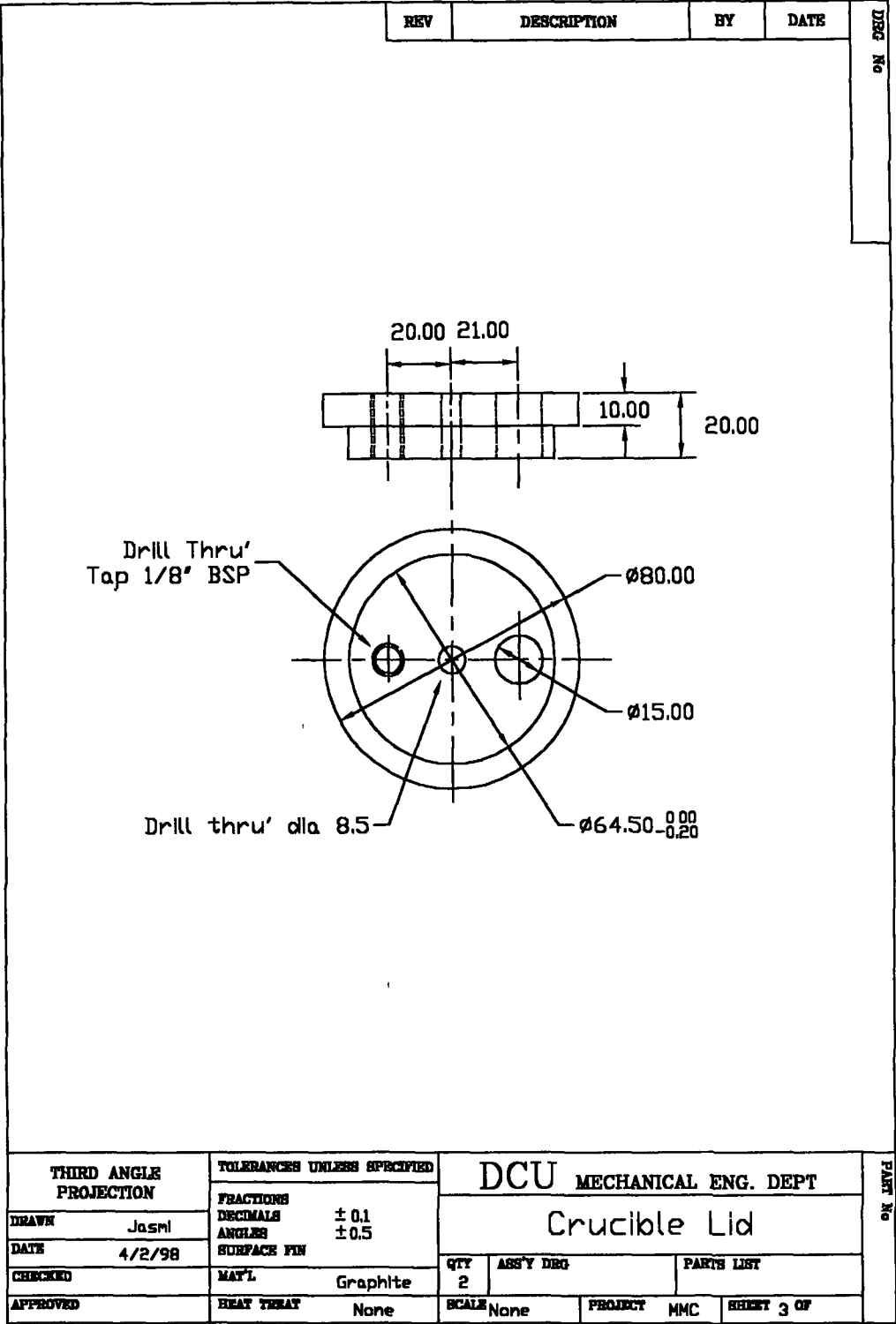


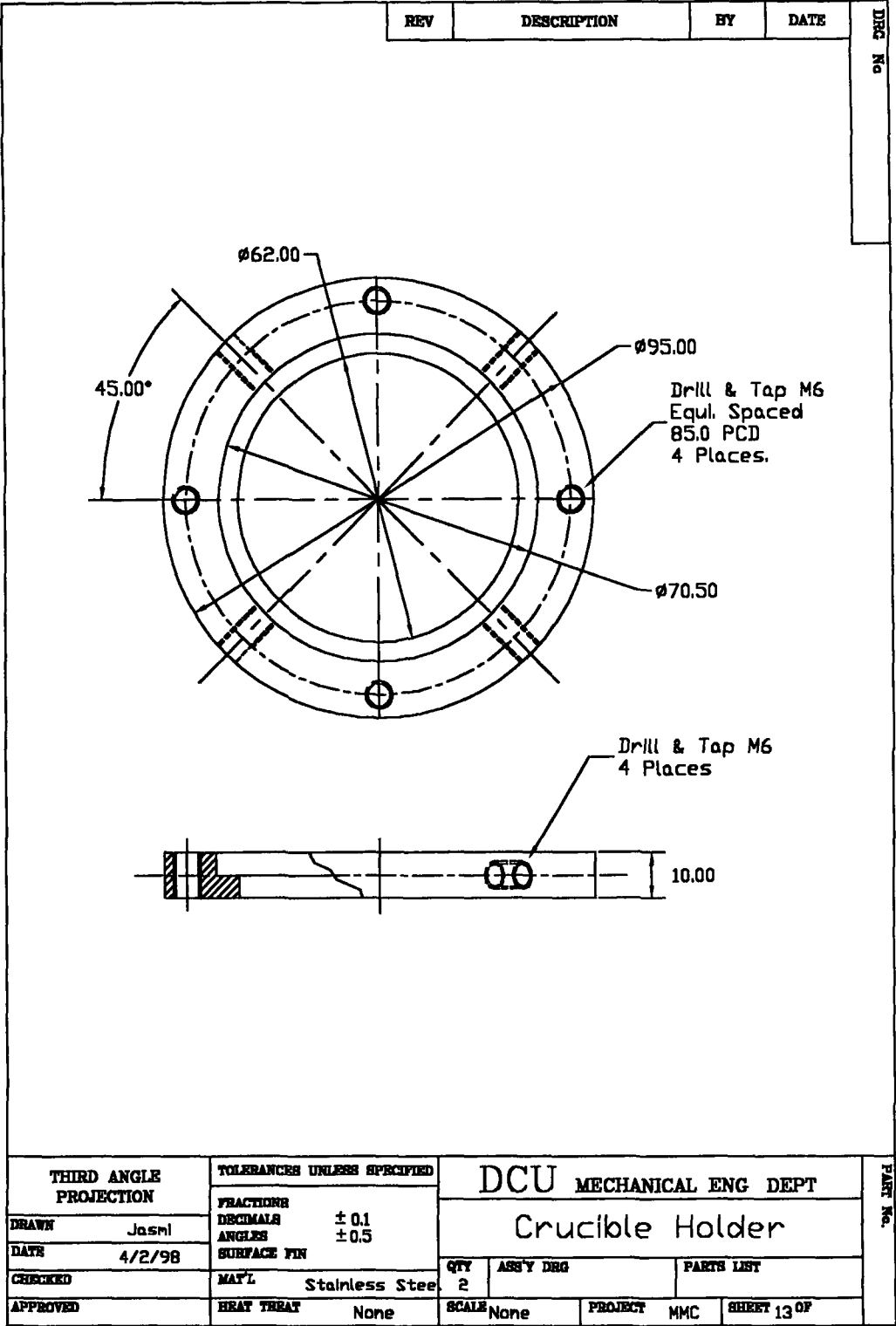


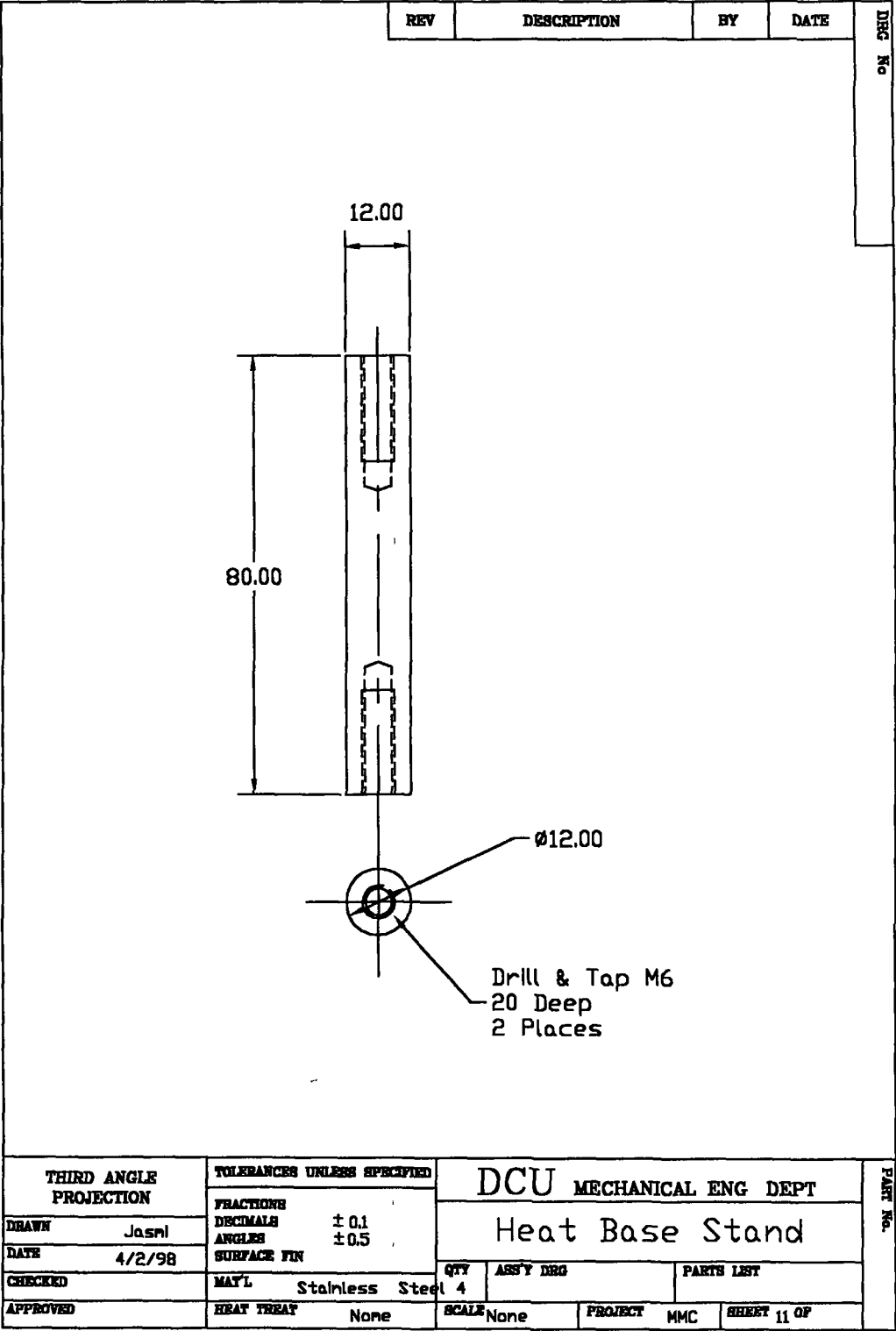


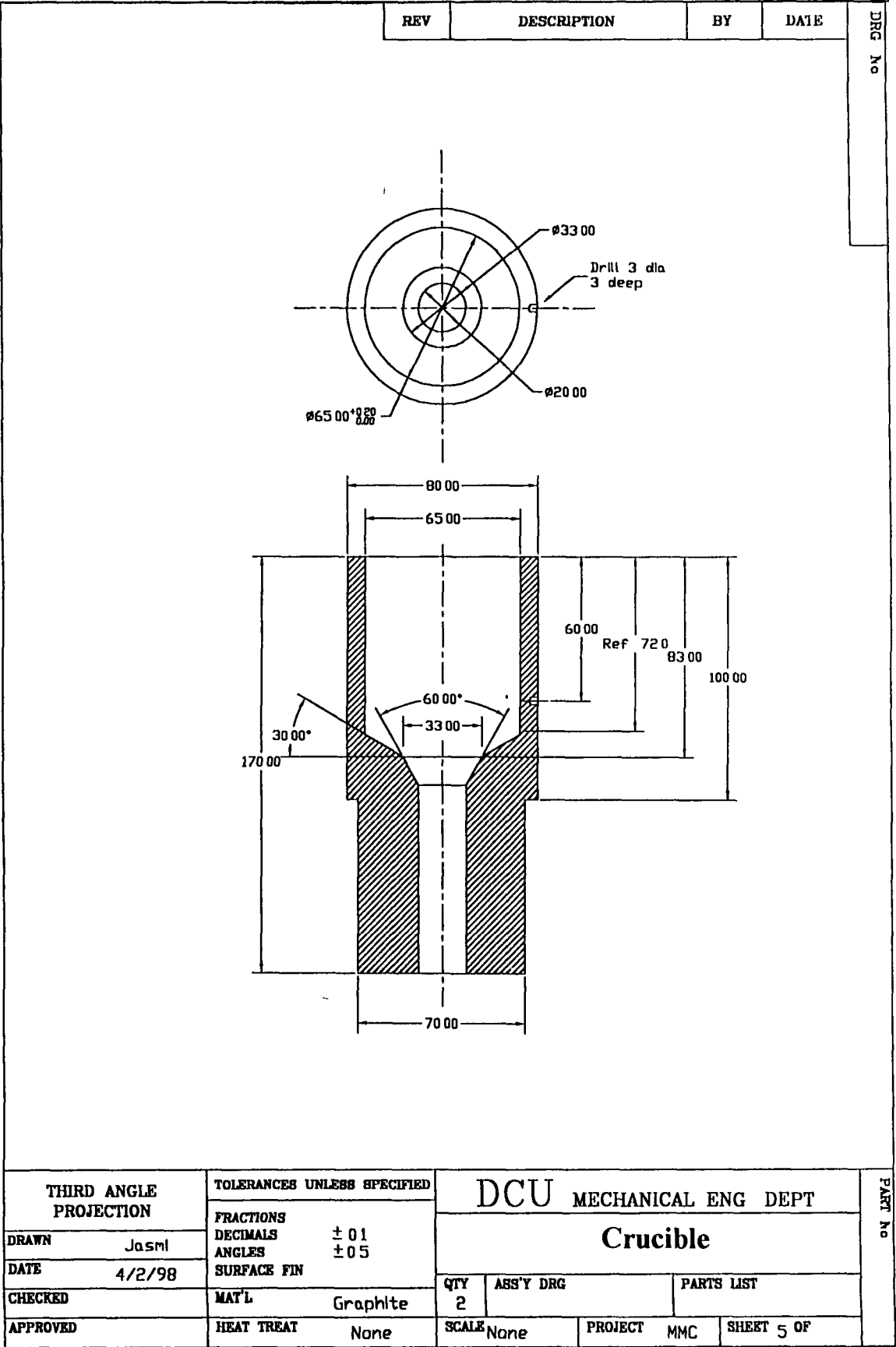


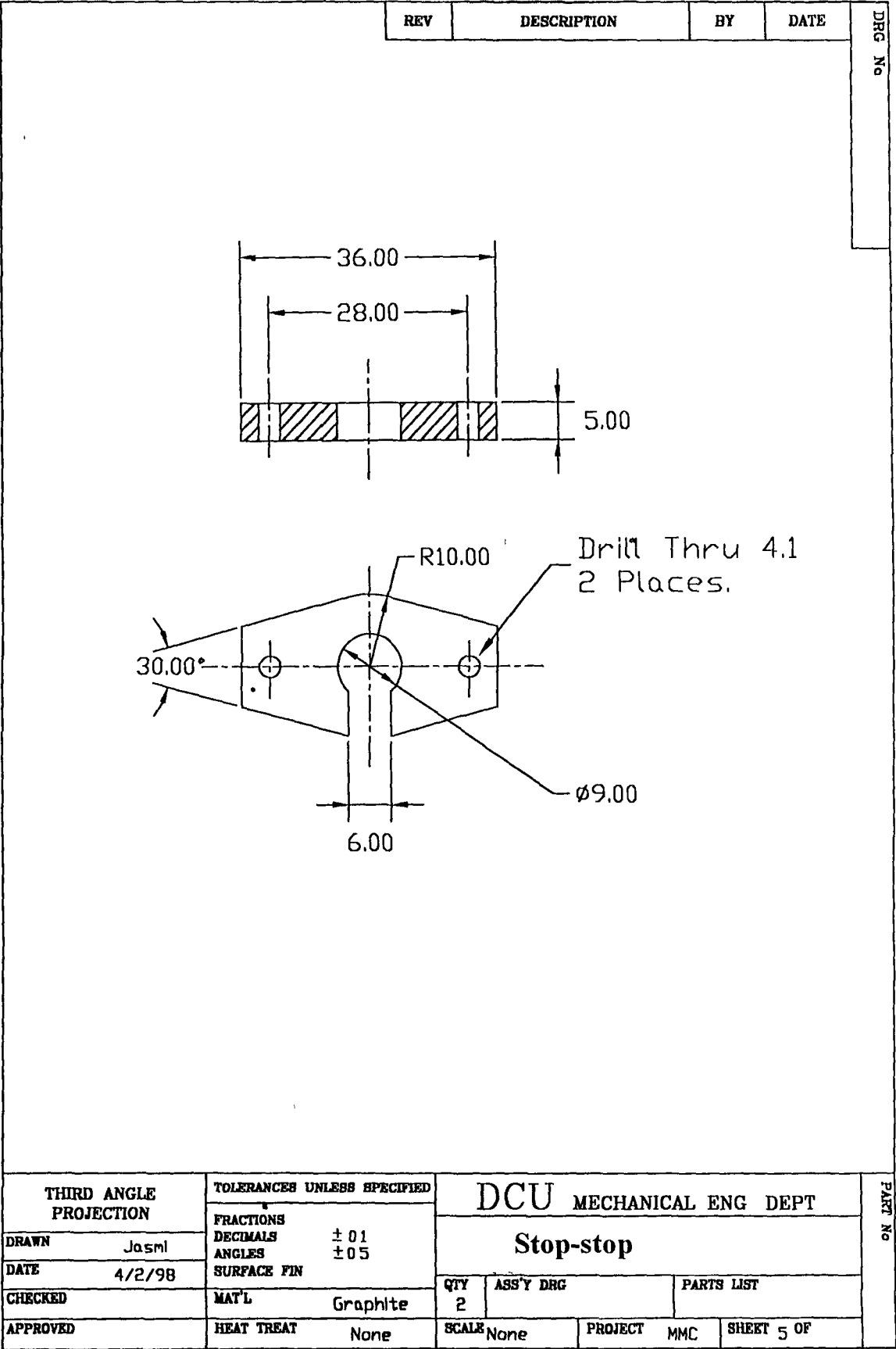






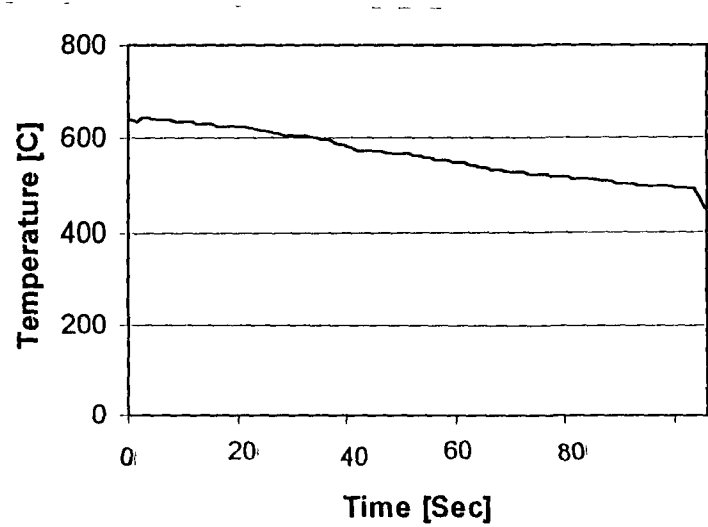






Appendix C

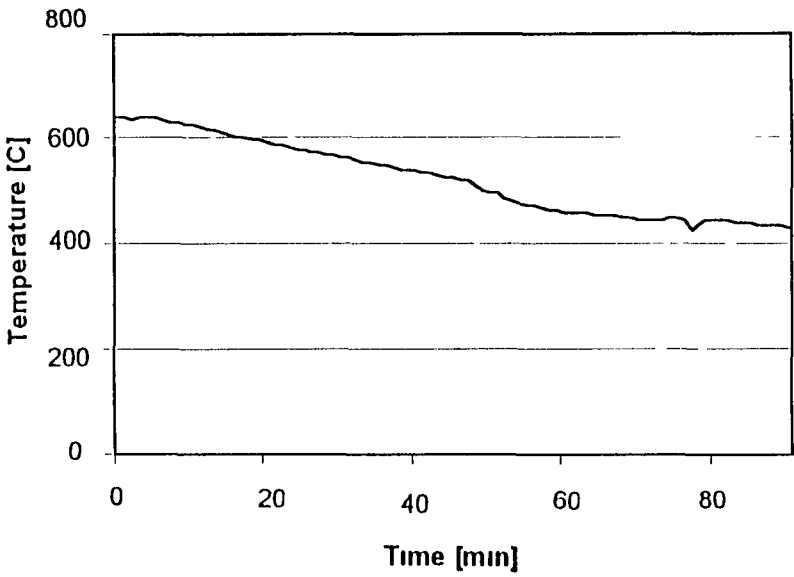
Temperature Measurements



Temperature as a function of time, to measure the cooling rate for the steel mould

Result from temperature measurement of the steel mould during casting,
which gives the cooling rate of 0.803°C/s

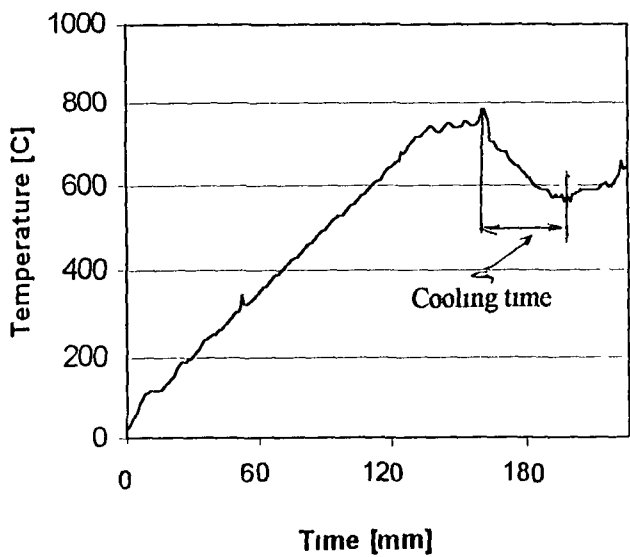
Temperature [C]	Time [Sec]	Temperature [C]	Time [Sec]	Temperature [C]	Time [Sec]
639.25	2	593.01	74	525.63	146
635.25	4	590.31	76	524.33	148
642.36	6	586.76	78	523.11	150
642.53	8	586.78	80	521.77	152
638.5	10	581.36	82	520.32	154
637.02	12	575.42	84	518.73	156
637.19	14	572.27	86	517.35	158
636.89	16	571.66	88	516.28	160
635.97	18	570.66	90	515.33	162
634.96	20	569.96	92	514.42	164
633.8	22	569.15	94	513.23	168
633.8	24	567.91	96	511.66	170
631.01	26	566.16	98	511.68	172
629.38	28	566.18	100	510.11	174
628.01	30	566.18	102	508.59	176
627.13	32	564.14	104	507.14	178
626.45	34	561.98	106	505.63	180
625.93	36	559.96	108	504.05	182
625.37	38	558.1	110	502.71	184
623.68	40	555.86	112	501.92	186
623.7	42	553.52	114	500.96	188
622.18	44	551.15	116	499.79	190
621.13	46	549.132	118	498.61	192
617.69	48	547.38	120	497.44	194
614.22	50	544.84	122	497.44	196
612.63	52	544.86	124	496.72	198
610.75	54	541.88	126	496.23	200
609.04	56	539.51	128	495.59	202
606.04	58	537.41	130	494.75	204
606.18	60	535.53	132	493.67	206
605.64	62	533.62	134	492.32	208
604.51	64	531.51	136	490.83	210
602.82	66	529.77	138	477.88	212
601.05	68	528.51	140	446.45	214
599.36	70	527.16	142		
595.5	72	525.61	144		



Temperature as a function of time, to measure the cooling rate for the graphite mould

Result from temperature measurement of the graphite mould during casting,
which gives the cooling rate of 1 475°C/s

Temperature [C]	Time [Sec]	Temperature [C]	Time [Sec]	Temperature [C]	Time [Sec]
640 73	2	561 02	64	455 73	126
637 77	4	557 53	66	454 49	128
636 37	6	554 86	68	452 61	130
638 76	8	551 96	70	450 62	132
640 47	10	549 17	72	448 62	134
638 8	12	546 12	74	448 59	136
635 39	14	543 39	76	446 58	138
632 68	16	540 36	78	444 83	140
629 08	18	537 64	80	442 58	142
624 5	20	537 64	82	440 96	144
624 52	22	534 38	84	440 09	146
620 69	24	531 26	86	442 63	148
617 07	26	528 42	88	443 78	150
613 64	28	525 42	90	443 8	152
610 39	30	521 86	92	442 35	154
605 34	32	519 68	94	423 71	156
602 24	34	516 84	96	433 9	158
599 28	36	509 32	98	441 05	160
595 76	38	500 21	100	441 71	162
595 76	40	494 63	102	440 71	164
591 49	42	494 65	104	439 68	168
588 32	44	486 42	106	438 33	170
585 01	46	480 34	108	436 34	172
581 26	48	476 03	110	434 63	174
578 29	50	472 14	112	432 96	176
575 44	52	468 8	114	432 96	178
572 79	54	464 9	116	431 5	180
570 04	56	461 82	118	430 41	182
567 08	58	459 79	120	428 63	184
567 1	60	456 77	122		
564 18	62	455 73	124		



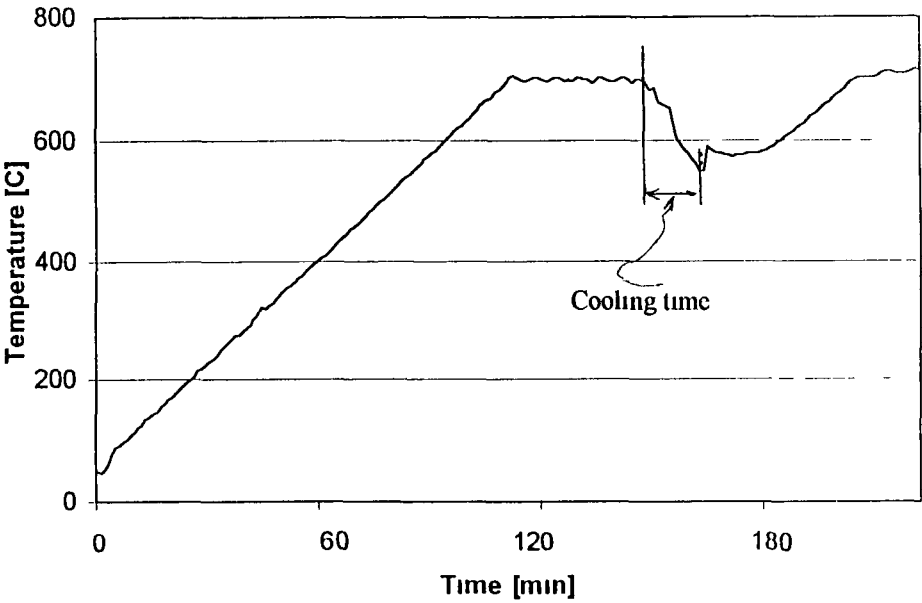
Temperature profile for wettability test-5 (iii), with 'cooling time of 41 minutes

Result form temperature measurement of MMC slurry during wettability test 5 (iii), which gives 'cooling time' of 41 minutes

Temperature[C]	Time [min]	Temperature[C]	Time [min]	Temperature[C]	Time [min]
24 76	1	305 17	51	545 03	101
34 16	2	309 76	52	549 79	102
45 66	3	341 15	53	554 54	103
58 73	4	318 43	54	559 15	104
71 9	5	322 53	55	563 92	105
84 35	6	326 97	56	568 38	106
95 07	7	331 76	57	573 01	107
103 39	8	336 83	58	577 51	108
109 12	9	342 11	59	582 13	109
112 58	10	347 43	60	587 25	110
114 24	11	352 81	61	592 41	111
114 77	12	357 84	62	597 53	112
114 53	13	362 94	63	602 71	113
114 06	14	367 9	64	607 76	114
114 64	15	372 68	65	612 42	115
116 73	16	377 26	66	617 3	116
120 8	17	381 94	67	626 87	117
126 84	1	386 77	68	631 74	118
134 3	19	391 53	69	636 7	119
143 08	20	396 66	70	641 67	120
152 22	21	401 89	71	646 76	121
161 78	22	406 99	72	651 18	122
175 51	23	412 25	73	655 11	123
180 87	24	417 32	74	654 94	124
184 53	25	422 49	75	680 02	125
187 11	26	427 49	76	676 29	126
188 86	27	432 48	77	682 01	127
190 23	28	437 24	78	688 77	128
192 18	2	442 2	79	696 04	129
199 18	30	447 09	80	702 6	130
204 27	31	452 18	81	708 26	131
210 41	32	457 24	82	713 3	132
216 83	33	462 29	83	717 67	133
223 75	34	467 47	84	722 48	134
230 16	35	472 48	85	728 13	135
236 87	36	477 41	86	734 37	136
241 1	37	482 37	87	740 2	137
245 41	38	487 29	88	741 82	138
249 22	39	492 15	89	738 45	139
252 73	40	497 04	90	733 19	140
256 07	41	501 98	91	728 72	141
259 49	42	507 12	92	728 7	142
263 41	4	512 19	93	733 01	143
267 67	44	517 05	94	739 1	144
272 72	45	521 79	95	745 21	145
278 08	46	526 48	96	748 75	146
283 83	47	526 48	97	747 64	147
289 63	48	531 15	98	743 09	148
295 09	49	535 77	99	738 03	149
300 33	50	540 38	100	735 76	150

Continue

738 21	151	642 55	177	578 25	203
743 61	152	637 42	178	581 11	204
754 51	153	632 04	179	583 56	205
754 6	154	629 64	180	585 16	206
750 66	155	620 24	181	585 74	207
745 25	156	615 72	182	585 91	208
741 33	157	617 34	183	586 31	209
743 19	158	605 66	184	587 42	210
747 92	159	599 34	185	588 93	211
754 2	<u>160</u>	595 65	186	588 91	212
785 75	161	590 8	187	588 81	213
785 4	162	585 61	188	592 07	214
770 33	163	589 98	189	596 27	215
760 79	164	587 46	190	600 3	216
704 25	165	579 43	191	604 02	217
700 8	166	570 69	192	591 47	218
701 66	167	569 9	193	595 33	218
689 7	168	578 22	194	599 77	220
685 08	169	570 28	195	605 92	221
679 96	170	567 81	196	614 28	222
680 55	171	577 74	197	622 93	223
677 4	172	561 02	198	658 82	224
663 71	173	572 03	199	632 58	225
655 89	174	572 43	200		
652 49	175	560 39	201	641 37	226
647 53	176	575 57	<u>202</u>		



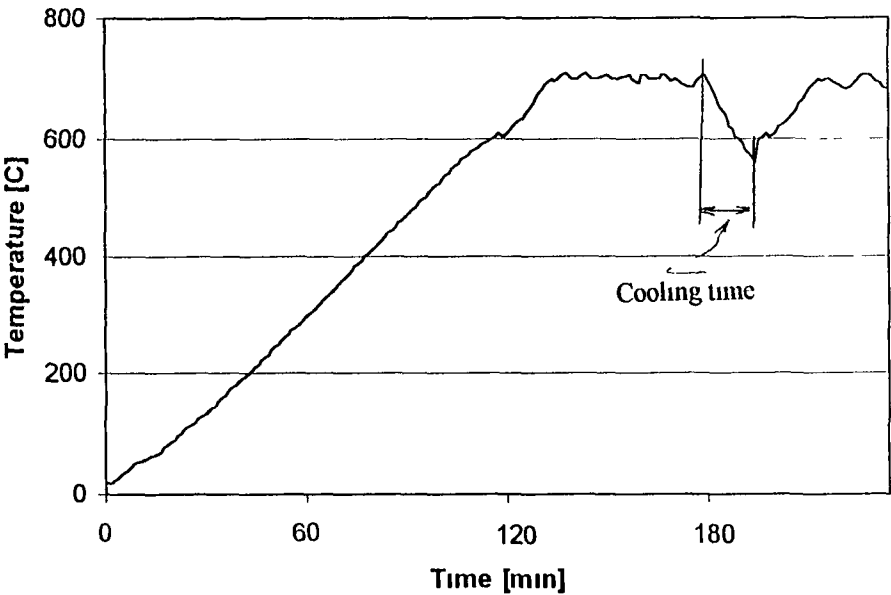
Temperature profile during wettability test-5 (iii), with
'cooling time of 21 minutes

Result form temperature measurement of MMC slurry during wettability test 5 (iii), which gives 'cooling time' of 21 minutes.

Temperature[C]	Time [min]	Temperature[C]	Time [min]	Temperature[C]	Time [min]
		343.77	52	630.91	102
49.72	3	348.88	53	636.37	103
46.63	4	354.22	54	641.61	104
54.36	5	359.11	55	649.42	105
66.72	6	365.88	56	655.89	106
78.47	7	371.66	57	661.53	107
87.72	8	375.56	58	667.32	108
91.41	9	383.45	59	671.01	109
98.11	10	388.57	60	679.34	110
101.69	11	394.67	61	684.34	111
107.99	12	398.72	62	691.01	112
113.19	13	405.98	63	697.22	113
121.16	14	409.25	64	701.89	114
125.07	15	415.76	65	706.49	115
133.07	16	421.41	66	703.88	116
138.77	17	427.31	67	699.65	117
144.94	18	433.23	68	697.54	118
148.79	19	439.41	69	699.12	119
157.56	20	443.61	70	702.42	120
162.07	21	451.22	71	704.43	121
167.97	22	456.88	72	702.67	122
171.88	23	462.56	73	698.01	123
178.51	24	468.32	74	697.04	124
183.87	25	474.23	75	698.12	125
191.26	26	478.24	76	702.63	126
197.28	27	486.32	77	703.31	127
201.07	28	491.67	78	701.19	128
207.04	29	497.34	79	697.23	129
214.76	30	503.57	80	698.49	130
218.79	31	509.35	81	697.37	131
224.79	32	515.36	82	702.77	132
232.26	33	518.54	83	702.21	133
235.12	34	524.71	84	701.16	134
242.45	35	532.42	85	697.91	135
249.44	36	538.35	86	693.51	136
255.44	37	542.42	87	697.89	137
261.86	38	548.13	88	702.36	138
267.71	39	556.74	89	703.16	139
273.26	40	561.55	90	698.34	140
275.81	41	567.48	91	697.75	141
281.12	42	573.54	92	697.77	142
286.91	43	579.1	93	698.11	143
292.84	44	584.01	94	703.41	144
300.85	45	588.07	95	702.58	145
309.11	46	596.22	96	698.11	146
322.69	47	602.31	97	693.81	147
317.17	48	608.06	98	698.12	148
324.62	49	614.13	99	698.71	149
328.88	50	618.12	100	697.16	150
336.68	51	622.1	101	687.11	151

Continue

682 9	152	576 5	177	674 53	202
685 23	153	577 78	178	680 5	203
664 2	154	578 64	179	685 92	204
660 75	155	579 28	180	691 26	205
655 34	156	579 87	181	696 36	206
652 25	157	581 07	182	700 59	207
617 39	158	583 07	183	703 12	208
600 66	159	586 18	184	703 56	209
595 22	160	590 41	185	702 75	210
586 63	161	594 69	186	702 06	211
578 36	162	599 57	187	702 78	212
568	163	604 91	188	705 12	213
560 85	164	608 91	189	708 33	214
550 58	165	612 59	190	711 3	215
548 36	166	616 66	191	712 7	216
588 21	167	621 61	192	712 22	217
584 5	168	627 34	193	710 65	218
582 6	169	633 2	194	709 2	219
580 58	170	639 1	195	709 28	220
578 25	171	644 18	196	711 09	221
576 16	172	648 78	197	714	222
574 58	173	653 2	198	716 5	223
573 97	174	657 83	199	717 41	224
574 24	175	663 17	200		
575 2	176	668 66	201		



Temperature profile during wettability test-5 (iii), with
'cooling time of 14 minutes

Result form temperature measurement of MMC slurry during wettability test 5 (iii), which gives 'cooling time' of 14 minutes

Temperature[C]	Time [min]	Temperature[C]	Time [min]	Temperature[C]	Time [min]
19 03	3	238 07	52	519 6	101
21 35	4	243 83	53	525 33	102
24 67	5	249 66	54	531 04	103
28 92	6	255 16	55	536 74	104
33 4	7	260 53	56	542 52	105
38 04	8	265 85	57	548 34	106
42 37	9	271 17	58	554 03	107
46 37	10	276 58	59	558 72	108
49 98	11	282 14	60	563 5	109
53 05	12	287 82	61	568 12	110
55 86	13	293 55	62	572 47	111
58 4	14	299 45	63	578 87	112
60 94	15	305 37	64	582 03	113
63 2	16	311 22	65	585 12	114
66 03	17	317 03	66	589 02	115
69 14	18	322 79	67	593 37	116
73 1	19	328 47	68	596 93	117
77 38	20	334 07	69	599 68	118
82 04	21	339 48	70	603 93	119
87 29	22	345 11	71	610 64	120
92 57	23	350 78	72	602 31	121
98 03	24	356 5	73	607 46	122
103 17	25	362 16	74	612 81	123
108 15	26	368 12	75	618 01	124
112 58	27	374 08	76	622 57	125
116 78	28	379 83	77	628 16	126
120 69	29	385 73	78	633 86	127
124 5	30	391 64	79	640 84	128
128 29	31	397 24	80	648 18	129
132 46	32	402 99	81	655 79	130
137 07	33	408 56	82	664 72	131
141 78	34	414 42	83	673 06	132
147 19	35	420 09	84	680 76	133
152 9	36	426 09	85	687 3	134
158 62	37	431 88	86	692 92	135
164 49	38	437 73	87	697 64	136
170 07	39	443 76	88	695 39	137
175 63	40	449 53	89	697 11	138
180 68	41	455 49	90	703 33	139
185 65	42	461 22	91	709 41	140
190 34	43	466 92	92	703 09	141
195 03	44	472 63	93	697 6	142
199 68	45	478 61	94	697 11	143
204 41	46	484 35	95	697 85	144
209 68	47	490 23	96	705 75	145
215	48	496 14	97	707 42	146
220 5	49	502 03	98	704 45	147
226 46	50	508 08	99	698 87	148
232 27	51	513 86	100	697 88	149

Continue

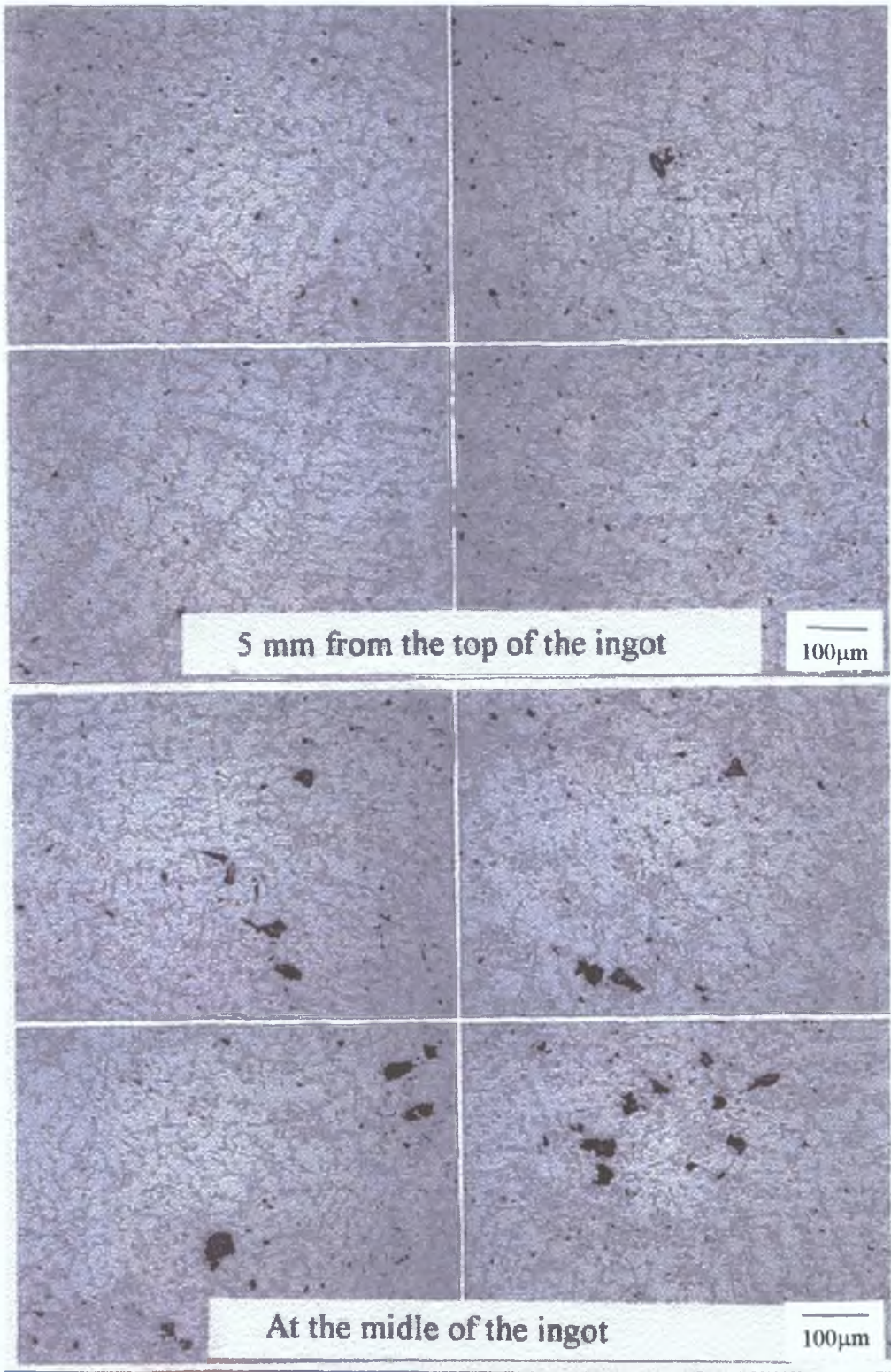
696 72	150	689 4	179	640 84	208
702 42	151	696 19	180	648 18	209
705 6	152	704 73	181	655 79	210
703 55	153	703 51	182	664 72	211
697 7	154	691 21	183	673 06	212
698 75	155	677 26	184	680 76	213
697 54	156	670 13	185	687 3	214
702 53	157	653 39	186	692 92	215
702 39	158	641 91	187	697 64	216
703 59	159	639 21	188	695 39	217
697 8	160	618 84	189	698 46	218
695 66	161	616 04	190	698 59	219
692 45	162	603 27	191	695 87	220
705 63	163	599 66	192	691 47	221
703 44	164	592 28	193	686 67	222
698 51	165	583 01	194	682 94	223
698 7	166	576 42	195	681 36	224
697 11	167	565 99	196	682 74	225
698 21	168	557 63	197	687 3	226
704 33	169	599 68	198	694 39	227
704 51	170	603 93	199	701 3	228
697 65	171	610 64	200	705 47	229
693 21	172	602 31	201	706 2	230
698 24	173	607 46	202	704 32	231
694 59	174	612 81	203	700 39	232
692 45	175	618 01	204	695 3	233
686 74	176	622 57	205	689 61	234
683 35	177	628 16	206	684 34	235
684 62	178	633 86	207	680 58	236

Appendix D

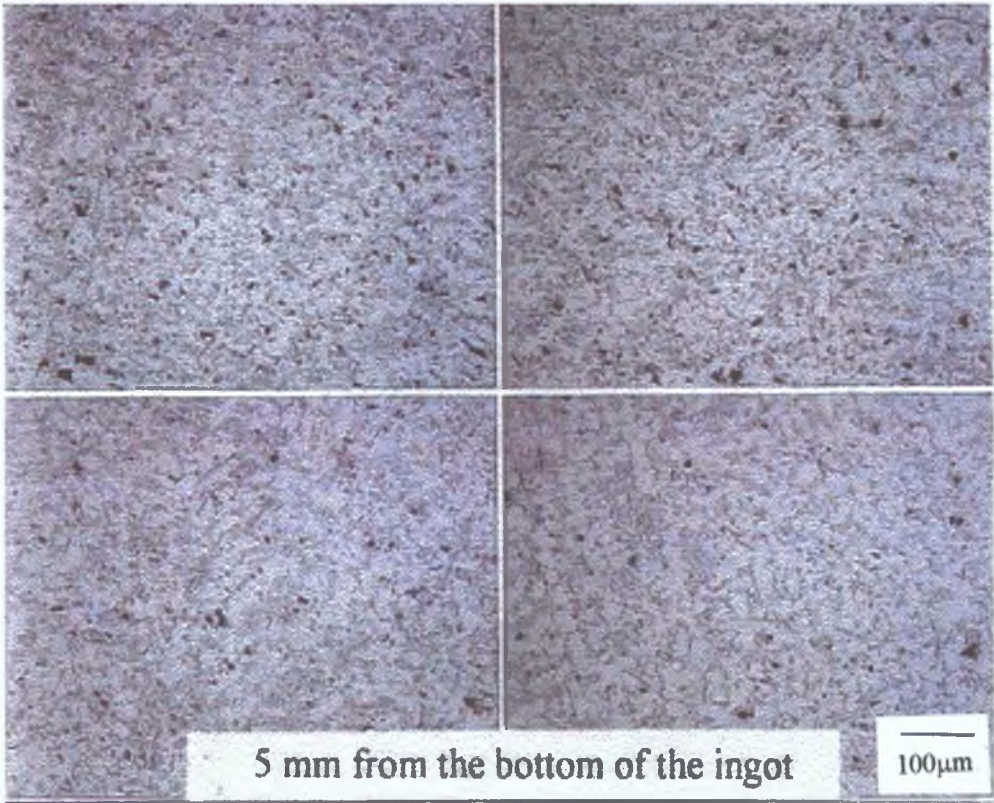
Graphical Method of Wettability Measurements

(Accept for micrograph in page D1 and D2, all the micrographs
were taken at the middle of the ingot)

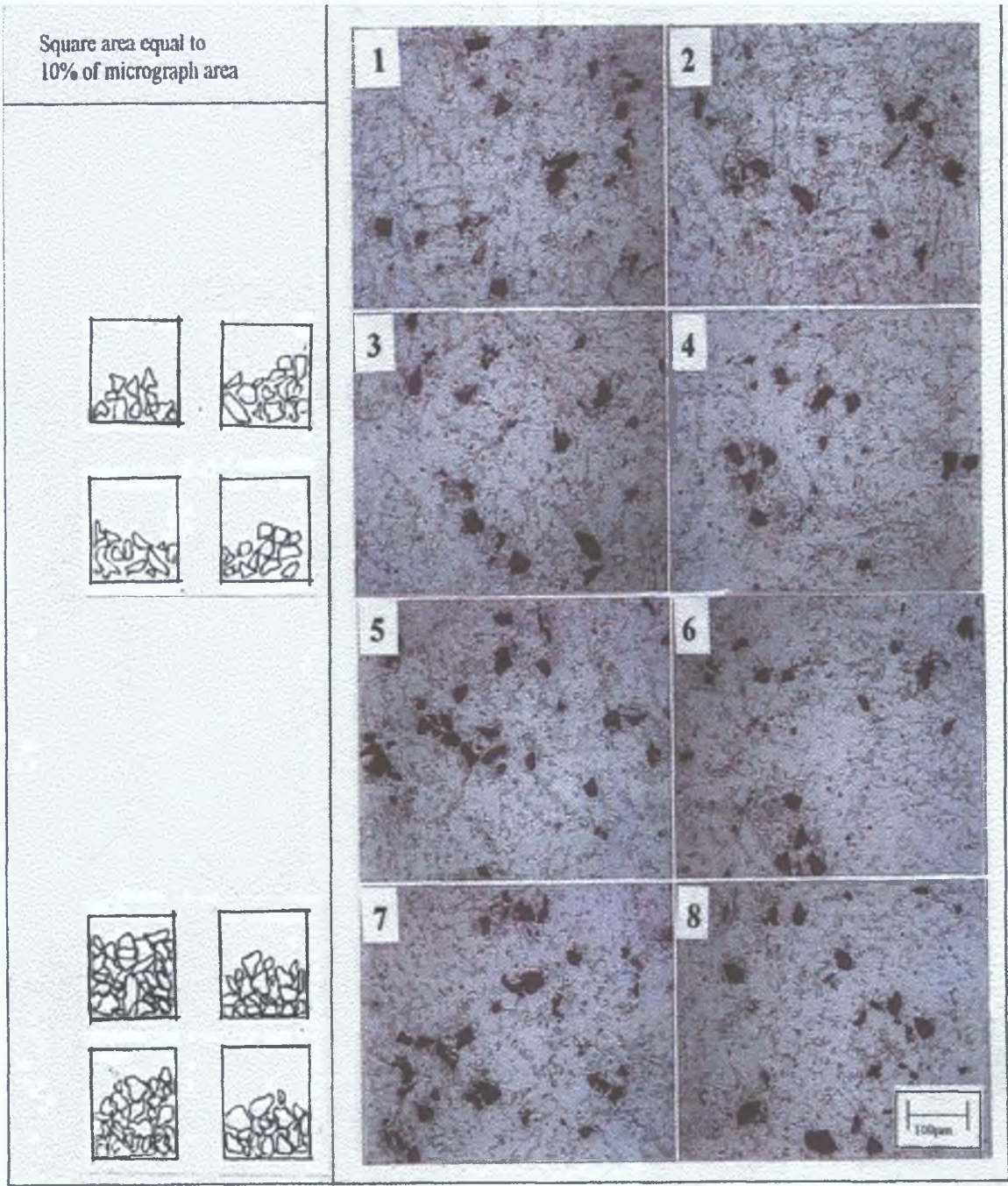
Micrograph of cast MMC, stirring in fully state condition. The wettability is zero or negligible.



Micrograph of cast A359/SiC/25p, for the cooling time during stirring of about 5 minutes (Continued).

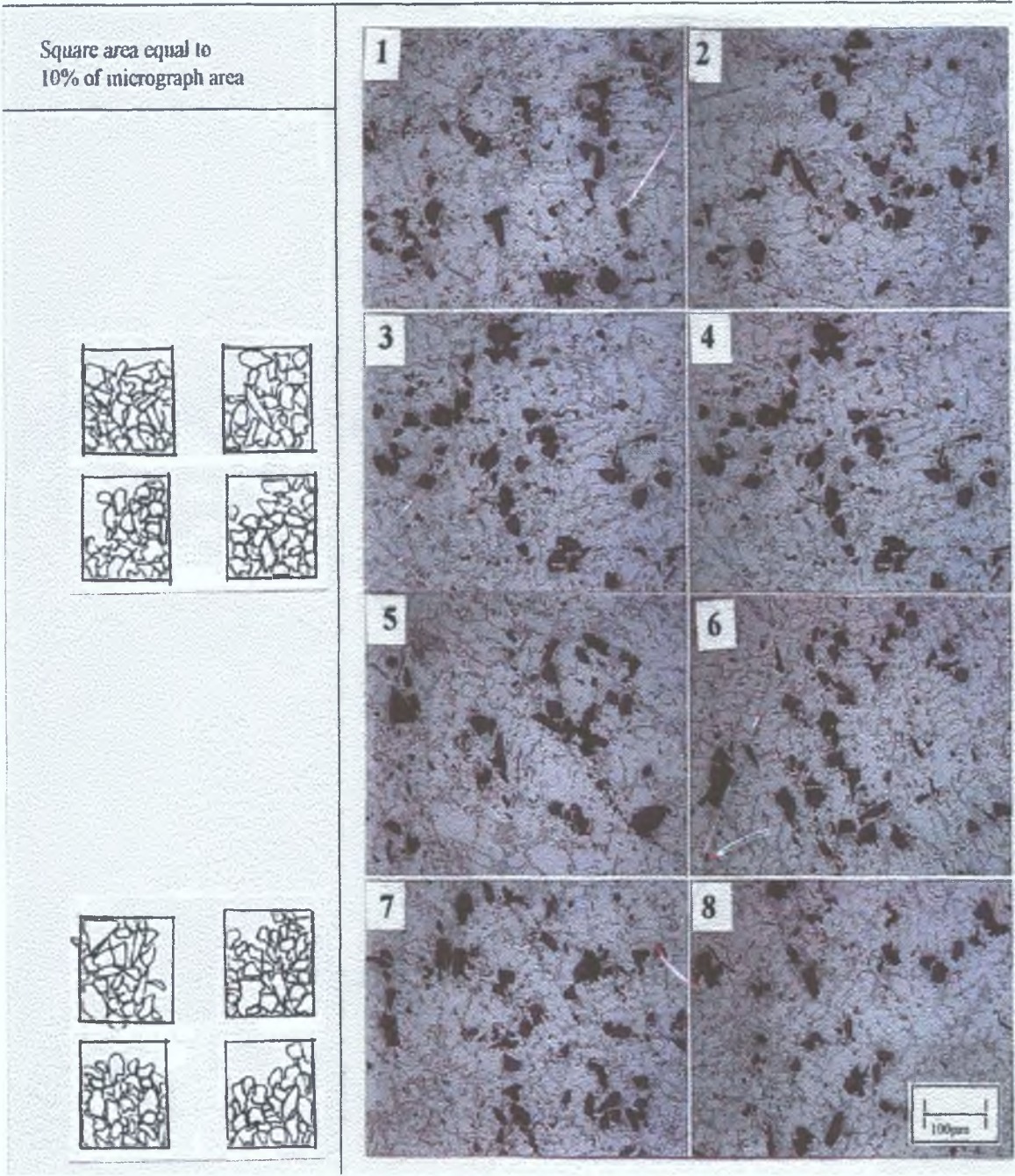


Micrograph of cast A359/SiC/10p, for the cooling time during stirring of about 40 minutes



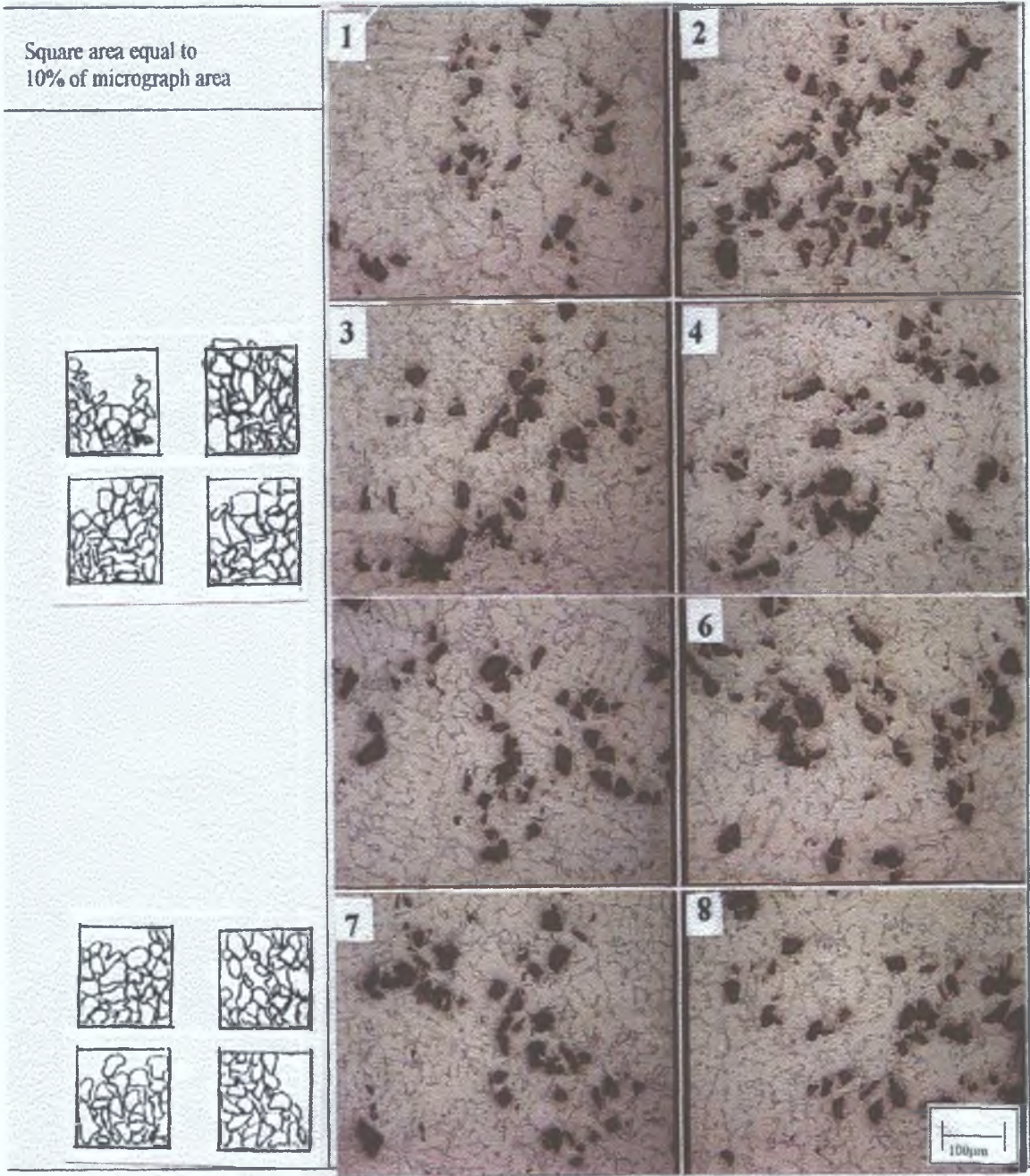
Wettability Measurement [%]									
Picture No	1	2	3	4	5	6	7	8	Average [%]
Percentage of wettability [%]	20	30	20	30	70	40	65	45	39.63

Micrograph of cast A359/SiC/10p, for the cooling time during stirring of about 21 minutes



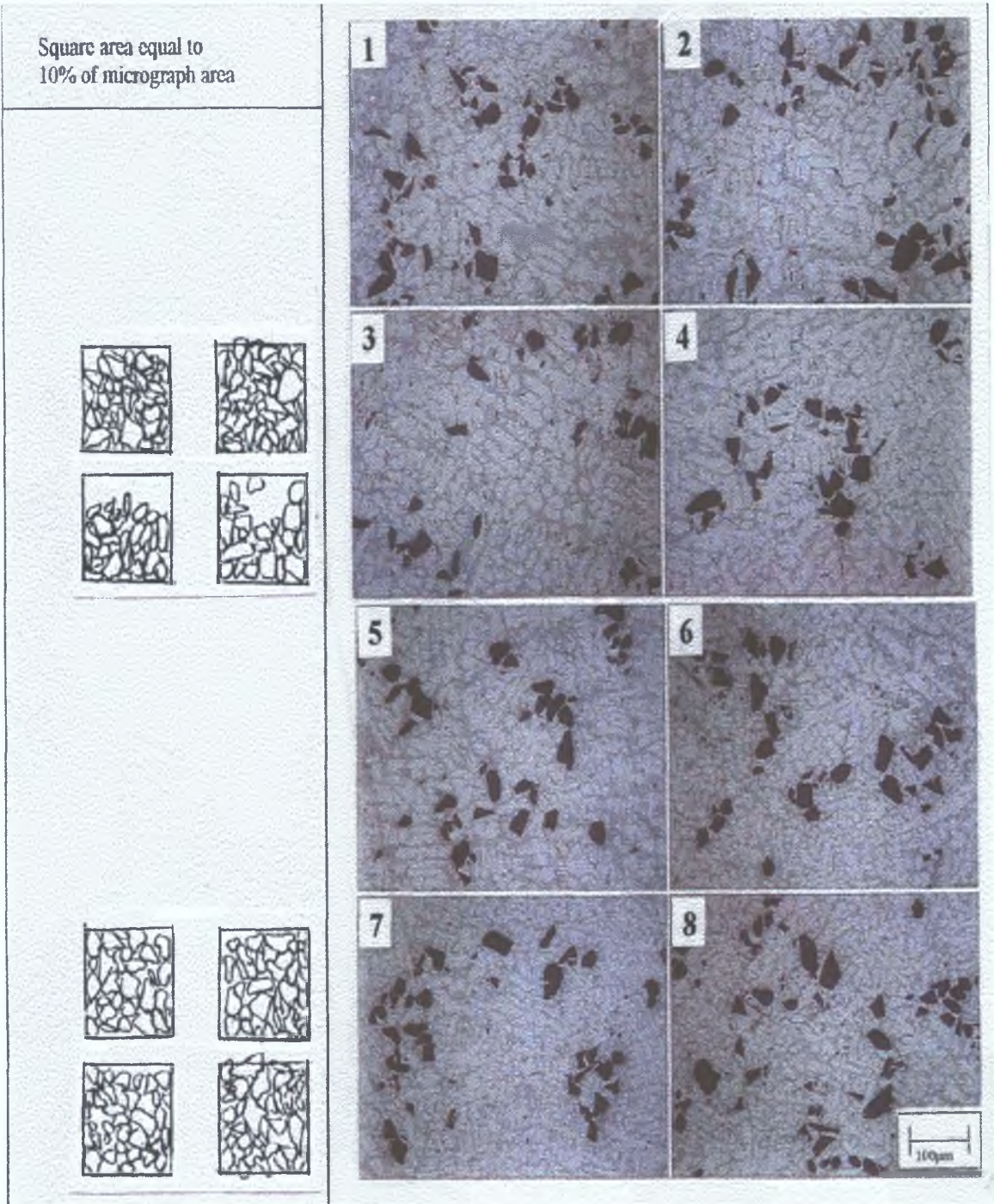
Wettability Measurement [%]									
Picture No	1	2	3	4	5	6	7	8	Average [%]
Percentage of wettability [%]	75	70	65	70	60	70	75	70	69.39

Micrograph of cast A359/SiC/10p, for the cooling time during stirring of about 14 minutes



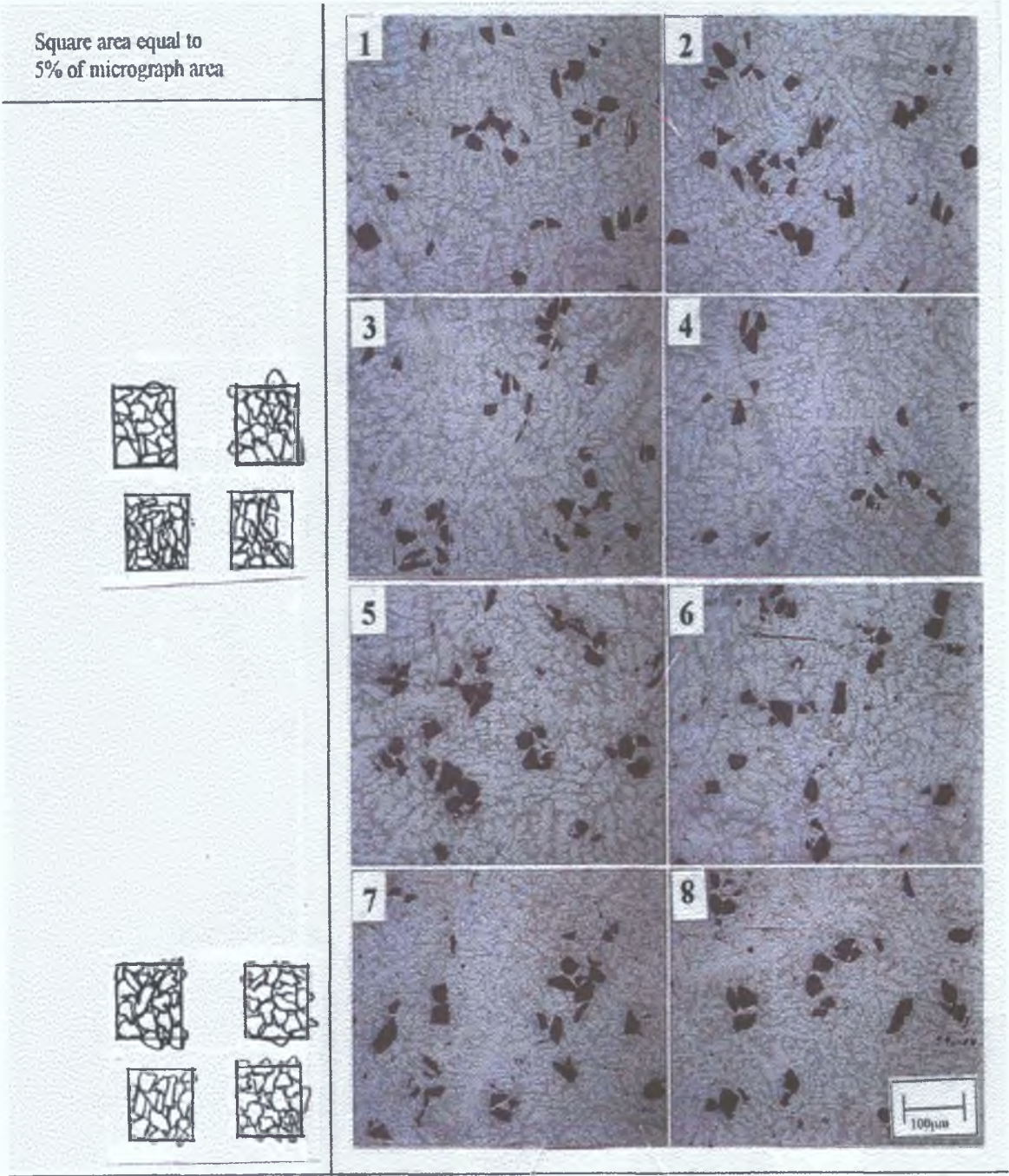
Wettability Measurement [%]									
Picture No	1	2	3	4	5	6	7	8	Average [%]
Percentage of wettability [%]	50	100	75	70	80	75	80	75	75.63

Micrograph of cast A359/SiC/10p, for the cooling time during stirring of about 5 minutes



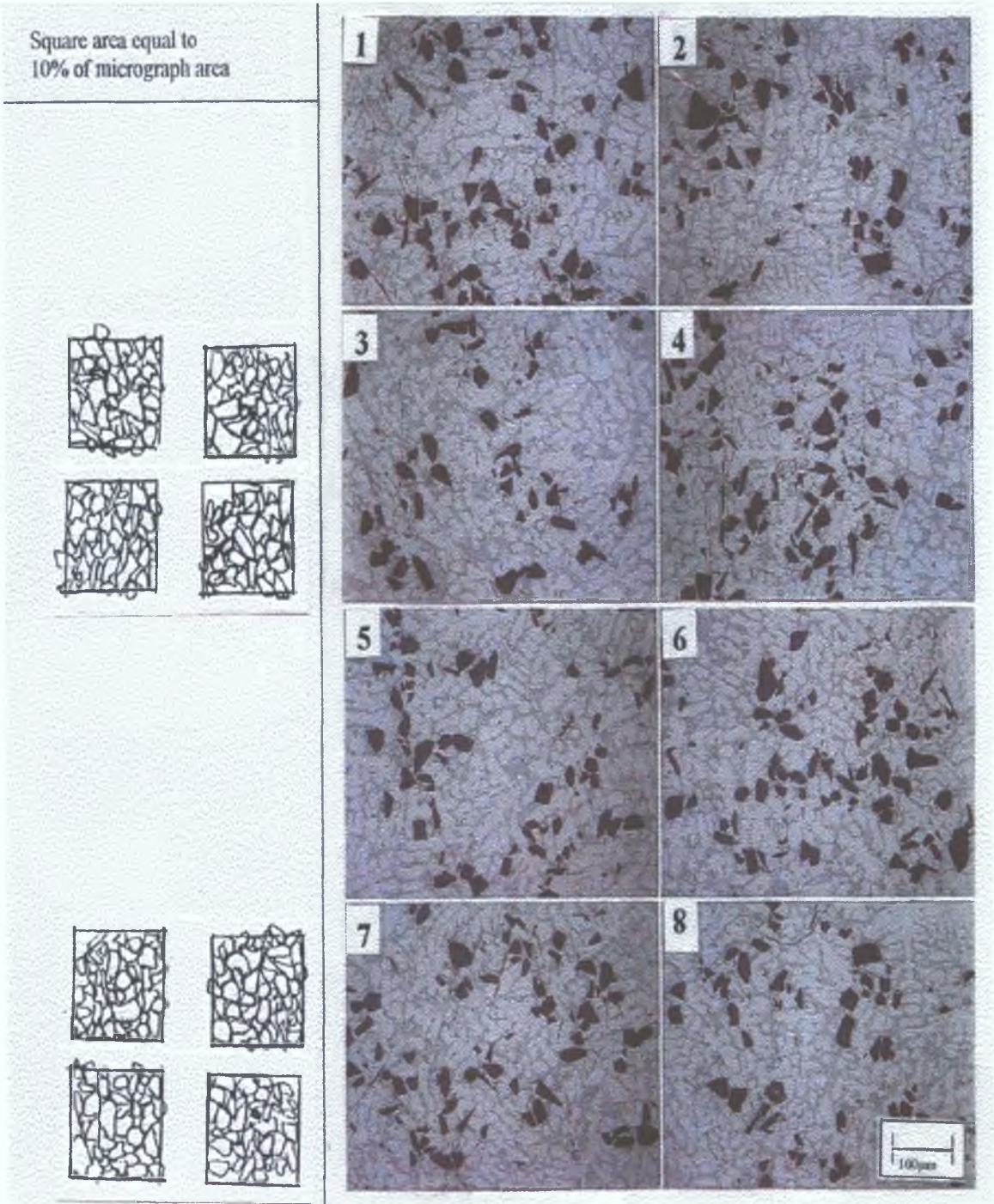
Wettability Measurement [%]									
Picture No	1	2	3	4	5	6	7	8	Average [%]
Percentage of wettability [%]	90	97	75	70	95	95	90	97	88.63

Micrograph of cast A359/SiC/5p, for the cooling time during stirring of about 5 minutes



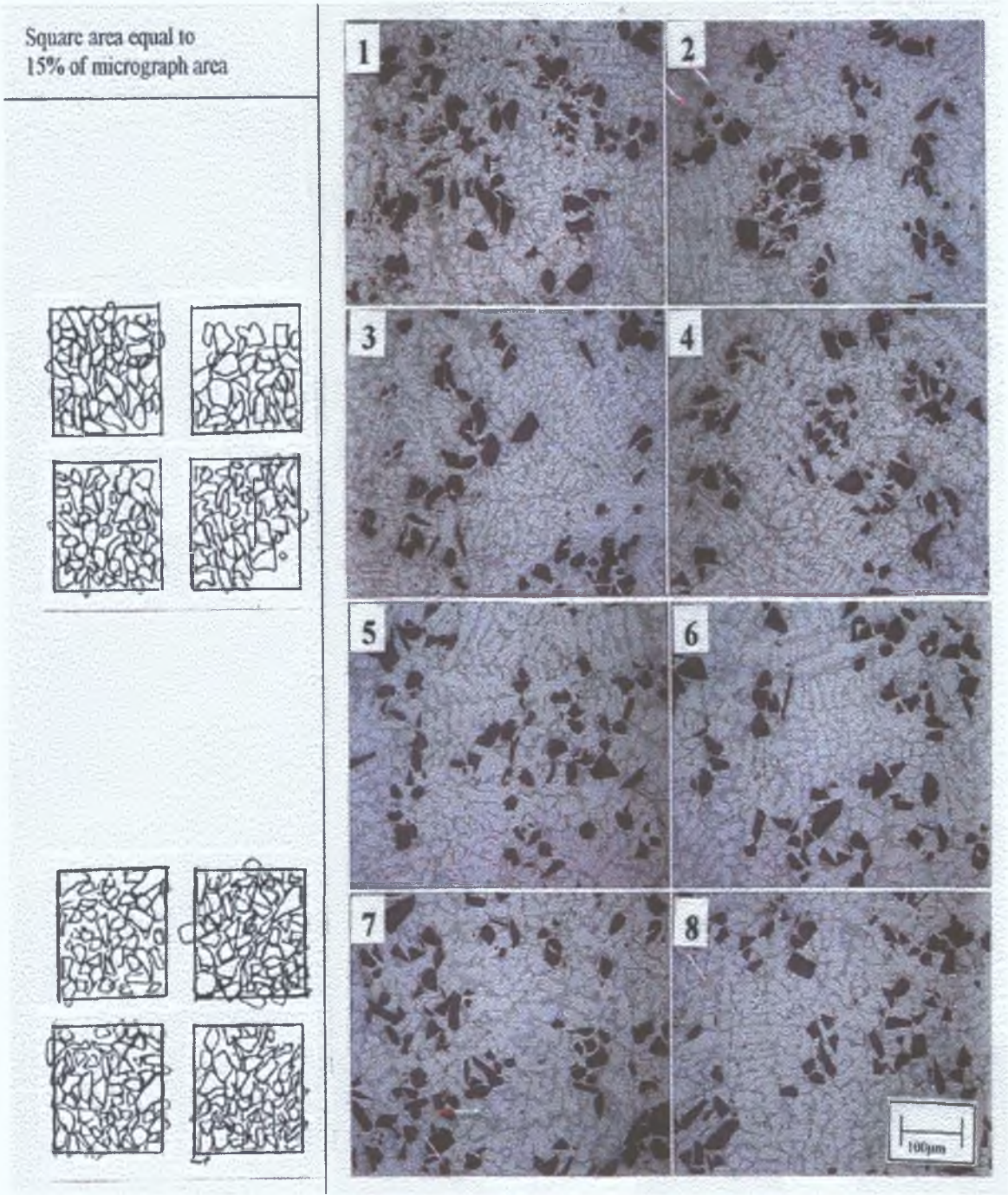
Wettability Measurement [%]									
Picture No	1	2	3	4	5	6	7	8	Average [%]
Percentage of wettability [%]	95	100	95	90	100	97	95	100	96.5

Micrograph of cast A359/SiC/10p, for the cooling time during stirring of about 5 minutes



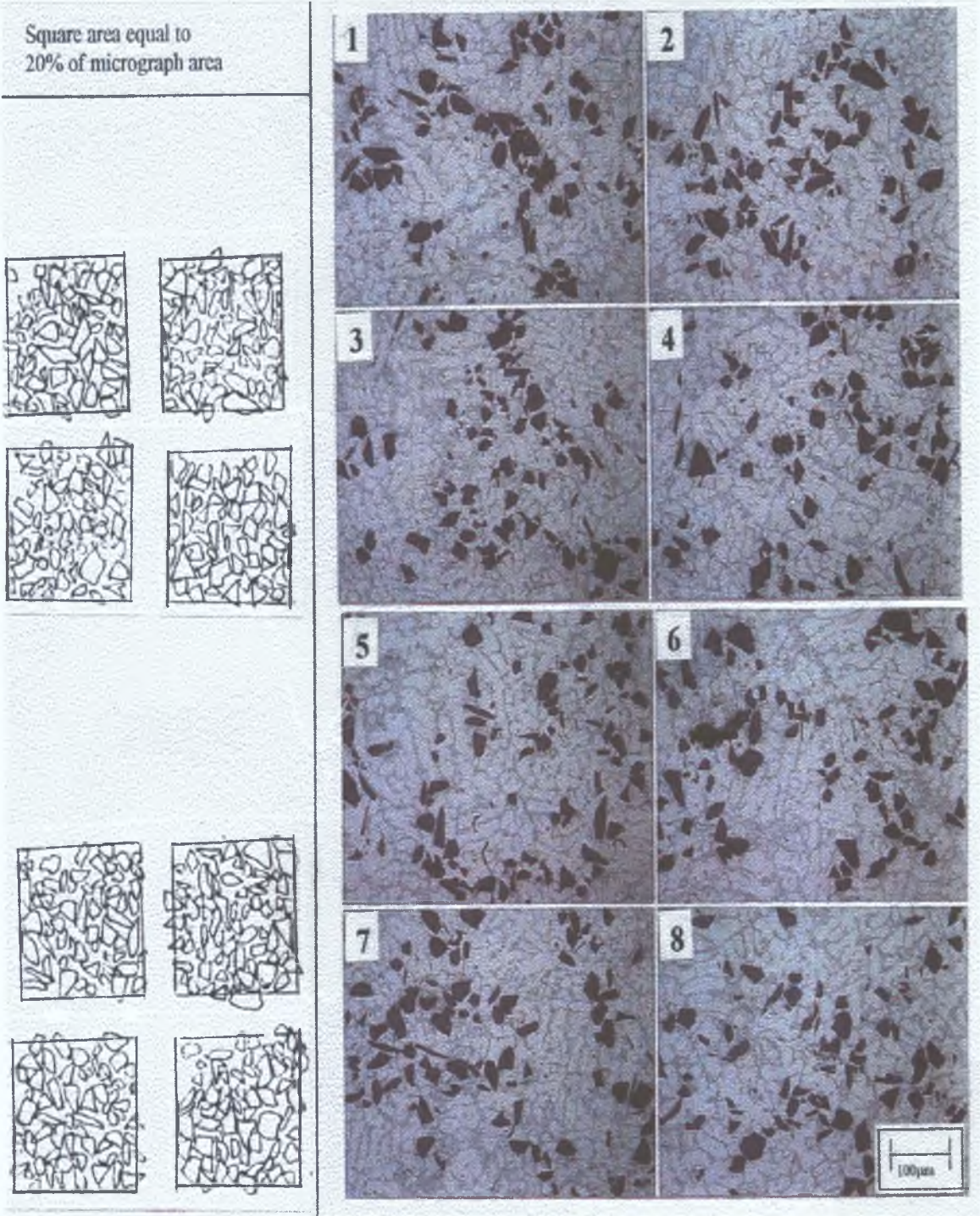
Wettability Measurement [%]									
Picture No	1	2	3	4	5	6	7	8	Average [%]
Percentage of wettability [%]	95	90	85	90	90	90	90	90	90.00

Micrograph of cast A359/SiC/15p, for the cooling time during stirring of about 5 minutes



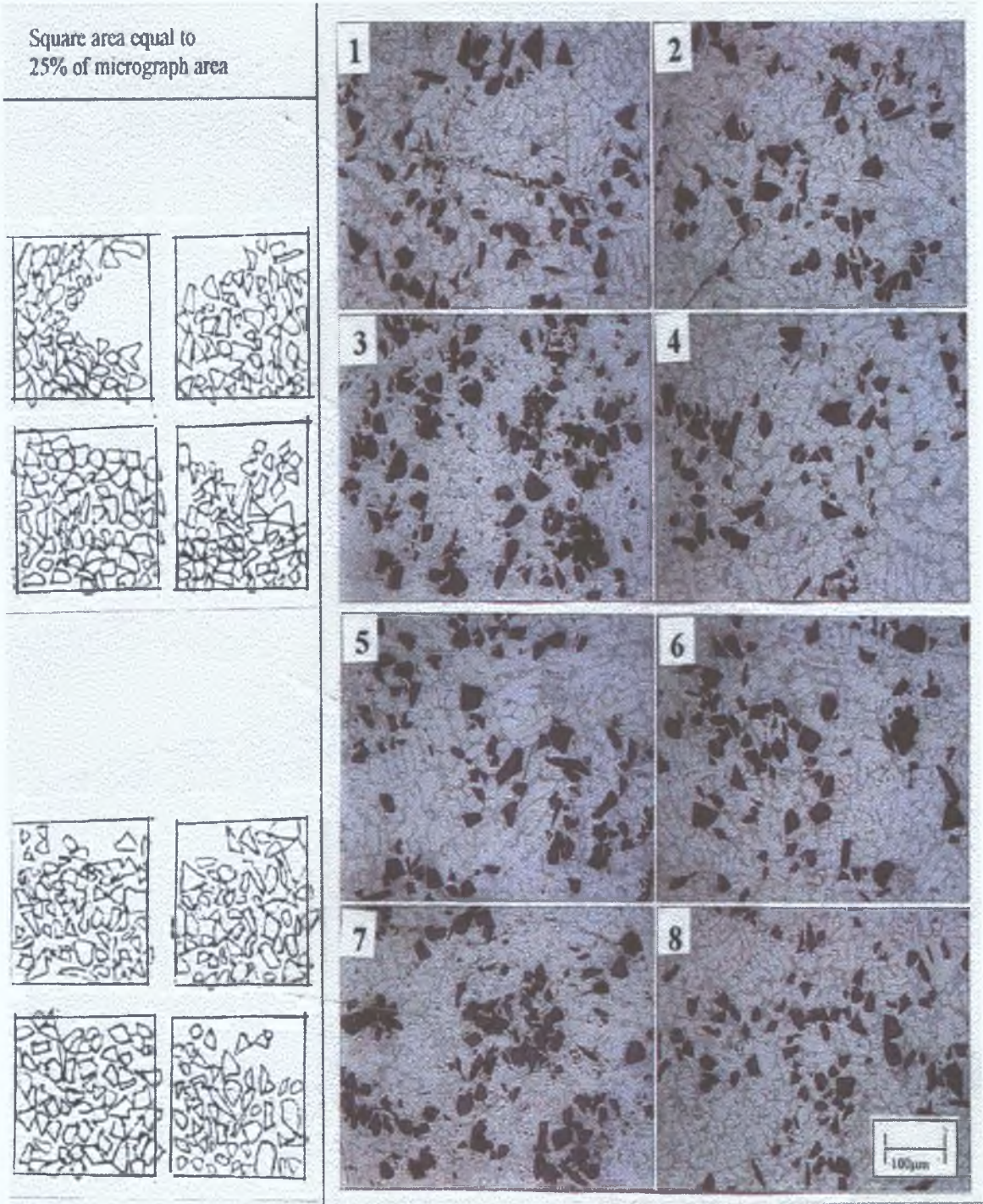
Wettability Measurement [%]									
Picture No	1	2	3	4	5	6	7	8	Average [%]
Percentage of wettability [%]	95	80	85	85	90	97	97	95	90.5

Micrograph of cast A359/SiC/20p, for the cooling time during stirring of about 5 minutes



Wettability Measurement [%]									
Picture No	1	2	3	4	5	6	7	8	Average [%]
Percentage of wettability [%]	80	80	80	80	80	80	80	75	79.38

Micrograph of cast A359/SiC/25p, for the cooling time during stirring of about 5 minutes



Wettability Measurement [%]									
Picture No	1	2	3	4	5	6	7	8	Average [%]
Percentage of wettability [%]	70	75	80	70	70	70	80	70	73.13

Appendix E

,

Density Measurements

Density measurement for ingot B, steel mould

Sample	Diameter [mm]	Thickness [mm]	Weight In Air [g]	Volume (Calculate)	Measured Density M/V	Porosity [%]
ALS-1	16 77	6 86	3 934	1 513	2 600	2 98
ALS-2	16 83	6 77	3 965	1 504	2 636	1 64
ALS-3	16 77	6 29	3 612	1 387	2 604	2 83
5S-1	17 00	6 83	3 986	1 550	2 572	4 95
5S-2	16 77	8 28	4 785	1 827	2 619	3 21
5S-3	16 78	8 42	4 868	1 862	2 614	3 39
10S-1	16 74	7 31	4 169	1 6019	2 591	5 16
10S-2	16 92	6 73	3 896	1 513	2 575	5 75
10S-3	16 76	6 43	3 751	1 419	2 643	3 26
10S-3	17 04	7 93	4 66	1 808	2 581	5 52
15S-1	16 75	6 87	3 996	1 512	2 643	4 17
15S-2	16 84	8 00	4 684	1 782	2 628	4 71
15S-3	16 82	8 69	5 125	1 931	2 654	3 77
15S-4	16 89	7 34	4 303	1 642	2 620	5 00
17S-1	16 77	6 90	3 993	1 522	2 623	5 24
17S-2	16 84	7 76	4 585	1 728	2 653	4 15
17S-3	16 83	7 81	4 554	1 735	2 624	5 20
17S-4	16 82	7 32	4 298	1 626	2 643	4 52
20S-1	16 98	7 21	3 767	1 633	2 306	17 17
20S-2	16 82	8 01	4 187	1 779	2 353	15 48
20S-3	16 83	7 55	4 030	1 677	2 403	13 68
20S-4	16 89	7 19	3 781	1 609	2 349	15 62
25S-1	16 99	8 73	4 931	1 977	2 494	11 24
25S-2	16 83	9 22	5 229	2 048	2 553	9 15
25S-3	16 91	8 93	4 909	2 003	2 451	12 77

Density measurement for ingot B, graphite mould

Sample	Diameter [mm]	Thickness [mm]	Weight In Air [g]	Volume (Calculate)	Measured Density M/V	Porosity [%]
ALG-1	17 06	7 28	4 376	1 664	2 629	1 90
ALG-2	17 38	6 65	4 115	1 577	2 608	2 98
ALG-3	17 22	7 01	4 270	1 632	2 615	2 42
5G-1	17 32	8 50	5 248	2 003	2 62	3 17
5G-2	17 37	7 70	4 769	1 822	2 616	3 32
5G-3	17 39	6 56	4 059	1 556	2 608	3 62
5G-4	17 26	7 31	4 480	1 710	2 619	3 21
10G-1	16 79	7 43	4 289	1 643	2 610	4 46
10G-2	17 30	6 97	4 269	1 638	2 606	4 61
10F-3	17 30	6 97	4 201	1 6007	2 624	3 95
15G-1	17 34	8 26	5 017	1 951	2 571	6 78
15G-2	17 38	8 46	5 188	2 007	2 585	6 27
15G-3	17 35	8 32	5 123	1 965	2 607	5 47
17G-1	17 32	7 43	4 479	1 750	2 559	7 55
17G-2	17 28	7 44	4 437	1 745	2 543	8 13
17G-3	17 28	7 35	4 409	1 724	2 557	7 62
17G-4	17 26	7 44	4 438	1 741	2 549	7 91
20G-1	17 26	7 48	4 414	1 750	2 522	9 41
20G-2	17 37	7 76	4 503	1 837	2 451	11 96
20G-3	17 31	8 07	4 753	1 897	2 505	10 02
20G-4	17 30	8 32	4 919	1 956	2 510	9 84
20G-5	17 19	7 20	4 093	1 669	2 452	11 92
20G-6	17 31	7 49	4 450	1 761	2 527	9 23
20G-7	17 34	8 17	4 842	1 929	2 510	9 84
20G-8	17 33	8 87	5 164	1 89	2 472	11 20
25G-1	17 35	6 52	3 796	1 539	2 466	12 24
25G-2	17 35	6 35	3 811	1 499	2 542	9 54
25G-3	17 54	7 90	4 702	1 909	2 463	12 35
25G-4	17 44	7 46	4 470	1 782	2 508	10 75

Density measurement for ingot A, steel mould

Sample	Diameter [mm]	Thickness [mm]	Weight In Air [g]	Volume (Calculate)	Measured Density M/V	Porosity [%]
ALS-1	10 19	9 39	2 014	0 764	2 636	1 64
ALS-2	10 15	10 09	2 130	0 815	2 613	2 50
ALS-3	10 11	10 43	2 204	0 835	2 639	1 52
ALS-4	10 15	11 42	2 435	0 922	2 641	1 45
ALS-5	10 14	9 35	1 979	0 755	2 621	2 20
5S-1	10 12	12 00	2 539	0 965	2 631	2 77
5S-2	10 16	11 91	2 524	0 965	2 615	3 36
5S-3	10 16	11 83	2 528	0 959	2 636	2 58
5S-4	10 16	11 55	2 459	0 936	2 627	2 92
10S-1	10 19	11 59	2 479	0 943	2 628	3 80
10S-2	10 16	12 29	2 592	0 996	2 602	4 75
10S-3	10 20	11 86	2 536	0 969	2 617	4 20
10S-4	10 14	11 60	2 455	0 937	2 620	4 09
10S-5	10 18	11 49	2 491	0 935	2 664	2 48
15S-1	10 19	10 83	2 342	0 881	2 658	3 63
15S-2	10 19	12 43	2 673	1 012	2 641	4 24
15S-3	10 16	11 83	2 439	0 959	2 543	7 79
17S-1	10 19	12 00	2 440	0 977	2 497	9 79
17S-2	10 18	11 42	2 370	0 929	2 551	7 84
17S-3	10 17	12 54	2 594	1 017	2 5506	7 81
17S-4	10 15	13 02	2 719	1 051	2 587	6 54

Density measurement for ingot A, steel mould (continue)

Sample	Diameter [mm]	Thickness [mm]	Weight In Air [g]	Volume (Calculate)	Measured Density M/V	Porosity [%]
20S-1	10 17	12 46	2 553	1 010	2 528	9 19
20S-2	10 15	11 47	2 440	0 926	2 635	5 35
20S-3	10 10	11 39	2 339	0 912	2 565	7 87
20S-4	10 14	11 09	S 213	0 895	2 473	11 17
25S-1	10 18	12 61	2 672	1 026	2 604	7 33
25S-2	10 19	11 94	2 473	0 972	2 544	9 47
25S-3	10 13	12 27	2 621	0 987	2 655	5 52
25S-4	10 20	13 11	2 741	1 071	2 559	8 93
25S-5	10 18	11 92	2 517	0 970	2 590	7 83

Density measurement for ingot A, graphite mould

Sample	Diameter [mm]	Thickness [mm]	Weight In Air [g]	Volume (Calculate)	Measured Density M/V	Porosity [%]
ALG-1	10 00	10 65	2 227	0 836	2 6638	0 6
ALG-2	10 09	11 22	2 359	0 895	2 6357	1 65
ALG-3	10 07	10 59	2 205	0 842	2 6187	2 28
ALG-4	10 21	10 85	2 333	0 886	2 6331	1 75
5G-1	10 05	12 39	2 574	0 981	2 6238	3 03
5G-2	10 04	12 17	2 530	0 963	2 6272	2 91
5G-3	10 13	11 83	2 505	0 951	2 634	2 66
5G-4	10 11	11 16	2 347	0 894	2 6253	2 98
10G-1	9 97	12 74	2 594	0 993	2 6122	4 38
10G-2	10 13	11 89	2 512	0 956	2 6276	3 82
10G-3	10 06	12 49	2 584	0 993	2 6022	4 75
10G-4	10 13	12 29	2 575	0 988	2 606	4 61
15G-1	10 02	11 31	2 335	0 892	2 6177	5 08
15G-2	10 06	11 69	2 425	0 929	2 6103	5 35
15G-3	10 18	12 67	2 635	1 031	2 555	7 36
17G-1	10 12	10 89	2 269	0 876	2 590	6 43
17G-2	10 07	11 85	2 434	0 942	2 584	6 65
17G-3	9 97	11 44	2 327	0 891	2 612	5 64
17G-4	9 99	11 01	2 236	0 862	2 594	6 29
17G-5	10 17	11 34	2 359	0 919	2 567	7 26
20G-1	10 12	10 71	2 247	0 861	2 609	6 28

Density measurement for ingot A, graphite mould (continue)

Sample	Diameter [mm]	Thickness [mm]	Weight In Air [g]	Volume (Calculate)	Measured Density M/V	Porosity [%]
20G-2	10 06	12 22	2 452	0 971	2 525	9 30
20G-3	10 13	11 27	2 371	0 906	2 616	6 03
20G-4	10 05	11 14	2 328	0 882	2 639	5 21
25G-1	10 12	10 24	2 053	0 824	2 492	11 31
25G-2	10 05	10 84	2 082	0 858	2 426	13 66
25G-3	10 21	11 62	2 380	0 949	2 508	10 75

Appendix F

**Micro Hardness Measurements
-As cast Condition**

Micro hardness measurement for A359 matrix alloy as cast condition

Sample	Microhardness [Hv]					Microhardnes [Hv] Average value
	Reading 1	Reading 2	Reading 3	Reading 4	Reading5	
AL -1 (50G)	74 8	64 6	73 6	59 1	69 6	68 34
AL-2	73 5	63 9	64 6	71 5	74 8	69 66
AL-3	64 6	71 5	63 9			66 67
VICKERS HARDNESS FOR A359 MATRIX ALLOY						68.22

Microhardness measurement for A359/SiC/5p

Sample	Microhardness [Hv]				Distance form the top [mm]
	Reading 1	Reading 2	Reading 3	Reading 4	
5G-1	78 5	96 7	90 4	90 0	5
5G-2	111	106	108	94 9	11 6
5G-3	132	129	114	94 5	19 9
5G-4	97 6	98 5	102	116	27 6
5G-5	123	117	121	105	35 4
5G-6	103	109	96 2	127	43 9
5G-7	126	108	120	120	51 2
5G-8	80 5	92 8	98 5	90 8	59 9
5G-9	68 3	103	103	90 4	67 3
5G-10	66 8	89 6	82 9	98 5	74 5

Microhardness measurement for A359/SiC/5p

Sample	Microhardness [Hv]				Distance from the top [mm]
	Reading 1	Reading 2	Reading 3	Reading 4	
5G-1	96 2	94 9	81 8	98 9	5
5G-2	116	90 8	101	94 9	12 3
5G-3	97 6	107	87 2	96 7	19 9
5G-4	105	94 1	93 6	98 9	27 8
5G-5	88 8	104	94 9	106	35 3
5G-6	94 9	116	99 4	89 2	42 8
5G-7	96 7	116	102	90 8	50 6
5G-8	99 4	105	98 5	86 9	58 3
5G-9	88 8	99 4	79 5	97 6	66 8
5G-10	93 6	85 0	97 1	90 8	74 9
5G-11	102	91 6	86 9	85 4	82 9
5G-12	86 9	75 1	91 6	102	92 8

Microhardness measurement for A359/SiC/15p

Sample	Microhardness [Hv]			Distance form the top [mm]
	Reading 1	Reading 2	Reading 3	
15G-A	69 1	76 0	95 8	5
15G-B	83 6	82 9	72 4	14 9
15G-C	80 5	99 4	90 8	23 2
15G-D	76 0	116	72 7	30 3
15G-E	88 4	90 0	85 8	36 7
15G-F	88 8	91 2	90 4	44 8
15G-G	93 6	90 8	88 0	51 3
15G-H	90 4	91 6	85 4	60 0
15G-J	93 6	99 4	69 9	75 2
15G-K	83 2	83 6	87 6	80 5
15-M	78 5	83 6	78 2	99.8

Microhardness measurement for A359/SiC/25p

Sample	Microhardness [Hv]				Distance form the top [mm]
	Reading 1	Reading 2	Reading 3	Reading 4	
25G-1	85 8	82 5	81 8	68 0	11.8
25G-2	88 8	78 5	93 2	72 4	17.3
25G-3	83 9	86 9	101	83 2	24 0
25G-4	92 8	108		83 6	30 5
25G-5	98 5	82 9	84 7	84 3	37 3
25G-6		92 4	95 3	98 0	44 2
25G-7	88 4	93 6	107		58.0
25G-8	83 6	86 5	76 9		71.6
25G-9	79 5	79 8	86 9		78.9

Microhardness measurement for A359/SiC/15p

Sample	Microhardness [Hv]				Distance form the top [mm]
	Reading 1	Reading 2	Reading 3	Reading 4	
15G-1	80 8	98 0	94 5	89 2	5
15G-2	100	82 5	92 8	89 6	13 3
15G-3	95 3	104	96 7	91 2	20 7
15G-4	87 6	103	105	93 6	29 0
15G-5	91 2	97 6	103	94 1	35 8
15G-6	105	90 8	92 8	99 8	44 3
15G-7	92 4	87 2	97 6	94 9	51 4
15G-8	87 6	98 5	96 7	102	59 6
15G-9	102	101	93 6	102	67 4
15G-10	98 0	98 8	102	78 5	75 3
15G-11	95 8	80 2	104	97 1	83 7
15G-12	93 2	94 1	92 4	99 8	91 3

Microhardness measurement for A359/SiC/25p

Sample	Microhardness [Hv]				Distance form the top [mm]
	Reading 1	Reading 2	Reading 3	Reading 4	
25G-A	126	108	117	120	5
25G-B	124	124	130	141	11 4
25G-C	133	126	146		18 4
25G-D	114	128	116	117	24 9
25G-E	106	119	99 4	91 2	32 4
25G-F	99 8	101	80 4	98 5	40 0
25G-G	81 8	85 0	86 9		47 2
25G-H	89 6	107	102		54.5
25G-I	116	110	74 2		62.4
25G-J	80 5	103	91 2		69 8
25G-K	95 8	106	101		76 3

Microhardness measurement for A359/SiC/5p

Sample	Microhardness [Hv]				Distance form the top [mm]
	Reading 1	Reading 2	Reading 3	Reading 4	
5S-1	91 2	123	105	134	5
5S-2	116	109	97 6	116	12 3
5S-3	98 5	128	108	99 4	19 8
5S-4	82 2	102	99 8	94 9	25 6
5S-5	107	94 9	108	116	32.4
5S-6	104	79 2	108	97 6	39 7
5S-7	101	112	98 0	105	47 1
5S-8	78 8	126	103	88 8	55 5

Microhardness measurement for A359/SiC/10p

Sample	Microhardness [Hv]				Distance form the top [mm]
	Reading 1	Reading 2	Reading 3	Reading 4	
10S-1	87 2	94 9	93 6	96 7	5
10S-2	116	95 3	98 0	116	11 7
10S-3	110	102	116	105	18 1
10S-4	109	93 6	101	97 6	24 9
10S-5	111	90 8	93 2	89 6	32 0
10S-6	92 0	110	110	96 2	38.2
10S-7	106	110	110		44 7
10S-8	111	116	93 2	116	51 7
10S-9	110	116	91 6	97 6	58 7

Microhardness measurement for A359/SiC/15p

Sample	Microhardness [Hv]				Distance form the top [mm]
	Reading 1	Reading 2	Reading 3	Reading 4	
5S-1	110	105	102	108	5
15S-2	128	124	111	83 6	12.9
15S-3	105	99 4	110	116	21 0
15S-4	116	99 8	111	104	28.6
15S-5	116	110	97 1	116	36 7
15S-6	107	105	98 9	115	44 3
15S-7	116	116	107	116	51 4
15S-8	98 9	105	109	112	58 9

Microhardness measurement for A359/SiC/15p

Sample	Microhardness [Hv]				Distance form the top [mm]
	Reading 1	Reading 2	Reading 3	Reading 4	
15S-1	78 5	75 4	83 2		5
15S-2	90 4	90 8	78 5	75 4	12 0
15S-3	94 9	101	99 8	92 0	19 3
15S-4	110	109	108		26 3
15S-5	100	104	109		34 0
15S-6	99 4	109	110	116	41 3
15S-7	83 2	86 9	105		50.0
15S-8	87 6	98 0	88 8		57 3

Microhardness measurement for A359/SiC/25p

Sample	Microhardness [Hv]				Distance form the top [mm]
	Reading 1	Reading 2	Reading 3	Reading 4	
25S-1	75 4	83 9	74 8	83 9	5
25S-2	94 9	103	90 8	96 2	12 6
25S-3	101	105	94 9	87 6	19 7
25S-4	95 3	116	105	104	26 9
25S-5	110	105	109	109	34 9
25S-6	95 8	108	95 8	113	44.0
25S-7	100	79 2	107	85 4	52.1

Microhardness measurement for A359/SiC/25p

Sample	Microhardness [Hv]				Distance form the top [mm]
	Reading 1	Reading 2	Reading 3	Reading 4	
25S-1	103	86 1	103	93 2	5
25S-2	67 8	103	98 5	72 4	17 2
25S-3	89 2	89 6	103	116	25 7
25S-4	103	93 6	88 0	91 2	35 1
25S-5	103	96 2	105	102	43 9
25S-6	82 2	101	111	97 6	52 8
25S-7	86 5	88 0	85 4		59 0

Appendix G

Micro Hardness Measurements -After T6 Treatment

Micro hardness measurement after t6 treatment for
A359 matrix alloy

Samples	Aging time	Hardness
1	2	85 8
2	2	71 9
3	2	81 8
1	4	85 0
2	4	89 2
3	4	86 5
1	6	89 2
2	6	98 0
3	6	95 8
1	8	82 2
2	8	79 5
3	8	96 2
1	10	95 3
2	10	104
3	10	101

Microhardness measurements after t6 treatment for A359/SiC/5p

Samples	Aging time [hr]	Hardness [Hv]
1	2	74 2
2	2	76 3
3	2	85 0
1	4	115
2	4	97 6
3	4	96 7
1	6	113
2	6	110
3	6	101
1	8	123
2	8	115
3	8	121
1	10	116
2	10	104
3	10	111

Microhardness measurements after t6 treatment for A359/SiC/10p

Samples	Aging time [hrs]	Hardness [Hv]
1	2	64 8
2	2	83 2
3	2	71 9
1	4	94 5
2	4	90 8
3	4	96 7
1	6	119
2	6	112
3	6	111
1	8	115
2	8	112
3	8	101
1	10	85 4
2	10	87 2
3	10	93 2

Micro hardness measurements after t6 treatment for
A359/SiC/15p

Samples	Aging time [hrs]	Hardness [Hv]
1	2	70 2
2	2	83 9
3	2	90 8
1	3	79 2
2	3	77 6
3	3	90 4
1	4	88 8
2	4	81 8
3	4	82 5
1	5	94 5
2	5	97 6
3	5	107
1	6	96 2
2	6	106
3	6	105
1	7	99 4
2	7	98 0
3	7	109 0
1	8	96 2
2	8	101
3	8	104
1	10	105
2	10	104
3	10	106

Microhardness measurements after t6 treatment for A359/SiC/17p

Samples	Aging time [hrs]	Hardness [Hv]
1	2	102
2	2	90 0
3	2	98 0
1	3	102
2	3	114
3	3	111
1	4	127
2	4	111
3	4	106
1	5	107
2	5	109
3	5	112
1	6	97 6
2	6	112
3	6	104
1	7	99 8
2	7	116
3	7	106
1	10	106
2	10	110
3	10	112

Microhardness measurements after t6 treatment for
A359/SiC/20p

Samples	Aging time [hrs]	Hardness [Hv]
1	2	106
2	2	96 7
3	2	99 4
1	3	87 2
2	3	84 7
3	3	89 6
1	4	93 6
2	4	85 8
3	4	79 5
1	6	77 2
2	6	96 7
3	6	95 8
1	7	102
2	7	104
3	7	95 8
1	8	91 6
2	8	109
3	8	110
1	10	85 0
2	10	86 5
3	10	81 2

Microhardness measurements after t6 treatment for A359/SiC/25p

Samples	Aging time [hrs]	Hardness [Hv]
1	2	97 6
2	2	107
3	2	93 2
1	3	93 2
2	3	85 8
3	3	98 2
1	4	103
2	4	100
3	4	94 5
1	5	98 0
2	5	86 5
3	5	82 2
1	7	99 8
2	7	112
3	7	96 7
1	8	102
2	8	110
3	8	99 8
1	10	123
2	10	120
3	10	116

Microhardness measurements after t6 treatment for
A359 matrix alloy

Samples	Aging time [hrs]	Hardness [Hv]
1	2	106
2	2	89 2
3	2	88 8
1	4	105
2	4	110
3	4	105
1	6	108
2	6	107
3	6	107
1	8	103
2	8	121
3	8	126
1	10	112
2	10	114
3	10	110

Microhardness measurements after t6 treatment for A359/SiC/10p

Samples	Aging time [hrs]	Hardness [Hv]
1	2	105
2	2	92.8
3	2	102
1	4	104
2	4	104
3	4	102
1	6	101
2	6	112
3	6	108
1	8	121
2	8	100
3	8	101
1	10	104
2	10	110
3	10	106

Micro hardness measurements after t6 treatment for
A359/SiC/15p

Samples	Aging time [hrs]	Hardness [Hv]
1	2	98 0
2	2	98 0
3	2	94 1
1	3	82 9
2	3	82 5
3	3	90 0
1	4	94 5
2	4	107
3	4	103
1	5	107
2	5	93 2
3	5	104
1	6	102
2	6	107
3	6	106
1	7	115
2	7	109
3	7	112
1	9	98 9
2	9	112
3	9	108
1	10	93 6
2	10	90 0
3	10	112

Micro hardness measurements after t6 treatment for
A359/SiC/17p

Samples	Aging time [hrs]	Hardness [Hv]
1	3	93 2
2	3	79 5
3	3	99 4
1	5	84 3
2	5	89 6
3	5	95 8
1	6	103
2	6	86 1
3	6	86 9
1	7	101
2	7	111
3	7	93 2
1	9	107
2	9	88 0
3	9	97 6

Micro hardness measurements after t6 treatment for A359/SiC/20p

Samples	Aging time [hrs]	Hardness [Hv]
1	2	83 9
2	2	96 2
3	2	105 0
1	3	101
2	3	116
3	3	101
1	4	110
2	4	109
3	4	112
1	5	100
2	5	107
3	5	102
1	7	79 6
2	7	90 0
3	7	92 0
1	8	84 3
2	8	79 8
3	8	75 1
1	9	94 1
2	9	78 5
3	9	93 2

Micro hardness measurements after t6 treatment for
A359/SiC/25p

Samples	Aging time [hrs]	Hardness [Hv]
1	2	95 3
2	2	84 7
3	2	96 2
1	3	88 8
2	3	91 6
3	3	93 2
1	4	115
2	4	104
3	4	93 2
1	5	80 2
2	5	95 8
3	5	86 5
1	6	97 1
2	6	93 2
3	6	97 6
1	7	116
2	7	108
3	7	113
1	8	103
2	8	95 8
3	8	104
1	9	97 6
2	9	99 8
3	9	97 6
1	10	93 2
2	10	98 9

Appendix H

Compression Testing

Compression testing result - as-cast condition

Sample	Diameter [mm]	Initial length [mm]	Length after loading [mm]	Load at fracture [kN]
AL-1	10 07	10 29	7 26	
AL-2	10 04	10 69	7 49	
AL-3	10 16	11 35	6 26	
AL-4	10 13	11 09	7 06	
AL-5	10 17	10 81	7 85	
5G-1	10 09	12 18	6 70	-
5G-2	10 09	12 65	8 52	-
5G-3	9 82	10 13	7 13	-
5G-4	9 99	11 48	8 15	-
5G-5	10 03	11 95	8 78	-
10G-1	10 00	10 62	6 88	-
10G-2	10 05	11 14	7 22	33 53
10G-3	10 12	12 34	7 86	32 91
10G-4	10 09	12 36	8 38	-
10G-5	10 12	12 99	8 48	26 29
17G-1	10 17	11 07	5 92	40 32
17G-2	9 97	12 49	10 05	42 17
17G-3	10 05	11 51	7 44	38 72
17G-4	10 01	11 07	6 54	48 67
17G-5	10 07	11 44	7 39	44 23
20G-1	10 15	11 70	9 50	41 85
20G-2	10 21	11 31	7 48	31 34
20G-3	10 16	12 53	9 39	48 28
20G-4	10 16	11 91	6 83	41 38
25G-1	10 01	12 19	8 90	24 20
25G-2	10 18	13 25	10 32	27 83
25G-3	10 09	11 70	9 15	29 72
25G-4	10 19	10 86	9 02	21 08
25G-5	10 08	10 24	8 78	27 78
25G-6	10 19	11 01	8 90	25 85

Appendix I

Tensile Testing

Tensile testing result before and after t6 treatment for A359 matrix alloy

Samples	Aging time [hrs]	Tensile strength [n/mm2]
1	0	103 75
2	0	104 95
1	2	179 56
2	2	237 09
1	4	244 19
2	4	179 02
1	6	249 96
2	6	260 49
1	8	262 68
2	8	230 70

Tensile testing result before and after t6 treatment for
A359/SiC/5p

Samples	Aging time [hrs]	Tensile strength [N/mm ²]
1	0	157 73
2	0	170 94
3	0	132 95
1	2	198 66
2	2	230 70
3	2	188 62
1	4	215 91
2	4	225 95
3	4	246 36
1	6	208 48
2	6	231 41
3	6	241 99
1	8	161 17
2	8	223 17
3	8	175 69
1	10	234 14
2	10	217 22

Tensile testing result before and after t6 treatment for A359/SiC/10p

Samples	Aging time [hrs]	Tensile strength [N/mm ²]
1	0	141 25
2	0	140 81
3	0	153 19
1	2	217 87
2	2	190 53
3	2	148 99
1	4	196 92
2	4	167 39
3	4	116 79
1	6	120 78
2	6	141 46
3	6	272 39
1	8	135 89
2	8	210 56
3	8	217 93
1	10	238 61
2	10	220 38
3	10	189 44

Tensile testing result before and after t6 treatment for
A359/SiC/15p

Samples	Aging time [hrs]	Tensile strength [N/mm ²]
1	2	115 10
2	2	152 16
3	2	152 22
1	4	118 54
2	4	174 37
3	4	182 29
1	6	174 59
2	6	180 05
3	6	180 05
1	8	166 08
2	8	191 84

0 2 Proof Stress before and after t6 treatment for
A359 matrix alloy

Samples	Aging time [hrs]	0 2 Proof Stress [N/mm ²]
1	0	57 85
2	0	60 58
1	2	121 00
2	2	181 74
1	4	198 66
2	4	176 28
1	6	245 05
2	6	259 24
1	8	234 14

0 2 Proof Stress before and after t6 treatment for
A359/SiC/5p

Samples	Aging time [hrs]	0 2 Proof Stress [N/mm ²]
1	0	76 9
2	0	74 23
3	0	71 49
1	2	198 66
2	2	187 20
3	2	173 56
1	4	216 13
2	4	225 95
3	4	234 14
1	6	208 49
2	6	225 98
3	6	228 68
1	8	266 89
2	8	222 68
1	10	228 68
2	10	217 22

0.2 Proof Stress before and after t6 treatment for
A359/SiC/10p

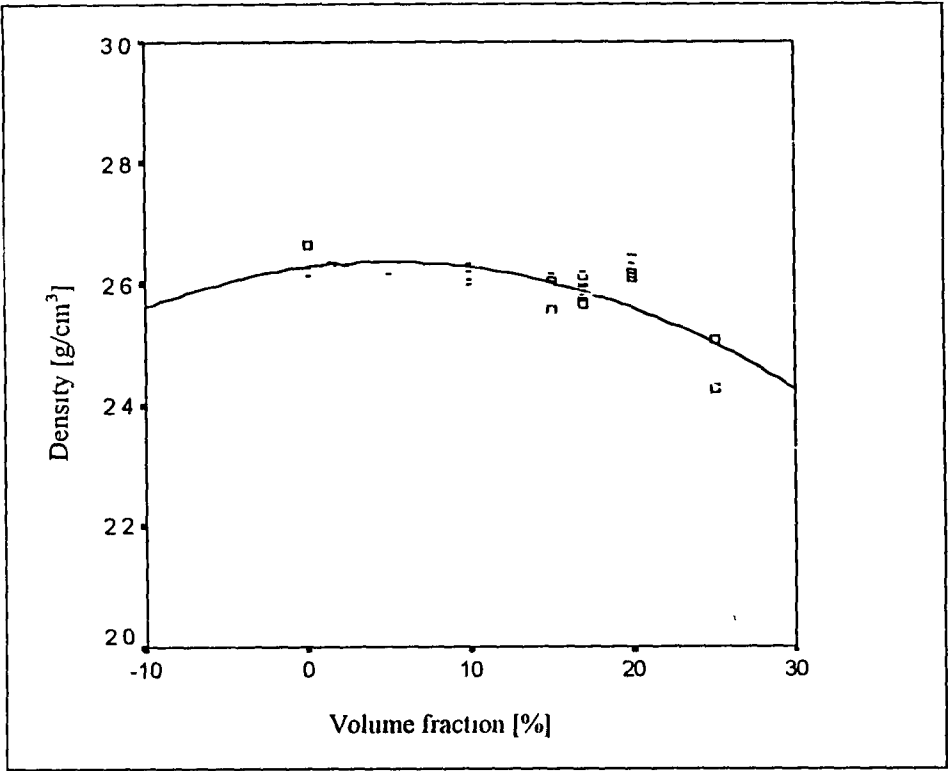
Samples	Aging time [hrs]	0.2 Proof Stress [N/mm ²]
1	0	57.85
2	0	46.39
3	0	55.12
1	2	189.93
2	2	173.56
1	4	173.56
2	4	159.37
1	6	211.76
2	6	211.76
1	8	211.76
2	8	204.12
1	10	217.76
2	10	217.76
3	10	187.20

0.2 Proof Stress before and after t6 treatment for A359/SiC/10p

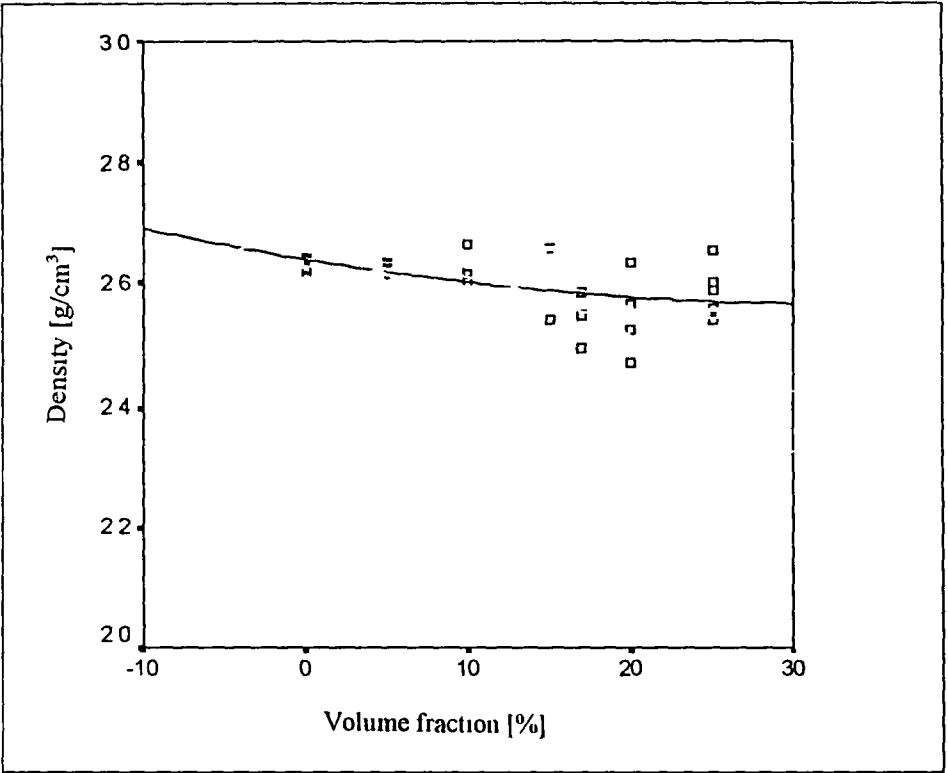
Samples	Aging time [hrs]	0.2 Proof Stress [N/mm2]
1	2	121.71
2	2	113.46
1	4	144.08
2	4	135.89
1	6	170.28
2	6	171.37
1	8	168.09
2	8	143.54

Appendix J

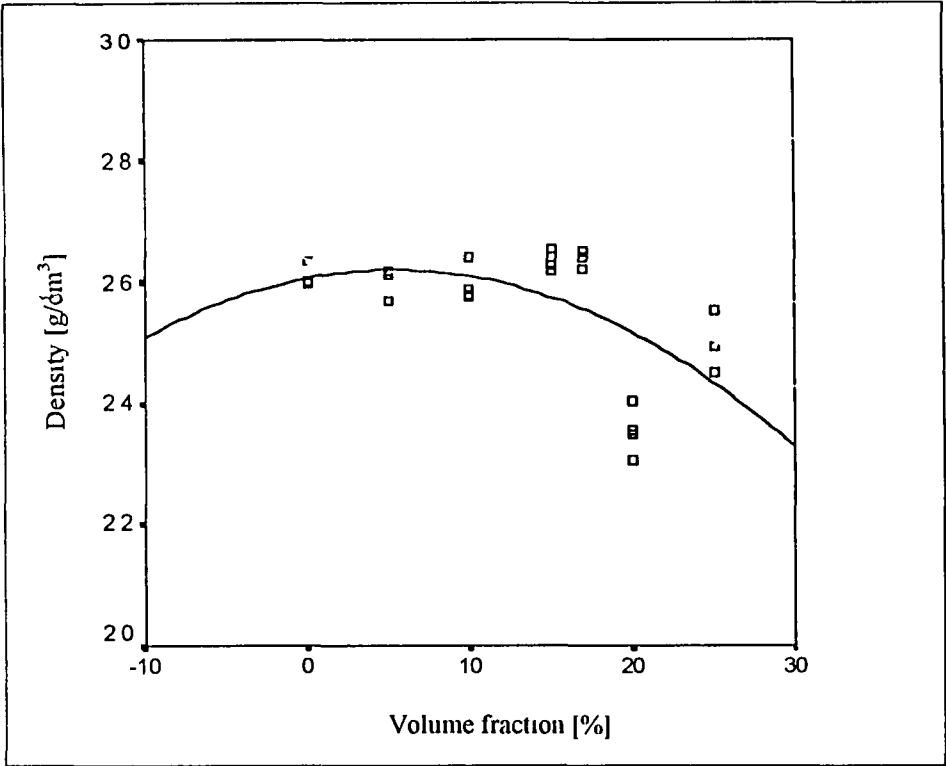
Graphs



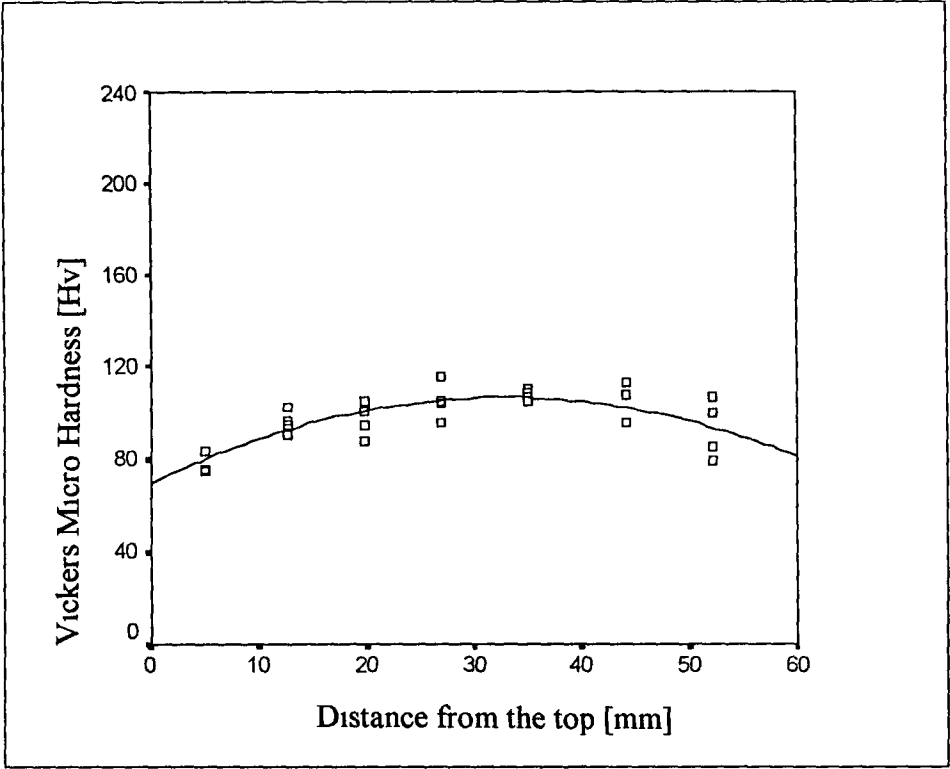
Porosity as a function of silicon carbide content for graphite mould- A



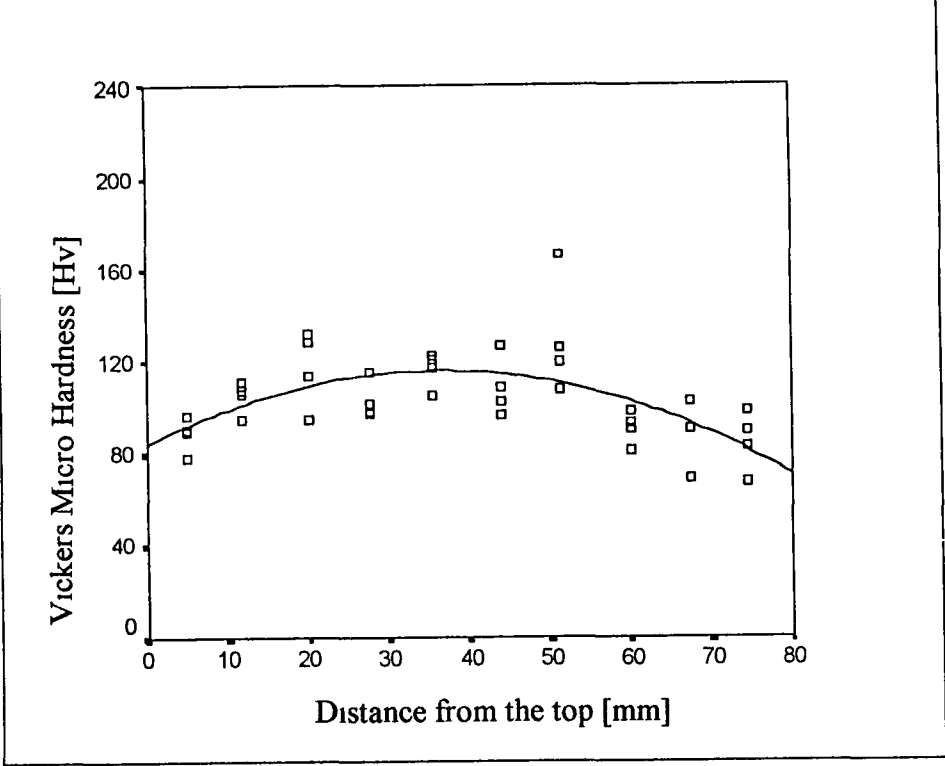
Porosity as a function of silicon carbide content for steel mould- A



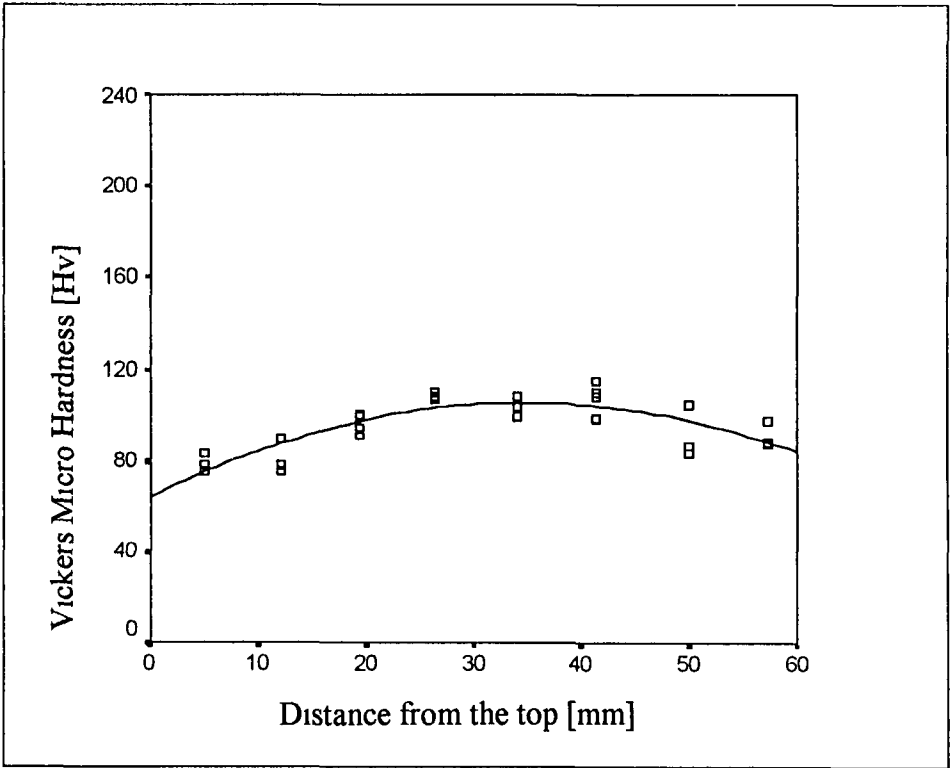
Porosity as a function of silicon carbide content for steel mould- B



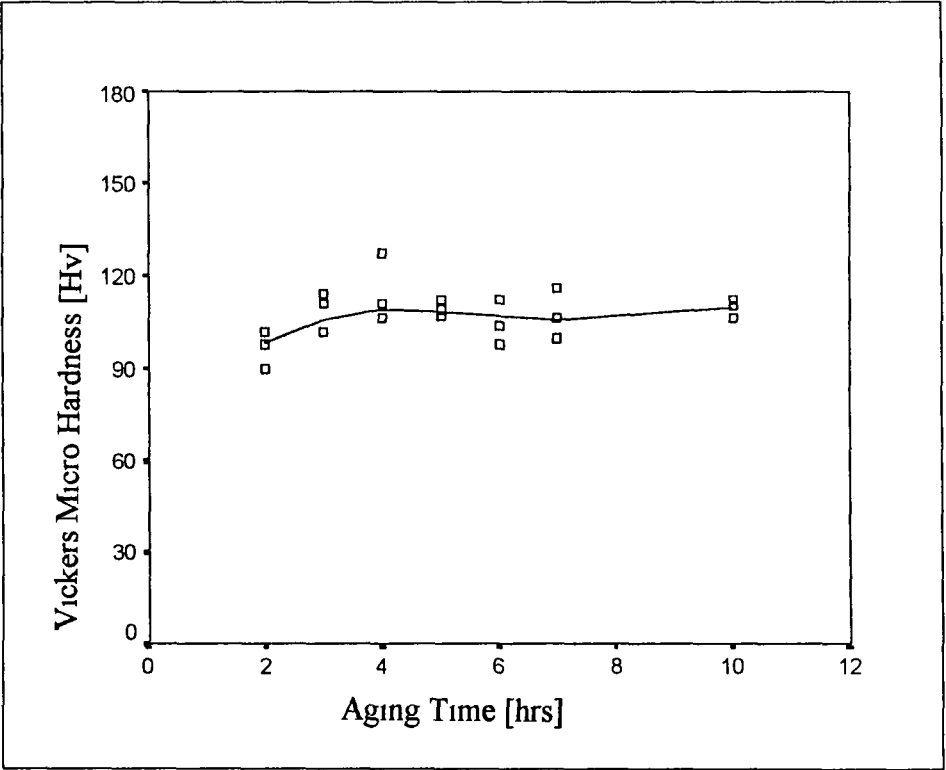
Micro hardness as a function f ingot's distance from the top for A359/SiC/5p (as cast)



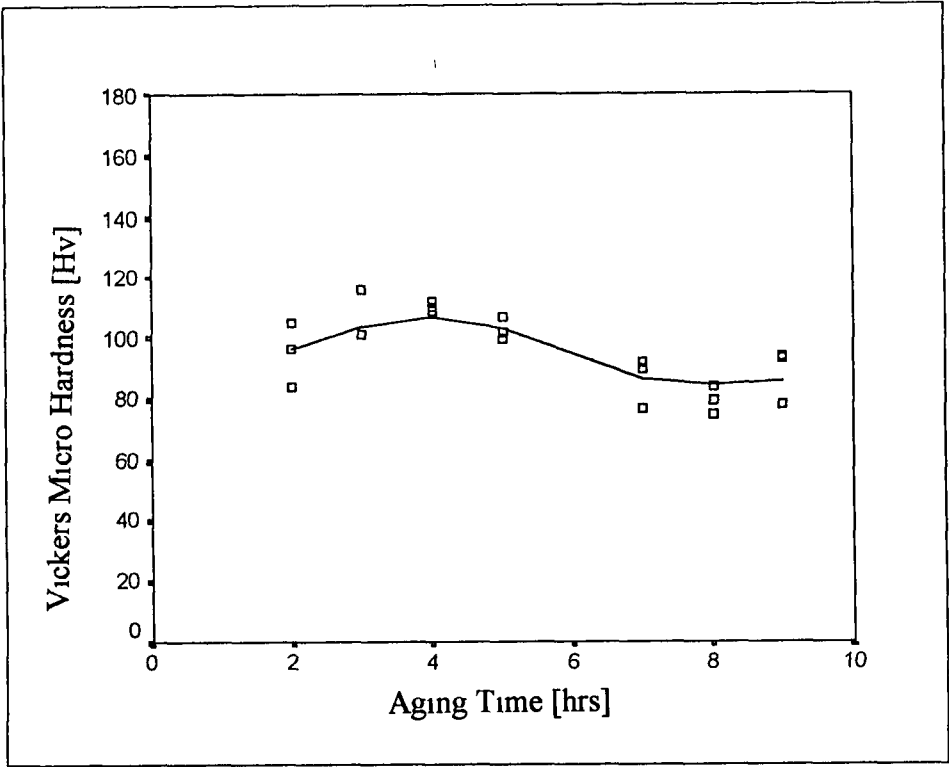
Micro hardness as a function f ingot's distance from the top for A359/SiC/5p (as cast)



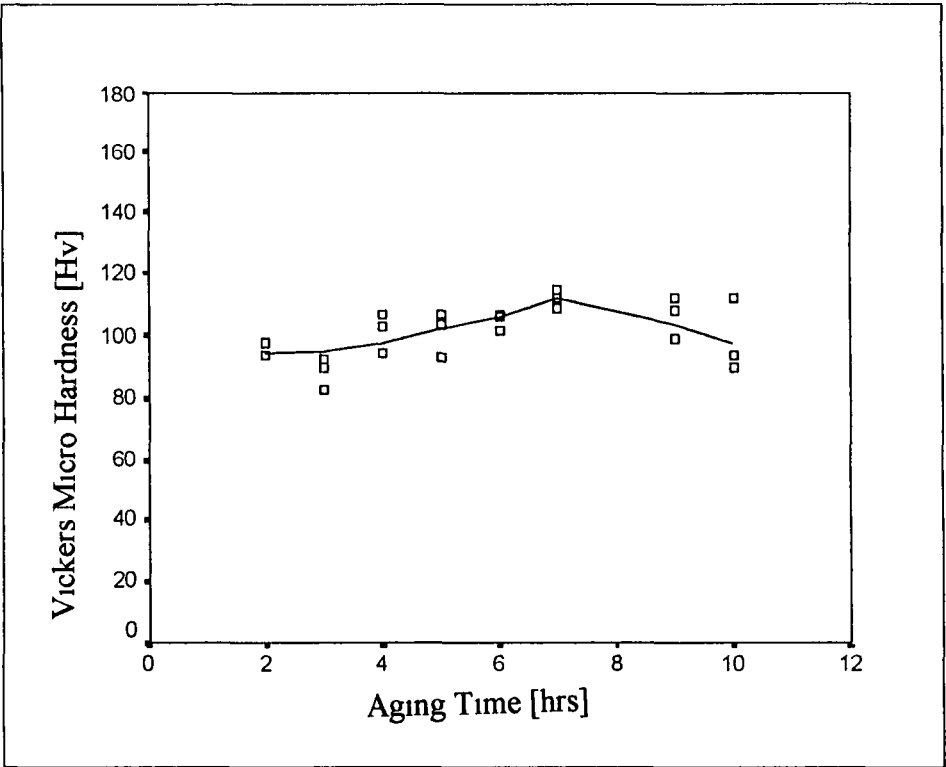
Micro hardness as a function f ingot's distance from the top for A359/SiC/15p (as cast)



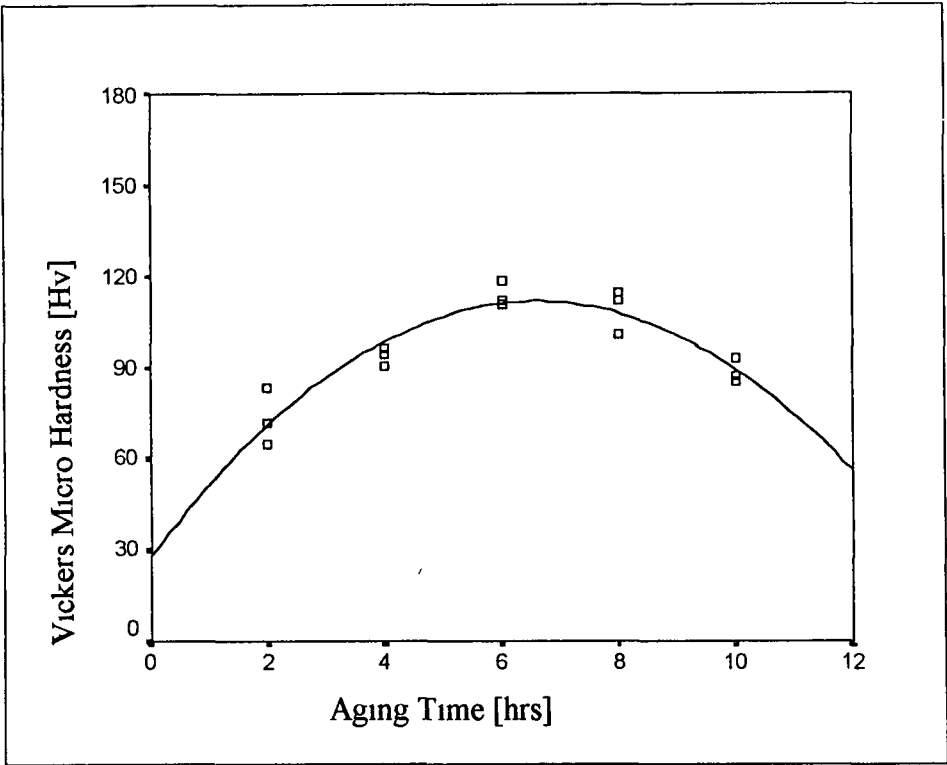
Micro hardness as a function of aging time for A359/SiC/17p



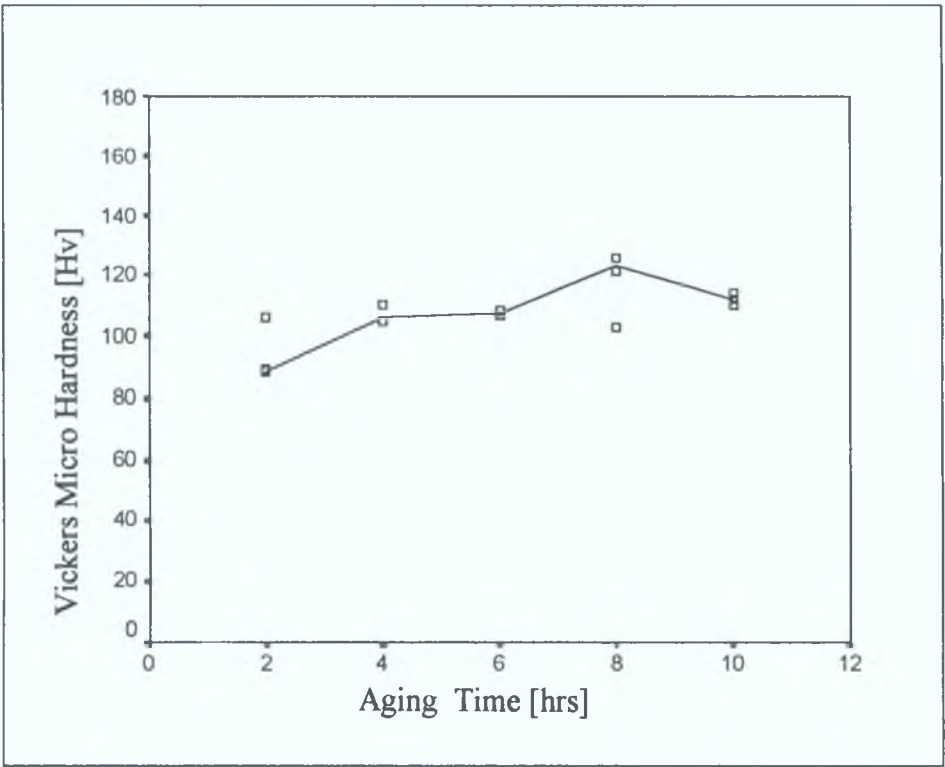
Micro hardness as a function of aging time for A359/SiC/20p



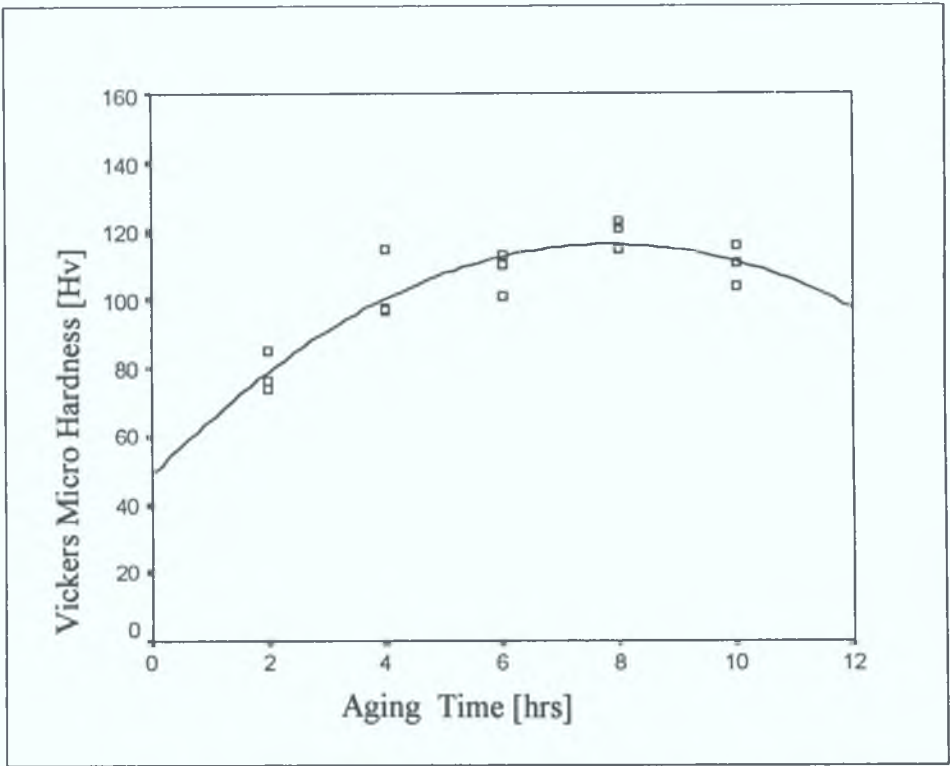
Micro hardness as a function of aging time for A359/SiC/15p



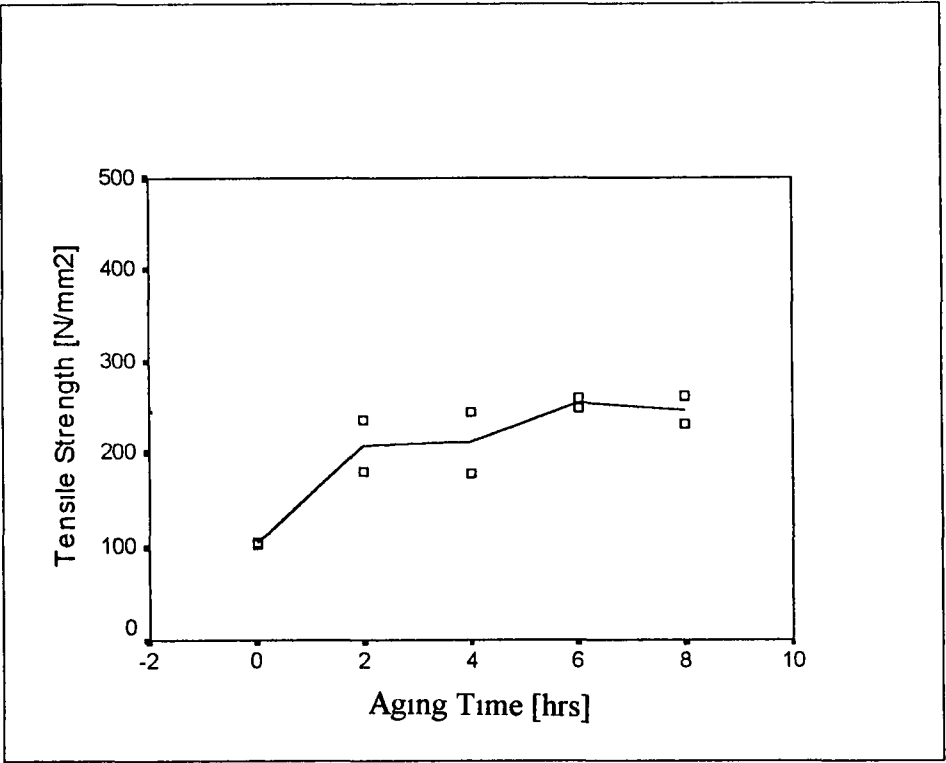
Micro hardness as a function of aging time for A359/SiC/10p



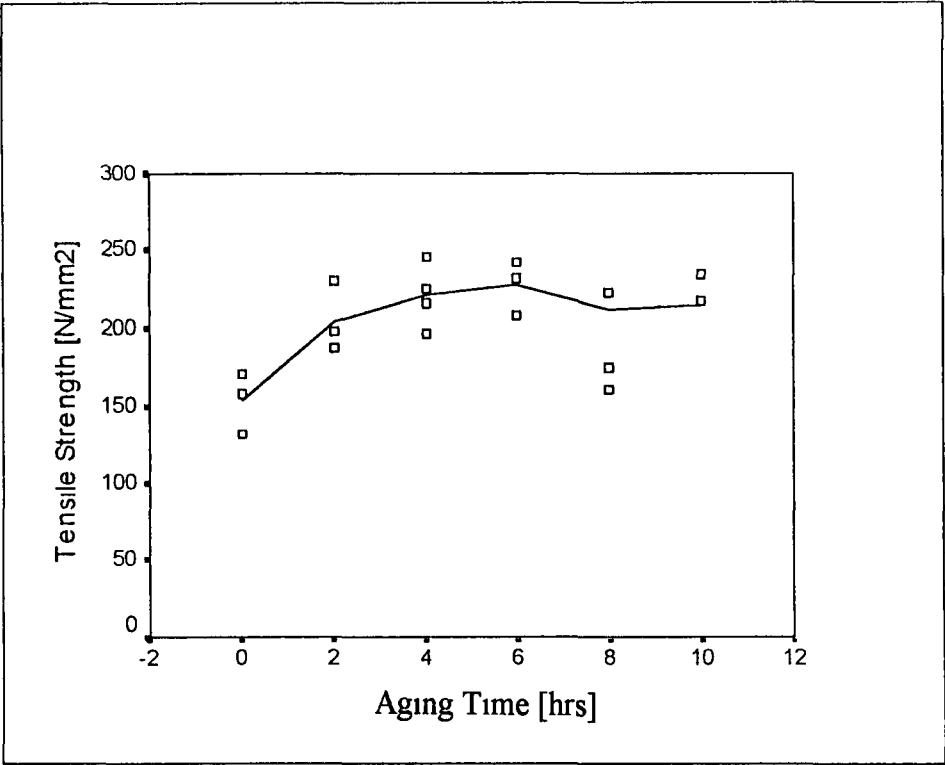
Micro hardness as a function of aging time for A359 alloy



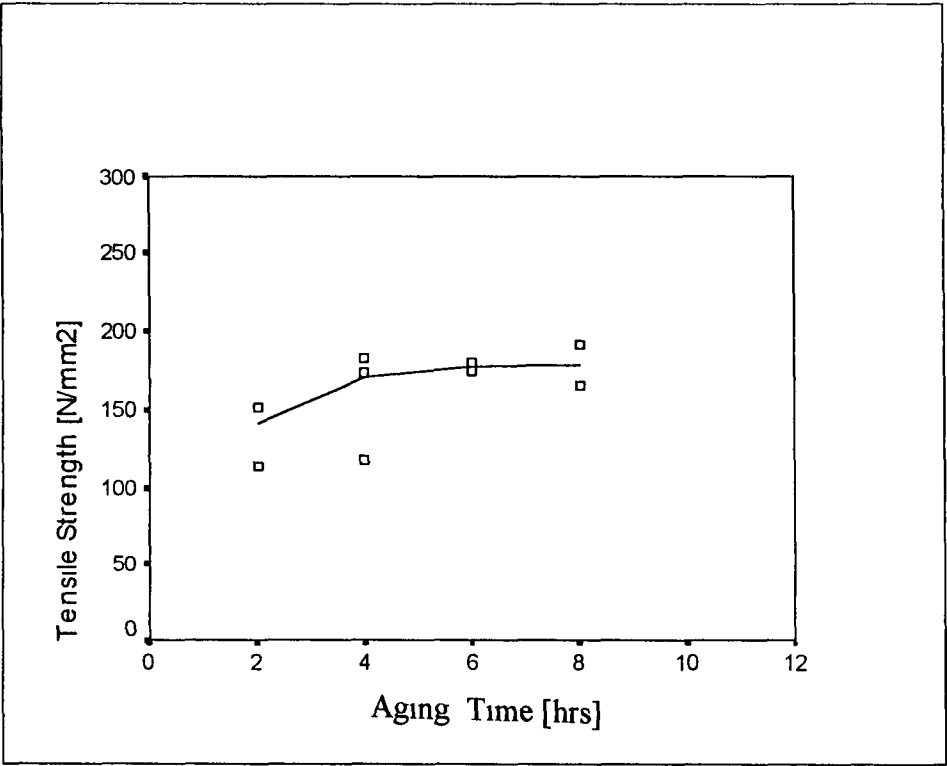
Micro hardness as a function of aging time for A359/SiC/5p



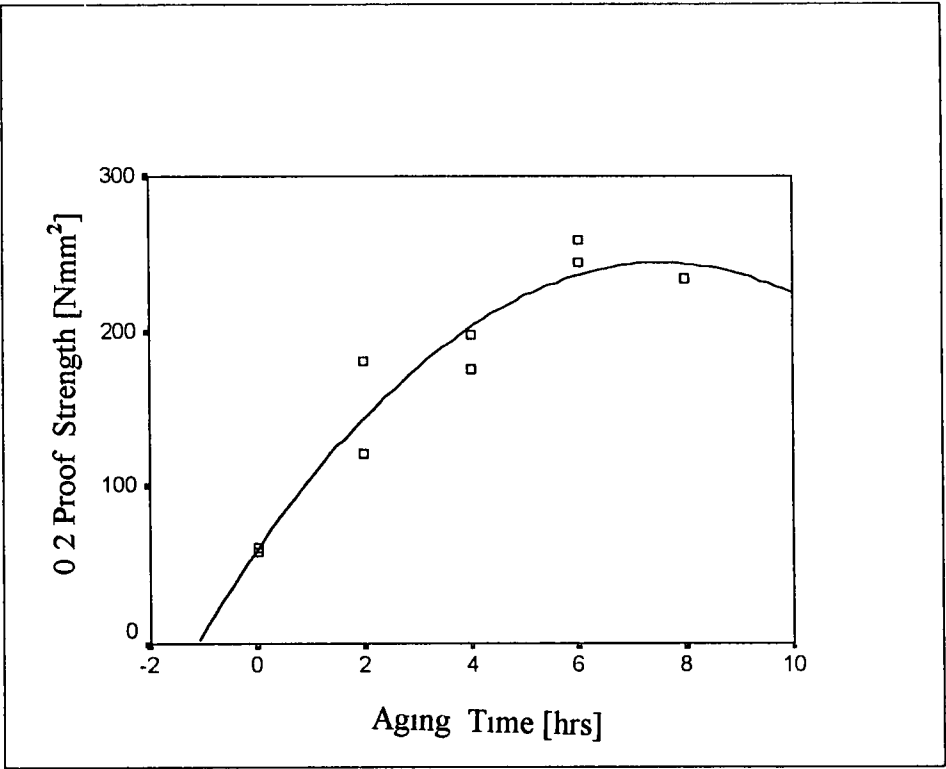
Tensile Strength as a function of aging time for A359 alloy



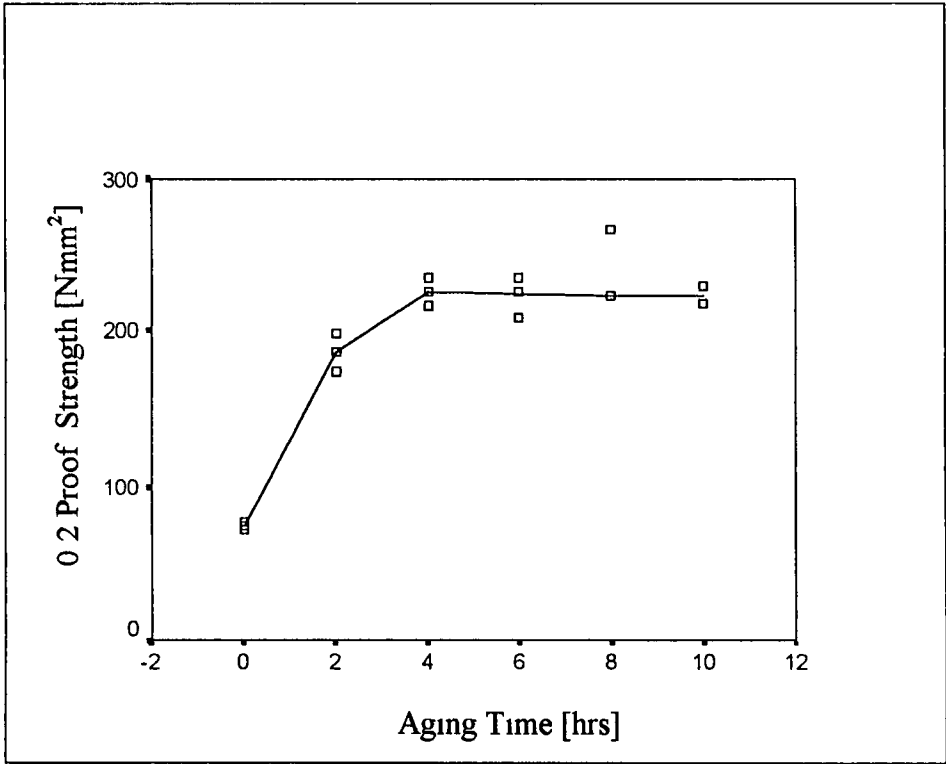
Tensile Strength as a function of aging time for A359/SiC/5p



Tensile Strength as a function of aging time for A359/SiC/15p



Proof Strength as a function of aging time for A359 alloy



Proof Strength as a function of aging time for A359/SiC/5p

Appendix K

Publications

PUBLICATIONS

- 1 Hashim J , Looney L and Hashmi M S J, Metal Matrix Composites Production by the Stir Casting Method, Proceeding of the International Conference on Advances in Materials and Processing Technologies, Universidade do Minho, Portugal, July 1997, pp 1-8
- 2 Hashim J, Looney L and Hashmi M S J , Particle Distribution In Cast MMCs - Part I, Proceeding of the International Conference, Advances on Materials and Processing Technologies, Kuala Lumpur, Malaysia, August 1998, pp 349-358
- 3 Hashim J, Looney L and Hashmi M S J , Particle Distribution In Cast MMCs - Part II, Proceeding of the International Conference, Advances on Materials and Processing Technologies, Kuala Lumpur, Malaysia, August 1998, pp 358-366
- 4 Hashim J, Looney L and Hashmi M S J , The Enhancement of Wettability of SiC Particles in cast Aluminium Matrix Composites, Proceeding of the International Conference Advances on Materials and Processing Technologies, Dublin City University, Ireland, August 1999, pp 47-57

- 5 Hashim J, Looney L and Hashmi M S J, The of Wettability of SiC by Molten Aluminium Alloy, Proceeding of the International Conference, Advances on Materials and Processing Technologies, Dublin City University, Ireland, August 1999, pp 57-69